ISWS/BUL-64/80
BULLETIN 64
STATE OF ILLINOIS
ILLINOIS INSTITUTE OF NATURAL RESOURCES

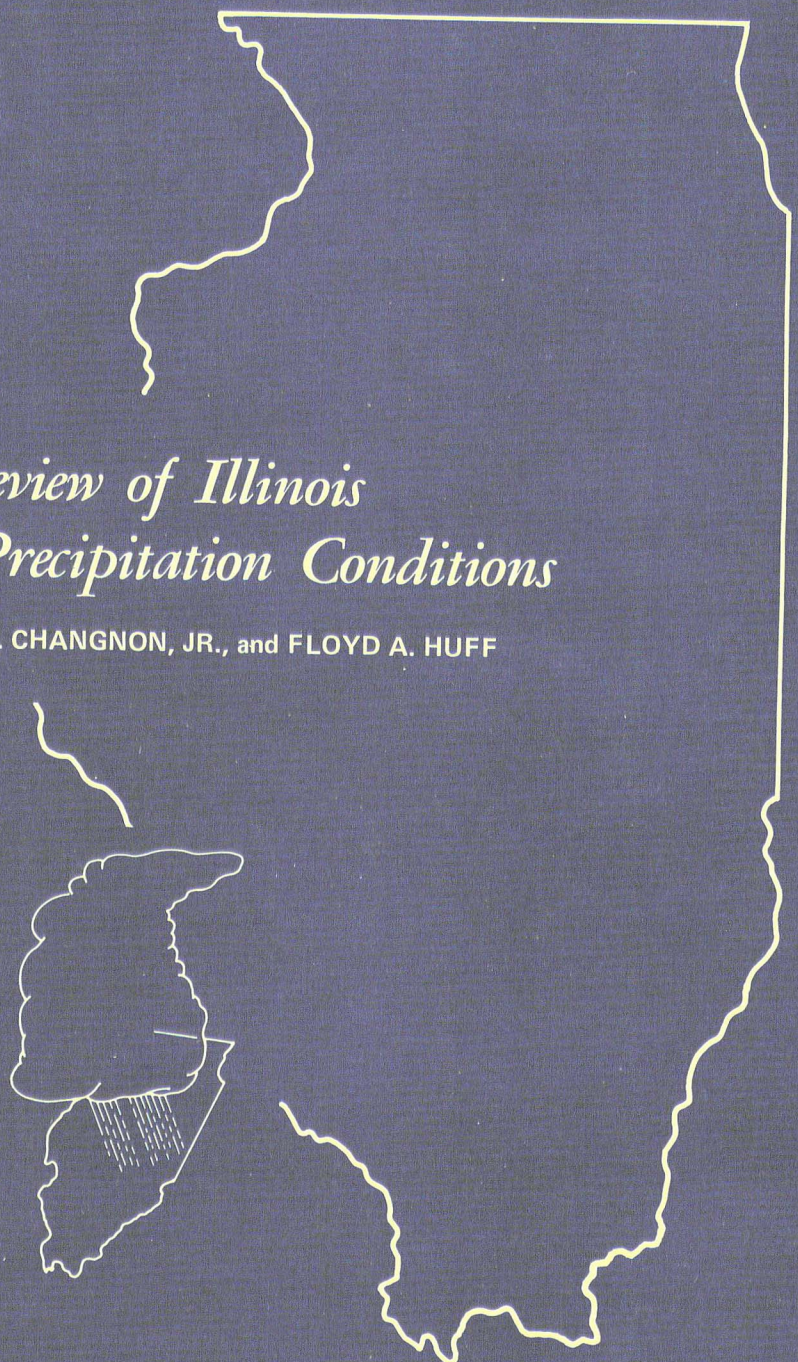

Review of Illinois Summer Precipitation Conditions

by STANLEY A. CHANGNON, JR., and FLOYD A. HUFF

ILLINOIS STATE WATER SURVEY
URBANA
1980

BULLETIN 64

Review of Illinois Summer Precipitation Conditions

by STANLEY A. CHANGNON, JR., and FLOYD A. HUFF

Title: Review of Illinois Summer Precipitation Conditions

Abstract: This report summarizes key findings regarding all aspects of precipitation in the convective season gleaned from 30 years of research at the Illinois State Water Survey. Examples of information that dimensionalize midwestern precipitation phenomena extracted from published papers, reports, and grant-contract studies have been included. These examples are accompanied by extensive graphs, maps, and tables to provide a useful information document pertinent to the areas of forecasting, modification of summer convective elements, or midwestern precipitation conditions in general. As an equally important purpose, the report provides listings of nearly a hundred supporting references that serve as a guide to more extensive information. The material covers general climatic aspects of the state, ranging from average annual, monthly, and daily rain distributions through severe rainstorms and droughts. More detailed information on relationships of precipitation with atmospheric moisture and various weather types, on organized storms and substorm entities, on vertical and horizontal characteristics of individual storm cells, and on external and internal cloud characteristics is also included.

Reference: Changnon, Stanley A. Jr., and Floyd A. Huff. Review of Illinois Summer Precipitation Conditions. Illinois State Water Survey, Urbana, Bulletin 64, 1980.

Indexing Terms: climatology, convection, droughts, heavy rainstorms, hydrometeorology, mesometeorology, radar meteorology, rainfall, synoptic weather conditions, weather modification.

STATE OF ILLINOIS
HON. JAMES R. THOMPSON, Governor

INSTITUTE OF NATURAL RESOURCES
FRANK H. BEAL, M.U.P., Director

STATE WATER SURVEY DIVISION
STANLEY A. CHANGNON, JR., M.S., Chief

URBANA
1980

Printed by authority of the State of Illinois
(4-80-1500)
P.O.19331

CONTENTS

Review of Illinois Summer Precipitation Conditions

by Stanley A. Changnon, Jr., and Floyd A. Huff

ABSTRACT

This report summarizes key findings regarding all aspects of precipitation in the convective season gleaned from 30 years of research at the Illinois State Water Survey. Examples of information that dimensionalize midwestern precipitation phenomena extracted from published papers, reports, and grant-contract studies have been included. These examples are accompanied by extensive graphs, maps, and tables to provide a useful information document pertinent to the areas of forecasting, modification of summer convective elements, or midwestern precipitation conditions in general. As an equally important purpose, the report provides listings of nearly a hundred supporting references that serve as a guide to more extensive information.

The material covers general climatic aspects of the state, ranging from average annual, monthly, and daily rain distributions through severe rainstorms and droughts. More detailed information on relationships of precipitation with atmospheric moisture and various weather types, on organized storms and substorm entities, on vertical and horizontal characteristics of individual storm cells, and on external and internal cloud characteristics is also included.

INTRODUCTION

The emergence of various programs in Illinois relating to the study of precipitation in the convective season has shown the need for a document that will touch on key findings of prior Water Survey research. Studies of forecasting and of modification of summer convective elements in Illinois can be aided by a host of findings from 30 years of research by scientists of the Illinois State Water Survey. Findings from a variety of published papers, state reports, and grant-contract reports have been chosen for presentation herein. These serve two purposes. One is to present examples of information that dimensionalize the phenomena. The second is to provide listings of the supporting references that allow one to find further, more extensive information than can be brought forward in a single summary document. Thus, this is both a guide and an information document, presenting most information in the form of graphs, maps, and tables.

A variety of topics are treated within the realm of precipitation. They have been chosen both to allow greater understanding for midwestern scientists and to dimensionalize the phenomena for those unfamiliar with midwestern conditions. Importantly, results presented do not represent all pertinent results, but only those rather hurriedly and arbitrarily chosen from an extremely large library of information. Apologies are offered to those who perceive that important documents or information have not been included.

The material presented begins on a larger or state scale, both in time and space, and progresses to smaller time and space elements by the end of the report. English and metric units are used interchangeably throughout this report. Most of the

material has been abstracted directly from Water Survey reports and technical papers over a span of 25 to 30 years. English units were used exclusively in the earlier publications, whereas a change to the metric system has occurred in recent years. For the purpose of this report, it was deemed unnecessary and too time-consuming to convert all of the many numerical values to a single measurement system.

The initial division of the report is entitled "General Climatic Aspects." Various information (maps and graphs) is presented to reveal the average daily, monthly, seasonal, and annual distributions of rainfall and rain-related phenomena (hail, thunderstorms, tornadoes, etc.). A special section is devoted to their diurnal distributions followed by a section devoted to field studies of rain events, or storms, over fixed areas. Next, certain conditions related to summer droughts in Illinois are presented.

The next major division of the report deals with "Rainfall Relations with Atmospheric Conditions." Here, the relationships of atmospheric moisture to precipitation and the occurrence of precipitation with various weather types are examined, as is information on pre-rain conditions related to forecasting.

The third major division of the report deals with organized storm or substorm entities, treated for their lifetimes and not over a fixed area. Within this section, information on organized lines and poorly organized groups of cells are presented.

The fourth major division of the report deals with information available on individual storm cells. Within this division, considerable information is presented in a section on the vertical characteristics of individual storm cells. Another section focuses on the horizontal characteristics of these phenomena as seen aloft by radar and at the surface.

The final division of this report deals with available information on various external and internal cloud characteristics from Survey studies. It should be noted that a variety of useful climatic results relevant to summer rainfall in the Midwest can be found in *High Plains Climatography* (Changnon et al., 1975).

Acknowledgments

The various research projects upon which this report is based have been carried out by numerous individuals within the Atmospheric Sciences Section, under the general direction of William C. Ackermann, now Chief Emeritus of the Illinois State Water Survey. Material assembled in this report has been abstracted from a large number of reports and research papers published by Survey scientists. The various research projects have drawn financial support from a wide range of sources. In addition to the state of Illinois, precipitation research at various times has been partially supported by such federal agencies as the National Science Foundation, Department of Energy, Armed Forces (Army, Navy, Air Force), and the Department of the Interior. Much of the hail research has been supported by the Crop-Hail Insurance Actuarial Association.

Credit is extended to the Survey's Graphic Arts Unit under the guidance of John W. Brother, Jr., and especially to William Motherway, Jr., for their considerable efforts in locating or redrawing the numerous figures from previous publications. Thanks are also due J. Loreena Ivens and Patricia A. Motherway for editing the final manuscript, and Marilyn J. Innes for preparing the camera-copy.

GENERAL CLIMATIC ASPECTS

Average Annual, Monthly, and Daily Distributions

Figure 1 presents the pattern of average annual precipitation in Illinois, based on 1901-1944 data (Changnon, 1958). Basically, a north-to-south distribution is shown ranging from 32 inches in the north to 46 inches in the hill area of extreme southern Illinois. Previous research (Huff et al., 1975) has shown that this hill area has an effect on warm season rainfall leading to 10 to 15% increases, on the average.

Figure 2 presents average precipitation patterns for the 3-month seasons as defined for the Illinois climatic regime. The winter (December-February) pattern is dominated by a north-south latitudinal distribution of precipitation, whereas the summer distribution (figure 2b) reveals a generally flat pattern, ranging from 9.5 to 11.5 inches. Notably, the summer distribution indicates slightly higher rainfall, on an average, in western Illinois. This reflects a greater incidence of nocturnal thunderstorm activity during summer (June-August) in western Illinois. Changnon (1957) shows that 70 to 80% of the summer rain comes from thunderstorms *(see* figure 4c).

A further subdivision of the warm season rainfall into that for the July-August period, when the greatest benefit of rainfall is realized in agricultural crop production, is shown in figure 3 (Huff and Vogel, 1977). Again, a relatively flat pattern is shown with the highest amounts, those greater than 18 cm, found in the western extremes of Illinois, the lowest being slightly less than 15 cm in northeastern Illinois.

Figure 4a presents the pattern based on the average number of days with thunderstorms in Illinois indicated by the 1901-1944 data (Changnon, 1957). This shows a pattern similar to the annual rainfall (figure 1), ranging from 38 thunder days in the northeast to 58 days in the south. Figure 4b shows the annual average precipitation from thunderstorms. Tables 1 and 2 present additional information on the monthly and seasonal distributions of thunderstorm events throughout Illinois (Changnon, 1968). Shown in table 1 are frequencies of thunderstorm days and hours derived from 1948-1961 data at three stations. These include Moline (MLI) in northern Illinois; Springfield (SPI) in central Illinois; and Evansville (EVV) in southwestern Indiana (considered representative of southern Illinois). A latitudinal variation is shown in most months, although in summer the Springfield frequency of days and hours of thunderstorms exceed those in southern and northern Illinois. Also shown in table 1 are the average number of hours with thunder on days when thunder occurs. This reveals the typical duration on a thunderstorm day. In the warm season, thunderstorm events tend to be longer than in any other season of the year. Table 2 presents extremes in the hourly duration of thunderstorm events between three stations; these yield some estimate of their range at a point.

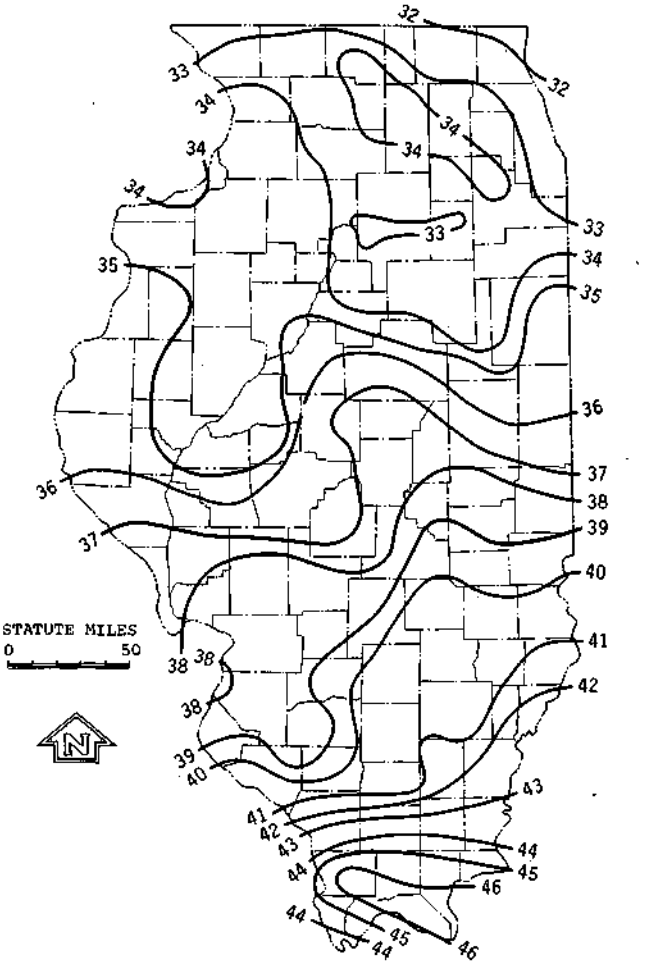

Figure 1. Average annual Illinois precipitation, inches, derived from 1901-1944 data

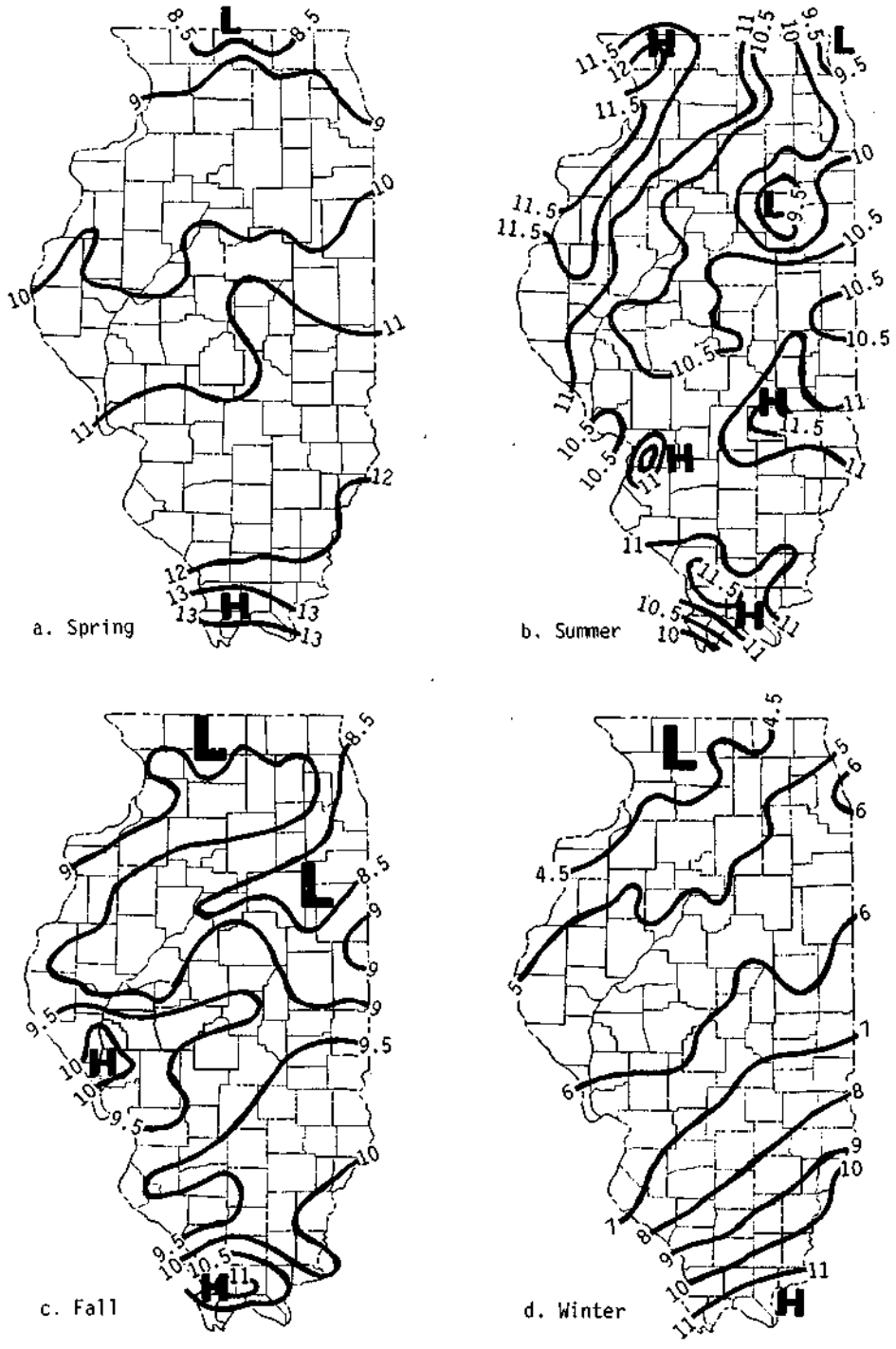

Figure 2. Average seasonal precipitation, inches

Figure 5 reveals the temporal frequency of thunderstorm days within the state of Illinois, as determined by state records over a 50-year period (Changnon, 1962a). Several interesting facts are shown, including 1) that within any given month there are periods of marked high and low frequencies of thunderstorm activity, including a maximum in early June, late July, and mid-August, and 2) that the distribution is not uniform throughout the summer season. Studies of singularities in precipitation days (Changnon, 1960) have shown that there are periods during June, July, and August when, on the average, precipitation events are more or less common than on days just before or after *(see* figure 12a).

Figure 6 presents a pattern based on the number of hail days in an average 20-year period in Illinois (Changnon, 1963a). This shows that hail is generally more frequent in central Illinois than in other parts, although there are isolated parts of western and northwestern Illinois with high frequencies. Most hail occurs during March-May, with decreasing frequencies in the summer months, June through August. A further inspection of the summer hail events is shown in figure 7 (Changnon, 1962b). Here the number of severe hail days, defined as those producing more than $10,000 in crop or property damage, are shown. In this instance, damaging hail events are shown to be most frequent in northern Illinois, with a secondary maximum in central Illinois averaging slightly more than one every third year. Basically, figures 6 and 7 show that hail is not a frequent event at a point, and that damaging hail is very infrequent at a point.

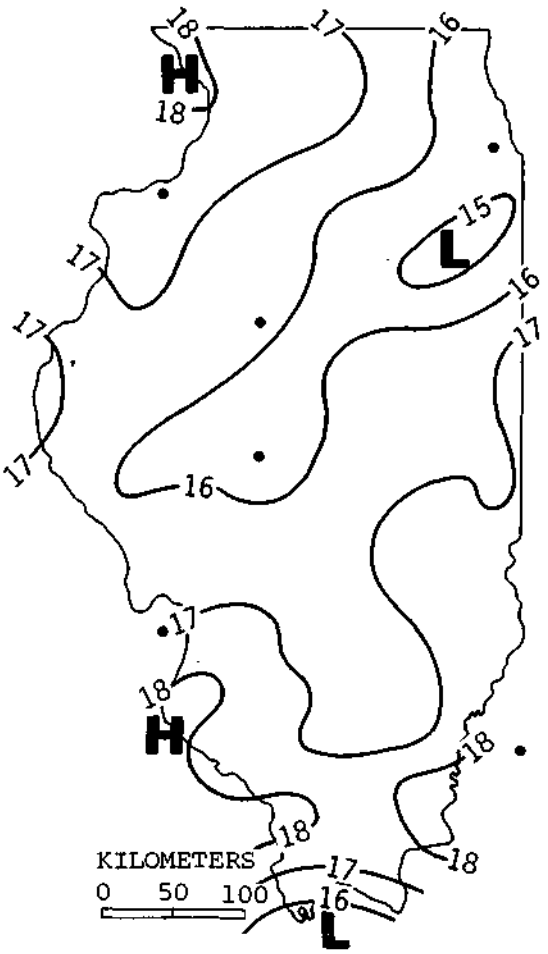

Figure 3. Normal rainfall (cm) for July-August in Illinois

Table 1. Average Number of Days and Hours of Thunderstorms during 1948-1961

Month	Number of days			Number of hours			Number of hours on thunderstorm days		
	MLI	*SPI*	*EVV*	*MLI*	*SPI*	*EVV*	*MLI*	*SPI*	*EVV*
Dec-Feb (winter)	1	2	4	2	4	7	1.5	1.6	1.9
Mar	2	3	4	5	5	7	2.1	1.9	2.0
Apr	4	4	4	11	10	10	2.7	2.7	2.2
May	5	6	5	10	14	13	2.2	2.3	2.4
Jun	7	9	7	19	23	17	2.7	2.4	2.3
Jul	7	8	7	16	22	14	2.3	2.8	2.0
Aug	6	6	5	14	13	9	2.3	2.2	2.0
Sep	4	5	2	8	11	5	2.3	2.4	2.2
Oct	2	2	1	6	5	2	2.8	2.6	1.5
Nov	1	1	2	2	2	4	2.1	1.8	1.8
Yearly totals	39	46	41	93	109	88	2.4	2.4	2.1
Long-term average (1901-1944)	47	50	50						

Note: MLI = Moline, SPI = Springfield, EVV = Evansville

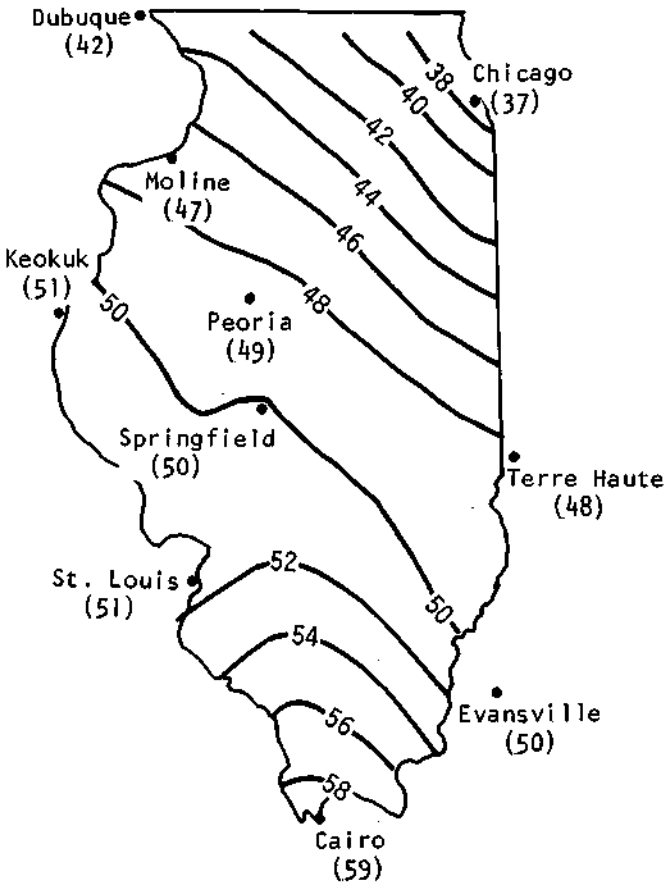

a. Average annual thunderstorm occurrences

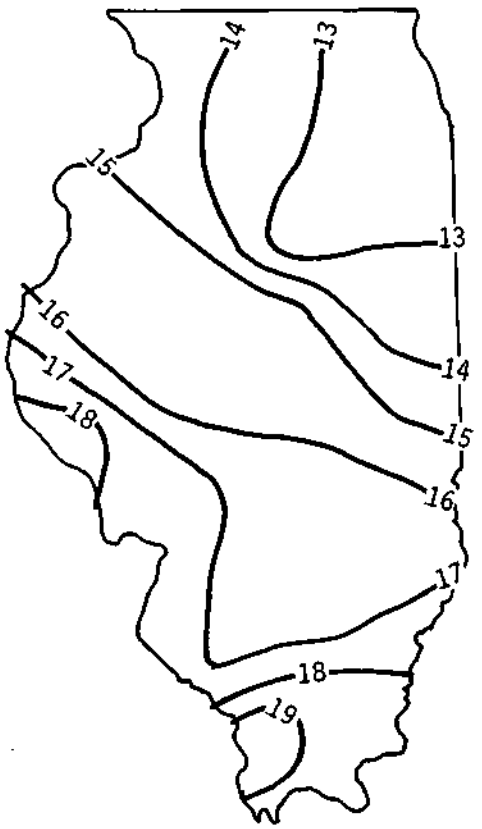

b. Average annual thunderstorm precipitation, inches

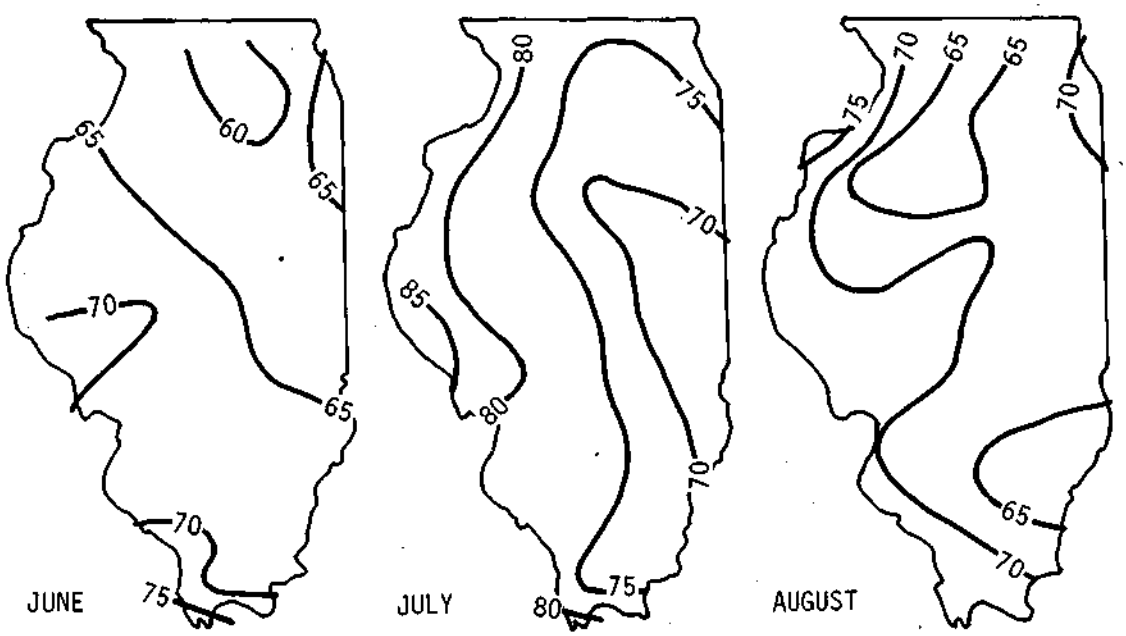

c. Average percent of normal monthly precipitation from thunderstorms during summer

Figure 4. Annual and seasonal thunderstorm information

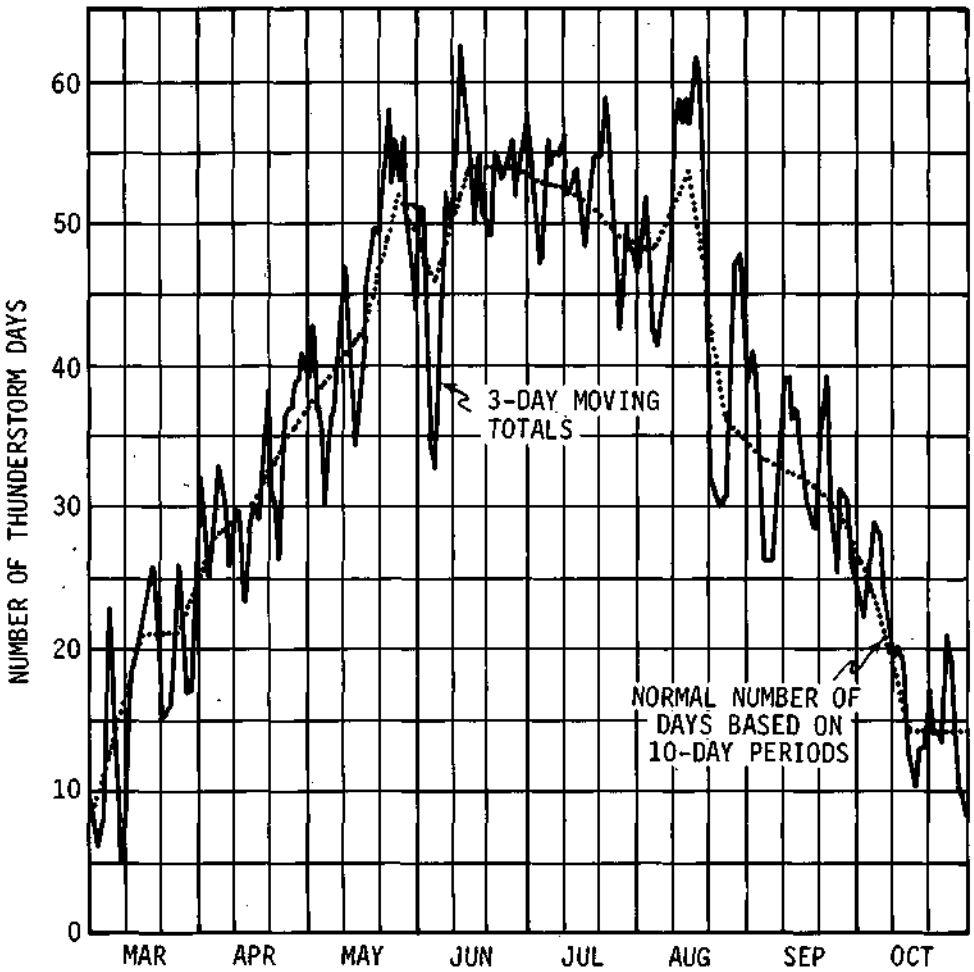

Figure 5. Temporal distribution of thunderstorm days (by date) in Illinois

Table 2. Extremes of Hourly Thunderstorm Occurrences during 1948-1961

	Extremes per month and year								
	Maximum number of hours in one day			*Maximum number of hours*			*Minimum number of hours*		
Month	*MLI*	*SPI*	*EVV*	*MLI*	*SPI*	*EVV*	*MLI*	*SPI*	*EVV*
Jan	3	5	7	4	6	11	0	0	0
Feb	2	3	4	2	5	4	0	0	0
Mar	6	4	7	9	9	12	1	1	1
Apr	14	8	8	27	20	21	0	4	0
May	10	5	7	15	25	28	2	3	4
Jun	8	9	8	31	37	31	12	9	6
Jul	8	7	6	26	35	23	6	16	6
Aug	9	5	5	27	31	25	5	6	1
Sep	5	7	5	13	23	14	2	3	0
Oct	17	6	3	22	10	15	2	0	0
Nov	4	4	6	7	5	12	0	0	0
Dec	2	2	3	2	3	5	0	0	0
Year	17	9	8	31	37	31	0	0	0

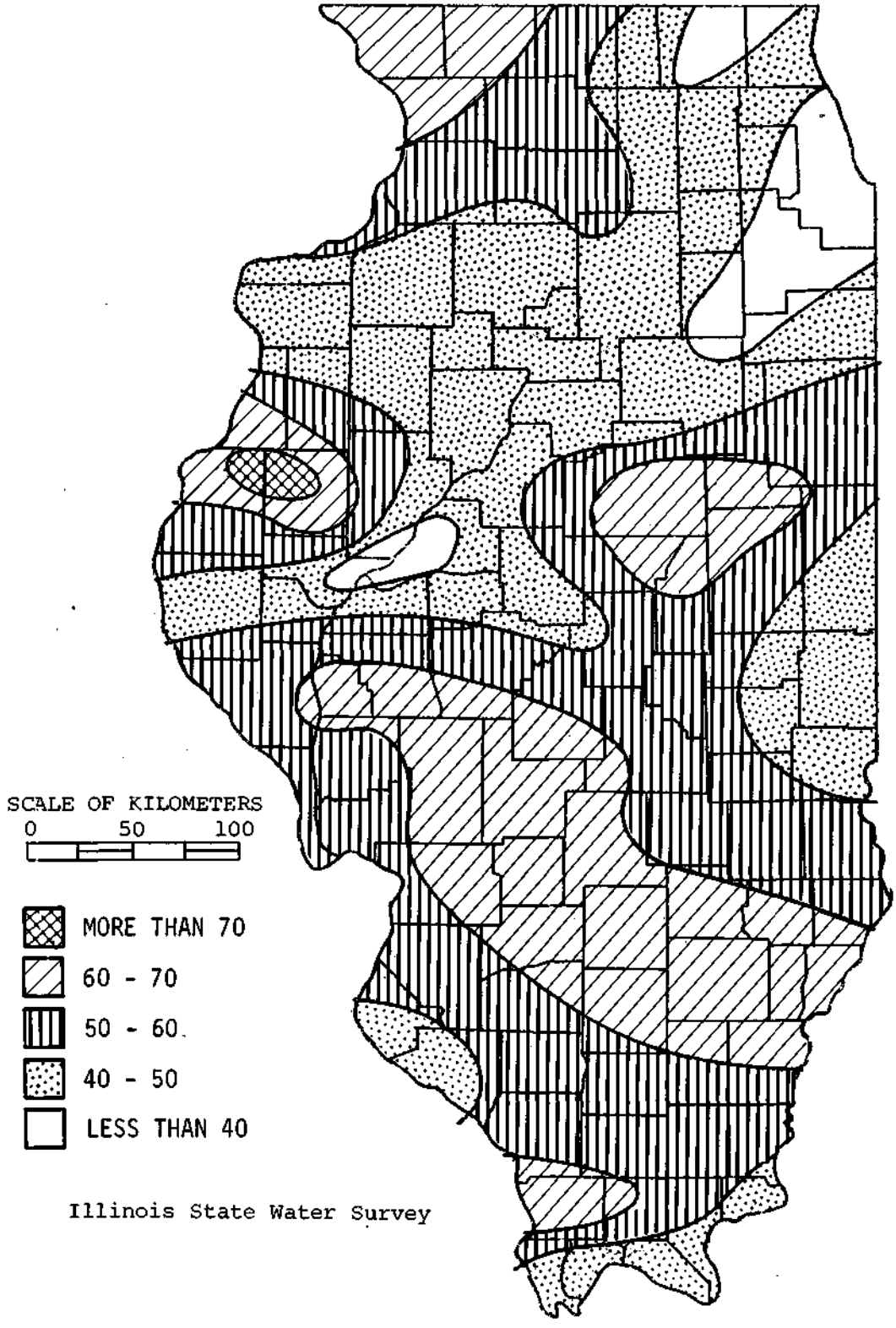

Figure 6. Number of hail days in an average 20-year period

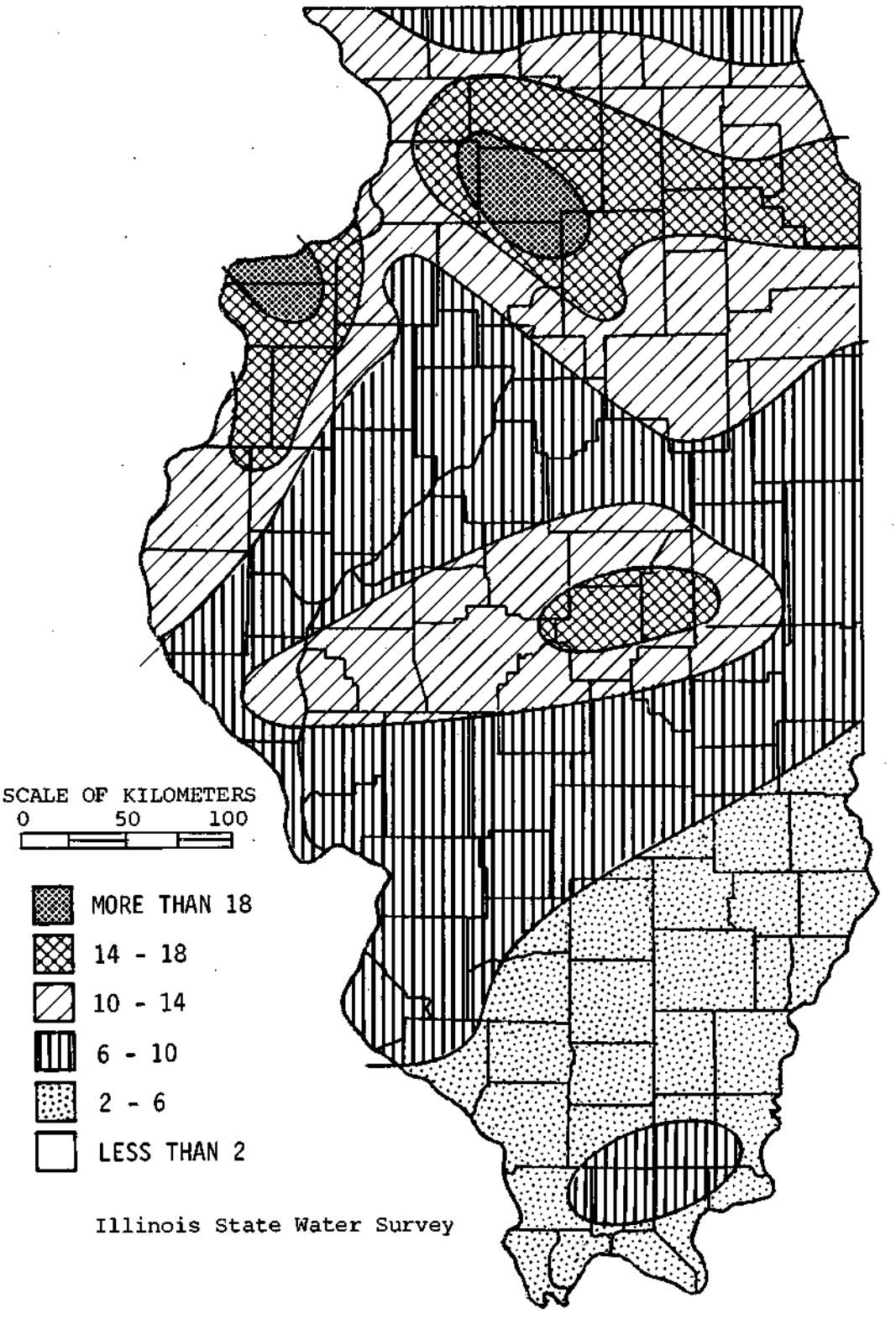

Figure 7. Number of severe summer hail days, 1910-1959

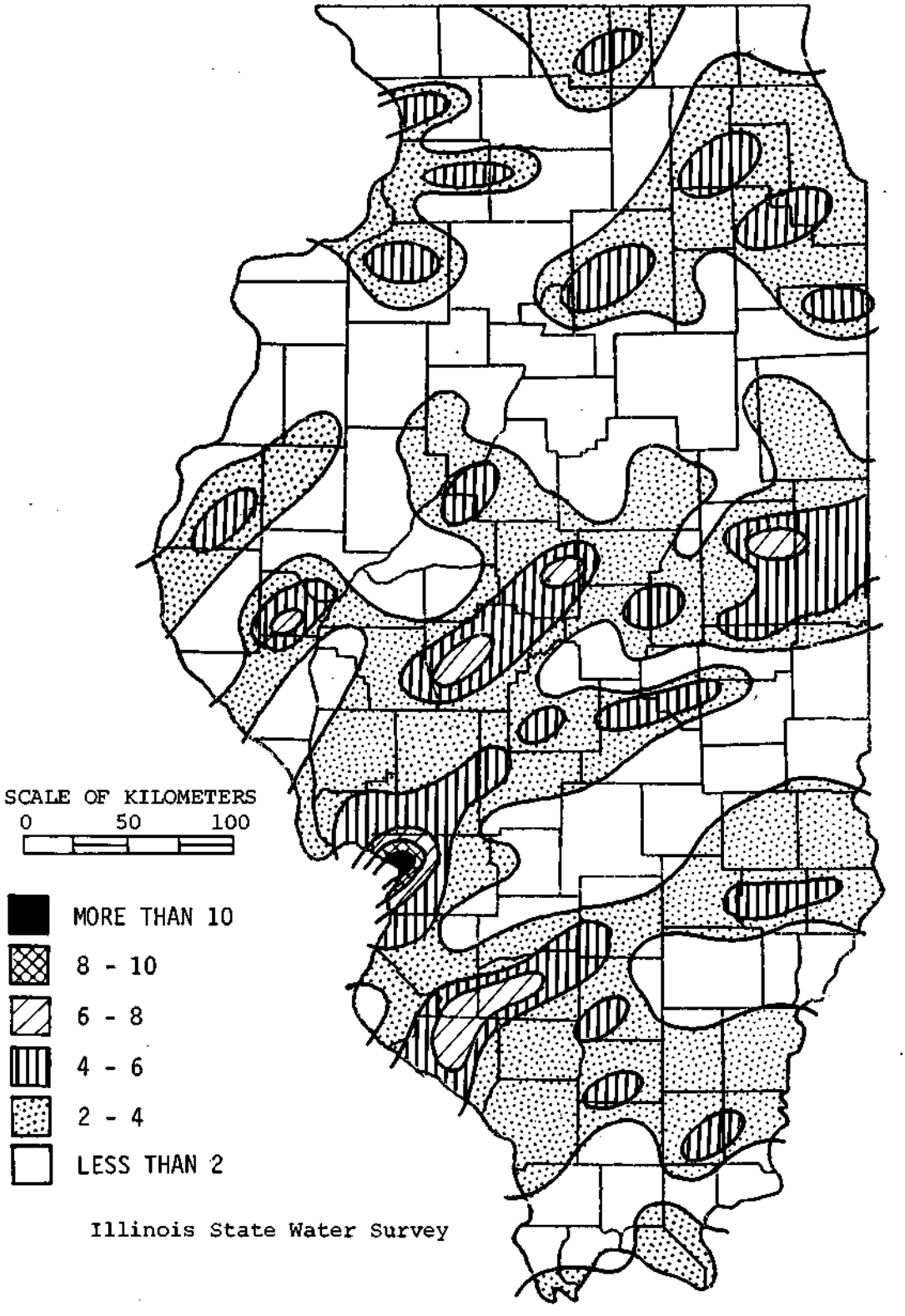

Figure 8. Distribution of tornadoes based on number per 100-mi^2 areas, 1914-1963

Figure 8 presents the pattern of tornadoes in Illinois based on an area-normalized figure (Wilson and Changnon, 1971). Basically, tornadoes are most frequent in a region extending ENE from the St. Louis area across central Illinois. A 50-year sample of tornadoes is, however, largely inadequate to define the average spatial pattern of tornadoes in Illinois.

Another important aspect of rainfall during July-August concerns its temporal fluctuations. Figure 9 presents values for the state and the three subdivisions of the state for 10-year periods beginning with 1895-1904. These reveal a general decline from 1895 through the 1925-1935 period of droughts, followed by increasing July-August rainfall in the subsequent 10-year periods. Considerable regional variation is apparent when one compares the state curve to those of the three subsections of the state. In general, most areas of the state reached, or were near to reaching, their all-time maximum 10-year rain during the 1965-1974 period (not shown).

Another illustration chosen to reveal the spatial and temporal variability of warm season rainfall is that presented in figure 10 (Stout, 1960). Shown here, from the network of 49 recording raingages in a 400-mi^2 area of central Illinois, are the single storm, the monthly, and ensuing warm season precipitation patterns for 1956. One figure shows the heavy rainfall pattern based on 3 August 1956, and its ensuing impact is shown in the August 1956 pattern. Another month (May)' of moderately heavy rainfall in 1956 with a steep south-north gradation is shown in figure 10. The resulting pattern for the warm season (May-August) of 1956 reveals widely different values in this 400-mi^2 area ranging from less than 12 inches to more than 18 inches. The largest gradient occurred across a distance of less than 3 miles.

Another way to portray the precipitation climate of Illinois is to look at the daily and weekly frequencies of rainfall. Figures 11 and 12 provide a variety of information on these periods (Changnon, 1967). For example, the probability of 0.1 inch and 1.0 inch in any given week for various areas of the state are shown in figure 11. Attention is drawn to the summer months, revealing a low likelihood of precipitation in mid-July with greater incidence of precipitation during a given week in mid-August. Notable are the differences in the regions. Figure 12 presents the probabilities, or chances, of a given day occurring in dry periods of varying lengths and of varying intensity. Again, varying likelihoods of wet and dry periods during July and August are shown. These results also indicate that there are sizeable regional differences in the likelihood of precipitation in Illinois during the warm months.

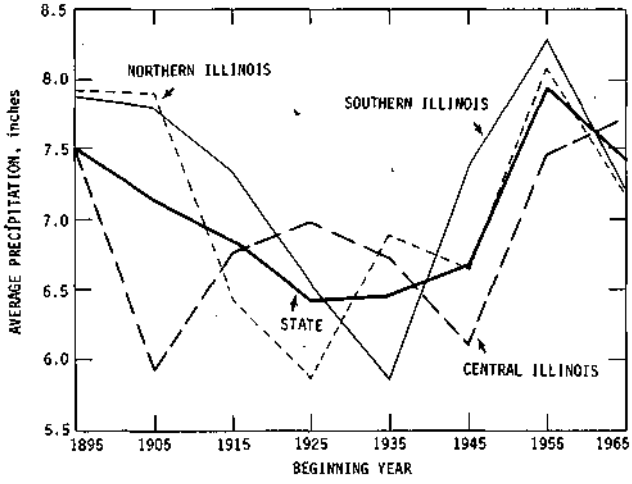

Figure 9. Average 10-year rainfall in July-August

Another key aspect of the precipitation climate in Illinois is revealed in figure 13. The data from a dense network of recording raingages in central Illinois were used to examine for profiles of precipitation over small areas (Huff, 1966). The most extreme profile is depicted in this figure. For the 10-year sampling period, considerable variation occurred, ranging from 186 inches to less than 165 inches over a 20-mile distance. Such variability, persisting over a 10-year period in a flat land, impacts on the evaluation of weather modification.

Large-Scale Patterns and Downwind Studies. An interesting question often raised about weather modification, and precipitation climate, in general, concerns the downwind effect, or the distribution of high and low rainfall areas over a large region. Water Survey studies (Schickedanz, 1973) have addressed this issue in a variety of ways. Table 3 presents the information about the spacing of discrete high rainfall areas, based on the study of summer rainfall in the Midwest over the 1950-1969 period. The mean distance to the nearest high downwind from another high varies from 100 to 116 miles, with a median from 76 to 100 miles. The most frequent interval lies in the range of 70 to 100 miles in high summer rain values.

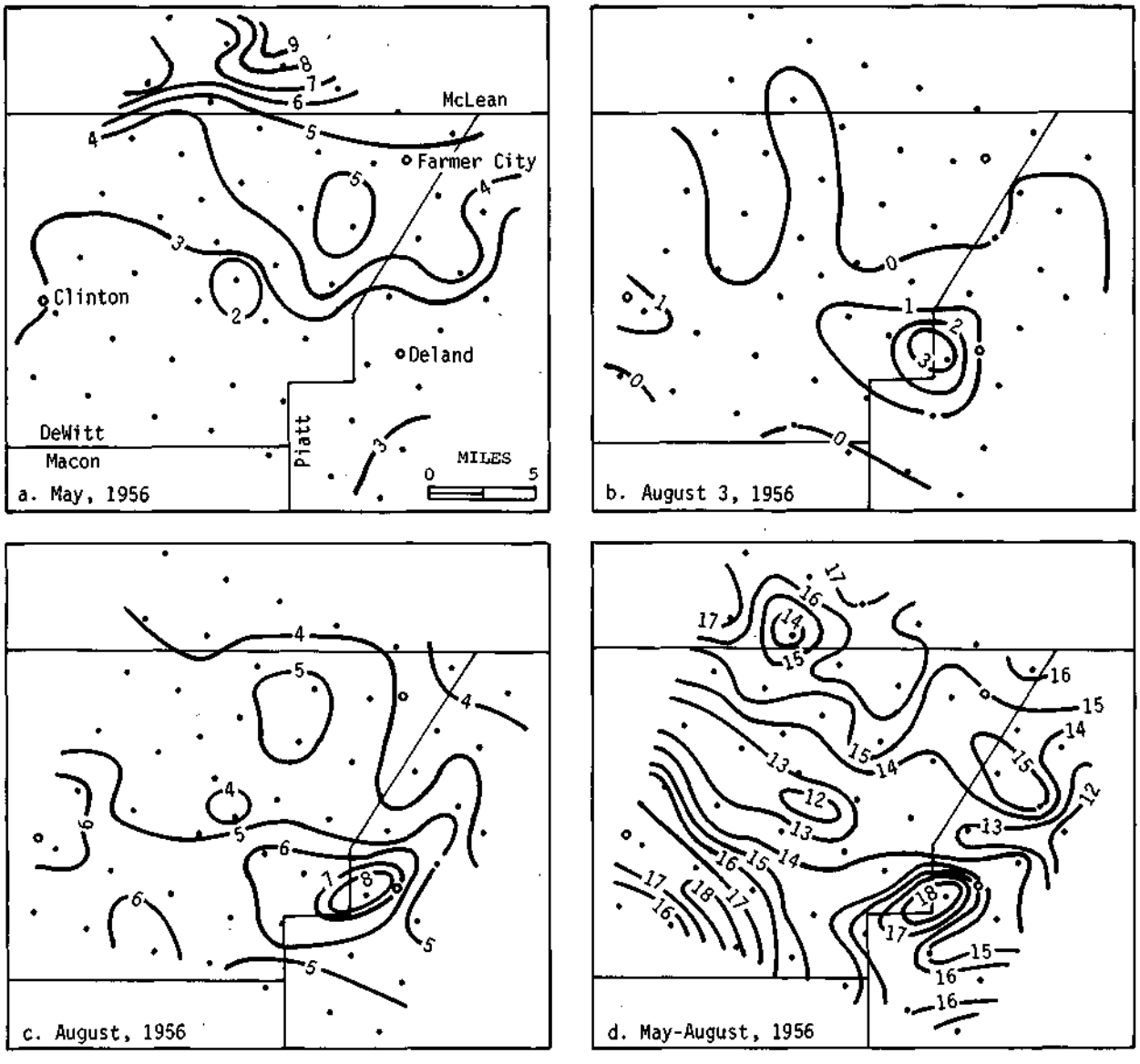

Figure 10. Storm, monthly, and growing season rainfall during summer in a 400-mi^2 network in central Illinois

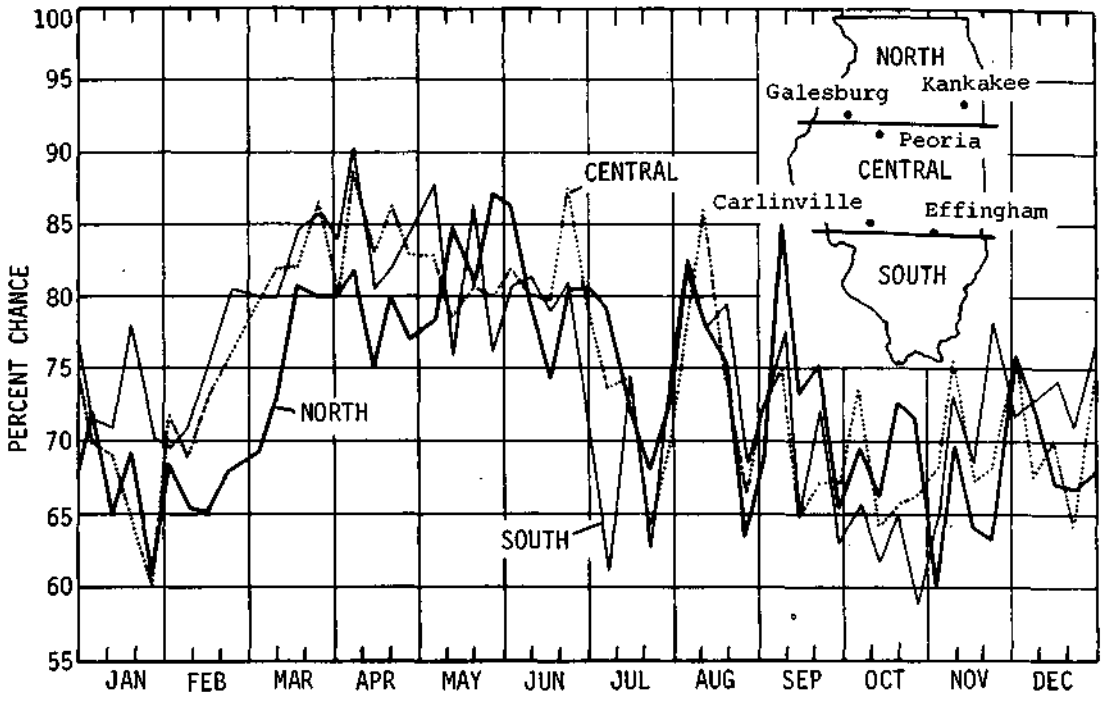

a. Chance of 0.1-inch or more rain in one week

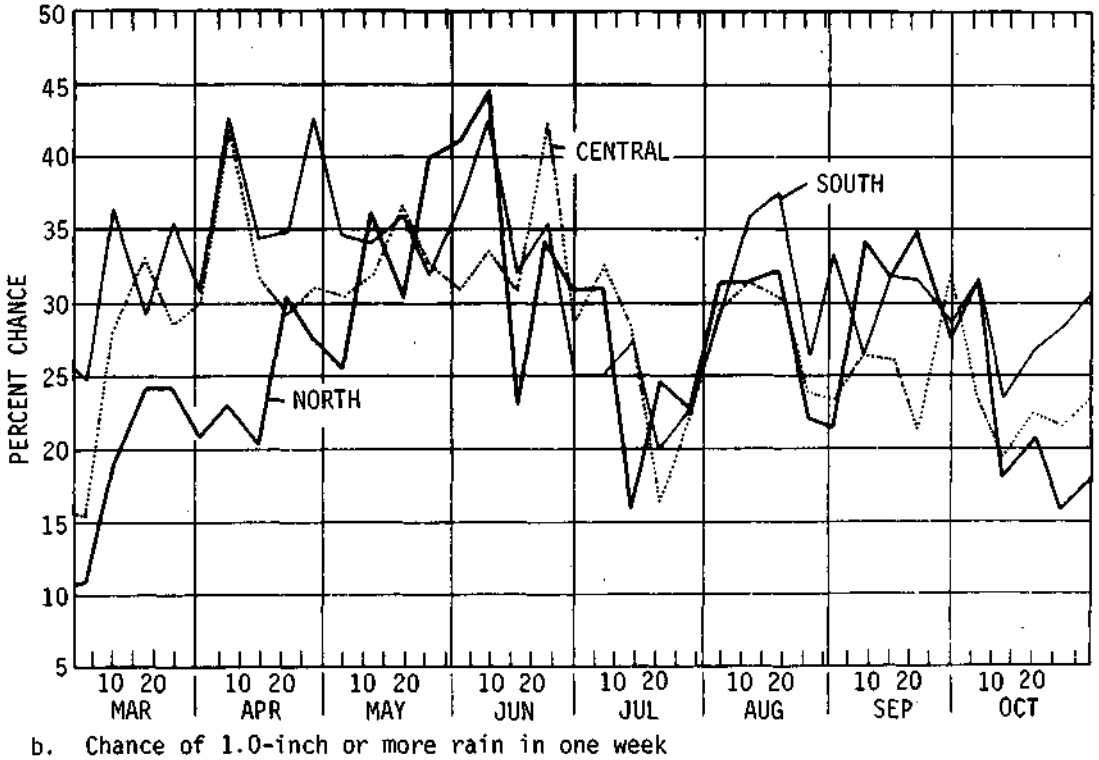

b. Chance of 1.0-inch or more rain in one week

Figure 11. Weekly probabilities of rain for various areas

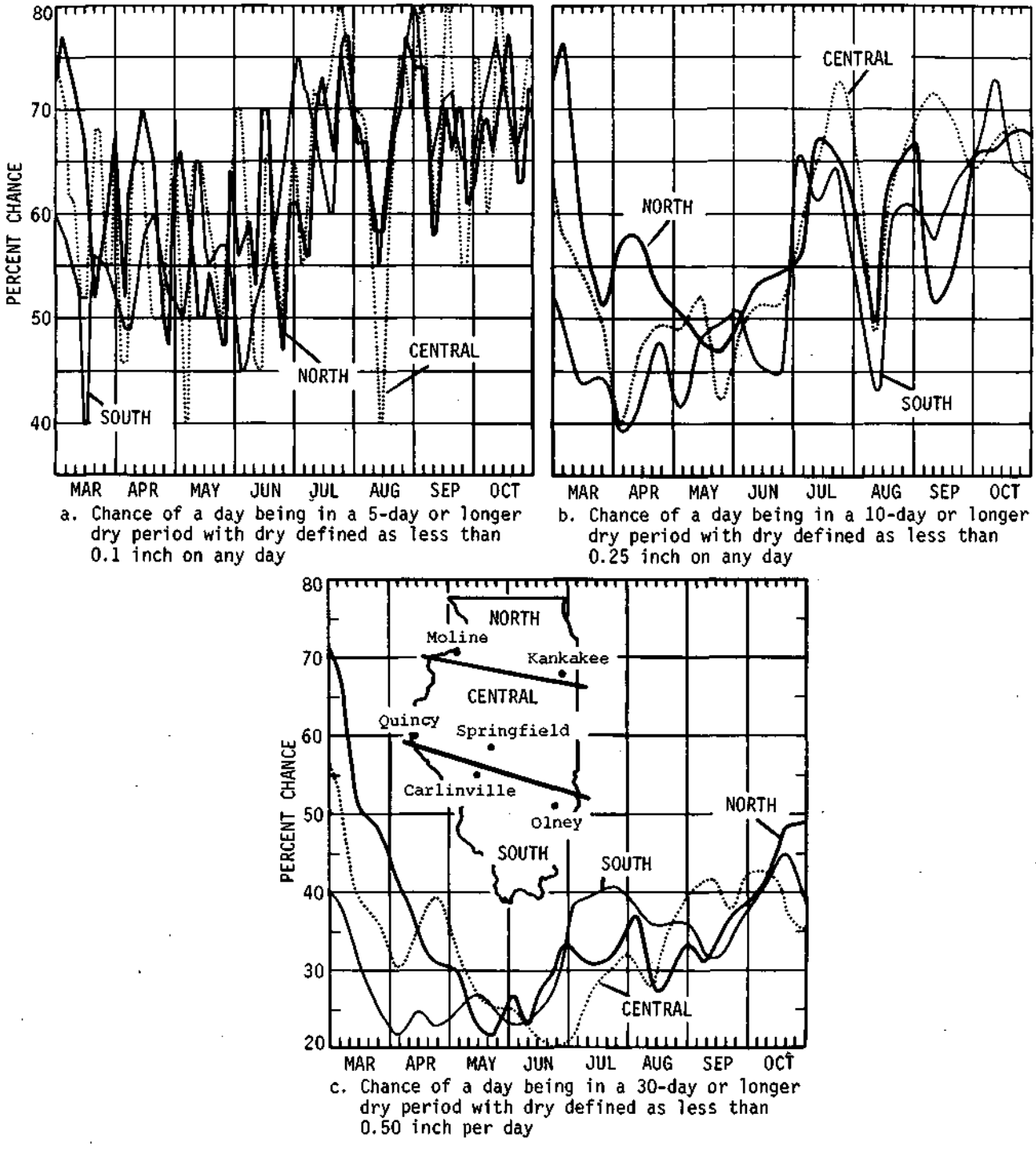

Figure 12. Probabilities of a given day occurring in dry periods of various length and intensity

Table. 3. The Spacing of Downwind Highs (5% Residuals) in 5-Year Monthly Rainfall Patterns as Determined by the Distance to the Nearest High

	Distance (mi) associated with the given percentile			*Mean*
Month	*0.20*	*0.50*	*0.80*	*(mi)*
June	60	84	136	105
July	56	76	140	100
August	52	100	148	116

Schickedanz (1973) presented the number of times that each sampling point in the Midwest was included in the high rainfall area (as defined statistically at the 5% level) for the summer rainfall patterns over a 20-year period. The resulting pattern (figure 14) shows various areas scattered throughout the Midwest. A high frequency is shown in western Kentucky and eastern Kentucky. Table 4 presents a measure of the variability between 5-year periods for the spacing and sizes of high rainfall areas. The average distance between highs during any 5-year period ranged from 67 to 136 miles for the summer patterns. The areal extents ranged from 518 to almost 1400 mi^2.

Figure 15 presents correlation patterns of summer rainfall at Salem (in southern Illinois) with other points throughout the Midwest. Note the tendency for the rainfall at Salem to be well correlated with points at relatively large distances; thus, isolated cores of relatively strong correlation are found as far as 250 miles away. The broadness of the correlation pattern indicates that one must be very cautious when postulating extra-aera effects from weather modification up to distances of 300 miles from the target. This problem is further stressed in the annual rainfall correlation patterns for Illinois in figure 16. Quite significant correlations (≥ 0.50) are found for a distance of 200 miles or more along the major axis of the correlation patterns, and strong correlations (≥ 0.70) occur for 100 miles or more.

Table 4. The Variability between 5-Year Periods of the Average Spacing and Size of Highs on 5-Year Patterns

Pattern	*Near-neighbor distances (mi)*	*Size (mi^2)*
Summer	67-136	518-1371
June	77-98	640-1520
July	63-124	578-1333
August	72-93	575-1055
December	80-230	640-2960

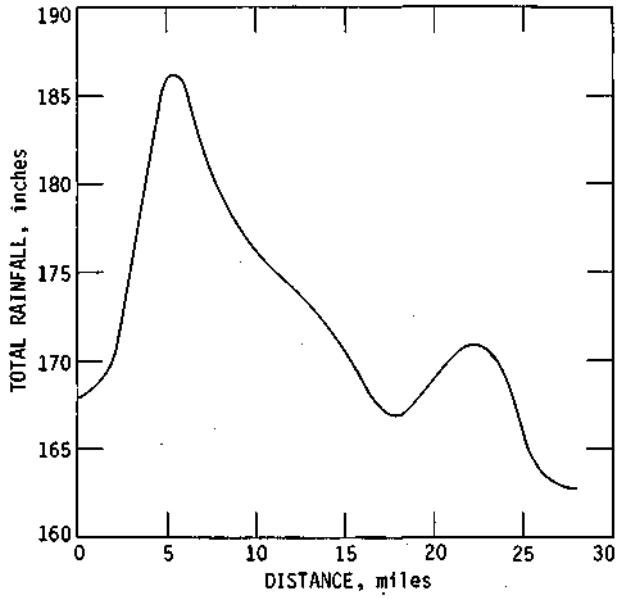

Figure 13. SW-NE profile of May-September total rainfall on East Central Illinois Network, 1955-1964

Diurnal Distributions

The diurnal distributions of rainfall and related weather conditions have been presented as a separate section in this document because of their relevance to the forecasting and modification of summer rainfall. A variety of results are available for four areas in Illinois and these areas are delineatedin figure 17 (Huff, 1971). Since most of the current interest concerns the North Central Section of Illinois, figure 18 presents, for the four seasons, the frequency of measurable precipitation events and the mean rainfall rates for that. area. In summer, rain occurrences (solid line) do not vary greatly on a diurnal basis, although they are slightly higher at night. The summer rainfall rates reach a minimum at 1100 CST and maximize during the hours of 2000 to 0100 CST.

Table 5 presents the annual and seasonal distributions of hourly precipitation for the four sections of Illinois (figure 17). These show the average hours of rain per year and the distribution by the various rainfall intensities. In summer, in the North Central Section, there are 90 hours of rain per year with 72% in the range of 0.01 to 0.1 inch per hour.

Figure 19 presents the diurnal distribution of the percentage frequency of total precipitation in the North Central Section. This shows that in summer, the minimum is reached in midday with

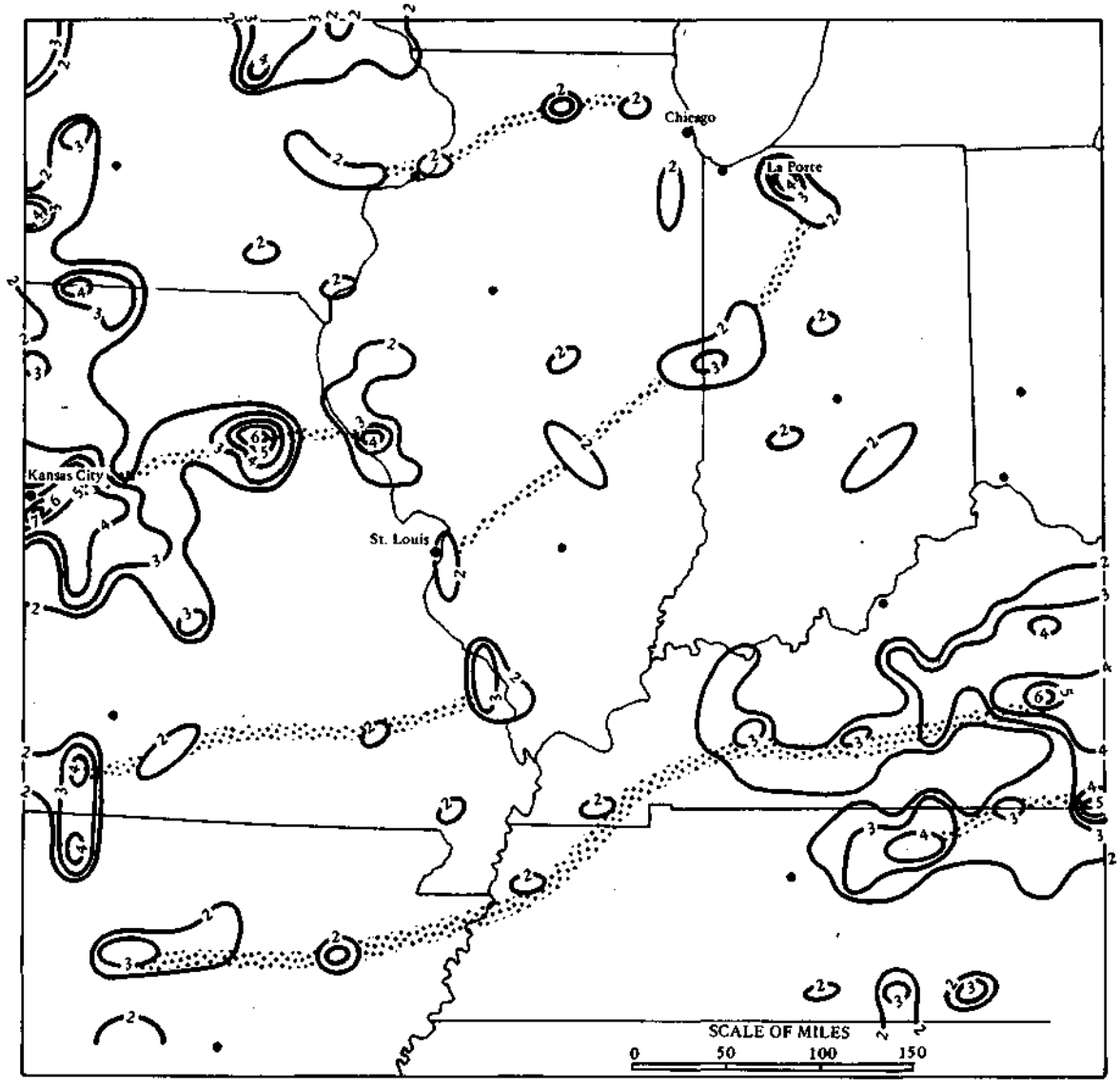

Figure 14. Number of times each sampling point was included in a high (5% residual) in the 1-year summer patterns during 1950-1969

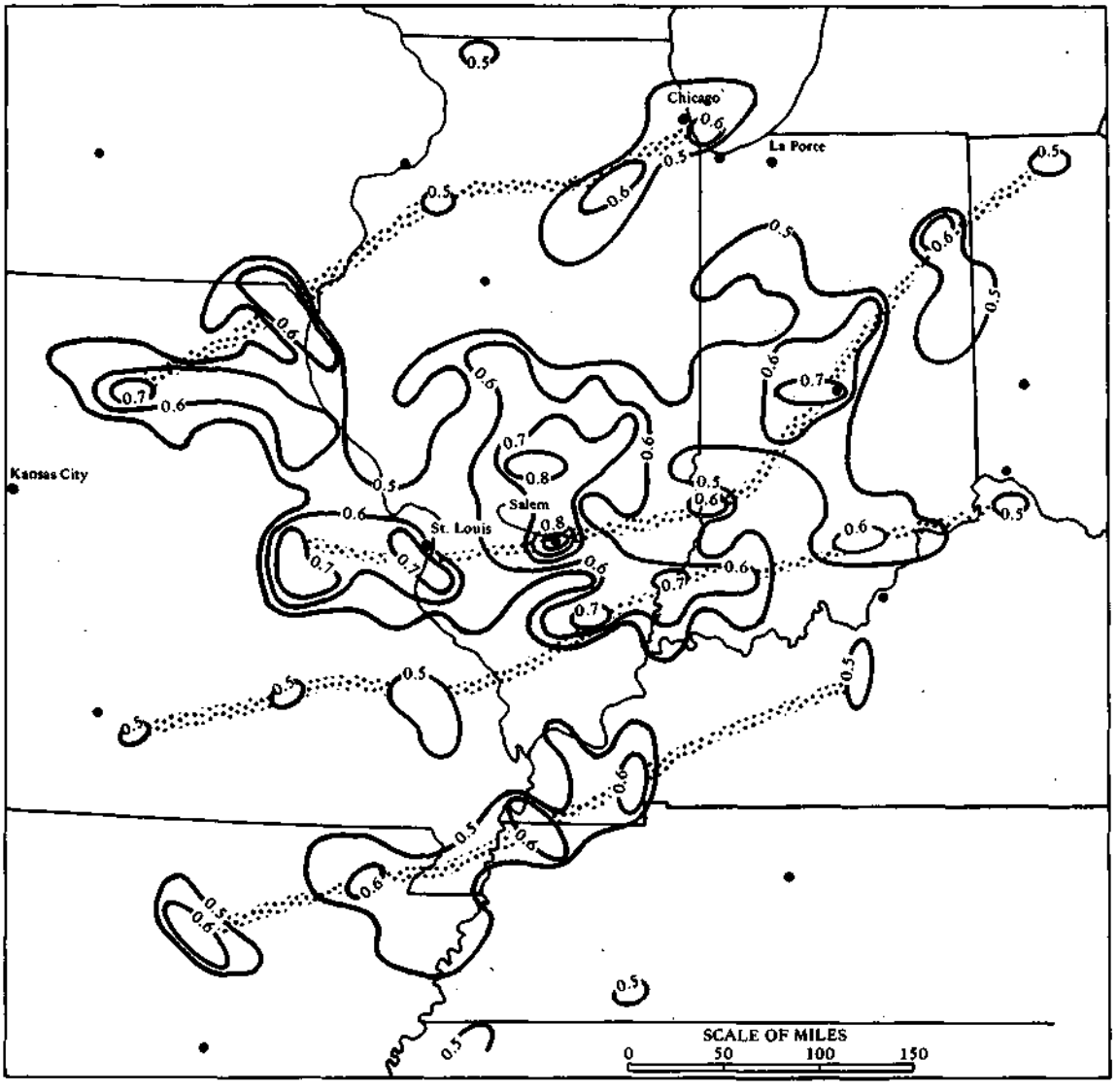

Figure 15. Correlation of summer rainfall at Salem with all other points in the PEP study area during 1950-1969

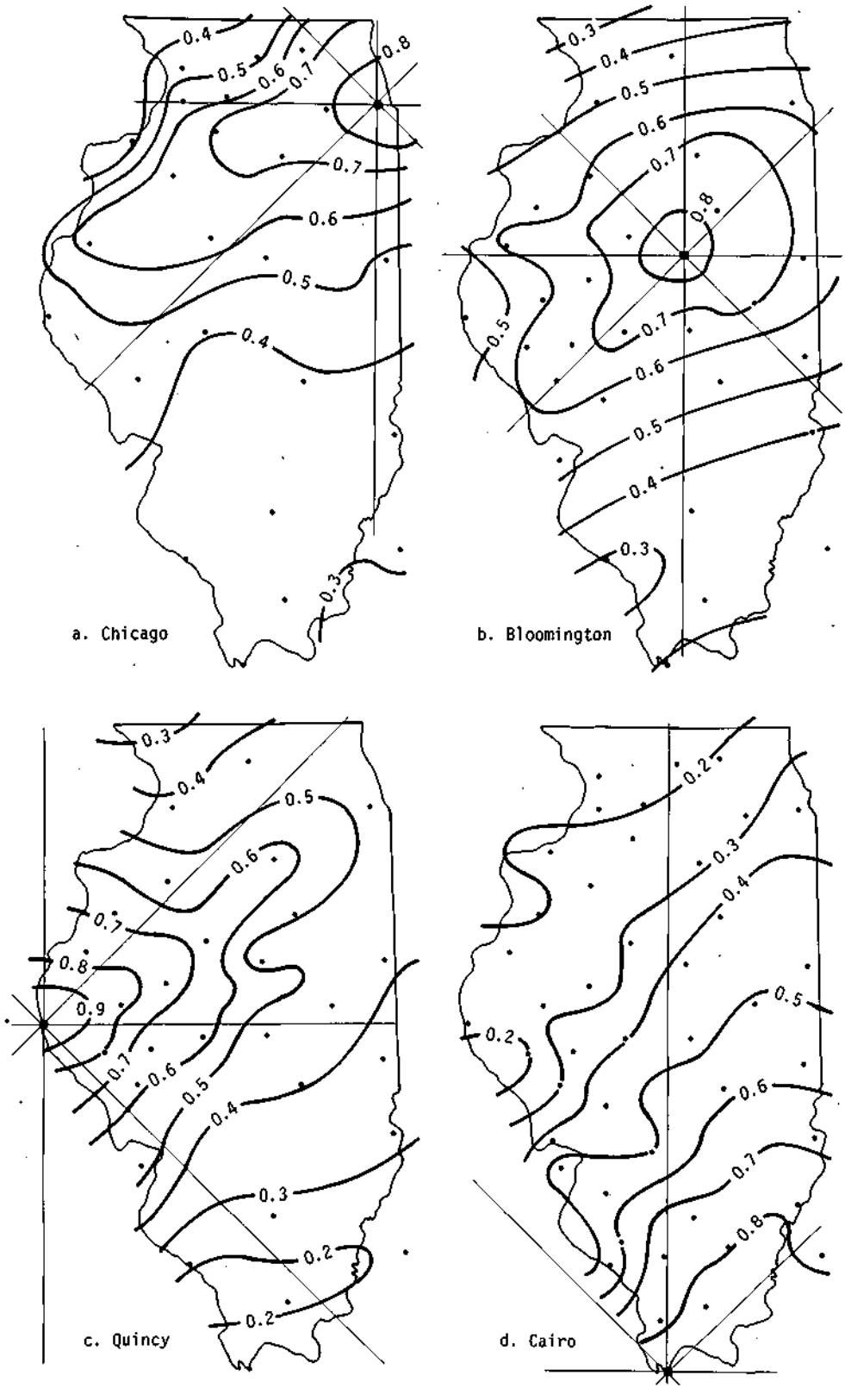

Figure 16. Correlation patterns ot annual precipitation in Illinois

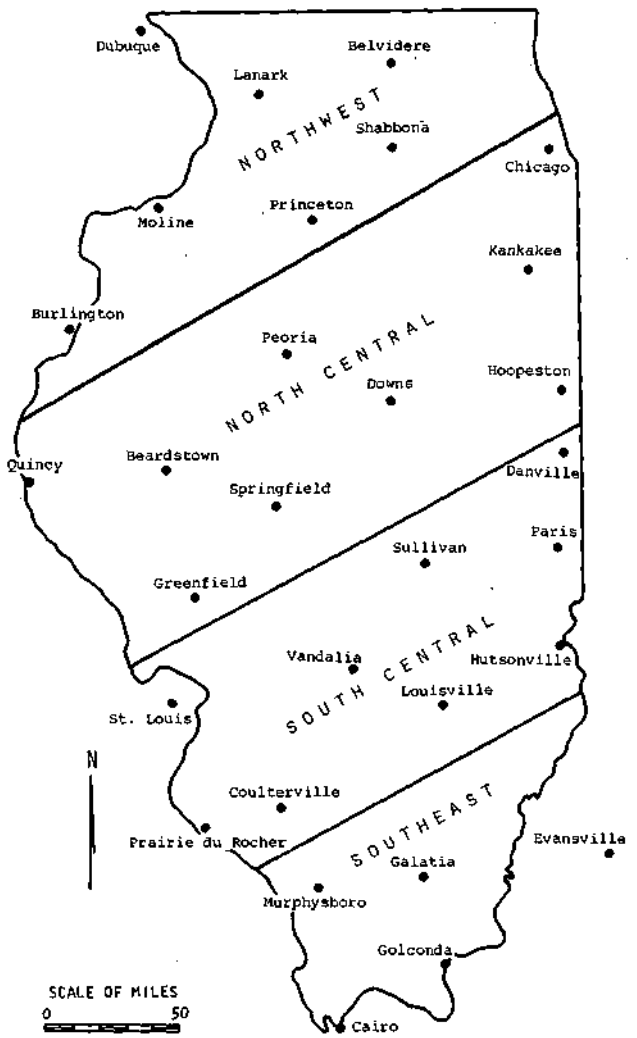

Figure 17. Recording raingage stations and climatological sections used in study

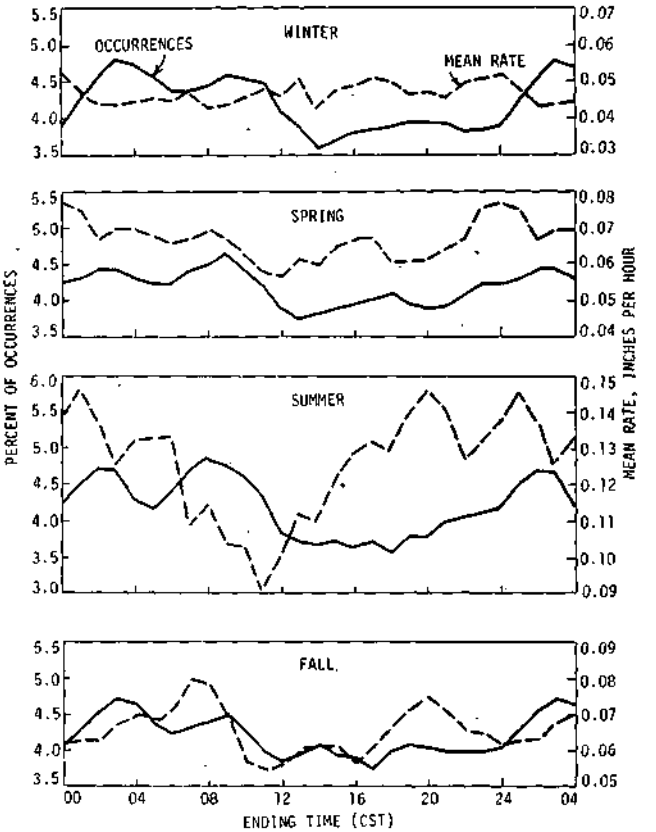

Figure 18. Percentage frequency of measurable precipitation occurrences and mean precipitation rate in North Central Section

the maximum in late evening. Considerable regional variations are found in central Illinois in the different seasons.

Changnon (1968) analyzed the diurnal distributions of thunderstorms, hail, and other weather events. The thunder data for three first-order stations in northern, central, and southern Illinois are presented in figure 20 and table 6. The thunder data show a late afternoon-early evening maximum; a secondary maximum in the 0100-0400 period (most pronounced in the north), and a minimum at midday. Damaging hail (figure 20) is shown to maximize in early afternoon with a secondary nocturnal maximum.

Another study of severe weather provided more diurnal information as displayed on figure 21 (Huff and Changnon, 1960). Importantly, all hailfall occurrences have a distribution similar to that shown for the damaging incidences in figure 20. Tornado occurrences (figure 21) show a very pronounced maximum between 1500 and 1900 with a minimum in the sunrise period of 0500 to 0900. The diurnal distribution of rain occurrences of 1 inch or more, in a 10-year period, is also shown on this figure. This distribution differs from that for hail and tornadoes, showing a gradual maximum developing at 1500 with a peak in 1-inch rainfall events between 2100 and 0100. However, the minimum is around 0800. Heavy rains, hail, and tornadoes, all have their minimums around sunrise, whereas thunderstorm minimums are achieved at noon in Illinois. As discussed in a later section, the diurnal distribution of precipitation events is related to several forcing factors, such as the nocturnal thunderstorm mechanism, the diurnal distribution of fronts, and the maximizing of solar heating in early afternoon.

Table 5. Annual and Seasonal Distribution of Hourly Precipitation by Section

Period	Average number of hours per year	Percent of total hours with given hourly amounts (inches) 0.01–0.10	0.11–0.25	0.26–0.50	0.51–1.00	Over 1.00
Northwest Section						
Winter	127	93.4	5.6	0.8	0.1	0.1–
Spring	155	86.2	10.6	2.4	0.7	0.1
Summer	99	71.8	16.4	7.1	3.5	1.2
Fall	87	83.5	12.5	2.8	0.9	0.3
Annual	468	84.6	10.8	3.1	1.1	0.4
North Central Section						
Winter	135	90.7	7.6	1.2	0.3	0.1–
Spring	151	84.8	11.2	3.0	0.8	0.2
Summer	90	72.1	15.0	8.0	3.7	1.2
Fall	89	84.2	11.4	3.4	0.9	0.1
Annual	465	83.8	11.1	3.5	1.3	0.3
South Central Section						
Winter	126	84.9	11.7	2.3	0.8	0.3
Spring	137	81.6	13.6	3.5	1.1	0.2
Summer	79	72.4	15.1	7.3	3.9	1.3
Fall	94	78.2	15.6	4.6	1.3	0.3
Annual	436	80.0	13.8	4.1	1.6	0.5
Southeast Section						
Winter	189	82.3	13.1	3.6	0.8	0.2
Spring	146	77.6	15.5	5.2	1.4	0.3
Summer	83	71.7	15.6	7.8	3.9	1.0
Fall	104	76.2	16.5	5.5	1.5	0.3
Annual	522	78.0	14.9	5.1	1.6	0.4

Table 6. Number of Occurrences of Thunderstorms per 2-Hour Periods (1949-1961)

Ending hour (CST)	Winter			Spring			Summer			Fall			Total		
	MLI	SPI	EVV	MLI	SPI	EVV	MLI	SPI	EVV	MLI	SPI	EVV	MLI	SPI	EVV
0200	0	2	12	30	40	37	76	89	45	27	20	18	133	151	112
0400	2	3	5	26	34	29	83	82	38	26	16	16	137	135	88
0600	3	3	3	25	38	32	77	65	43	20	17	12	125	123	90
0800	3	1	4	21	32	30	53	50	33	17	13	11	94	96	78
1000	1	2	4	9	19	25	39	35	24	15	9	4	64	65	57
1200	2	1	3	5	18	17	22	25	30	14	9	3	43	53	53
1400	2	1	4	15	17	15	22	53	52	12	20	5	51	91	76
1600	2	2	6	34	30	24	43	70	65	10	14	3	89	116	98
1800	2	8	2	25	36	36	60	66	60	18	24	8	105	134	106
2000	3	5	5	39	38	46	63	80	54	21	30	19	126	153	124
2200	2	1	12	49	46	47	71	80	35	21	35	22	143	162	116
2400	2	2	8	32	46	40	65	77	37	21	24	13	120	149	98
Total	24	31	68	310	394	378	674	772	516	222	231	134	1230	1428	1096

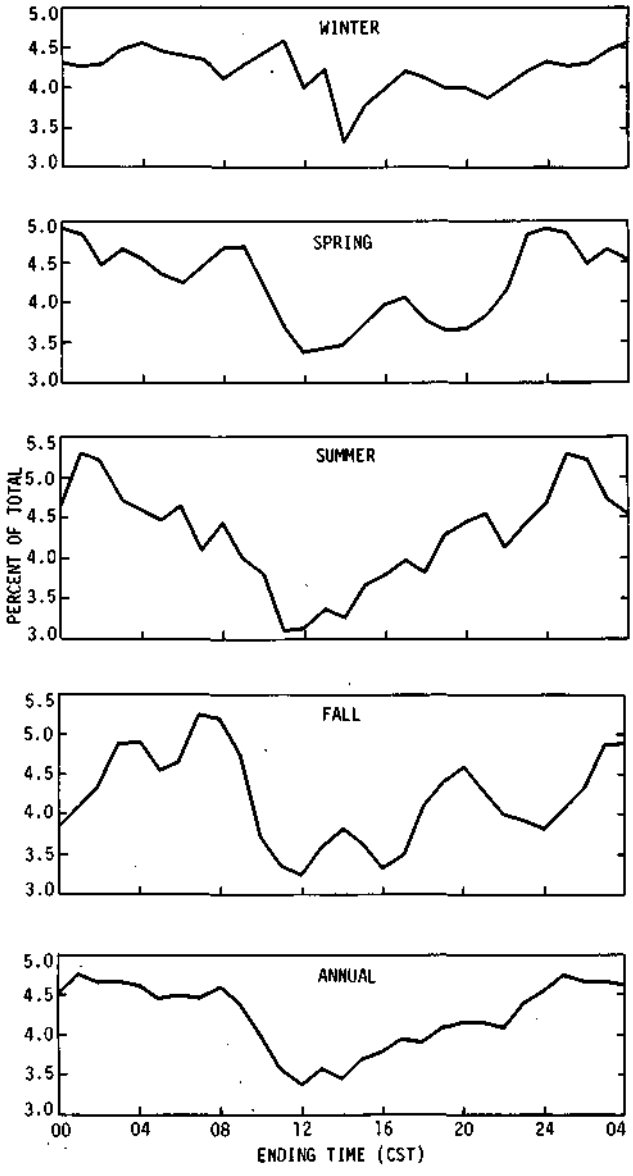

Figure 19. Percentage frequency of total precipitation in North Central Section

Rain Events (Storms) over Fixed Areas

Introduction and Definitions. The Water Survey's wide usage of dense raingage networks to serve a variety of rainfall studies (Huff and Changnon, 1966) has furnished a major amount of precipitation information for Illinois. These networks were largely composed of weighing-bucket recording raingages, and have been located in various parts of Illinois over areas ranging from 10 up to 4000 mi^2 *{see* figure 42). A major approach to the analysis of the data generated by these networks relates to the definition of individual rain events. Early in the analysis of network data in the 1950s, the Water Survey coined the term 'storm' (a potentially confusing label) to describe a discrete period of rainfall within a fixed network area. Most of the networks operated by the Water Survey from the late 1940s to the late 1960s covered areas ranging from 10 to 600 mi^2. Huff, in a study of rainfall on the central Illinois network of 400 mi^2, developed an objective definition of 'storm' as a discrete rain period produced by a specific synoptic weather system. The definition specified that "any rain period separated by more than 6 hours without rain *on the network"* was a storm. By this approach, most rain events were found to be related to or produced by different synoptic weather conditions.

Inspection of table 7, based on 5 years of data from a 550 mi^2 network in south-central Illinois, shows the frequency of storm events. This 6-hour separation for definition in the summer season produced more storms than days of rain, as shown in table 7. The summer (June-August) average was 50 storms compared with rain on 45 days. The average point duration for summer storms was 2.6 hours. The various other statistics in table 7 allow one to estimate the basic characteristics of network storms. The operation of larger networks covering 2000 mi^2 (METROMEX at St. Louis) and 4000 mi^2 (CHAP at Chicago) since 1970 required altered definitions of storms. An objective means of defining storms on these two larger networks consisted of time-space delineation of rain areas on the network based on distance separation of greater than-20 miles and more than 1 hour between rain events at any point (gage). These definitions were established to yield rain relationships with specific weather conditions that produce a rain entity or system.

Illustrations of Storms. Results from a paper involving the Little Egypt Network in southern Illinois (Changnon, 1963b) have been chosen to reveal some of the typical characteristics of network storms. Figure 22 presents certain types of storm isohyetal patterns, with regard to shape, configuration, and quantity of rainfall, found to be prevalent in various seasons. There were three frequent summer storm patterns found; one of a multicellular nature, another involving a single raincell crossing the network with light to moderate rain-

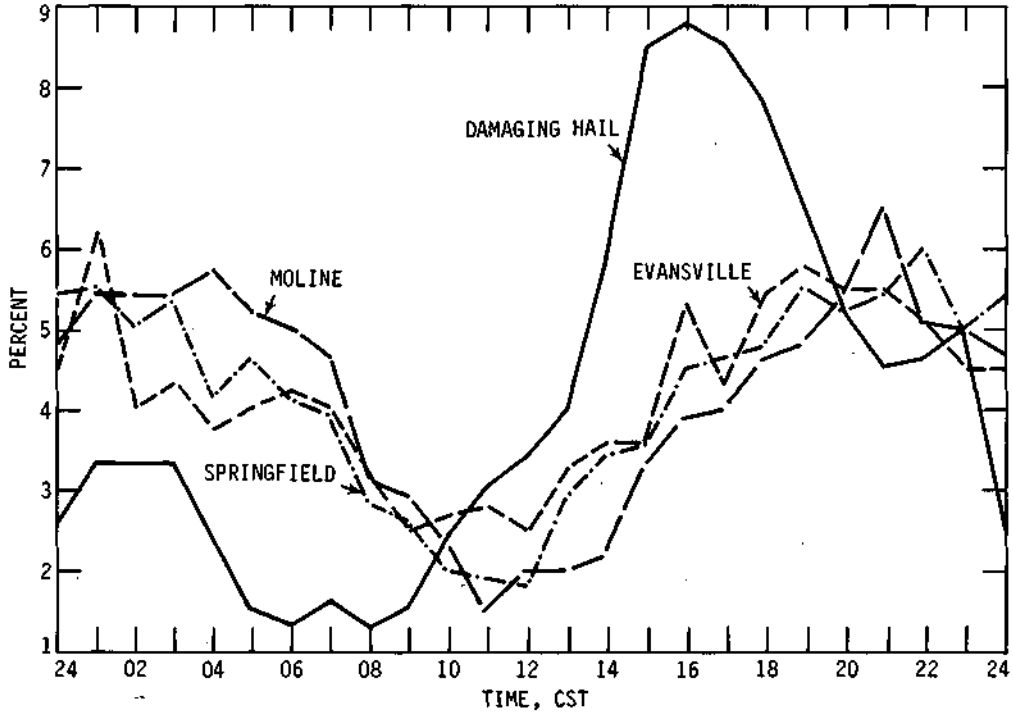

Figure 20. Number of thunderstorms and damaging hail occurrences expressed as a percent of the total occurrences

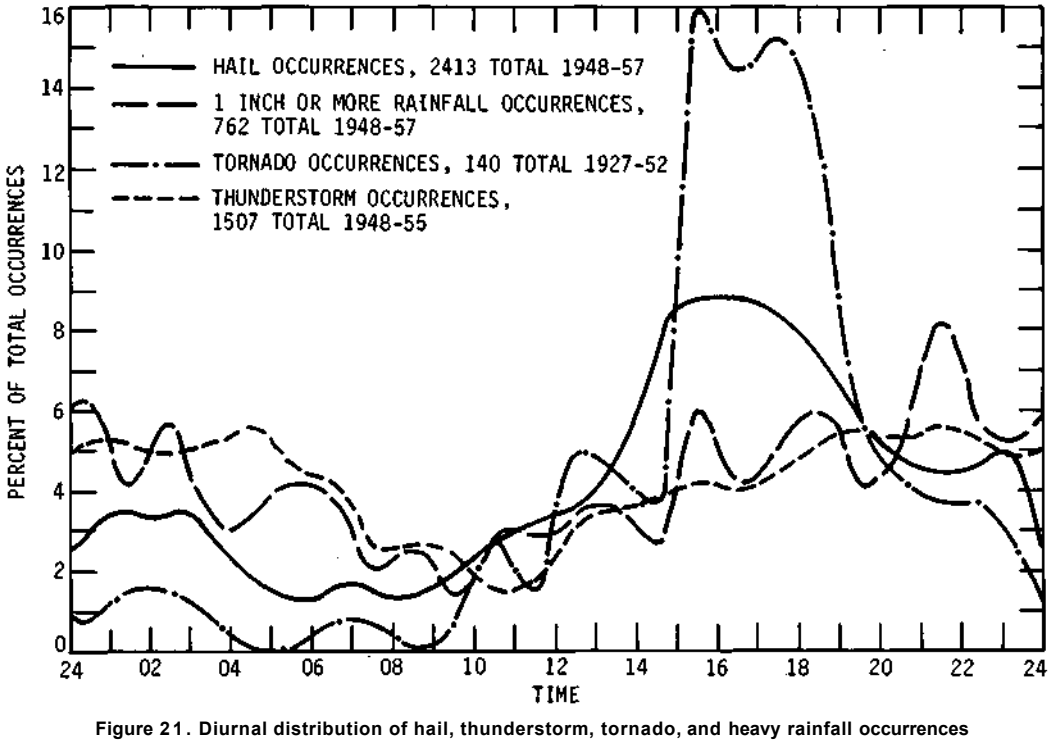

Figure 21. Diurnal distribution of hail, thunderstorm, tornado, and heavy rainfall occurrences

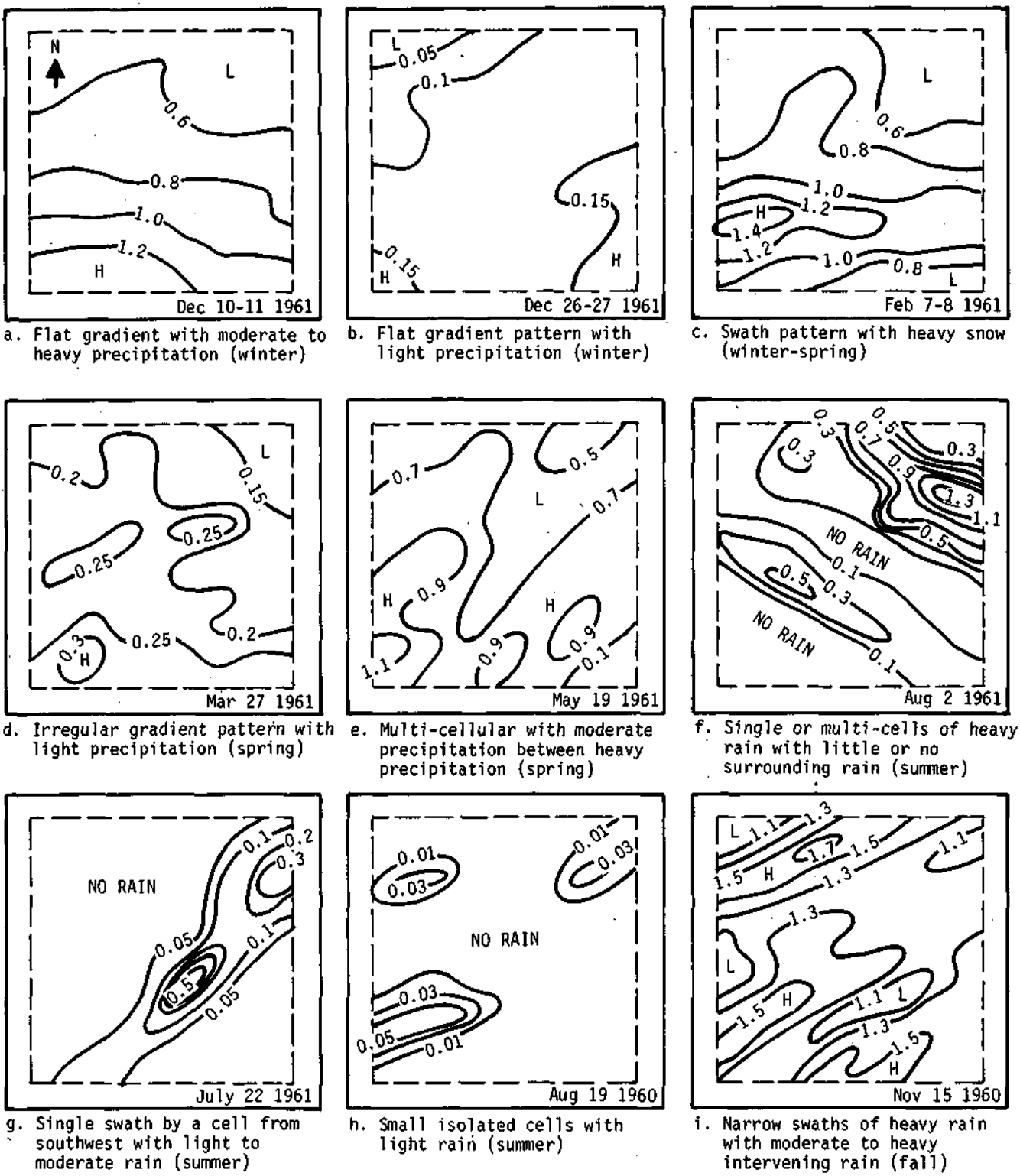

a. Flat gradient with moderate to heavy precipitation (winter)

b. Flat gradient pattern with light precipitation (winter)

c. Swath pattern with heavy snow (winter-spring)

d. Irregular gradient pattern with light precipitation (spring)

e. Multi-cellular with moderate precipitation between heavy precipitation (spring)

f. Single or multi-cells of heavy rain with little or no surrounding rain (summer)

g. Single swath by a cell from southwest with light to moderate rain (summer)

h. Small isolated cells with light rain (summer)

i. Narrow swaths of heavy rain with moderate to heavy intervening rain (fall)

Figure 22. Typical patterns of storm precipitation (inches) found for each season from network data

Table 7. Precipitation Conditions in Little Egypt Raingage Network

	Winter	*Spring*	*Summer*	*Fall*	*Annual*
Average number of days with precipitation in network	32	41	45	32	150
Average number of storms with network mean rainfall of:					
trace or more	23	37	50	30	140
0.25 inch or more	11	16	14	8	49
0.50 inch or more	6	9	7	5	27
1.0 inch or more	2	3	3	3	11
Average number of storms with					
thunderstorms	3	18	35	12	68
hail	1–	6	2	1–	9
excessive rainfall values	1–	4–	8	2	14
Average duration at a point, hours, for					
all storms	11.6	6.4	2.6	5.2	5.5
storms with network means of 0.5 inch or more	18.3	11.9	7.2	12.6	12.3
Percent of total time with rain	12	11	6	7	9

fall, and a third characterized by one or more isolated small cells of light rainfall.

To help illustrate what composes a typical network storm, figure 23 was chosen from the Little Egypt Network. These are maps of hourly rainfall of a typical summer storm showing the development and movement of a variety of cells across the network which combine to form the total storm rainfall map shown. Also from the data sample for this network, the areal distribution of storm initiations has been developed (figure 24). In the summer, most of the initiations were found in the northwest and southwest corners of the network, revealing frequent storm motions from the southwest and northwest. One-third of the 249 summer storms (in 5 years) initiated at the 10 'interior' raingages. This indicates the frequency of storm starts likely to occur within a 225 mi^2 area. In the period analyzed, 17 storms developed each year, on the average, within this internal area. Another illustration of storm distributions in the Little Egypt Network is portrayed in figure 25. Here, the number of storms that produced amounts equaling or exceeding the 2-year frequency values for any duration from 30 minutes to 24 hours at each raingage is portrayed. Considerable areal variation is apparent with the highest numbers of excessive storm rain events recorded at gages in the northwest and eastern parts of the network. These reveal the type of sampling differences that storms can produce over a 5-year period.

Huff (1967a) made a study of heavy rainstorms (network means of 0.5 inch or more) in the East Central Illinois Network (400 mi^2), over an 11-year period. The four examples of frequent storm patterns found are illustrated in figure 26. The closed and open elliptical patterns are quite likely similar and reflect only the position of the rainfall high, either within or on the edge of the network of 400 mi^2.

Figures 27 through 30 portray selected patterns of heavy storm rainfall from the larger METROMEX network at St. Louis (Changnon and Semonin, 1975). These were selected to reveal the typical patterns found with different synoptic weather conditions. Figure 27a shows a pattern with a squall zone area, produced by a series of semi-isolated and moving storms that were classified as air mass. Most of these METROMEX figures (27-30) also show the locations where thunder and hail events occurred. Figure 27b shows a post-cold frontal pattern based largely on isolated cell development, and figure 28a shows a typical rainfall pattern for a squall line. Figure 28b illustrates a pattern typical of cold-frontal passage through an area of this size. Figure 29 was chosen to show a sequence of three storms that occurred on a single August day. The early morning storm of isolated showers was of an air mass variety. During the day, two closely spaced squall lines passed producing moderately heavy rainfall. Then during the evening, storms with a cold front occurred and dis-

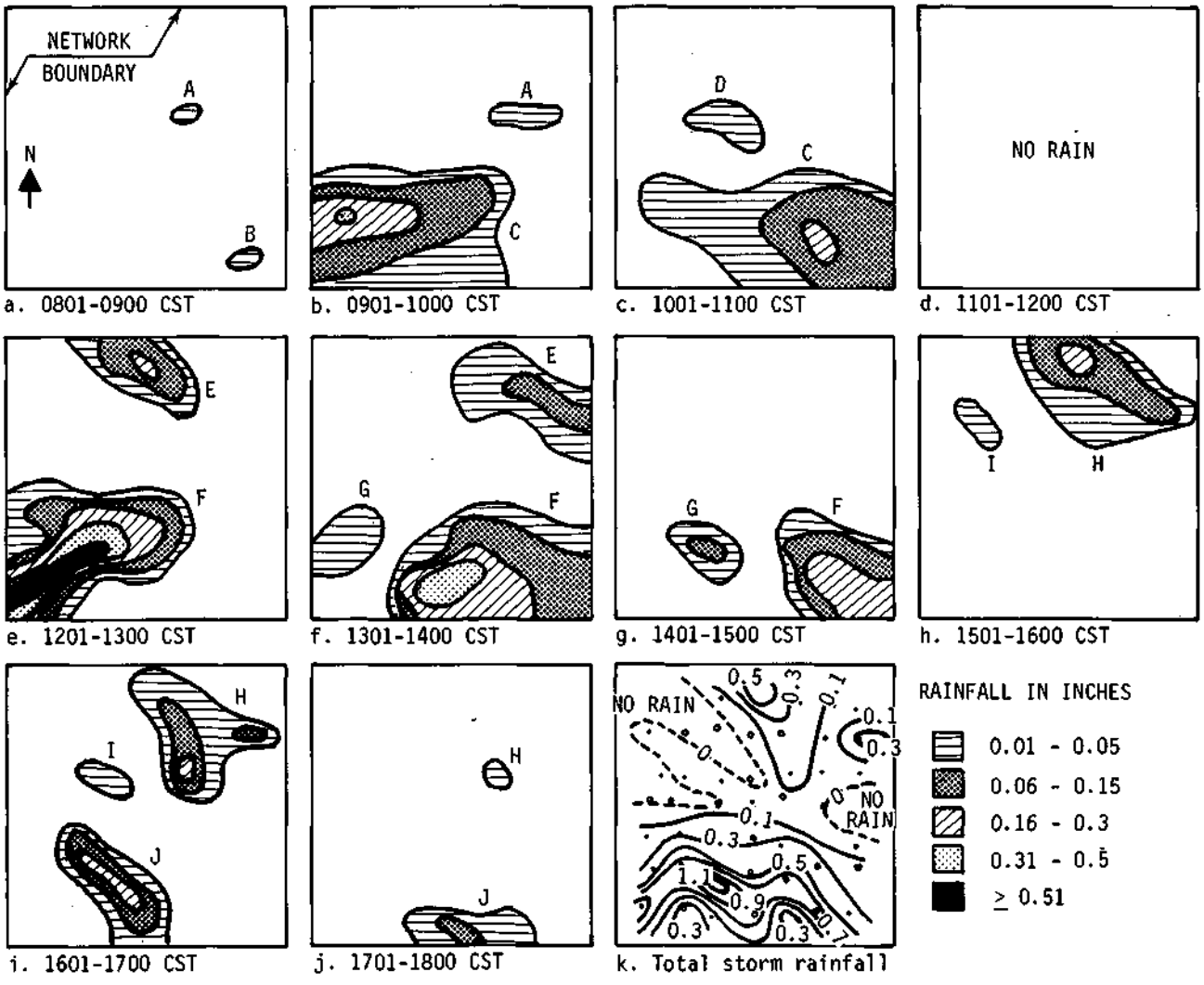

Figure 23. Maps of the hourly rainfall sequence and total rainfall for the storm of 21 August 1958

sipated as they moved across the network. Figure 30a presents a pattern for classical afternoon air mass thundershowers; these developed in the St. Louis metropolitan area and were somewhat self-sustaining by their own outflow. Figure 30b relates to the elements of a small squall line that developed within the network.

Precipitation Patterns Based on Storm Motions. One of the various storm analyses performed on the 5-summer METROMEX sample of 330 storms was to investigate the storms on the basis of their motion. Table 8 presents the frequency of summer storm movements. The patterns in figure 31 give some indication of the magnitude and distribution of rainfall associated with the four basic motions of storms. When southwest surface winds occurred during rainfall, 52% of that rainfall occurred with storms moving from the west-southwest. Additional information on storms based on their associated synoptic weather conditions appear in the later section on "Rainfall Relations to Atmospheric Conditions."

Table 9 shows the percentage distribution of rainfall in the METROMEX network grouped by storm motion and surface wind directions. Most of the summer rainfall (85%) is associated with SE or SW surface winds. Storms move most commonly from the WSW. Storms rarely move from the NE or SE quadrants.

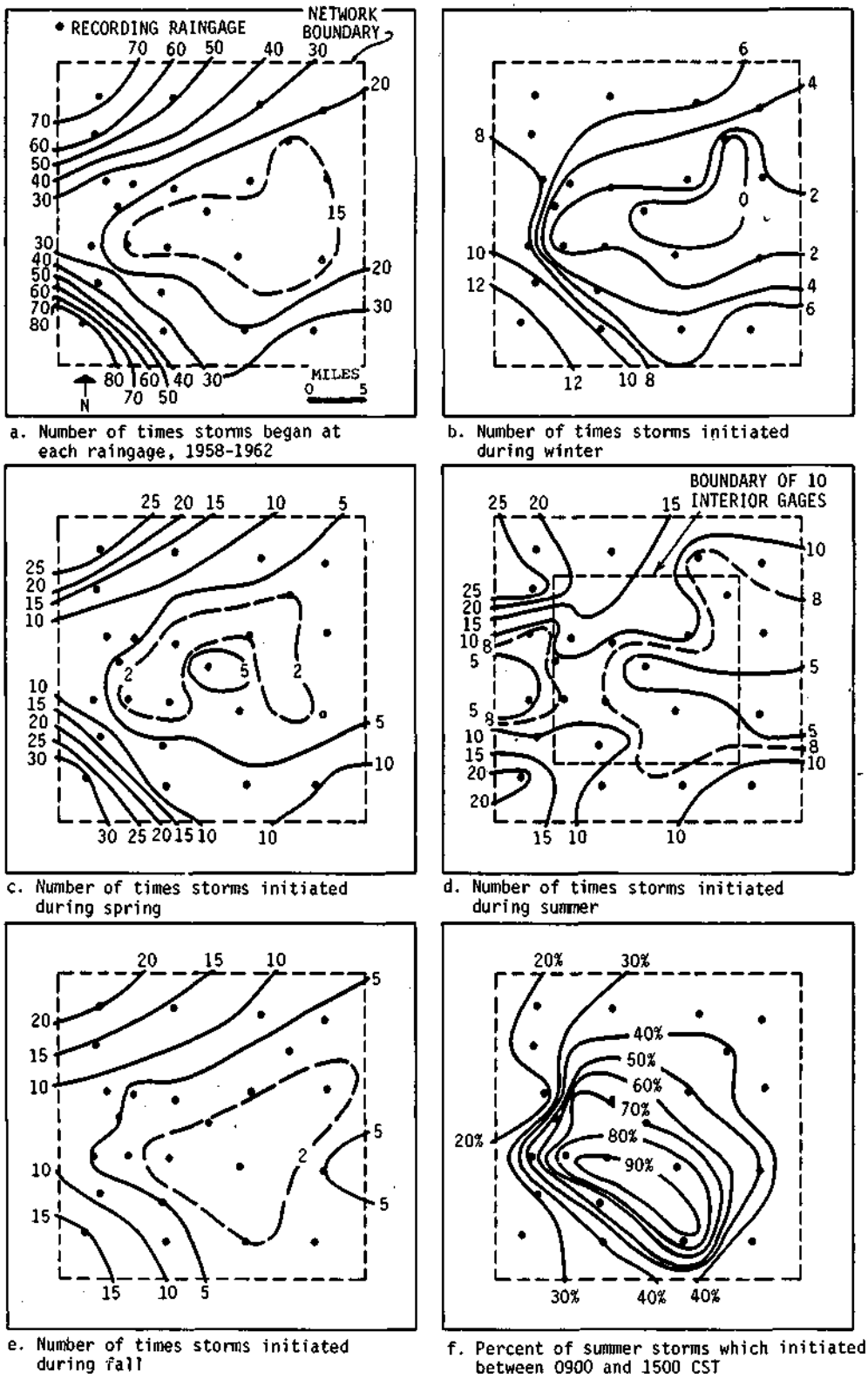

a. Number of times storms began at each raingage, 1958-1962

b. Number of times storms initiated during winter

c. Number of times storms initiated during spring

d. Number of times storms initiated during summer

e. Number of times storms initiated during fall

f. Percent of summer storms which initiated between 0900 and 1500 CST

Figure 24. Maps showing the annual and seasonal distributions of storm initiations, Little Egypt Network

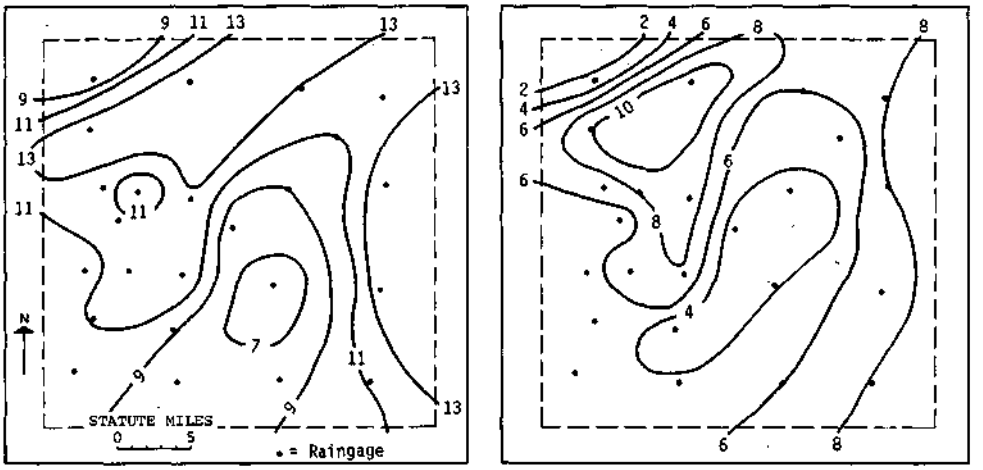

a. Number of storms that produced 2-year or greater recurrence interval values for any duration from 30-minutes to 24 hours, 1958-62

b. Number of times each gage recorded a 30-minute amount ≥ 2-year recurrence interval value (1.1 inch)

c. Number of times each gage recorded a 6-hour amount ≥ 2-year recurrence interval value (2.2 inches)

d. Number of times each gage recorded a 24-hour amount ≥ 2-year recurrence interval value (3.2 inches)

Figure 25. Number of times 2-year or greater recurrence interval rainfall occurred at each raingage in the network for selected durations

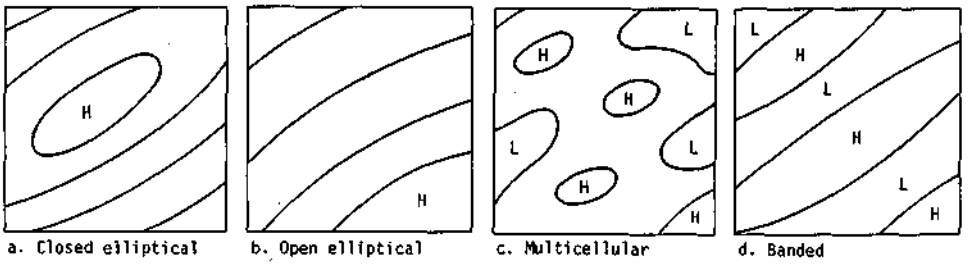

a. Closed elliptical b. Open elliptical c. Multicellular d. Banded

Figure 26. Major types of storm patterns

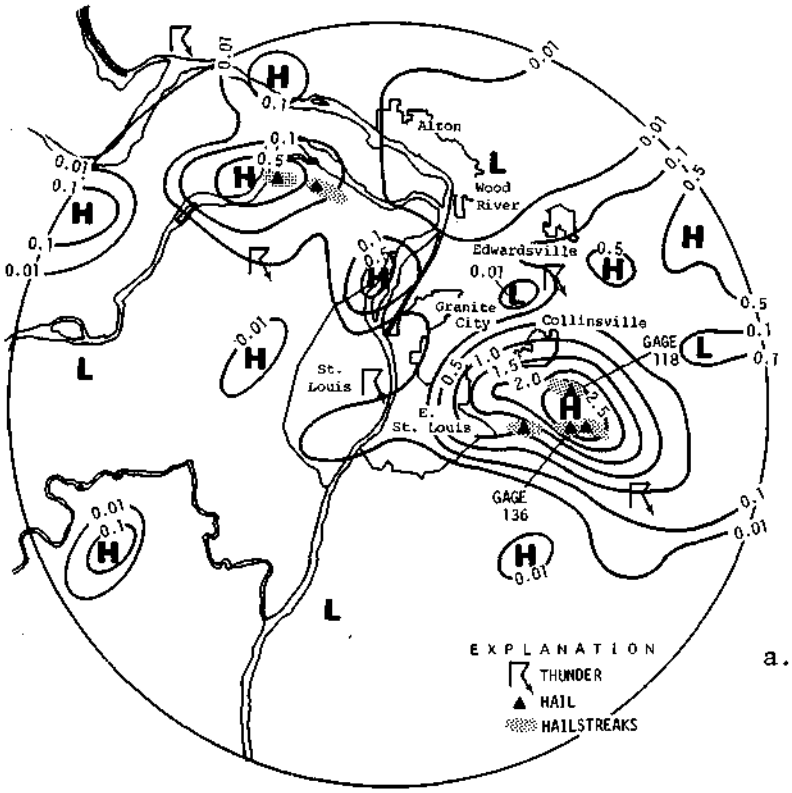

a. Total storm rainfall, inches, with squall zone on 11 August 1972

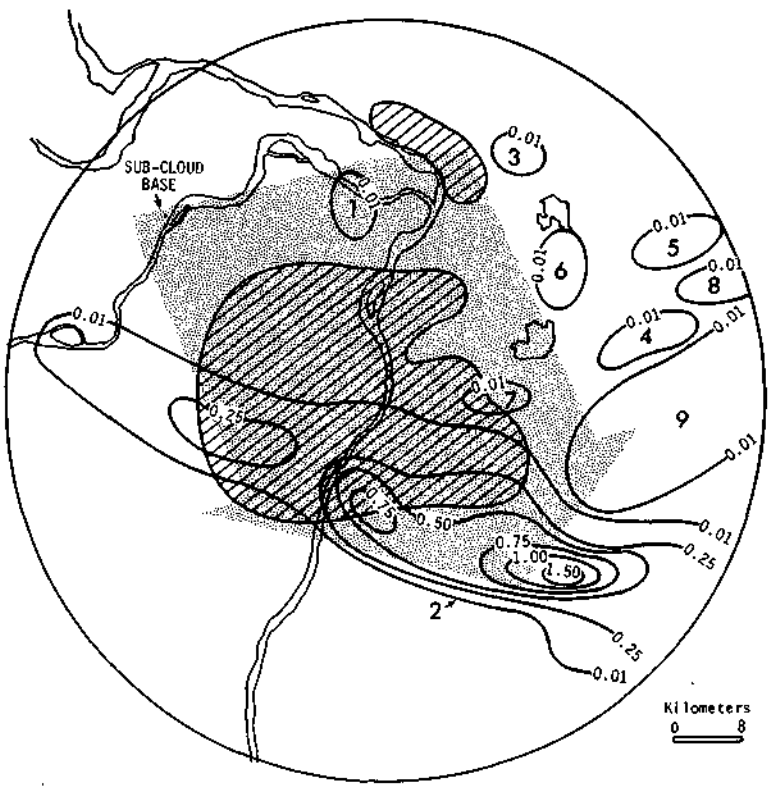

b. Total storm rainfall, inches, on 14 July 1973, post cold front

Figure 27. Storm rainfall patterns with different synoptic conditions, METROMEX network

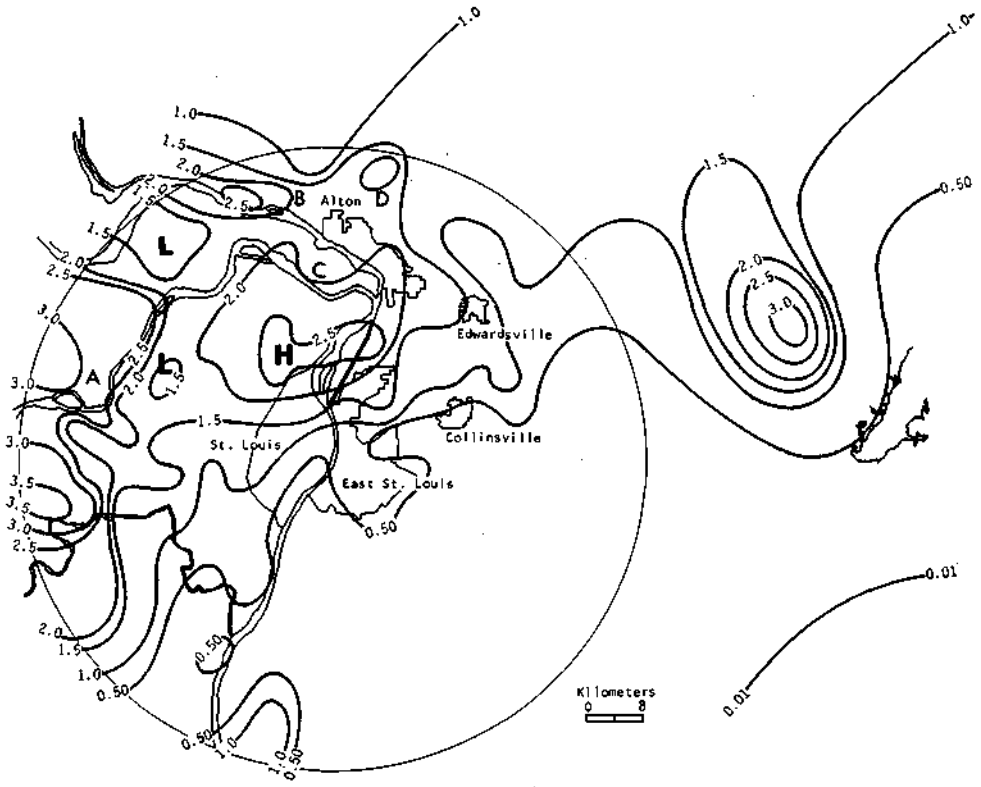

a. Rainfall, inches, squall line storm, 23 July 1973

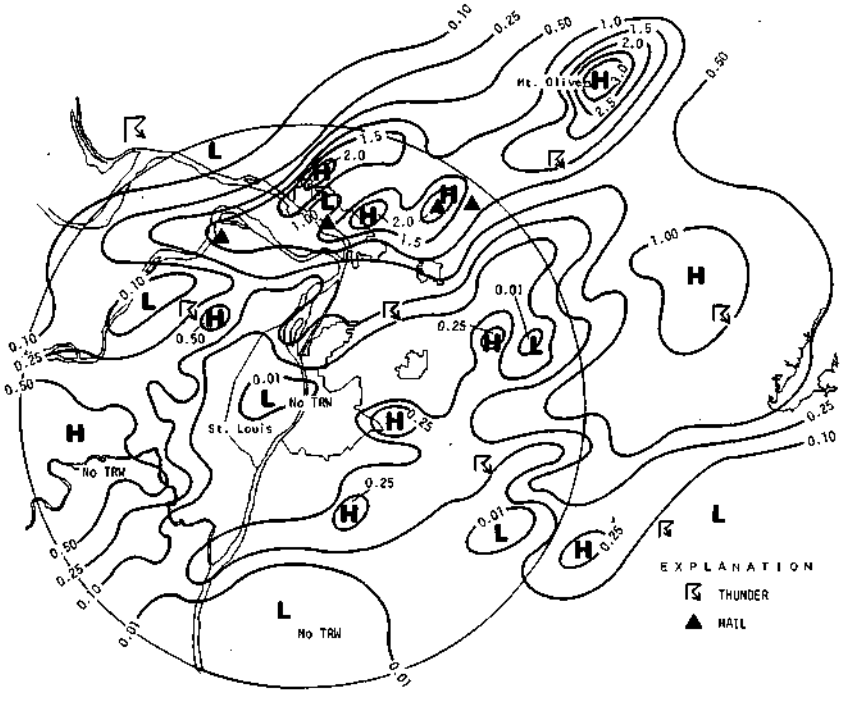

b. Rainfall, inches, cold front storm, 25-26 July 1973

Figure 28. Storm rainfall patterns with different synoptic conditions, METROMEX circle and extended network

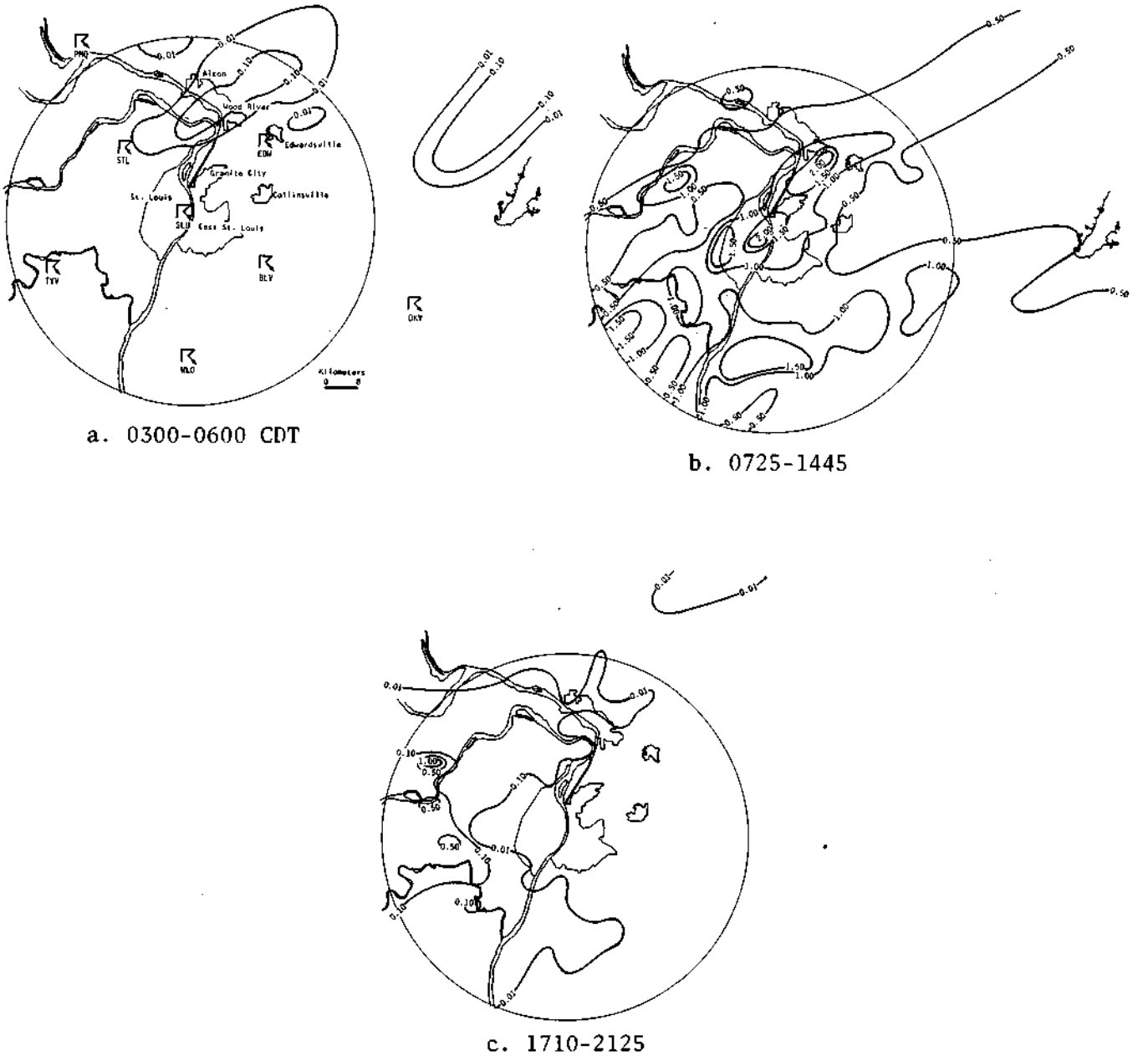

Figure 29. Total rainfall for three rain periods on 9 August — an air mass case at 0600, a squall line at 0725, and a cold front at 1710

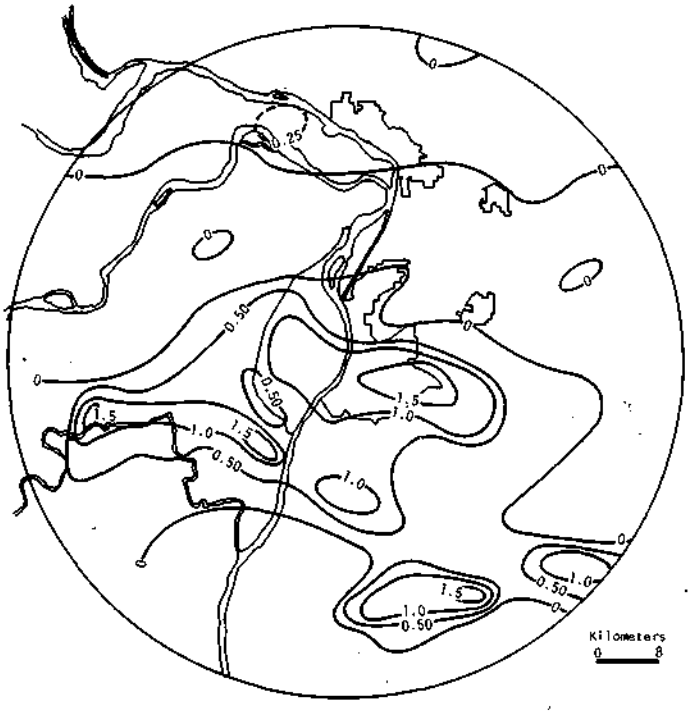

a. Total rainfall, inches,
air mass storm, 10 August 1973

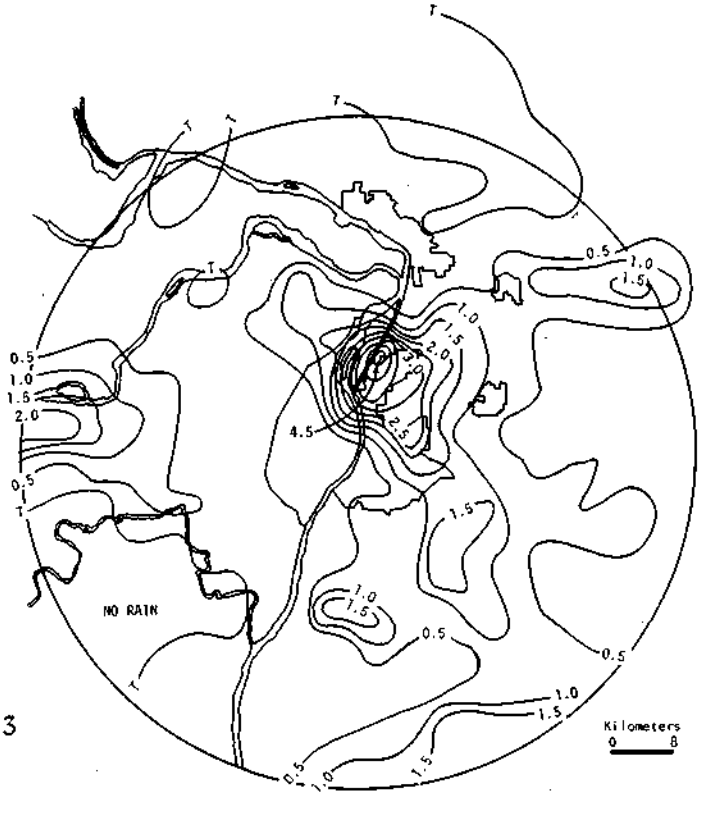

b. Total rainfall, inches,
squall line, 12 August 1973

Figure 30. Storm rainfall patterns with different synoptic conditions

Table 8. Frequency of Summer Storm Movements, 1971-1975, METROMEX

	Number of storms					*1971-1975*	
	1971	*1972*	*1973*	*1974*	*1975*	*Total number*	*Percent of total*
SSW	1	2	5	12	4	24	7
SW	10	16	11	11	16	64	20
WSW	13	13	17	17	17	77	23
WNW	9	11	9	13	11	53	16
NW	6	15	11	16	7	55	17
NNW	4	3	2	6	4	19	6
NNE	1	0	1	1	1	4	1
NE	0	0	0	0	0	0	0
ENE	0	0	0	0	0	0	0
ESE	0	0	0	0	1	1	0+
SE	0	0	0	2	1	3	1
SSE	1	2	0	0	1	4	1
Stationary	0	0	0	2	1	3	1
Indeterminate	2	7	9	0	5	23	7
Total	47	69	65	80	69	330	100

Table 9. Percentage Distribution of Rainfall Stratified by Storm Motion and Surface Wind Direction, Summers of 1971-1975 in METROMEX

	Percent of total rainfall			
Storm movement from	*SE surface winds*	*SW surface winds*	*NW surface winds*	*NE surface winds*
SSW	13	1	0	0
SW	20	13	2	1
WSW	29	52	58	67
WNW	15	13	25	29
NW	20	9	9	2
NNW	2	1	6	<0.5
NNE	0	1	<0.5	0
NE	0	0	0	0
ENE	0	0	0	0
ESE	<0.5	0	0	0
SE	1	0	0	1
SSE	0	<0.5	0	0
Indeterminate	<0.5	<0.5	<0.5	<0.5
Total rainfall, *cm*	48.9	43.9	7.2	8.3
Percent of all network rainfall	45	40	7	8

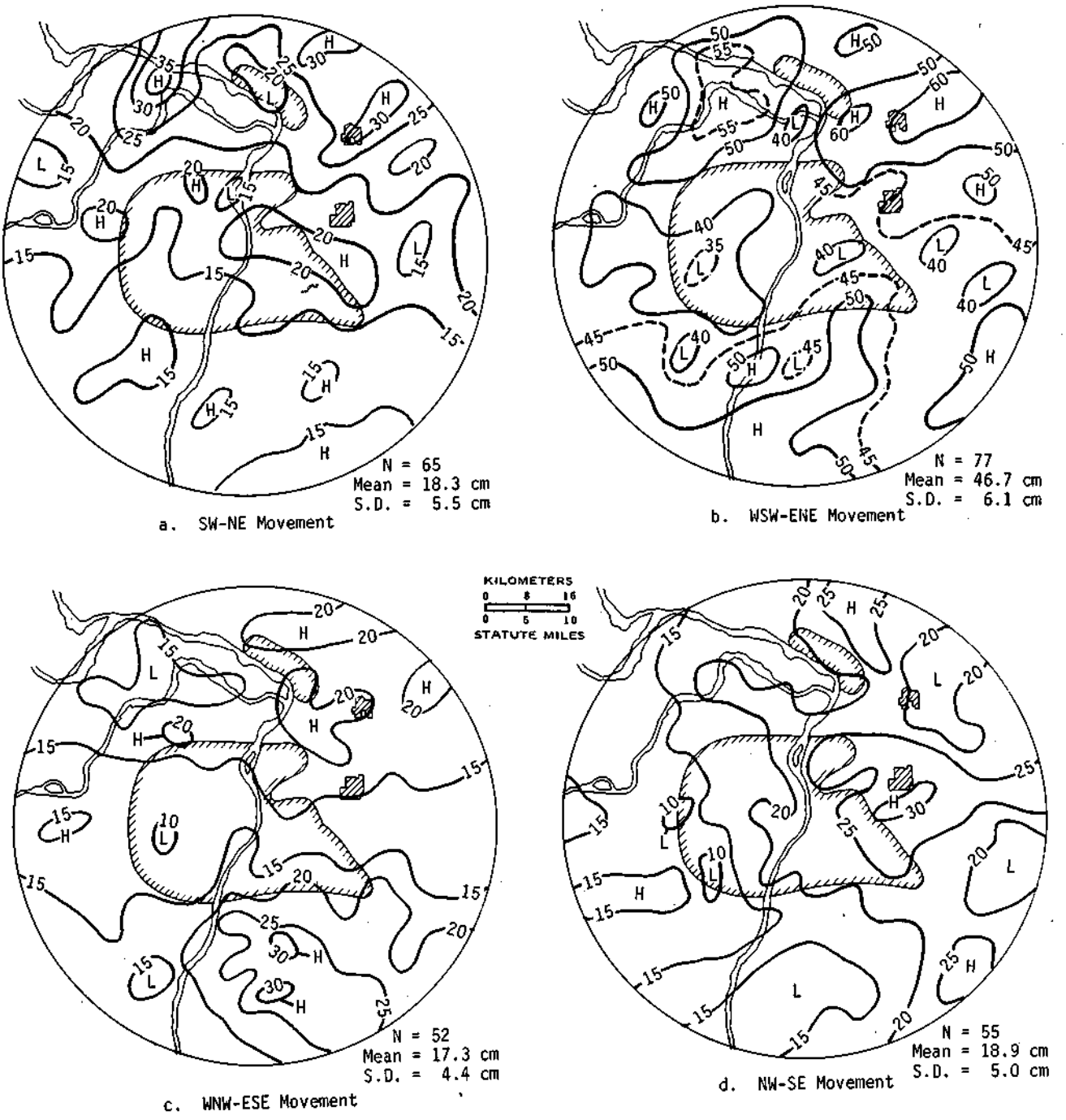

Figure 31. Rainfall patterns with various storm movements, METROMEX

Storm Characteristics. Very extensive studies of storms on the Survey's dense networks have often concerned the heavier storms, those producing point rainfalls of 1 inch or more, or mean network rainfalls of 0.5 inch or more (because of their hydrometeorological significance). A variety of results that essentially model these moderate-to-heavy storms have been generated and are described in the following text.

The first set of results are from Huff (1969a) based on an assessment of 12-year (May-September) data from the 400 mi^2 East Central Illinois Network *(see* figure 42). Table 10 shows how the climatological distribution of storm mean precipitation is related to storm duration. For example, reading horizontally, in the upper portion of the table it is seen that with storm durations equal to or less than 3 hours on the network, 28% of the storms, on the average, will produce a network mean exceeding 0.5 inch; whereas this percentage increases gradually to 95% for storms with durations greater than 24 hours. Similarly, for storms of durations of less than 3 hours, 80% of the storms have network means exceeding 0.1 inch compared with 7% exceeding 1 inch. The lower part of table 10 shows how storm duration affects the relation between storm mean rainfall and the distributions of storm occurrences. This table stresses the importance of the storm duration factor in the establishment of the distribution characteristics of storm rainfall in Illinois.

Figure 32 (Huff, 1969a) provides a measure of the distribution of total precipitation with respect

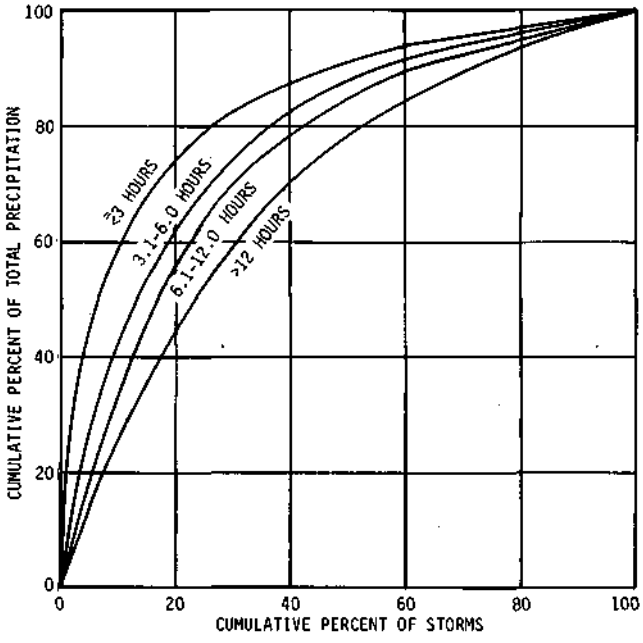

Figure 32. Relation between distributions of total precipitation and storm occurrences in Central Illinois network

to the frequency of storm occurrences. These sets of curves provide quantitative estimates of average distribution characteristics of network rainfall. It illustrates well the climatological trend for a large percentage of the total precipitation to fall in a small percentage of the total storm occurrences. For example, the curves indicate that 50% of the total precipitation occurring in storms with durations of less than 3 hours is recorded in 9% of the storms occurring (in an average year).

Table 11 indicates that differences in the distri-

Table 10. Average 12-Year Distribution of Network Storm Precipitation Grouped by Storm Duration in Central Illinois Network of 400 mi^2

Network mean storm precipitation exceeded (inches)	*Cumulative percent of total precipitation for given duration (hr)*					*Cumulative percent, all storms combined*
	≤3	*3.1-6.0*	*6.1-12.0*	*12.1-24.0*	*24.1-48.0*	
1.00	7	22	29	54	80	41
0.50	28	52	61	85	95	70
0.25	52	79	87	96	99	86
0.10	80	93	96	99	>99	95
	Cumulative percent of total storm occurrences for given duration (hr)					
1.00	<1	4	8	26	53	7
0.50	2	15	26	56	78	19
0.25	9	34	52	80	89	33
0.10	26	60	80	95	96	50

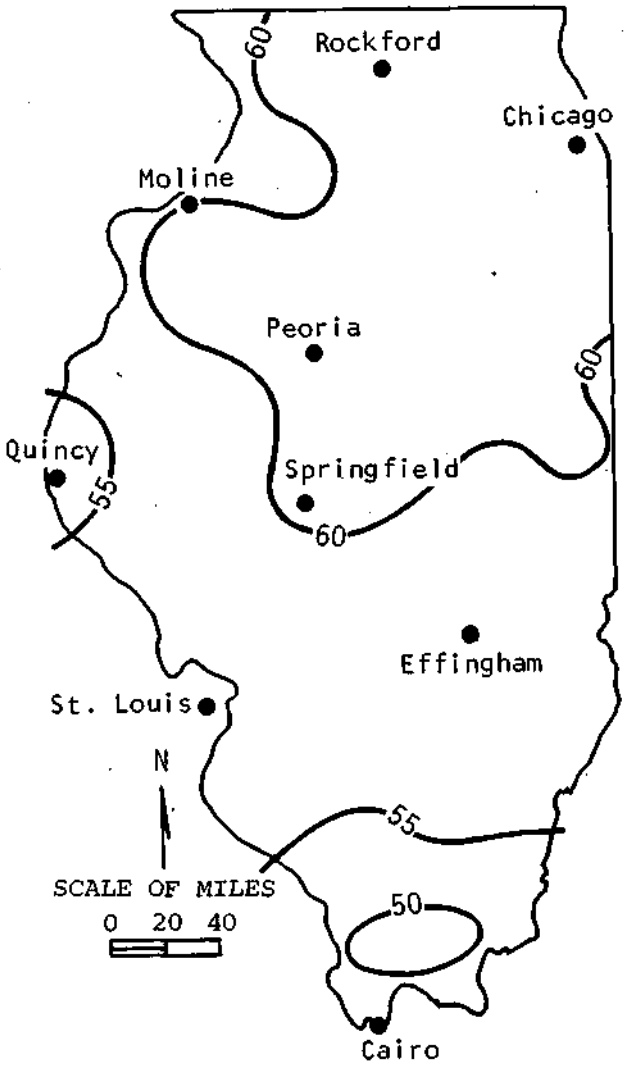

Figure 33. Average annual percentage of total precipitation from daily amounts of 0.11 to 1.00 inch

Table 11. Relation between Storm Precipitation Distributions on Selected Areas in Central Illinois Network

Areal mean precipitation (inches)	*Percent of total number of storms for given area (mi^2)* Gage 25	50	100	200	400	*USWB daily point*
≤0.10	38	45	46	46	47	38
0.11-0.50	37	34	34	33	34	40
0.51-1.00	15	13	12	13	12	14
>1.00	10	8	8	8	7	8
	Percent of total precipitation for given area (mi^2)					
≤0.10	4	5	6	6	5	5
0.11-0.50	24	25	25	25	25	29
0.51-1.00	28	29	28	28	29	30
>1.00	44	41	41	41	41	36

butional characteristics are small. This table shows comparisons of the average annual percent of storm occurrences for various intervals of mean precipitation on areas ranging from a single point (center gage of the network) up to 400 mi^2. Equivalent point values at the network center, based on long-term U.S. Weather Bureau records, are also presented.

Figure 3 3 illustrates the application of point precipitation records from climatic stations to obtain estimates of precipitation distribution characteristics. Inspection shows that 50 to 60% of the annual precipitation comes with daily amounts ranging from 0.11 to 1 inch.

Figure 34 presents a nomogram, developed from the precipitation distributions on the 400 mi^2 area, to facilitate the calculation of benefits from rain enhancement (Huff, 1969a). Figure 34 shows the effects of a 20% increase from a hypothetical seeding program on the total May-September rainfall for a variety of storms. These were classed as storms for a dry year and average year conditions, and for air mass type storms. Use of the nomogram

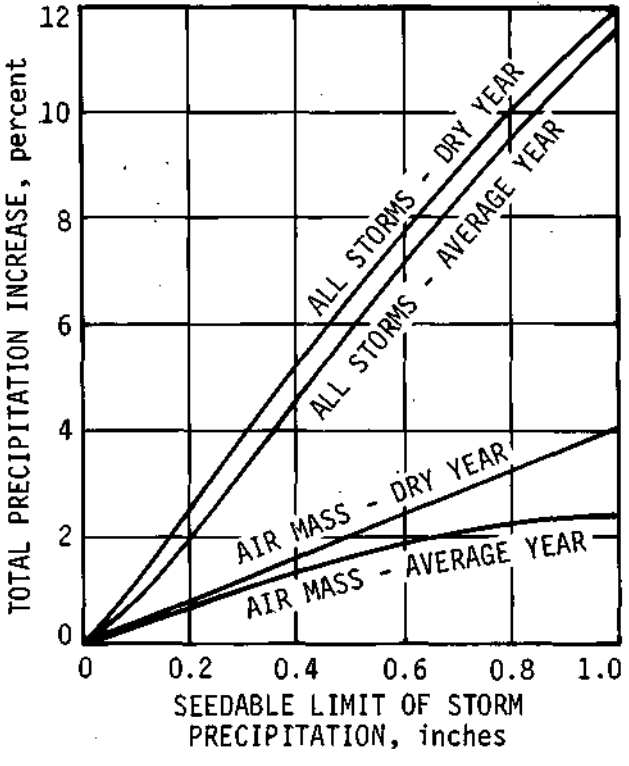

Figure 34. Effects of 20% seeding-induced increases on total May-September rainfall in Central Illinois Network (400 mi^3)

can be explained by an example. Assume a continuous seeding operation on a target area and that the seeding is capable of producing the 20% increase in storms once the areal mean rainfall produced naturally is 0.5 inch or less, but that the seeding of storms of greater intensity (of over 0.5 inch) will have no effect on the rainfall. The abscissa shows the upper limit of areal mean rainfall over a given assumption and the ordinate shows the percentage increase in total seasonal rainfall from a given capability. Thus, in a typical dry year (top curve) a realized rainfall increase of 6.4% is obtained as compared to 5.9% in an average year and there is no great difference from a practical standpoint. Figure 34 can also be used to determine potential seeding benefits within specific ranges of storm mean rainfall. Also, the effects of other assumed seeding increases such as 10 or 30% can be obtained by multiplying the nomogram answer by the ratio of the desired percentage to 20. Similarly, the nomogram can be used to calculate the potential effects of selective seeding.

It was shown by Huff (1969a) that the storm duration has a pronounced effect upon the mean rainfall distribution *(see* figure 32). Therefore, nomograms were constructed to permit consideration of duration in estimating potential cloud seeding benefits. Figure 35 shows that the realized increases in seasonal precipitation are relatively small, especially in the cold season, unless storms of relatively long duration can be successfully modified. Results shown in figures 34 and 35 indicate that it would be difficult to achieve seasonal increases of 10 to 20% in Illinois (and the Midwest) by seeding on days with natural rainfall unless 1) seeding intensifies heavy rainstorms (those of greater than 1 inch mean), and/or 2) very large percentage increases are produced in storms of light to moderate intensities. The results of the METROMEX research indicate that the urban modification of precipitation is due to influences on the heavier (greater than 1 inch) rainstorm events (Changnon et al., 1977).

Huff (1967a) in another exhaustive study of storms from an 11-year sample on the 400 mi^2 network in east central Illinois, focused on heavier storms, those in which the network mean exceeded 0.5 inch and/or one or more gages recorded an inch or more of rain (269 storms, qualified). This research examined the temporal characteristics of

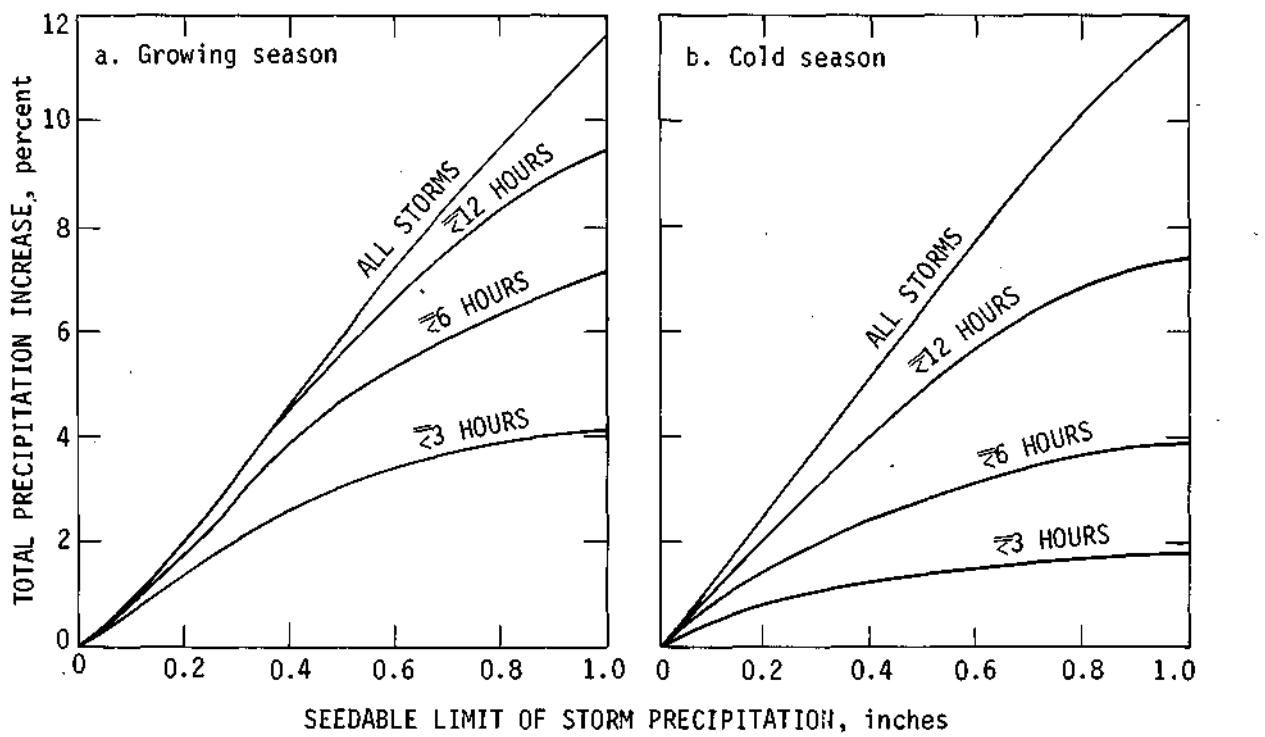

Figure 35. Effects of 20% seeding-induced increases in storms of selected duration on total seasonal rainfall

storms and attempted to model the rainfall distributions with time. A major portion of total storm rainfall occurs in a small part of the total storm time, regardless of storm duration, or mean rainfall, or the number of bursts in the storm. Therefore, Huff classified the storms into four groups, depending upon whether the heaviest rainfall occurred in the first, second, third, or fourth quarter of the storm. The frequency of these quartile storms is shown in table 12, revealing that those having the heaviest rainfall in the first or second quartile of the storm were more prevalent.

The time distributions were expressed in probabilistic terms because of the great variability in the characteristics of their distributions between storms. Figure 36 shows the probability distribution for first quartile storms. These are smoothed curves reflecting the average rainfall distribution with time and therefore do not exhibit the individual burst characteristics. Figure 37, a histogram for the 10-, 50-, and 90%-levels for the first quartile storms, shows percentages for total storm rainfall by 10% increments of storm times. The distributions for the three other storm classes are shown in figures 38-40.

Huff (1967a) also defined the rainfall burst characteristics in these 261 heavy storms. Bursts are the rapid increases in rainfall rate that relate to storm cores. In the first quartile storms, three bursts were most frequent, and with the second quartile storms, anywhere from one to three bursts typically occurred. Three to five bursts were most common for the third quartile storms and four bursts were common in the fourth quartile storms. Storms with two, three, or four bursts account for 53% of the storms. The number of bursts in the heavier rainstorms ranged anywhere from 1 to 14 and 4 is typical. The effect of total storm duration on the number of bursts was evaluated on the 400 mi^2 network. With storm durations of less than 3

Table 12. Percentage Frequency of Quartile Storms in Central Illinois

Quartile	*Frequency (%)*
First	30
Second	36
Third	19
Fourth	15

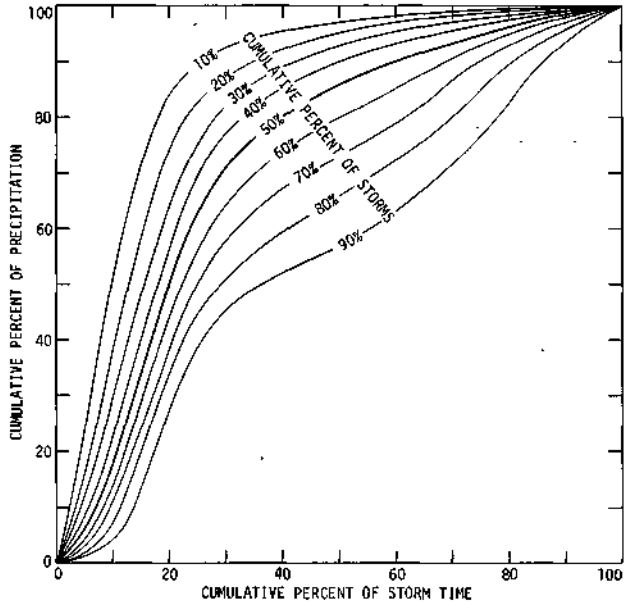

Figure 36. Time distribution of first-quartile heavy storms in Central Illinois network (400 mi^2)

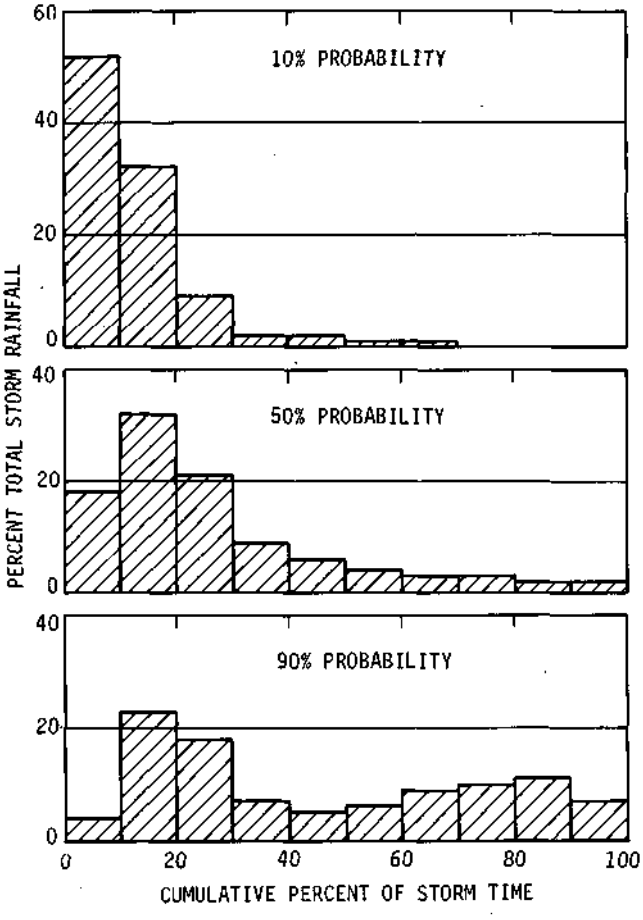

Figure 37. Selected histograms for first-quartile storms

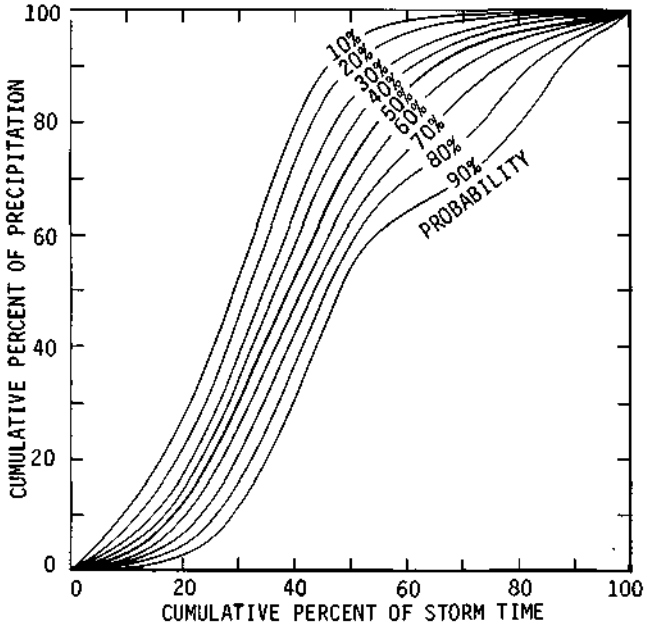

Figure 38. Time distribution of second-quartile storms in Central Illinois Network (400 mi^2)

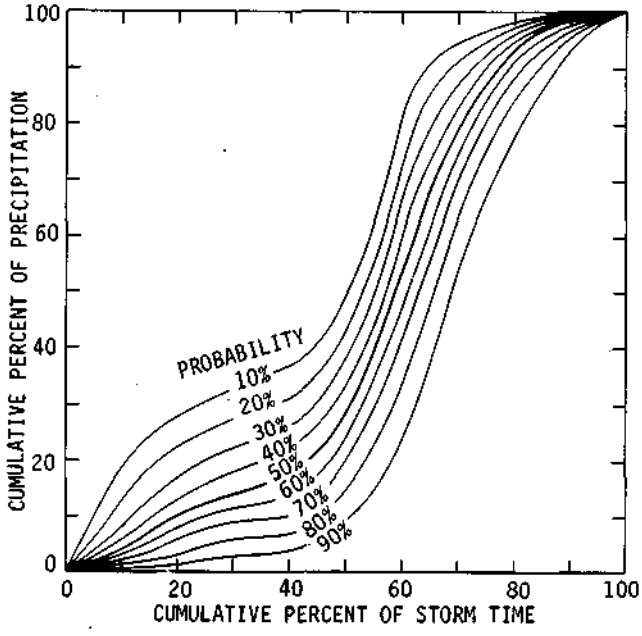

Figure 39. Time distribution of third-quartile storms in Central Illinois Network

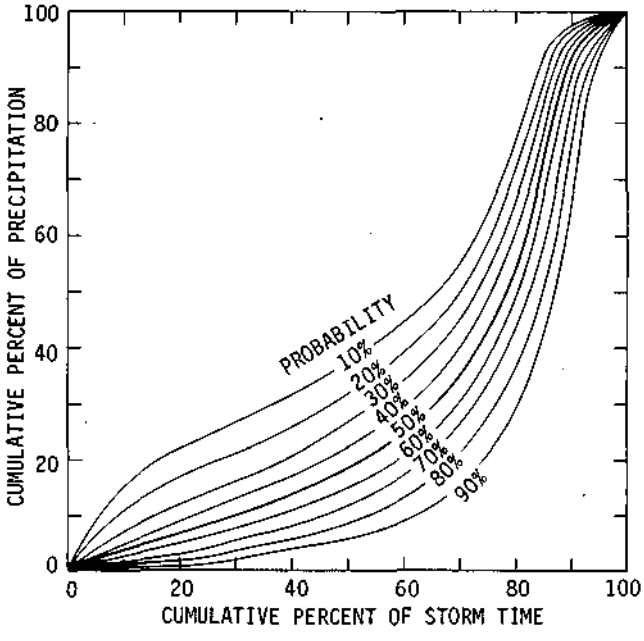

Figure 40. Time distribution of fourth-quartile storms in Central Illinois Network

Table 13. Distribution of 261 Heavy Storms by Quartile and Rain Type on 400 Square Miles, Central Illinois

Quartile	R,S*	R	RW	TRW	RW,R	TRW,RW	TRW,A	Number of cases
1	1.2	6.1	12.2	43.9	7.3	13.4	15.8	82
2	2.2	15.4	16.5	42.9	4.4	13.2	5.5	91
3	3.1	15.4	13.8	30.7	3.1	23.1	10.8	65
4	0.0	8.7	13.0	17.4	13.0	34.8	13.0	23
Combined	1.9	11.9	14.3	37.9	5.7	17.6	10.7	261

*R = Continuous rain, S = Snow, RW = Rainshower, TRW = Thunderstorm, A = Hail

hours, single burst storms predominated (52% of the cases). In storms with durations of 3 to 12 hours, double burst storms predominated, and storms typically had three to five bursts when durations exceeded 12 hours.

Table 13 presents the distributions of rain types for the quartile storms. Obviously, with storms of this type, the showery and convective type rains predominate. The TRW-only case predominated in the first, second, and third quartile storms, whereas the RW/TWR type predominated in the fourth quartile storms. These tended to be longer and were frequently associated with two or more closely related synoptic conditions.

Network data have been used to develop statistical models of heavy rainstorms for various uses (Stout and Huff, 1962; Huff and Changnon, 1964; Huff, 1967a). For example, Huff (1967a) created a statistical storm model for urban storm sewer design which used the typical first-quartile, 3-hour storm with a mean rainfall of 2 inches on a 100 mi^2 area. Storm parameters derived from median and mean values are shown in figure 41. The shape is most frequently elliptical, with an average ratio between the major and minor axis of the central isohyet of 1.7. The most frequent direction of movement is from the WSW and the most common storm type is cold front. The time distribution is based on the two-burst mode of the 3-hour storm, and on the time distribution for this type of storm. The lower part of figure 41 presents the average area-depth relation.

Another important study of network storms concerned the natural *spatial variability* of storm rainfall (Huff and Shipp, 1968). In this study data from four networks ranging in size from 10 to 550 mi^2 in central and southern Illinois were utilized. (All the Water Survey networks used for this and other research are portrayed in figure 42.) Network regression equations were developed by Huff and Shipp for a variety of conditions. Those for TRWs and RWs show the expected trend for relative variability (V) to increase with increasing area (A), and to decrease with increasing mean precipitation (P). These trends are illustrated quantitatively by the TRW curve in figure 43. As would be expected, substantially higher values of relative variability occurred with unstable precipitation types (TRW and RW) as shown in figure 44, where the relative variability for TRW is twice that for R (steady rain).

Analyses of the network data show the spatial variability to be an unstable precipitation parameter with large differences frequently observed between storms of similar average magnitude and precipitation types, as illustrated in figure 45. This shows the upper and lower 10% ranges about the average

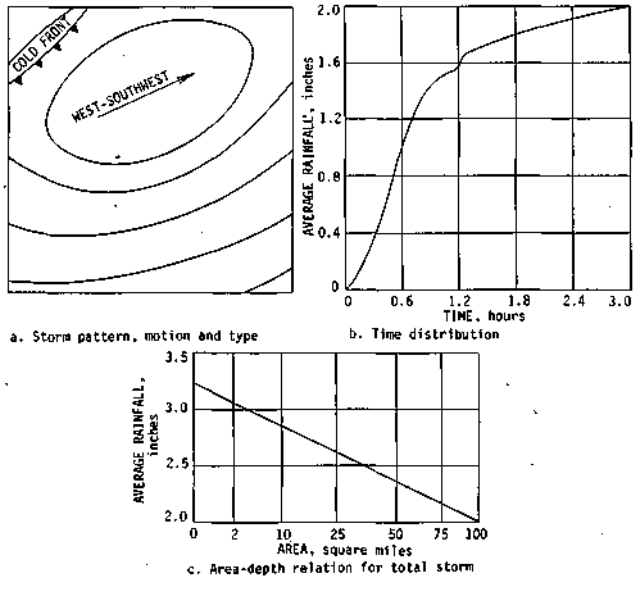

Figure 41. Statistical model of 3-hour, first-quartile storm on 100 mi^2 network in central Illinois

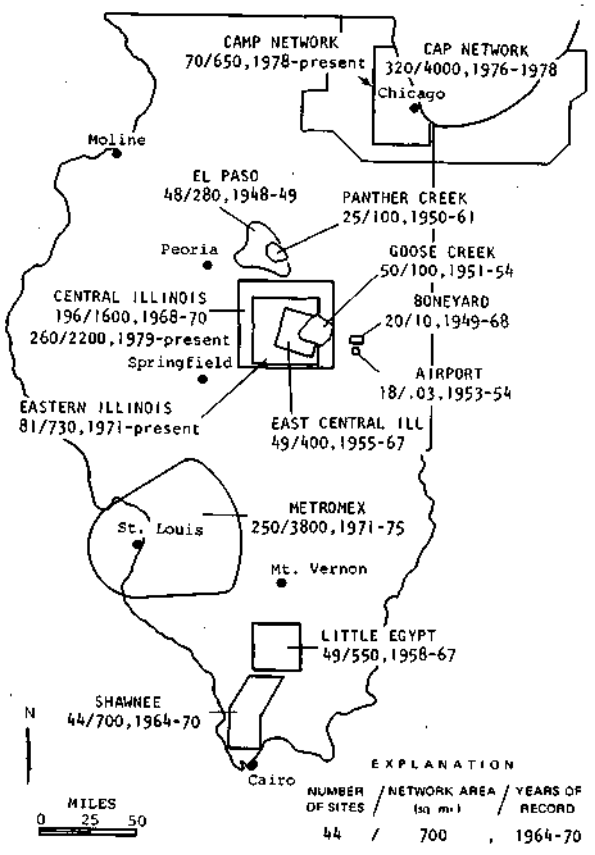

Figure 42. Recording raingage networks operated in Illinois by Water Survey, 1948-1978

relative variability for thunderstorms and steady rains on the East Central Network of 400 mi^2. Relative variability varied by a factor of approximately 5 between the upper and lower limits. The direct application of spatial variability as an evaluation parameter in weather modification experiments does not appear feasible in view of its great interstorm variance.

Huff and Shipp (1968) also grouped the data according to weather types. Representative relations for the large network are shown in figure 46. Throughout the range of precipitation, the highest relative variability occurred with air mass storms, and the least among low centers combined with occluded fronts. Obviously, air mass storms are more scattered than frontal storms and encompass less area on the average. Since high spatial variability intensifies the problem of rain modification evaluation, it is obvious (from figure 46) that the modification of air mass instability showers, such as pursued in some earlier cloud seeding experiments, presents an unusually difficult evaluation problem if surface rainfall is a primary verification tool.

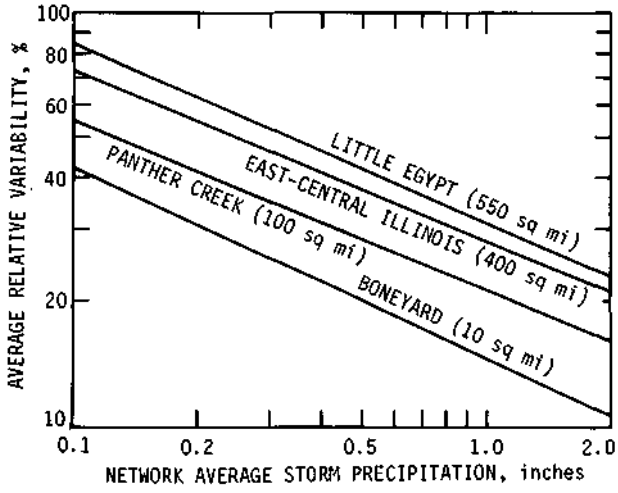

Figure 43. Relations between storm relative variability and mean precipitation in thunderstorms on various networks

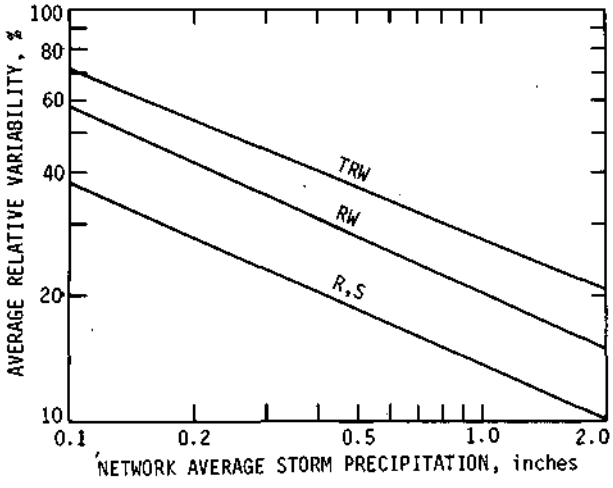

Figure 44. Relation between relative variability and precipitation type on a 400 mi^2 network in central Illinois

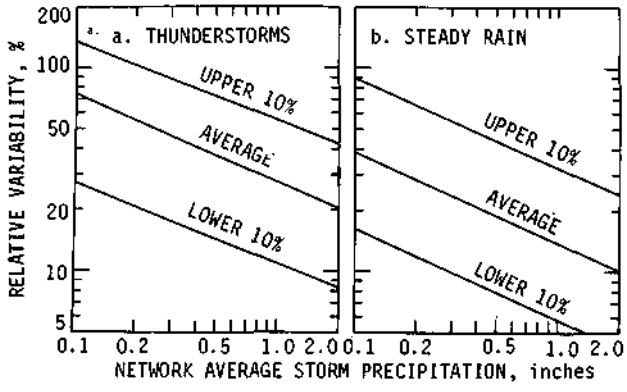

Figure 45. Range of storm relative variability on a 400 mi^2 network

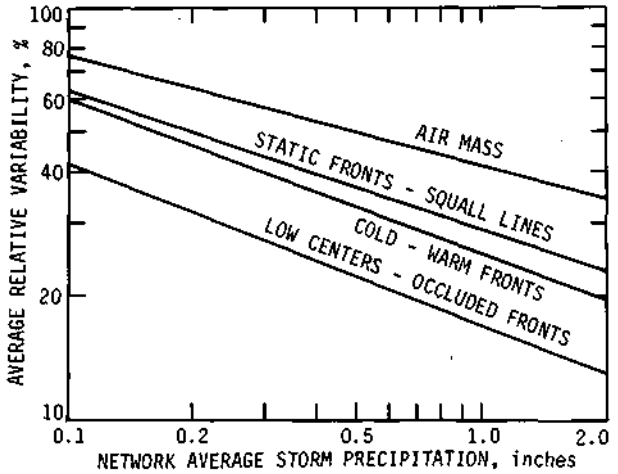

Figure 46. Relations between storm relative variability and synoptic storm type on 400 mi^1 network

The final example of storm rainfall patterns appears in figure 47. Here, 11 years of data at 49 recording raingages have been used to determine the 2-hour rainfall expected at a 2-year recurrence interval. This exhibits considerable variability and reveals the problems of a modest record of this length in determining expected heavy rainfall events (Stall and Huff, 1971).

In another study, climatological network stations were used to derive certain rainfall relations on an area of 7600 km^2 in central Illinois during 1954-1962. Computations were made of the average number of rain-free days, and the number of rain days with areal averages of a trace, 0.01-0.10 inch, 0.11-0.50 inch, over 0.50 inch, thunder, and hail.

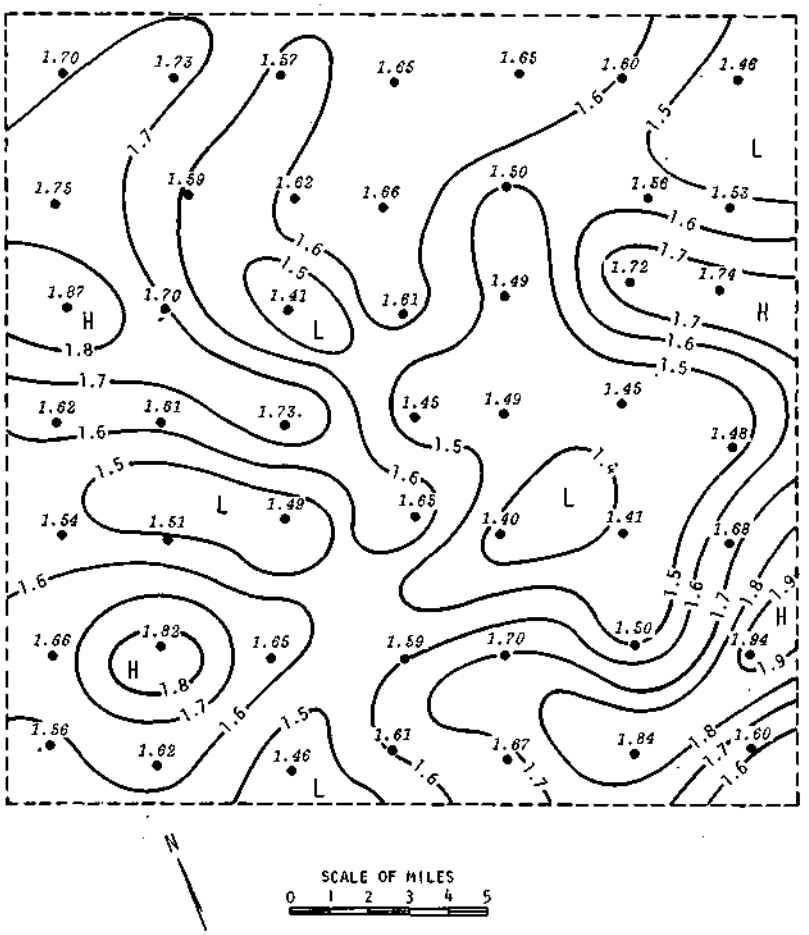

Figure 47. Two-hour storm rainfall, inches, expected at a 2-year recurrence interval as determined by the 11-year record at each of 49 gages in the 400 mi^2 East Central Illinois Network (Mean = 1.61 inches; standard deviation = 0.12 inch; coefficient of variation = 7%; data for clock hours)

Table 14. Average Percent of Possible Days with or without Rain*

	March	April	May	June	July	August	September	October
No-rain days	22.2	23.3	29.4	31.3	29.7	31.9	38.7	41.9
Trace rain	28.6	17.3	15.2	12.7	15.2	17.1	18.0	19.7
0.01—0.10 inch	33.1	33.7	29.4	30.0	25.5	26.1	23.0	20.6
0.11—0.50 inch	14.1	18.7	19.0	19.3	21.3	19.7	13.7	11.6
<0.50 inch	2.0	7.0	7.1	6.7	8.4	5.2	6.7	6.1
Trace—0.10 inch	61.7	51.0	44.6	42.7	40.7	43.2	41.0	40.3
Trace—0.50 inch	75.8	69.7	63.6	62.0	62.0	62.9	54.7	51.9
Days w/thunder	14.5	33.3	35.8	38.9	44.4	39.1	30.4	15.1
Days w/hail	6.5	8.5	7.5	6.7	5.7	3.2	4.8	1.1

**Within an area of 7600 km² in central Illinois, 1954-1962.*

Table 15. Distribution of Areal Mean Rainfall by Rainfall Amount in METROMEX Network, 1971-1975

Mean rainfall (inches)	Percent of storms equaling or exceeding given mean for given areas (mi²)					
	36	144	324	576	900	1296
0.10	54	44	39	37	33	31
0.25	35	26	23	21	18	16
0.50	21	14	13	11	9	8
0.75	13	9	8	7	6	5
1.00	8	6	5	4	3	3
N	150	191	220	253	279	303

The frequency of each of the above events was determined and normalized by dividing by the total number of days possible for each month of the 9-year period. The percent frequencies for the various categories are shown in table 14. With the exception of October, the combined frequency of the trace and 0.01-0.10 inch categories is always greater than the no-rain day frequency.

Assuming that light rain days are favorable for weather modification, these climatological data indicate a high frequency of cloud seeding opportunities during the warm season (40 to 60% of the days). Conversely, if useful weather modification is restricted largely to days with moderate to heavy natural rainfall (Huff, 1969a; Huff and Changnon, 1973; Changnon et al., 1977), only about 25% of the days, on the average, would be favorable for seeding (days with rain ≥ 0.11 inch).

Table 15 provides additional information for evaluating the potential of weather modification in the convective season. In this table, the percent of storms equaling or exceeding mean rainfalls of various amounts are shown for areas of various size. These results are based on the 5 years of sampling in the METROMEX network (1971-1975) in the St. Louis area.

Sampling Requirements for Storm Rainfall

Considerable emphasis has been placed on the raingage requirements for the measurement of precipitation, especially storm rainfall. Huff (1970) has summarized an evaluation of sampling errors in the measurement of storm mean rainfall, based upon data from several dense raingage networks. Differences in measurement requirements between seasons, precipitation types, synoptic type, storm intensity, and storm duration were investigated. In another study, Huff (1969b) determined sampling requirements for detection of storms of various magnitude over areas of various size. Also, rainfall gradients in warm season storms were evaluated in a 1967 study (Huff, 1967b).

The investigation of area-depth relations, which provide a mathematical expression of the areal rainfall pattern in rainstorms, has been pursued quite vigorously because of applications in both hydrology and weather modification. Huff (1968)

has shown how area-depth curves can be a useful tool in weather modification experiments, since they provide a measurement of the mean and maximum rainfall plus the rainfall gradient in target and control areas. Changes in these three important surface precipitation parameters should be useful in evaluation of weather modification effects. Furthermore, the area-depth relations can indirectly provide information on modification of the physical processes in treated cloud systems. A typical set of area-depth curves from a heavy rainstorm on the Little Egypt Network of 50 gages in 550 mi^2 is shown in figure 48.

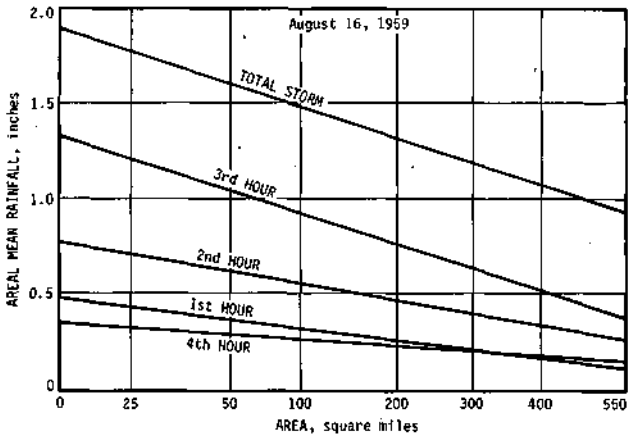

Figure 48. Area-depth relation in storm of 16 August 1959

At this point, it seems appropriate to mention previous research pertaining to the design and evaluation of rainfall modification experiments. Schickedanz and Huff (1971) used storm rainfall data from the Illinois dense raingage networks to determine the time required to obtain significance for various increases in storm rainfall due to weather modification. Investigation was made of the effect of stratifying the storm data on the detection of seeding effects for a given design. The efficiency of various rainfall parameters and statistical designs was also investigated. Results were presented to show the length of experimentation needed for detection of seeding effects when the data are stratified according to synoptic weather type, precipitation type, rainfall parameter, and statistical design employed. A summary of the more pertinent results is shown in table 16. The results in table 16 were based upon a 12-year sample from a dense raingage network of 400 mi^2 in central Illinois, and it was assumed all natural rain events are seeded; that is, all opportunities result in seeding operations. The other basic assumption was that seeding would only be successful in augmenting water output when natural precipitation of some type is occurring. Table 17 shows a general comparison of selected advantages and disadvantages of the various designs investigated.

Severe Rainstorms

Because of their hydrologic impact, severe rainstorms have been given considerable emphasis in the Survey's research. These are the storms which produce severe flash flooding in the convective season over areas ranging from a few hundred to several thousand square miles (Huff and Changnon, 1964). Studies have concentrated on both the surface distribution characteristics and the synoptic environment of these storms (Huff, 1978a; Huff, 1978b). These severe storm events are of major importance in weather modification also. Seeding operations should be aborted when synoptic conditions are favorable for their development. That is, they should be treated the same as severe hailstorms or tornadoes in operational planning. The location, areal extent, and intensity of several of these storms in 1956-1957 are shown in figure 49. The isohyetal pattern in a typical severe rainstorm is shown in figure 50. This storm produced 10-inch amounts in its core in a 12-hour period. Table 18 shows how the characteristics of the August 1959 storm compared with a statistical model derived from 10 such severe events.

The foregoing discussion has dealt with severe rainstorms that are relatively large in areal extent. Studies have shown that a smaller type of greater frequency also occurs in the convective season. In normal to above-normal rainfall periods, several of these are likely to occur in the convective season somewhere in Illinois. Except for 1957, we have seldom recorded more than one of the larger type per season in Illinois since studies started in 1948. Table 19 shows a statistical model of the surface and synoptic characteristics observed in the smaller type.

Droughts

Considerable Water Survey research has been done on droughts, beginning with an early extensive climatological study (Huff and Changnon,

Table 16. Comparison of Number of Years to Obtain Significance for Various Designs, Tests, and Types of Data Measurement ($\alpha = 0.05, \beta = 0.50$)

Design and data type	*Air mass* [warm] (% increases)			*Thunderstorms* [warm] (% increases)			*Cold fronts* [warm] (% increases)			*Steady rain* [cold] (% increases)			*Low centers* [cold] (% increases)		
	20	*40*	*60*	*20*	*40*	*60*	*20*	*40*	*60*	*20*	*40*	*60*	*20*	*40*	*60*
Crossover															
Areal means ≥0.005 inch	7	2	1	3	1	1	8	2	1	4	1	1	3	1	1
Areal means >0.10 inch	12	3	2	3	1	1	10	3	2	6	2	1	5	2	1
Areal means >1.0 inch	48	15	6	18	5	3	36	11	6	31	9	5	23	7	4
Maximum point rainfall	6	2	1	2	1	1	6	2	1	4	1	1	3	1	1
Areal mean gage values ≥0.01 inch	5	1	1	2	1	1	6	2	1	4	1	1	3	1	1
Random–historical (sequential)															
Areal means ≥0.005 inch	17	5	3	7	2	1	20	6	3	10	3	1	8	2	1
Areal means >0.10 inch	28	8	4	8	2	1	25	7	4	13	4	2	13	4	2
Areal means >1.0 inch	115	33	18	44	13	7	88	26	13	75	22	11	58	17	9
Maximum point rainfall	15	4	2	5	1	1	14	4	2	8	2	1	6	2	1
Areal mean gage values ≥0.01 inch	11	3	2	5	2	1	13	4	2	10	3	1	7	2	1
Target–control															
Areal means ≥0.005 inch	24	7	4	10	3	2	28	8	4	14	4	2	11	4	2
Areal means >0.10 inch	40	11	6	11	4	2	36	11	5	19	5	3	18	5	3
Areal means >1.0 inch	164	48	24	62	18	10	124	37	19	107	31	16	81	25	12
Maximum point rainfall	22	6	4	7	2	1	19	6	3	12	4	2	9	3	1
Areal mean gage values ≥0.01 inch	16	4	3	7	2	1	19	5	3	14	4	4	10	3	2
Random–experimental															
Areal means ≥0.005 inch	54	16	8	22	6	4	64	18	10	32	10	4	26	8	4
Areal means >0.10 inch	92	26	14	26	8	4	82	24	12	44	12	6	40	12	6
Areal means >1.0 inch	375	110	54	142	42	22	284	84	44	244	70	36	186	56	28
Maximum point rainfall	50	14	8	16	4	2	44	14	6	28	8	4	21	6	3
Areal mean gage values ≥0.01 inch	36	10	6	16	4	2	44	12	6	32	10	8	22	6	4

Table 17. A General Comparison of Selected Advantages and Disadvantages of Various Designs

	Advantages	*Disadvantages*
Crossover	1. Uses only experimental data 2. Randomization in design 3. Requires small sample sizes	1. Difficult to position target and control in order to avoid contamination
Continuous-historical (sequential)	**1.** Requires relatively small sample sizes	1. Historical data sample may not be adequate 2. Sequential test is sensitive to trends 3. Lack of randomization may produce bias
Continuous-historical (non-sequential)	1. Requires relatively small sample sizes	1. Historical data sample may not be representative 2. Lack of randomization may introduce bias
Random-historical (sequential)	1. Requires relatively moderate sample sizes 2. Randomization present	1. Historical data sample may not be representative 2. Sequential test is sensitive to trends
Target-control	1. Requires sample sizes smaller than that of random experimental	1. Requires a high degree of correlation between target and control
Random-historical (non-sequential)	1. Randomization present in design	1. Historical data sample may not be representative of experimental period
Random-experimental	1. Only experimental data are used in analysis 2. Randomization is present in design	1. Often requires large sample sizes

Table 18. Statistical Model of 12-Hour Severe Rainstorm and Comparison with 16-17 August 1959 Storm

	Model	*16-17 August*
Squall system orientation in rainstorm zone, *degrees*	255-75	255-75
Orientation of surface rainfall pattern, *degrees*	265-85	280-100
Squall system speed in storm zone, *mph*	9	10
Squall system speed outside storm zone, *mph*	22	27
Number of distinct bursts or storms	5	5
Average frequency of bursts, *hours*	2.4	2.4
850-mb wind	245°, 30 knots	250°, 35 knots
700-mb wind	255°, 30 knots	260°, 30 knots
500-mb wind	270°, 30 knots	270°, 25 knots
Surface dew point, departure from normal, °*F*	+9	+9
Precipitable water, surface to 400-mb, departure from normal, *percent*	+50	+61
Starting time of storm, *CST*	1900	1700
Maximization of storm, *CST*	2130-0330	2300-0500
Maximization point rainfall, *inches*	9.4	10.6
5000 mi^2 mean rainfall, *inches*	4.5	5.9

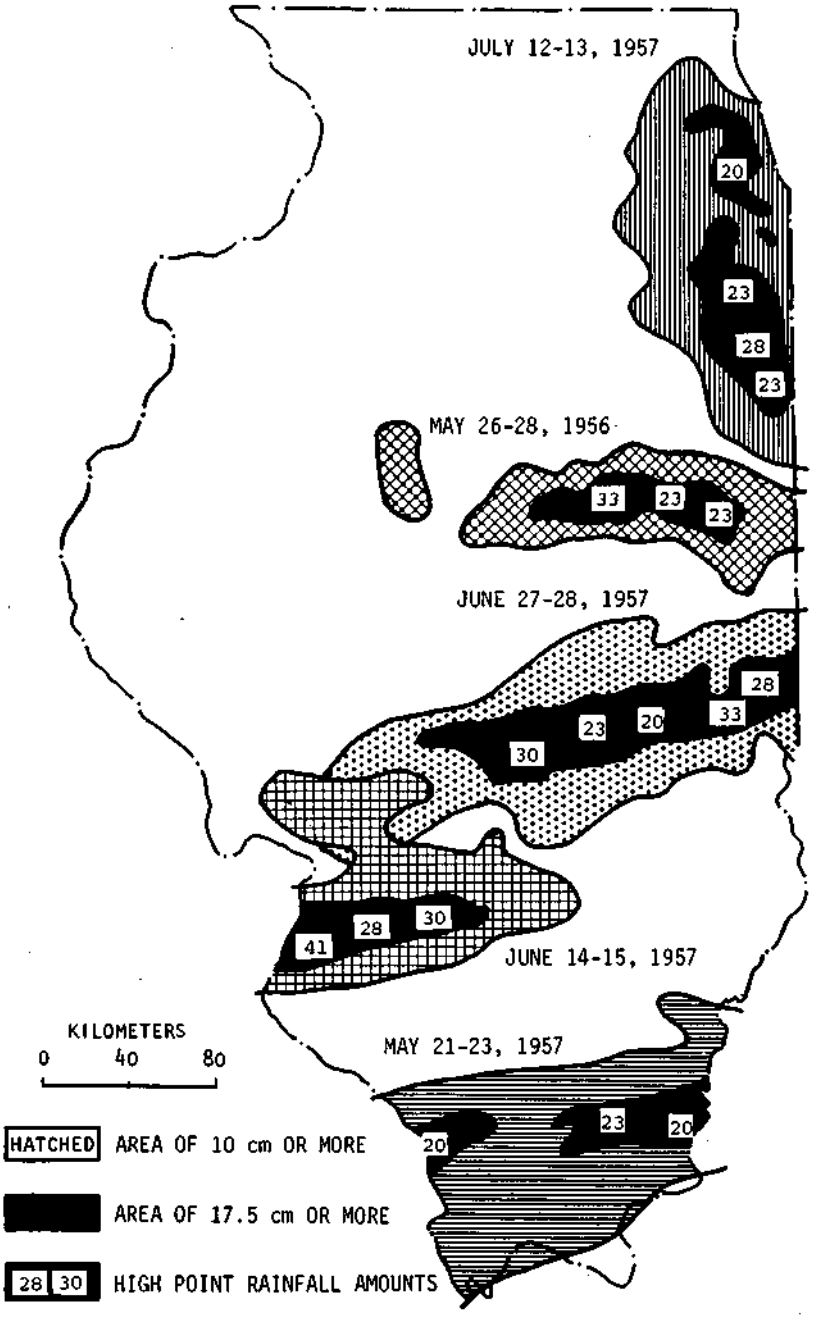

Figure 49. Severe rainstorms during 1956-1957

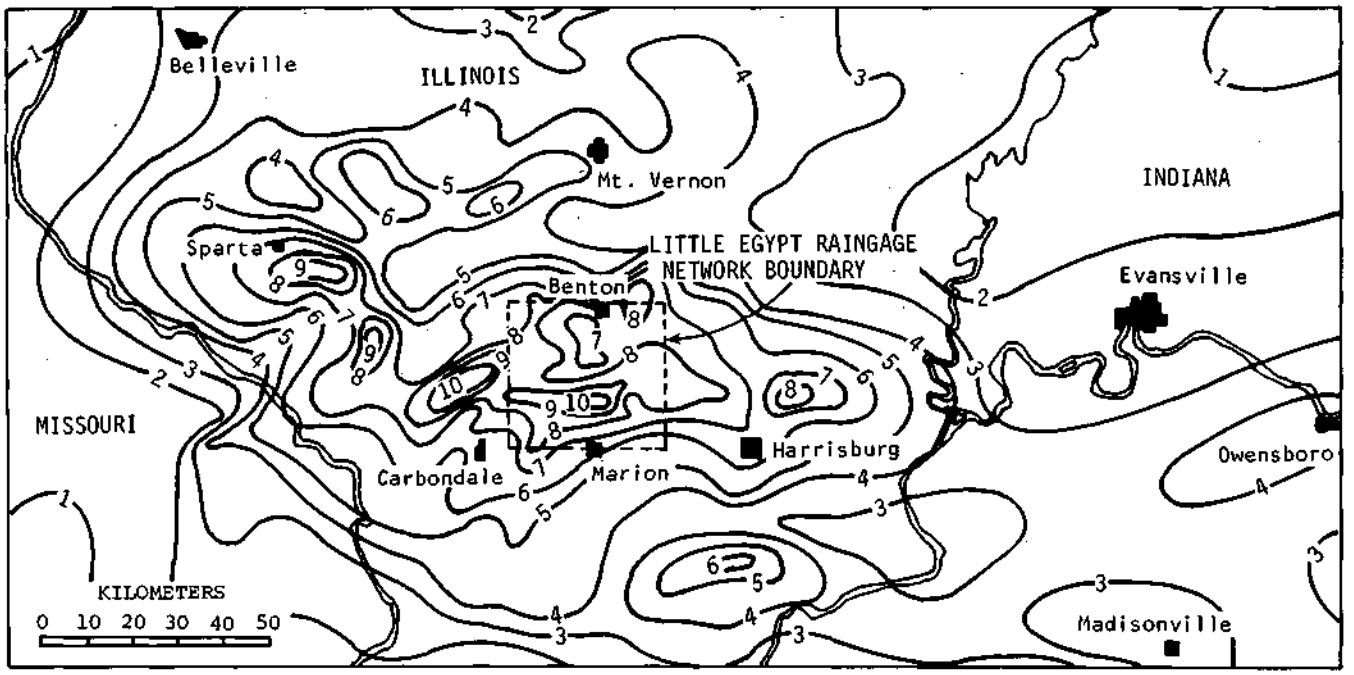

Figure 50. Isohyetal pattern, inches, in storm of 16-17 August 1959

Table 19. Statistical Model of Severe Rainstorms of the Small Type

Characteristic	*Model*
Storm duration, *hours*	4
Starting time of storms, *CST*	1600
Start of heaviest rain, *CST*	1630
Duration of heavy rain, *hours*	3
Area enveloped, km^2	500
Ratio, maximum/mean rainfall	2.30
Orientation of rain pattern	260°-080°
Ratio, major/minor axis of rain pattern	2.20
Number of bursts or merging cells	6
Average frequency of bursts, *hours*	0.50
Most frequent synoptic environment	mT air mass, non-frontal
Movement of convective entities	240°-060°
850-mb wind	240°, 12 knots
700-mb wind	240°, 17 knots
500-mb wind	250°, 22 knots
850 to 500 mb (layer)	245°, 17 knots
Surface dew point departure	+9°F
Precipitable water departure	+20%
Showalter Stability Index	-2
Rain burst interval, *hours*	0.5

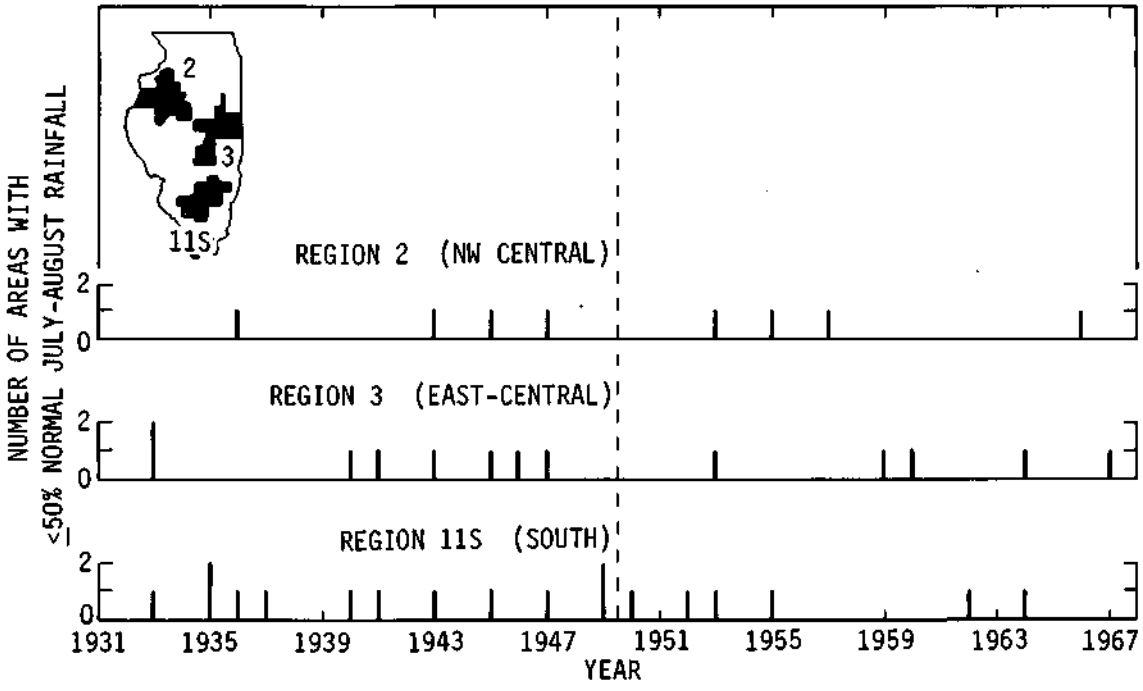

Figure 51. Regional distribution of dry areas

1963). Results from that extensive report have not been included here, largely because more recent studies have concentrated on summer droughts and the potential for precipitation modification during them.

Changnon and Huff (1971) made a climatic study of July-August dry periods in Illinois during the 1931-1968 period. Dry periods (or dry areas) were defined as July-August periods with less than 50% of the normal 2-month rainfall. A total of 75 distinct dry-areas were found in the 38-year study period. The average July-August rainfall in Illinois is 6.4 inches, ranging from 5.9 inches in the south-central area to 8.1 inches in northern Illinois. Fifty percent of normal July-August rainfall in most locations in Illinois ranges from 3 to 3.5 inches.

Certain areal and temporal frequency information on the dry periods (areas) appears in table 20. The annual average value was two dry areas. The yearly distribution of these dry periods indicates that 10 of the 38 years had no dry areas, 21 of the 38 years had two or more dry areas, and 2 years (1953, 1964) had five or more distinctly separate dry areas within Illinois.

The temporal distribution of dry areas for three regions is portrayed in figure 51. The data indicate decreasing frequencies of dry areas with time. For instance, 7 of the 12 dry areas that occurred in Region 3 occurred before the middle of the 1931-1968 period. Two occurred in 1976 and 1977. There has been a lack of any widespread occurrence in recent years. For instance, 1943, 1945, 1947, and 1953 had dry areas in all three regions, (figure 51), but no comparable widespread dry area has occurred in three regions since 1953.

The centers of dry areas in the three crop-weather regions are illustrated in figure 52. Placement of these annual values (lowest rain) reveals that even within the three regions, areas of extreme dryness seem to be non-randomly distributed. For instance, in Region 3 most of the driest areas were in the northeast or extreme so"uthwest. Half of the 12 dry periods in Region 3 occurred in the 1940-1947 period.

To investigate the possibility of detecting (and predicting) July-August dry periods (areas), the amounts of rainfall in the July 1-15 period for the 75 dry areas were calculated. Averaging of 75 regional percentages for July 1-15 rainfall indicated a mean value of 37% (about 0.6 inch) of normal. Rainfall in the July 1-15 period (of July-August dry periods) was 50% or less in 52 (70%) of the 75 dry periods. Prior rainfall in July 1-15 exceeded 100% of normal in only two dry periods. A second

Table 20. Statistics on Dry Areas (≤50% of Normal Rainfall) in July-August Period of 1931-1968

Frequency of areas	
1. 38-year state total	75
2. Annual average	2
3. Number of years in Illinois with	
No dry areas	10
1 or more	28
2 or more	21
3 or more	14
4 or more	9
5 or more	2
Sizes ofindividual areas (mi^2)	
Average	1,461
Median	435
Largest	19,200
Smallest	45
50% occurred in range between 240 and 960 mi^2	

study using long-term data from four stations revealed that only 23% of all July 1-15 periods with rain ≤37% of normal (the average for all 75 dry periods) were associated with July-August dry periods (totals ≤50%). Thus, it is not a good predictor.

The median size (table 20) of dry areas of 435 mi^2 is just slightly less than the average size of an Illinois county which gives some perspective as to the smallness of the typical July-August dry area. The largest dry area of 19,200 mi^2 occurred in 1936. This area represents 34% of the total state area, whereas the median dry area is slightly less than 1% of the total state area.

The areal distribution of the July-August dry areas based on the number of times each county was either partially or totally within a dry area was tabulated and iso-frequency lines are shown in figure 53. Inspection reveals that the highest frequency of dry areas is across southern Illinois with isolated high frequencies in western and east central Illinois.

The frequency of rain days during July-August dry periods is shown in table 21, expressed as a percent of average. Point averages are 6 days in July-August with ≥0.1 inch, 4 days with ≥0.25 inch, and 2.5 (5 days in 2 years) of ≥0.5 inch. The mean and median percentages of the averages for both the 0.1-inch and 0.25-inch classes were above normal. However, these were below normal for the 0.5-inch rain-day averages. The number of the 75 dry-area averages that were above 100% of the

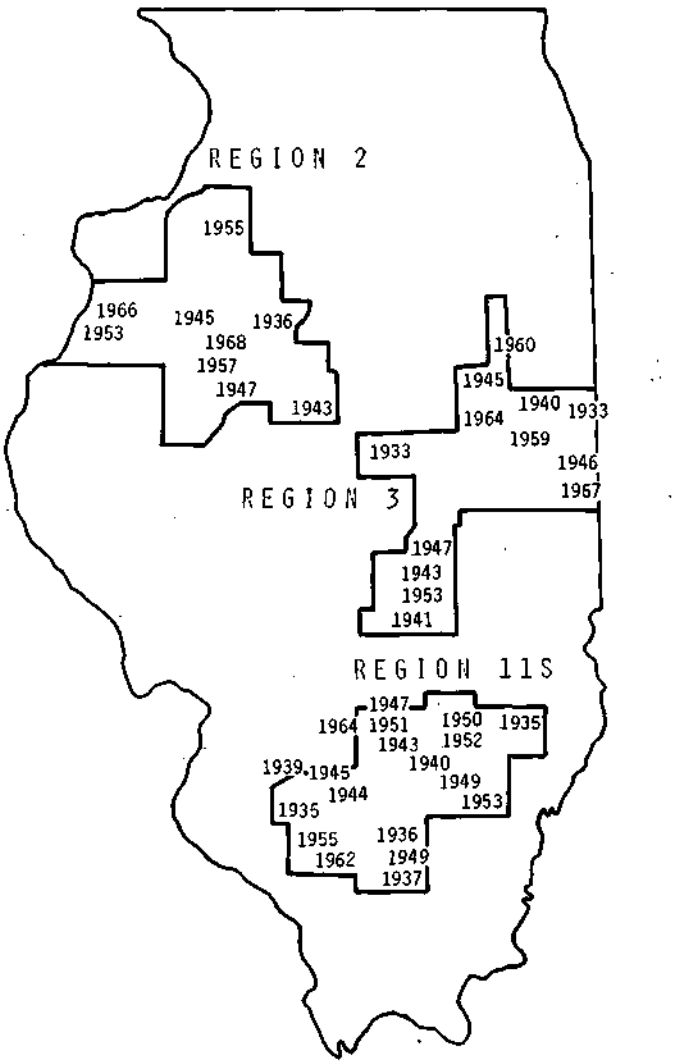

Figure 52. Dry-area centers within Crop Regions 2, 3, and 11S, 1931-1968

long-term normal, and the number that were equal to or less than 100% of normal are also shown in table 21. Fifty of the 75 dry areas had 0.1-inch frequencies that were above 100%, whereas 72 of the 75 dry areas had frequencies of 0.5-inch rain days that were 100% or below. The results suggest that there is no lack of light rainfall days in dry areas, but there is a distinct lack of 0.5-inch rain days, a condition noted in another study of Illinois droughts (Huff and Changnon, 1963). The occurrence of July-August dry areas is related to the lack of moderate to heavy rainfall days but does not seem to stem from a lack of rain conditions.

Huff and Vogel (1977) made an extensive 2-year study of Illinois precipitation droughts which has

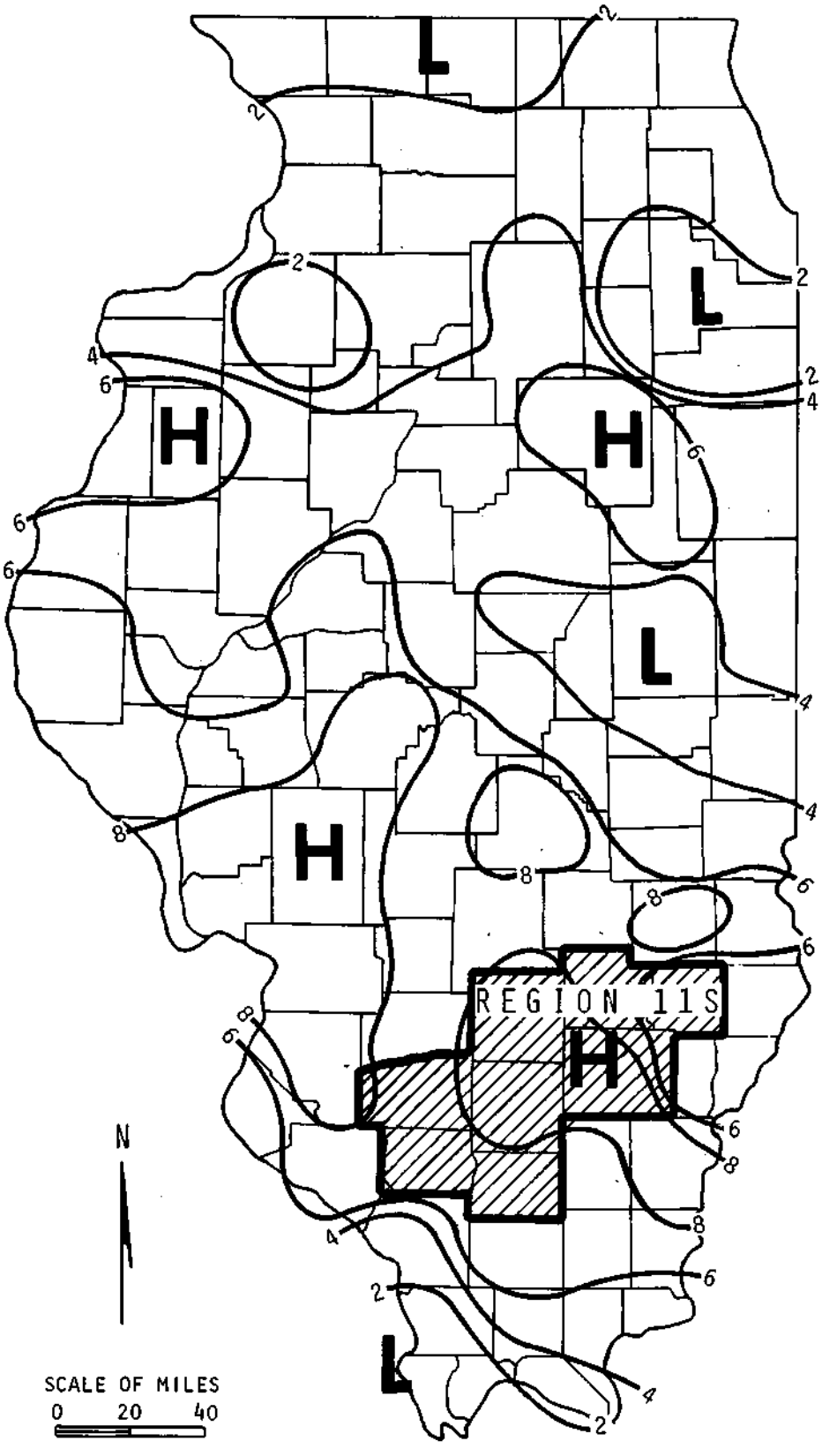

Figure 53. Frequency distribution of July-August dry areas per county, 1931-1968

Table 21. Rain-Day Frequency Information for 75 July-August Dry Areas (≤50%of Normal Rainfall), 1931-1968

	≥0.1 inch per day	≥0.25 inch per day	≥0.5 inch per day
Mean (%) of 75 dry-area averages	122	105	69
Mean (%) of 75 dry-area averages	120	111	89
Number times dry-area average >100% of normal	50	37	3
Number times dry-area average ≤100% of normal	25	38	72

Table 22. Average Percent of Normal Rainfall in July-August Droughts Grouped by Synoptic Type and Section of Illinois

	Percent of normal rainfall for given storm type				
Synoptic type	North section	Central section	South section	Multiple section	Combined sections
Cold front	63	59	73	65	65
Warm front	11	8	4	1	6
Static front	48	32	23	19	30
Occluded front	15	0	0	120	13
Air mass	9	9	22	0	13
Lows	86	31	51	43	50
Number of droughts	8	12	12	3	35
Number of storms	127	166	157	42	492

provided basic background information for evaluating weather modification potential in droughts of various intensity and areal extent. Selected results have been chosen to illustrate key features of these phenomena. Figure 54 presents examples of typical July-August drought patterns in various parts of the state. These reflect the types of drought conditions most apt to occur and those that future weather modification efforts must address. There are portions of the drought areas that tend to have non-drought rainfall.

From the standpoint of weather modification, it is apparent from table 22 that the greatest contribution to alleviating agricultural water shortages would come from successful treatment of cold front storms. Conversely, enhancement of non-frontal storms (air mass) would normally contribute little precipitation during drought periods. For example, air mass storms normally contribute 17% of the July-August rainfall in Illinois. However, in summer droughts, they average only 13% of their normal production. Average July-August rainfall in Illinois is approximately 6.5 inches, and air mass storms normally produce 1.1 inches. Multiplying the air mass normal (1.1) by 13%, shows only 0.14 inch would occur, on the average, in droughts. If one enhanced air mass rainfall by 50% in droughts, the July-August average would only increase 0.28 inch, producing an insignificant effect on crop production. Moderate increases of 20% through modification would increase the cold front total in average Illinois drought conditions to 2.0 inches which is 78% of the summer normal from this storm type. The foregoing example emphasizes the need to successfully treat cold frontal storms and other organized storm systems if substantial contributions are to be made in alleviating agricultural water shortages in Illinois and the Midwest.

As part of the Huff-Vogel (1977) research on droughts and weather modification, studies were made of clouds and various upper air parameters in Illinois. The primary purpose was to ascertain whether differences occurred in the characteristics of clouds, temperature, and moisture conditions between wet and dry periods. In the cloud studies, the frequency in areal coverage of cumulonimbus and middle clouds was determined to provide indices of the cloud activity under various degrees of normality of monthly precipitation. Altocumulus and alto-

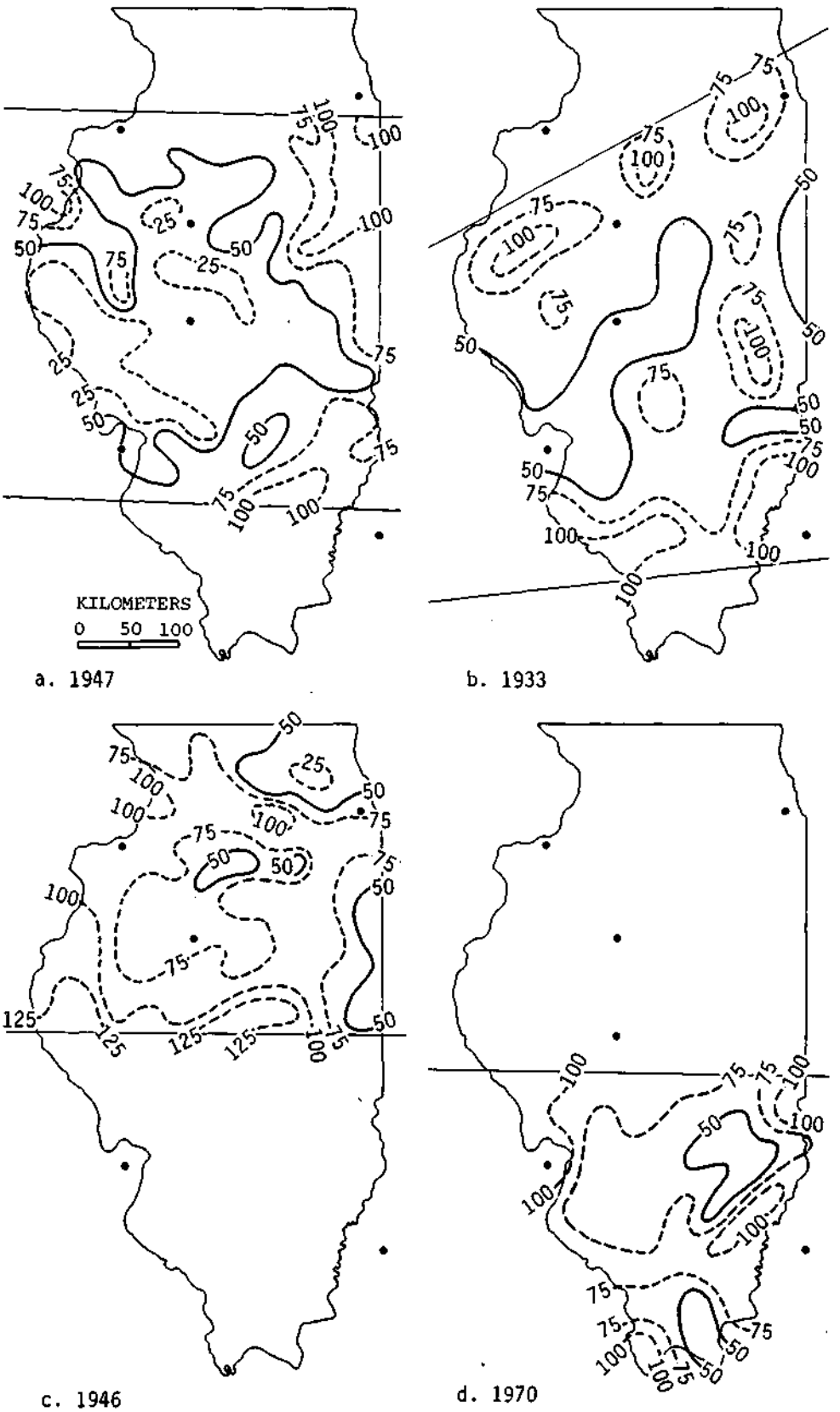

Figure 54. Examples of typical July-August drought patterns

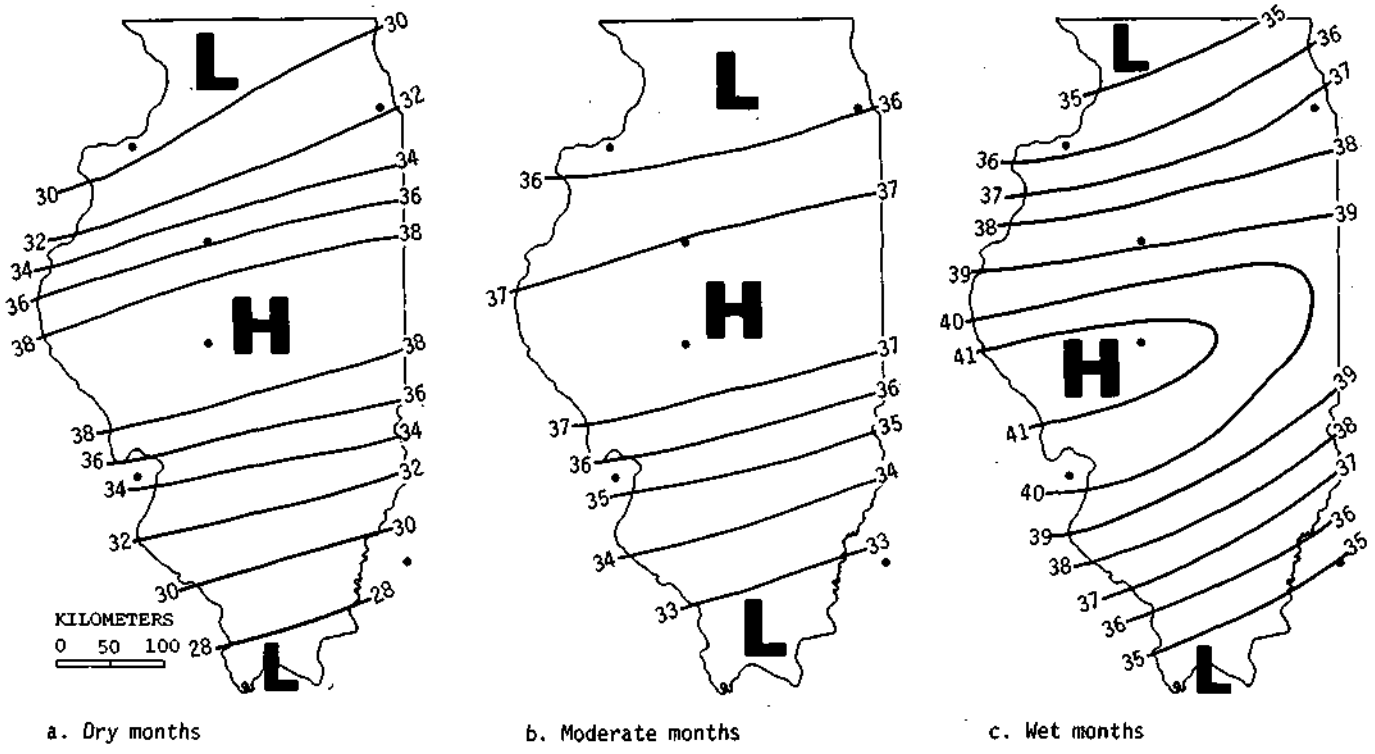

Figure 55. Monthly percentage frequency of middle cloud sky coverage during July-August, 1951-1964

stratus coverages were chosen to serve as an index of historical middle-level moisture conditions. As shown in figure 55, the areal differences in middle clouds were small between wet and dry periods. The greatest frequency of these clouds was found to occur in central Illinois. Analyses of the diurnal distribution of cumulonimbus (*see* figure 72) also showed that rain-producing clouds occurred most frequently during the night (1800-0600 CST), which compares favorably with findings on the nocturnal thunderstorm maximum. Basically, no strong relationship was established between the normality of precipitation and various upper-air parameters. These results are not really suprising, and tend to support the premise that the *synoptic-scale and meso-scale dynamics of the midwestern atmosphere exert a strong control over the initiation and then the intensity of convective precipitation.*

Relationship of Atmospheric Moisture and Precipitation

One of the initial research efforts of the Water Survey scientists concerned delineation of the hydrologic cycle in Illinois. The values resulting from a variety of studies are shown in figure 56 (Changnon, 1958). Shown are the average daily values of all phases of the hydrologic cycle. Important to precipitation and its modification is the fact that the atmospheric moisture of 2000 billion gallons a day (bgd) passes over the state and only 100 bgd, or 5% of the total moisture, is precipitated in Illinois. Furthermore, nearly three-fourths of the amount of precipitation is returned to the atmosphere through transpiration and evaporation. Hence, only 1 to 2% of the total atmospheric moisture passing across Illinois is retained in the state as streamflow or groundwater. Thus, 10 to 30% rain increases in the 100 bgd is small in relation to the total atmopheric reservoir. This does show that the atmosphere is basically very inefficient in the production of precipitation over large areas of the Midwest. It suggests that increasing precipitation efficiency should not seriously deplete the atmospheric moisture supply. This is not to say that other effects beyond the seeded area would not occur, but in general, the atmospheric moisture supply is large.

Huff (1963) made an extensive study of atmospheric moisture and its relationship to precipitation in Illinois. Figure 57 presents patterns of the average depth of precipitable water during January and July showing an average depth of 1.4 inches in central Illinois during July. Figure 58 presents

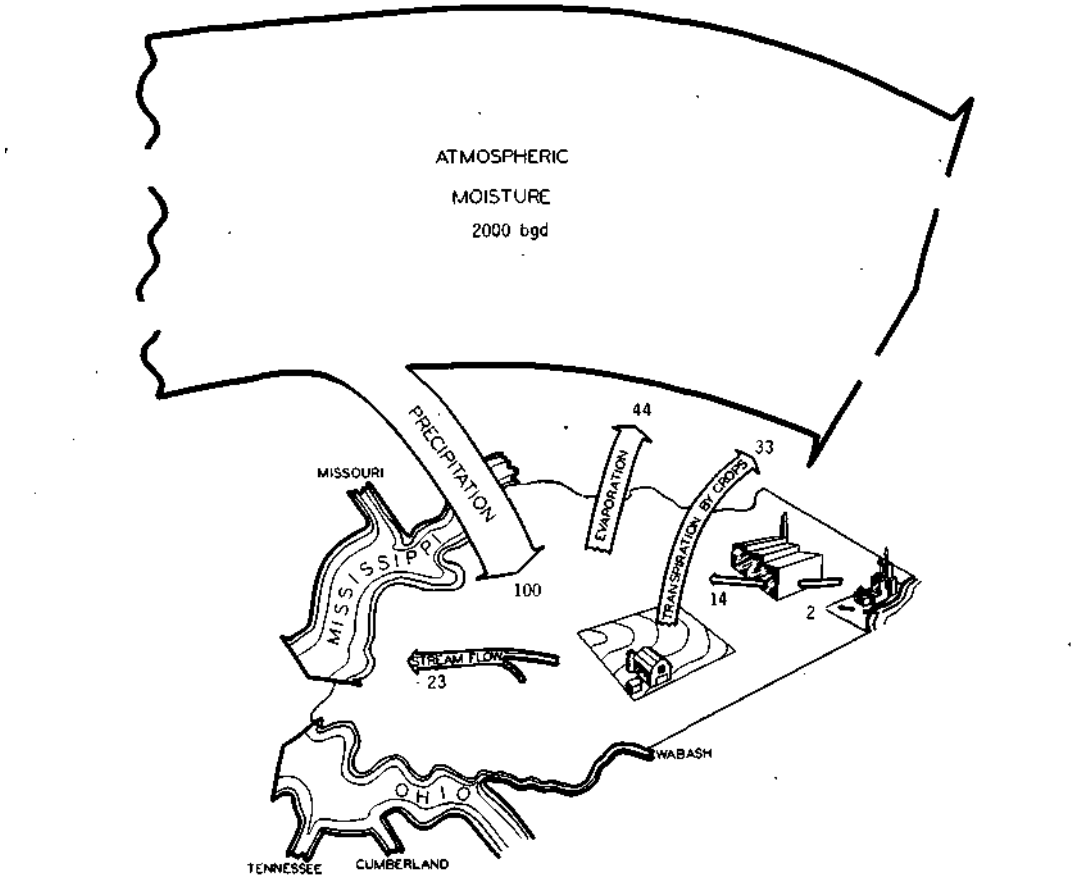

Figure 56. Hydrologic cycle for Illinois

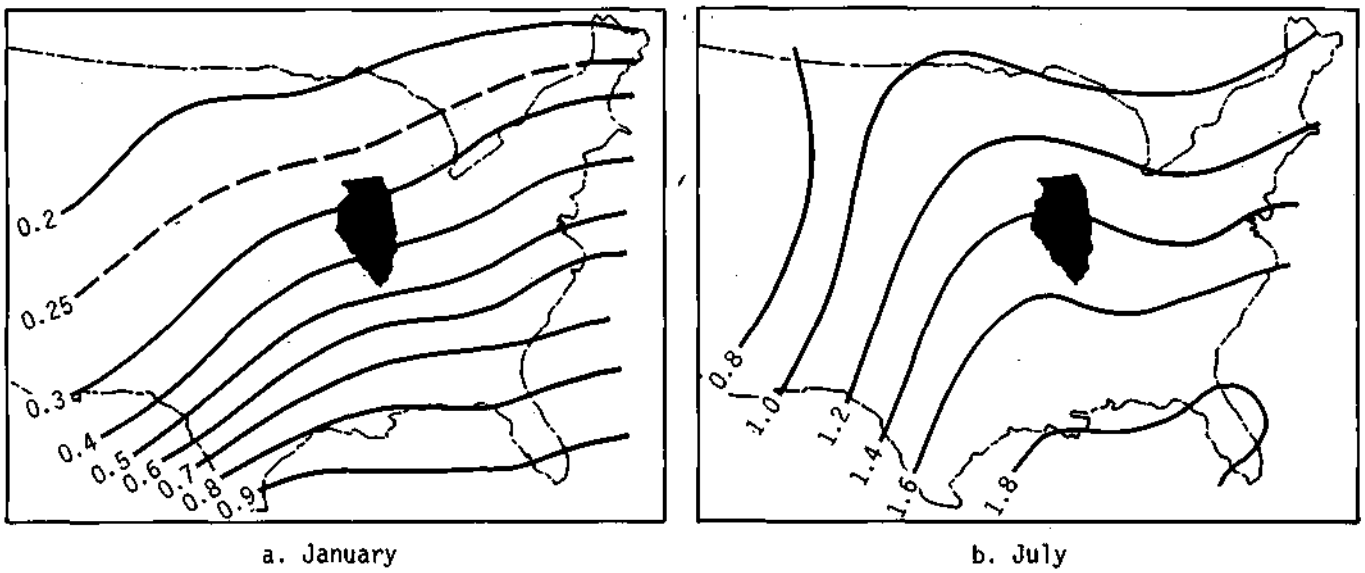

Figure 57. Average depth of precipitable water, inches, during (a) January and (b) July

mean monthly precipitable water (solid lines) and the average monthly precipitation pattern across the state. In general, precipitable water exhibits a latitudinal distribution as does precipitation in most months, except in summer when the rain pattern tends to be flat with slightly more in the western portions of the state.

Table 23 shows the distribution of precipitable water by layers by months and on an annual basis. This reveals that a goodly portion, 51%, of precipitable water is in the lowest 5000 feet of the atmosphere during July.

The percentage of available moisture precipitated to the surface as rain or snow is, on the average, greatest in the spring and least in summer and winter. The mean value was 5.6% with 70% of the monthly values falling in the range of 3 to 7%. The mean annual percentage precipitated showed little variation in the 3-year study period (1946-1948) ranging from 5.1 to 5.9%. During the 7 months when the precipitation was more than 1 inch above normal, the average amount precipitated was 8.8%, compared to 2.7% in the 7 months when precipitation was more than 1 inch below normal.

In another study (Huff, 1963), analyses were made of the atmospheric moisture on days with heavy rainstorms and widespread rainfall in Illinois, when the efficiency of precipitation production should be relatively high. Huff found that the percentage of inflowing moisture precipitated to the surface as rainfall averaged 17% with a range from

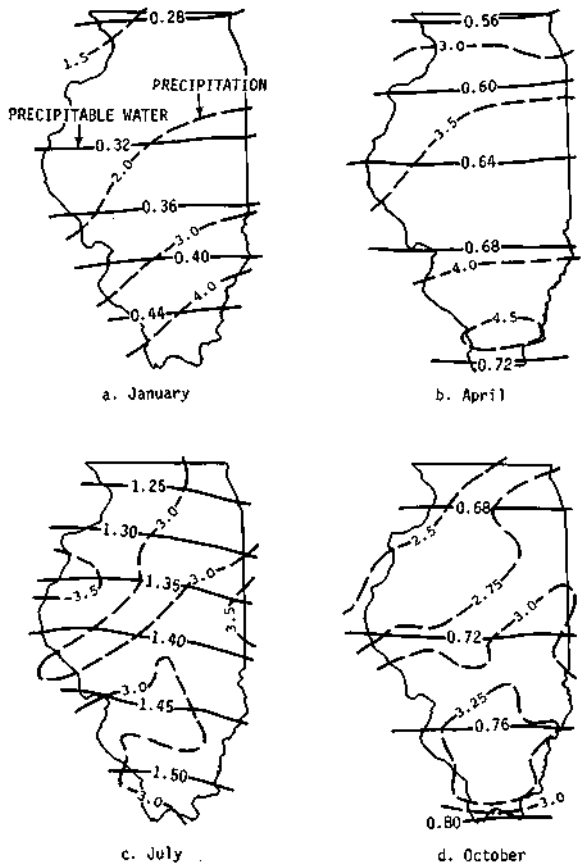

Figure 58. Mean monthly precipitable water and precipitation in Illinois, inches

10 to 25% on 14 very heavy rain days. Thus, even under optimum conditions, only a relatively small

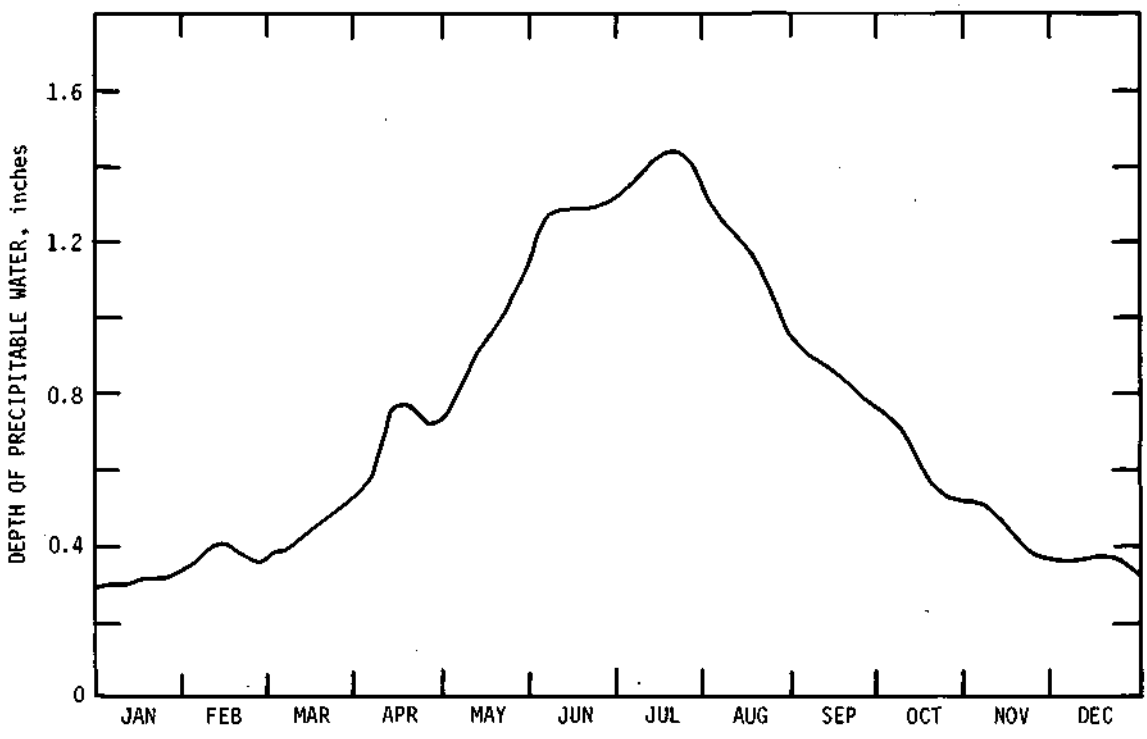

Figure 59. Fourteen-day moving averages of precipitable water in central Illinois

percentage of the available atmospheric moisture is used in producing surface precipitation.

Figure 59 shows the seasonal values of precipitable water in central Illinois, reaching the peak during the summer months. The Huff study also furnished information on the probability distribution of departures from normal precipitable water in Illinois (figure 60).

Figure 61 presents the mean monthly precipitable water value and those computed for days with rainfall of 0.1 inch and 0.5 inch. The data are based on radiosonde values at Rantoul and Peoria in central Illinois and, as expected, there is a greater average depth of precipitable water on rainy days. Precipitable water in summer does not apparently account much for the difference between rain days of 0.1 and 0.5 inch.

Table 24 presents correlation coefficients ob-

Table 23. Distribution of Precipitable Water by Layers

Layer, feet	*January*		*July*		*Annual*	
	(inches)	*(percent)*	*(inches)*	*(percent)*	*(inches)*	*(percent)*
Surface-5,000	0.14	44	0.71	51	0.36	49
5,000-10,000	0.10	31	0.41	30	0.22	29
10,000-15,000	0.06	19	0.19	14	0.12	16
15,000-25,000	0.02	6	0.07	5	0.04	6

Table 24. Correlation between Monthly Mean Precipitation and Atmospheric Moisture Factors

Atmospheric moisture factors	*Correlation coefficient*	*Coefficient of determination, percent*
Average depth of precipitable water	+0.40	16
Total moisture inflow	+0.55	30
Percentage of total moisture precipitated	+0.74	55

tained for monthly mean precipitation and atmospheric moisture factors. These include the average depth of precipitable water, total moisture inflow, and percent of the moisture precipitated. These reveal that precipitable moisture indices explain anywhere from 16 to 55% of the monthly mean precipitation.

Synoptic Weather Typing

A variety of Water Survey studies have focused on the typing of weather systems, particularly as they relate to precipitation. One study (Morgan et al., 1975) was based on 10 years of data and the surface weather maps as measured at 0600 CST. Figures 62 through 65 present cold-frontal and squall line patterns for the four warmest months of the year in the United States. The patterns are based on the number of frontal occurrences on 60 by 60 nautical mile grid squares. Examination of the cold front maps shows that Illinois is in a low

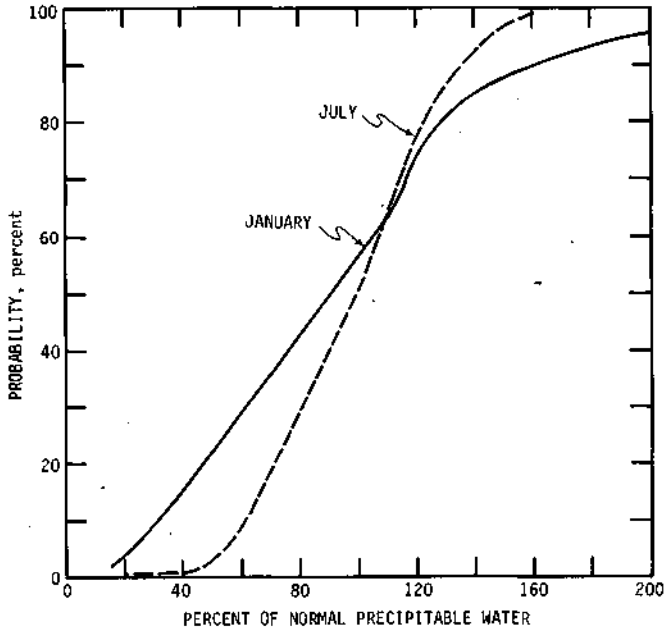

Figure 60. Probability of departures from normal precipitable water in Illinois

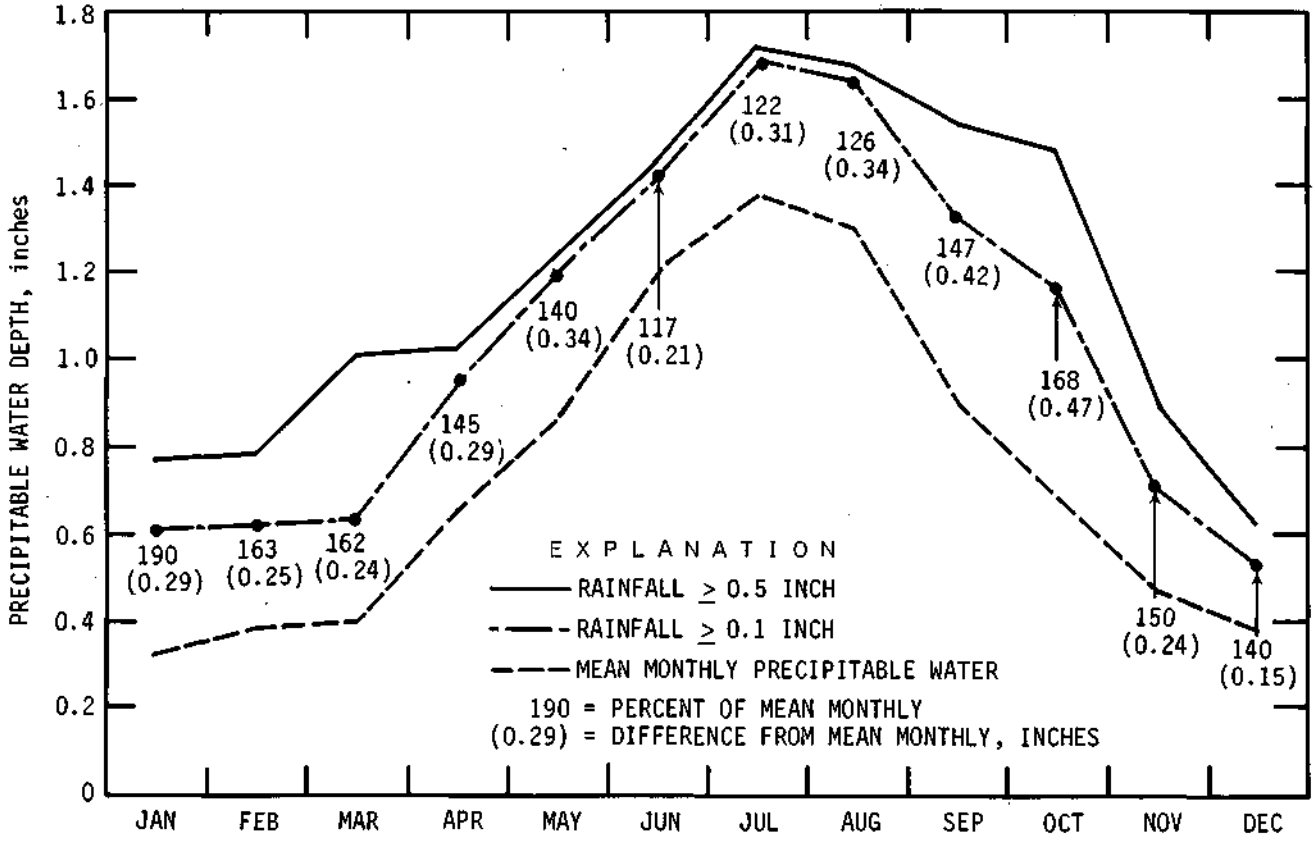

Figure 61. Comparison between monthly mean precipitable water and precipitable water on rainy days in Illinois

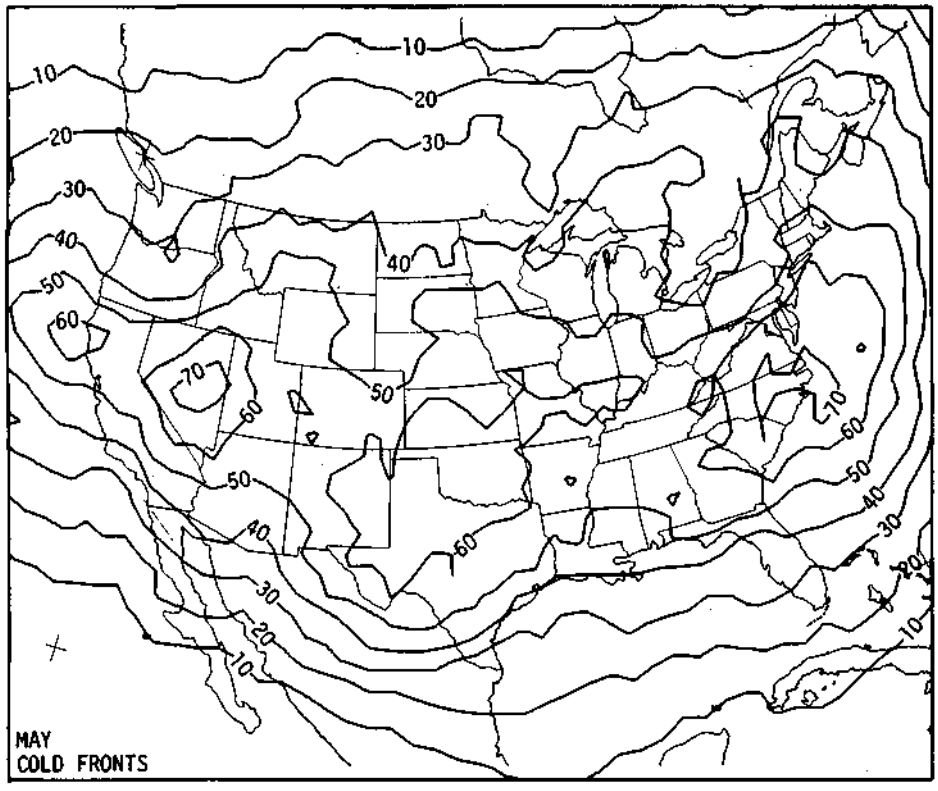

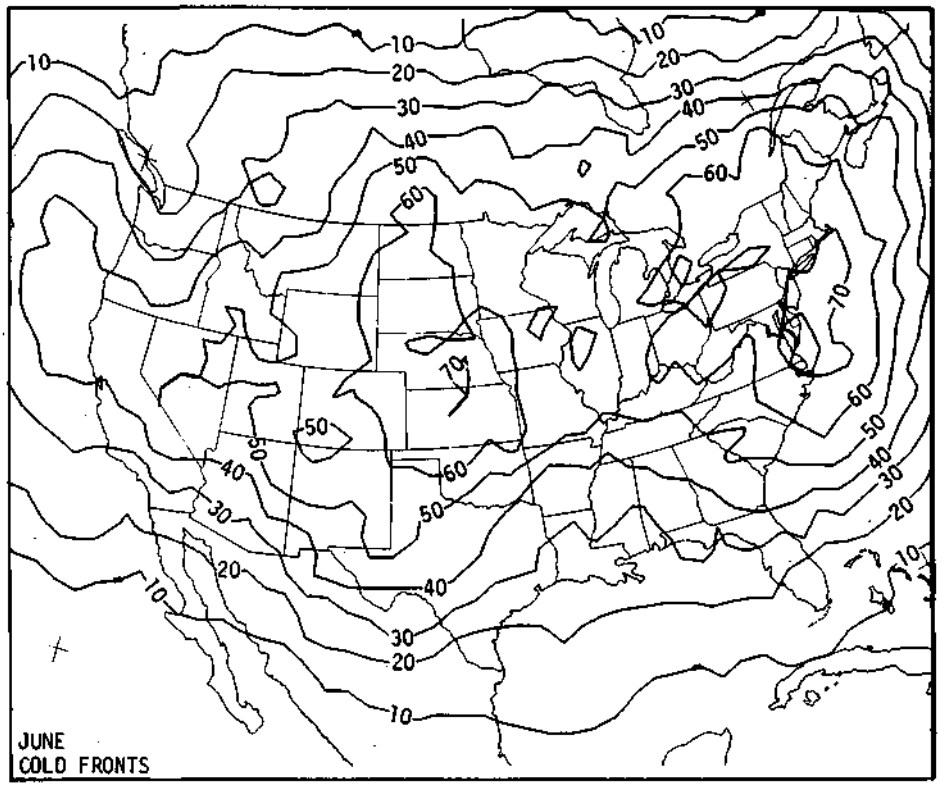

Figure 62. Number of days with cold fronts in 10 years in May and June

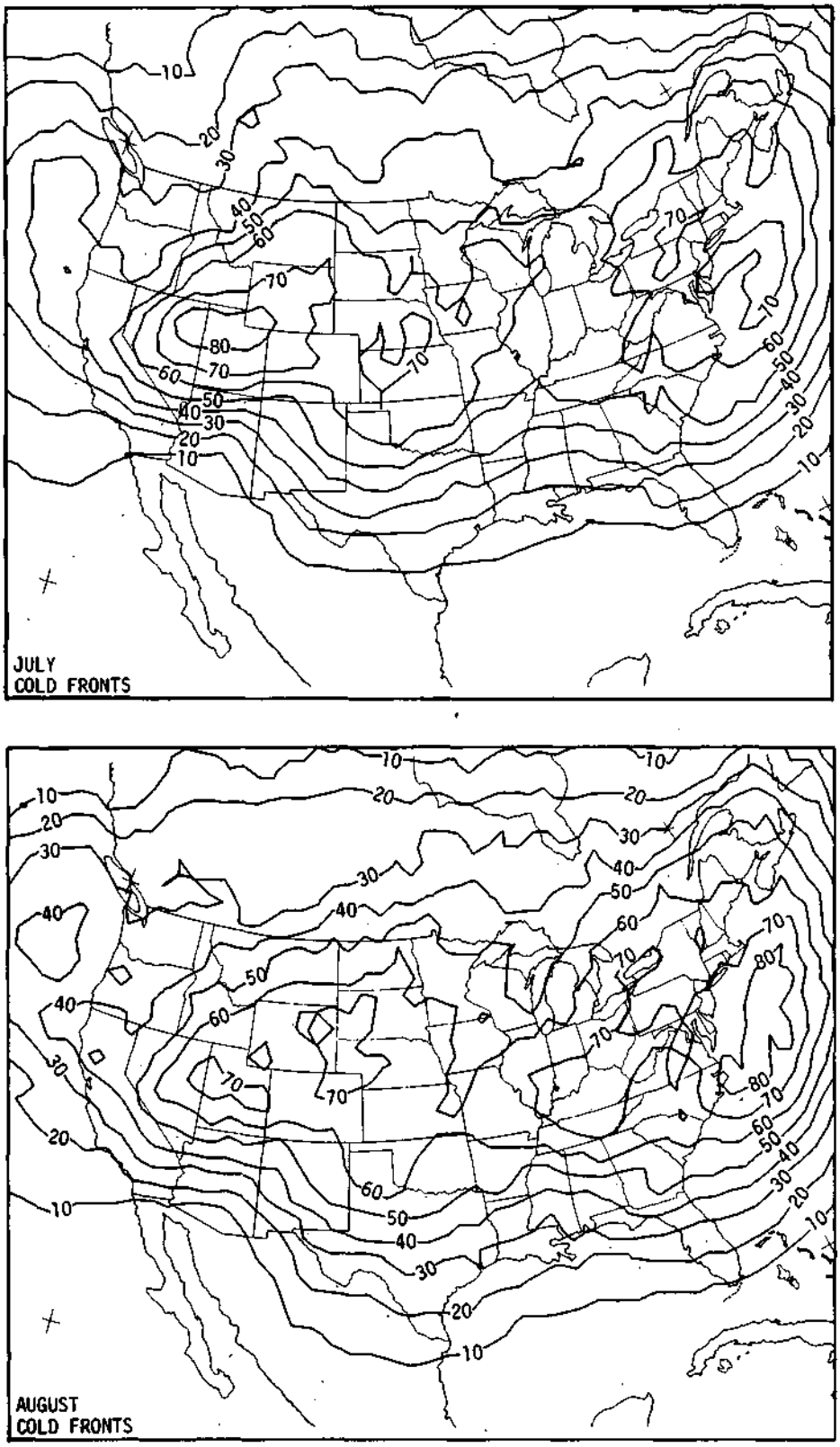

Figure 63. Number of days with cold fronts in 10 years in July and August

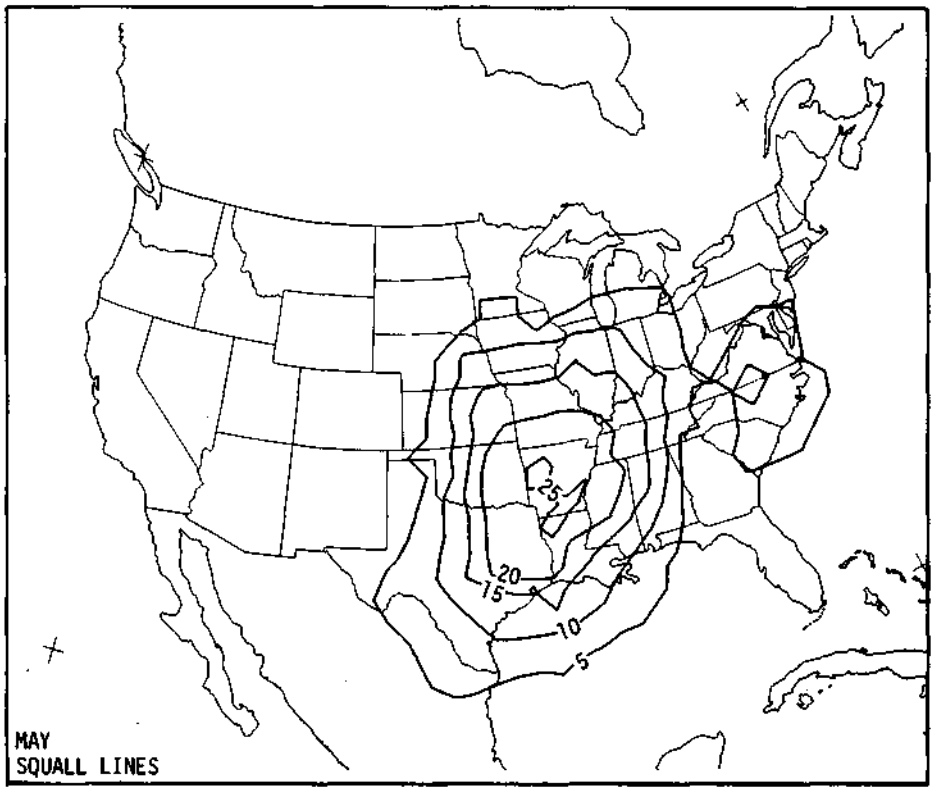

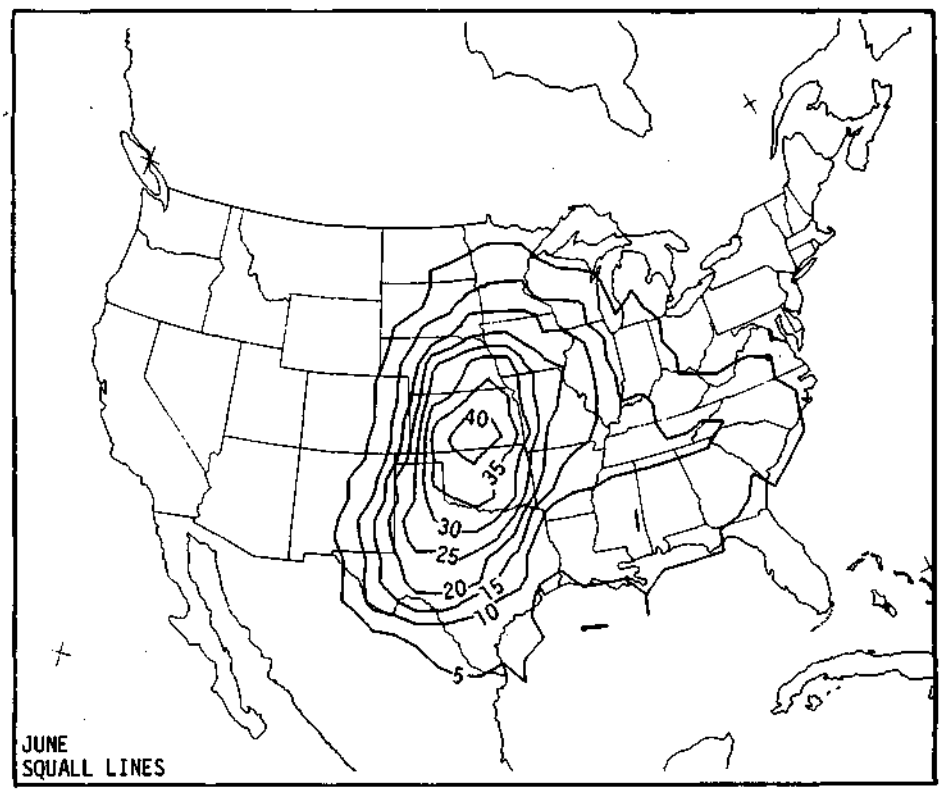

Figure 64. Number of days with squall lines in 10 years in May and June

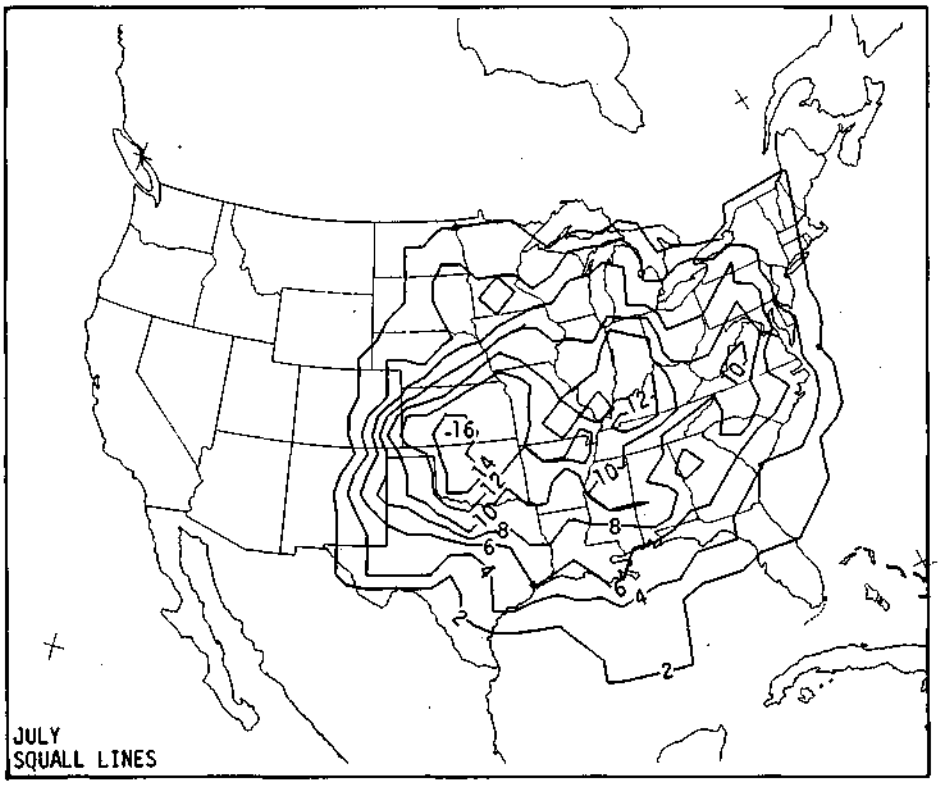

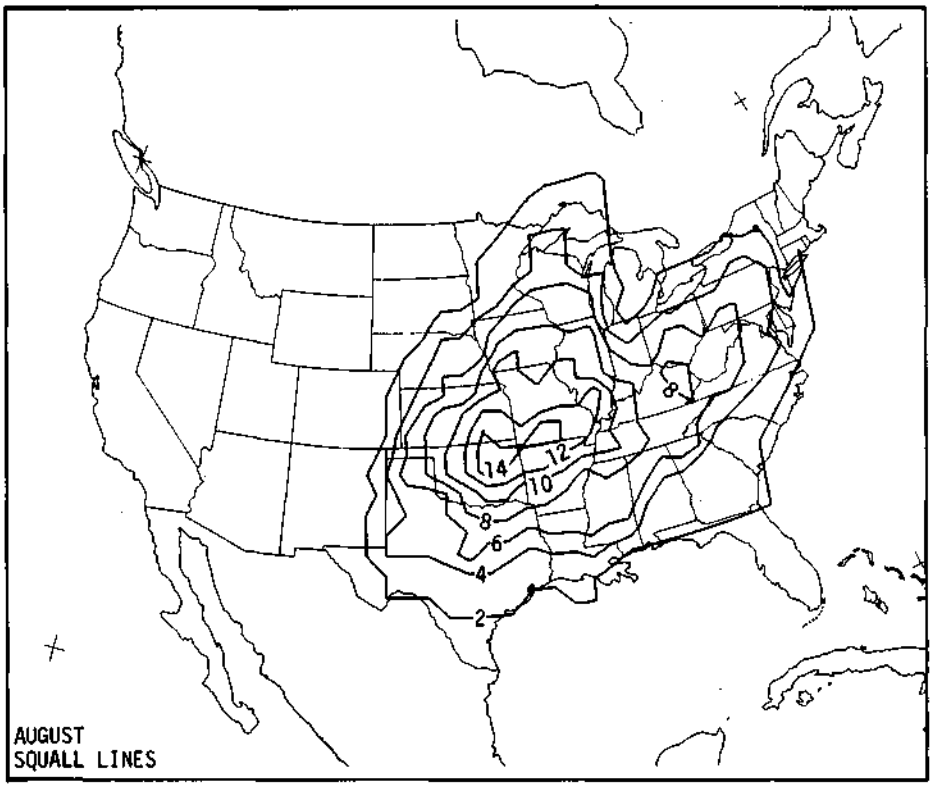

Figure 65. Number of days with squall lines in 10 years in July and August

in June, with areas of less than 50 days in north central Illinois, but growing to 60 (6 per year) in west central Illinois in July, and 70 in August.

Another important study conducted by Survey scientists was that done by Chiang (1961). Chiang used the standard surface and upper-air maps (1 per day) and a grid of 60 by 60 miles to study the frequency of fronts, air masses, and low and high pressure centers in and around Illinois during a 15-year period, 1945-1959. The 15-year frequency of all types of fronts is shown in figure 66. It reveals a maximum of frontal activity across south-central Illinois, and a minimum from western to northeastern Illinois. Figure 67 presents the frequency (per 625 mi^2 area) of summer fronts of varying types. For example, cold fronts were at a maximum in east-central Illinois with greater than 50.

Figure 68 presents patterns of the percentage frequencies of cP and mT air masses for the summer months. Inspection of the July pattern reveals that cP air masses represent 60% of those in northern Illinois, decreasing to less than 3 5% in extreme southern Illinois, with a reverse pattern for the mT air masses. In central Illinois, these air masses are equally likely during most summer months.

Figure *69* presents the frequency of high and low pressure centers per grid square during summer over the 15-year period. A center was counted only if a closed isobaric center was present, and it was then assigned to the grid square having the lowest or highest pressure within its boundaries. The frequencies of highs and lows are both relatively high in central Illinois. Chiang summarized his work with the patterns shown on figure 70. They are based on the frequency distributions of the fronts, high and low pressure centers, and typical air masses. In central Illinois (Region 5) we find frequent occurrences of fronts and of highs and lows, with the average ratio of continental to maritime air of 1.1.

Huff (1971), in a study of the diurnal distribution of precipitation, also presented results on frontal distributions in central Illinois. Figure 71 presents seasonal curves based on the frontal distributions passing through Urbana over a 30-year period. The annual curve shows excellent correspondence between the maximum and minimums of both fronts and precipitation. If these relations are true, it appears that the diurnal distribution of precipitation in central Illinois is attributable to three factors: 1) the nocturnal thunderstorm mechanism, 2) the frontal distributions (showing the double nocturnal maximum), and 3) the diurnal heating effect. The frontal distributions and nocturnal thunderstorm mechanisms may account largely for the night and early morning maximums, and the daytime heating for the afternoon and early evening maximums of precipitation. Of importance to summer weather modification operations is the lack of frontal frequencies during the 1200 to 1800 period.

Hiser (1956) made a study of the precipitation related to six major weather types at four Illinois first-order stations during a 10-year period. Precipitation was classified according to its source conditions including 1) cold front, 2) warm front, 3) stationary front, 4) squall line, 5) warm air mass, and 6) cold air mass. The warm air mass type was defined as that occurring within the warm sector in the absence of fronts. It typically included thermal convection in nocturnal showers usually with a trough aloft. A cold air mass type occurred in the cold air masses after the passage of the cold front, but was distinctly separated from the front by a zone of that precipitation, and normally represented instability showers. Tables 25 and 26 present the type distributions for each month at Springfield and for summer at three other stations, based on a 10-year period. Shown for Springfield, which is most typical of central Illinois, are the monthly amounts of precipitation with each weather type and the frequency of these events. This allows calculation of the average rainfall per event. Inspection of the summer (June, July, August) values shows that cold fronts, squall lines, and warm air masses were the major producers of rainfall. Calculation of the average precipitation per event for summer shows that the average rainfall from squall lines was 0.39 inch compared to 0.36 inch with cold fronts, and 0.30 inch with warm air mass conditions. Stationary fronts which were less frequent produced the highest yield per event, 0.51 inch. In the typing system used here, warm air mass storms would include some organized storm events in addition to the usual unorganized, scattered showers.

Huff and Vogel (1977) in a study of Illinois droughts made an investigation of the synoptic

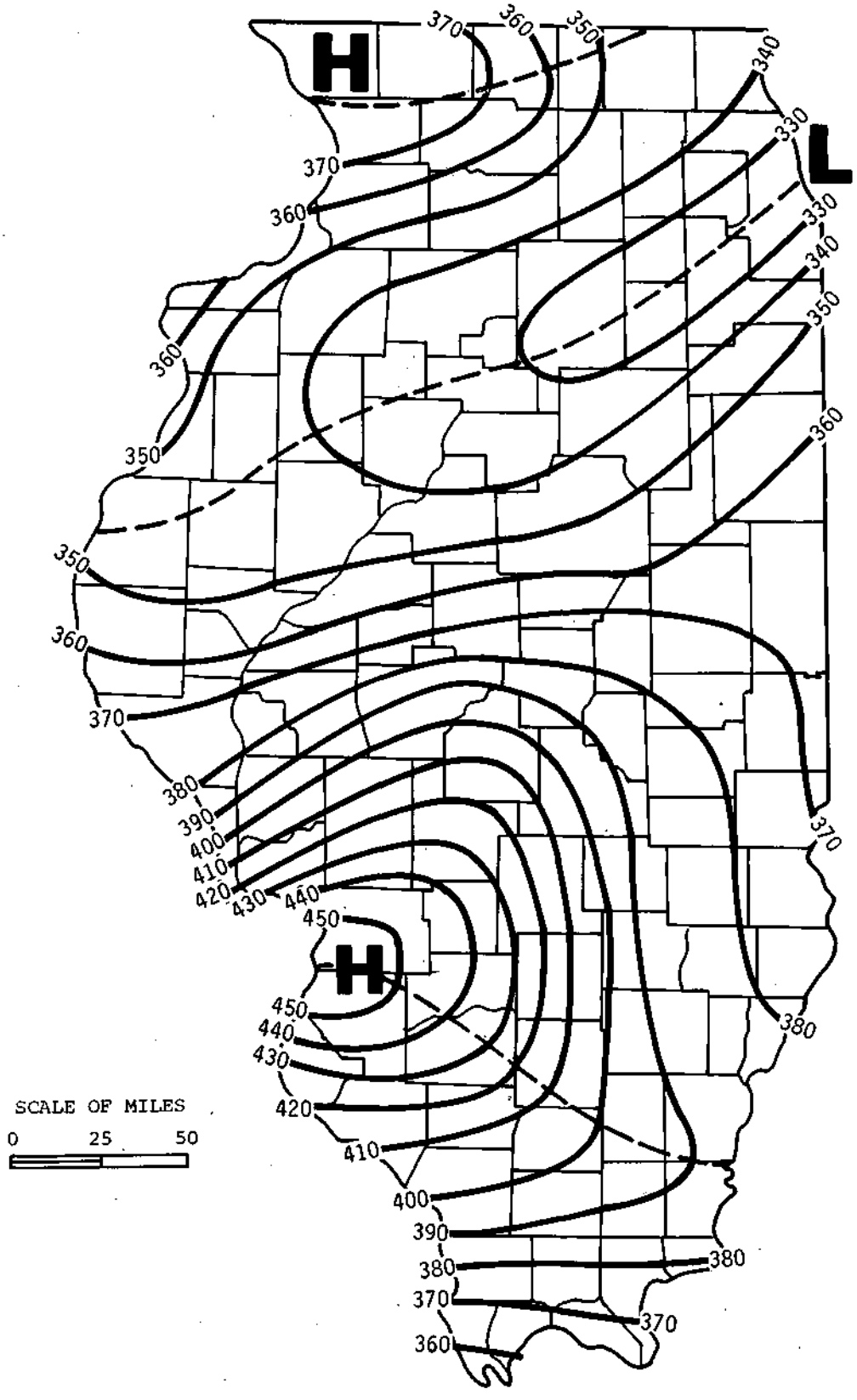

Figure 66. Frequency of all types of fronts, 1945-1959

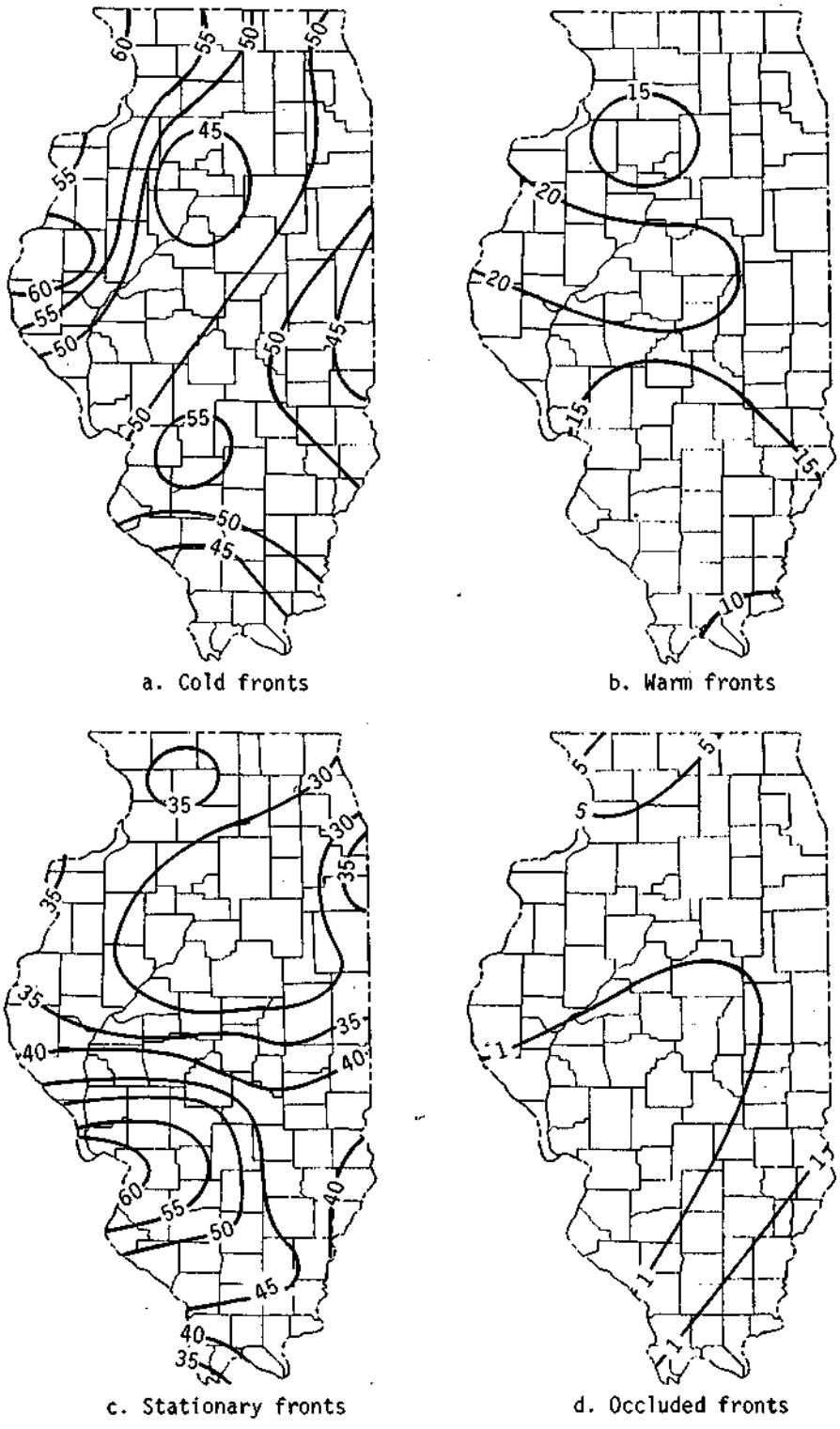

Figure 67. Frequency for summer of cold fronts, warm fronts, stationary fronts, and occluded fronts, 1945-1959

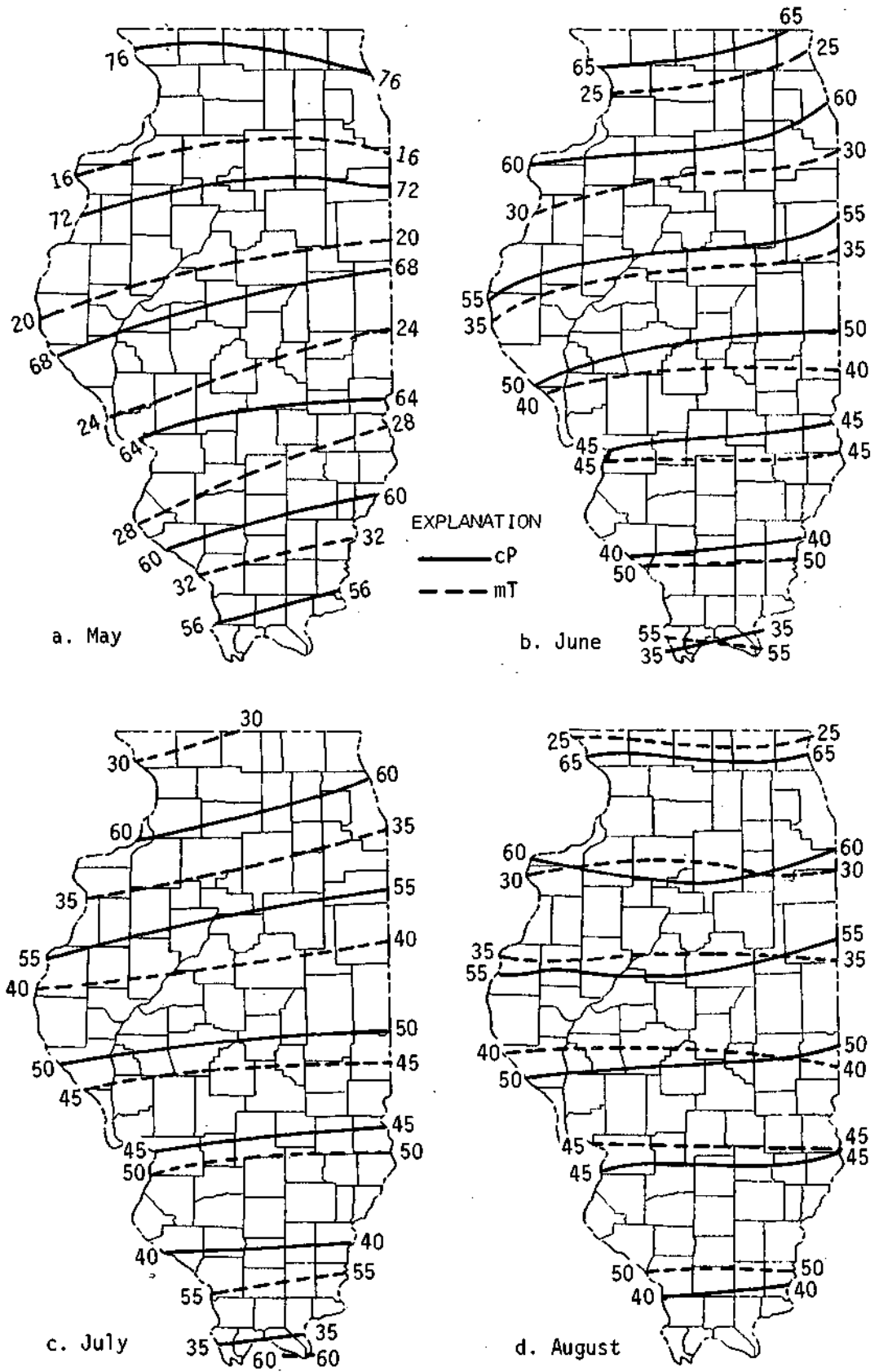

Figure 68. Percentage frequency of cP and mT air masses for May, June, July, and August in Illinois, 1945-1959

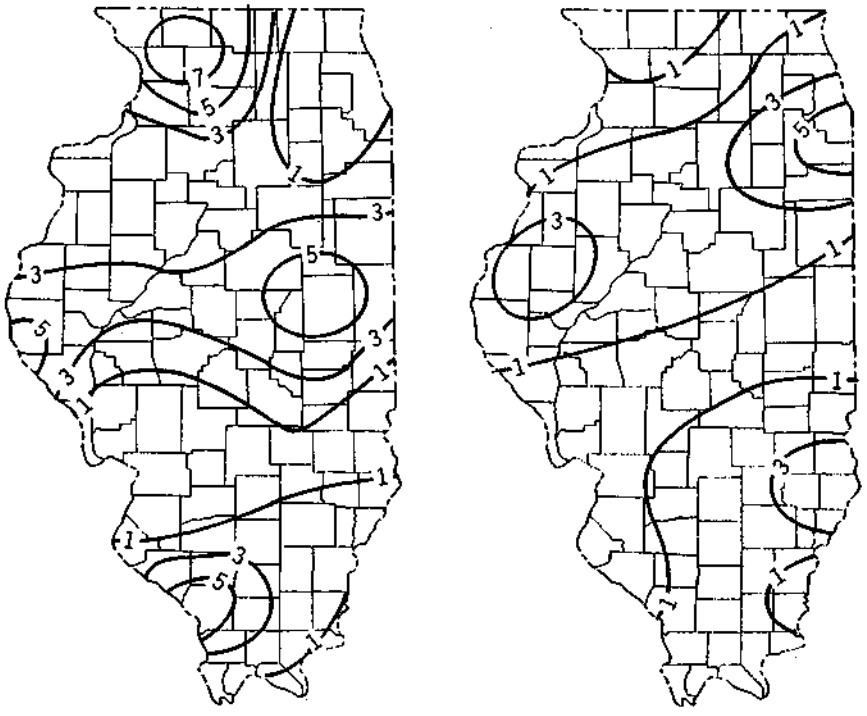

Figure 69. Frequency of high and low pressure centers for summer in Illinois. 1945-1959

weather types and their rainfall during July-August. Shown in table 27 are the normal percentage distributions of each type of event for Illinois. Included with the frontal types are the pre-frontal squall lines they produce. It is evident from table 27 that cold frontal activities are the major producers of summer rainfall in Illinois and the Midwest. The capability to modify precipitation with the three major frontal types appears essential to obtain a reasonably useful increase in rainfall for agricultural applications. Huff and Vogel presented the diurnal frequency of cumulonimbus clouds in Springfield during July and August shown in figure 72. An interesting difference is found during the late evening hours. In the midmorning, minimums are found with all types of conditions, but the wetter months show increasing frequency of Cb clouds from 1900 until 2200 CST, whereas dry conditions show a distinct lack of Cb after the late afternoon heating period. This would suggest a lack of the Cb-producing conditions in the mid and late nocturnal hours during droughts. This may be related to a decrease in frontal passages during droughts.

A major objective of the METROMEX research on urban effects on rainfall was the determination of the synoptic weather conditions during which local effects might have occurred and altered precipitation (Vogel and Huff, 1977, 1978). Previous synoptic weather typing of storms, or rain periods, was combined into slightly more refined analyses of eight major rain-producing storm types. The definition of these eight types is shown in table 28. During the five summer periods of 1971-1975, a total of 330 objective rainstorms and 228 rain days occurred in the 2000 mi^2 METROMEX circular network. The frequency of the eight types per year and for the 5 years is shown in table 29. This reveals the type of year-to-year variations in these events, as well as the difference between each condition over a small mesoscale area.

Table 30 presents the average point rainfall for the various weather types for all storms of the five summers. The average point value for squall lines of 1.19 cm, or 0.5 inch, is three times more than that of any other type. The second most productive is static fronts. The values in the lower part of table 30 are based on only gages with rain to com-

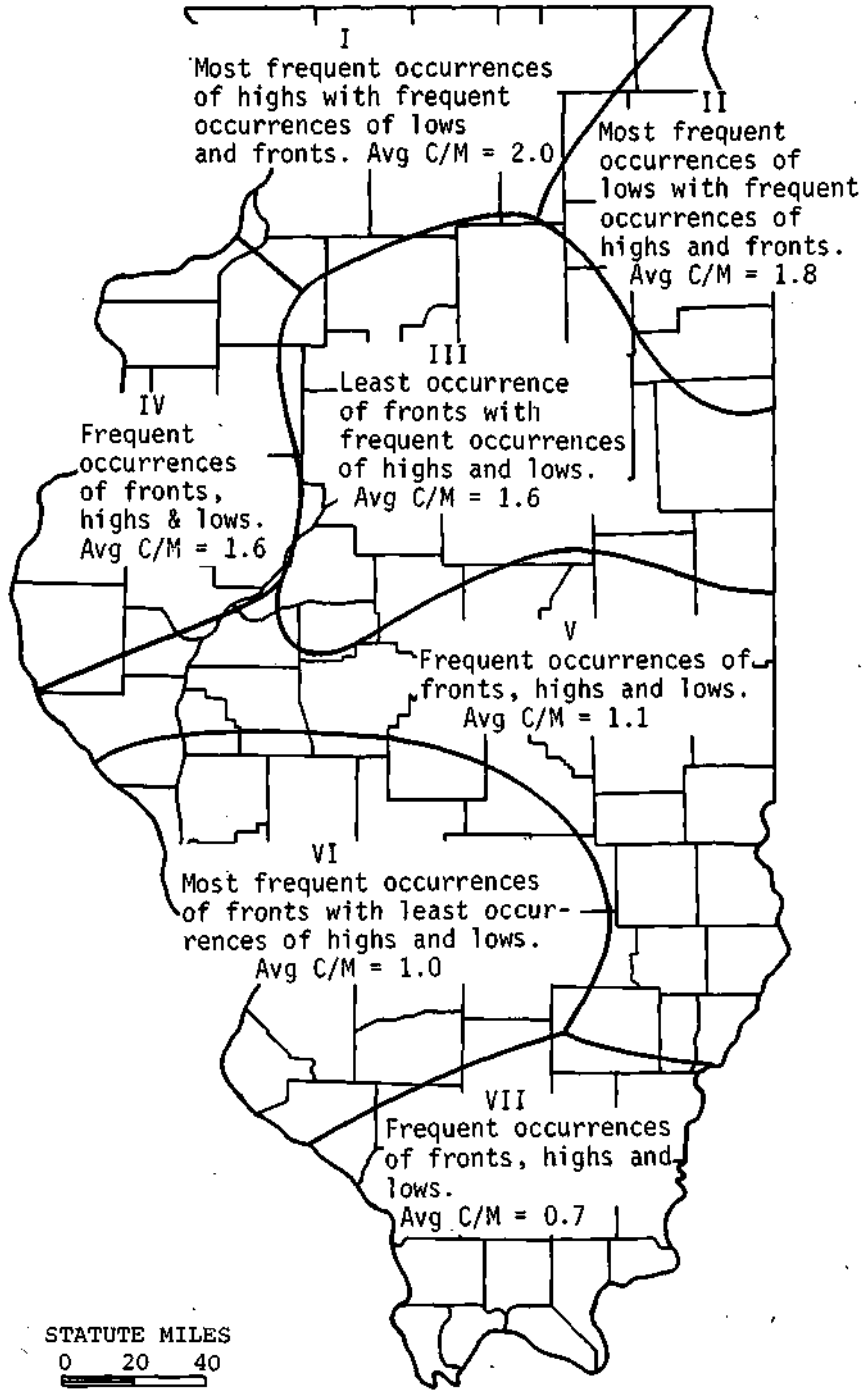

Figure 70. Climatic regions of Illinois for summer, based on frequency distributions of fronts, high and low pressure centers, and air masses, 1945-1959

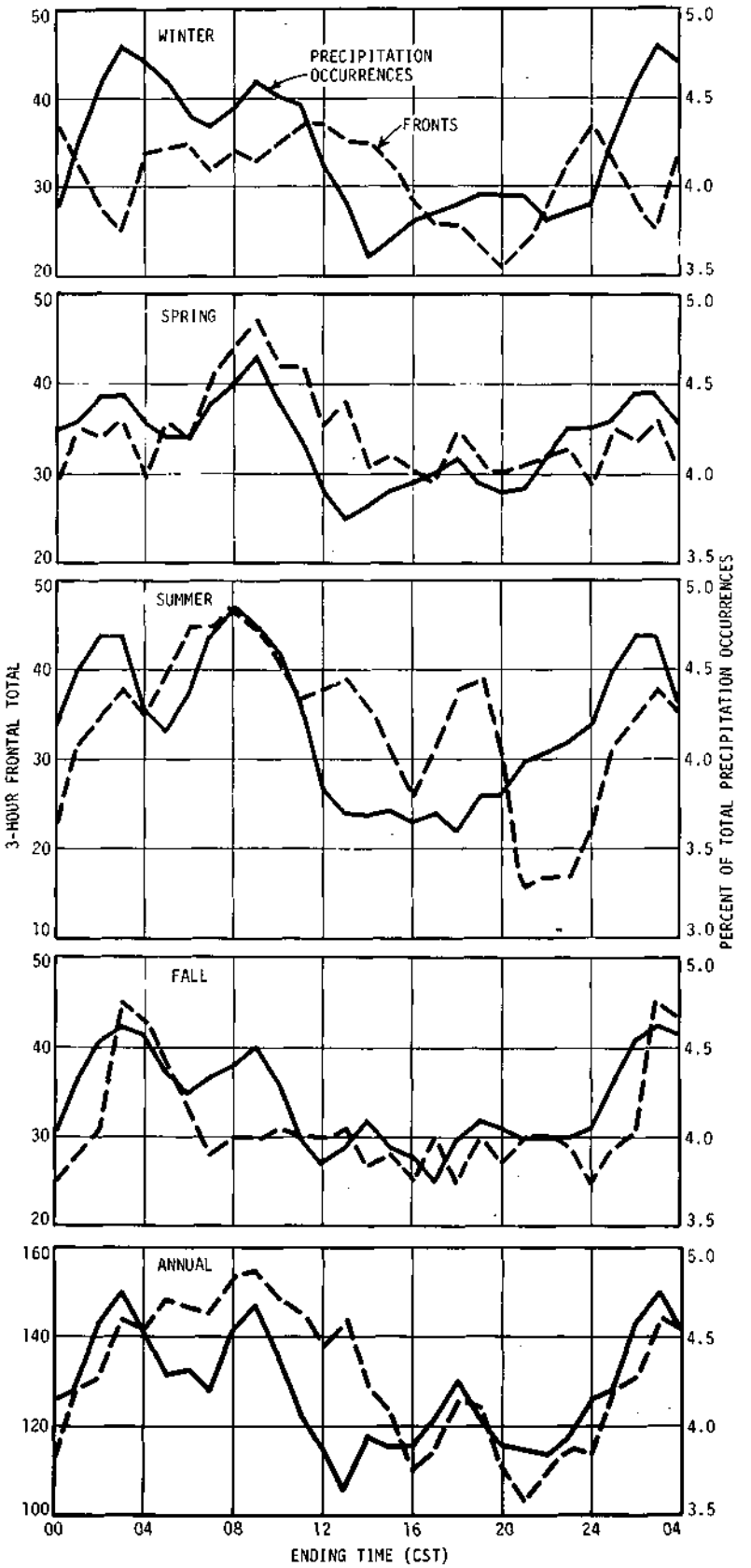

Figure 71. Comparison of Urbana frontal distributions with distribution of hourly precipitation occurrences in North Central Section

Table 25. Type Distributions of Precipitation by Months, 1944-1953, Springfield Airport

Month	Cold front Amt (inches)	Fq	Warm front Amt (inches)	Fq	Stat. front Amt (inches)	Fq	Squall line Amt (inches)	Fq	Warm air mass Amt (inches)	Fq	Cold air mass Amt (inches)	Fq
January	6.61	29	9.40	36	3.98	14	0.05	1	0.39	7	0.25	15
February	6.06	35	9.80	32	3.02	10			0.43	3	1.56	15
March	7.37	41	16.41	43	5.68	17	3.29	10	0.55	6	1.14	21
April	13.33	48	15.11	30	3.01	13	2.09	10	3.60	9	0.66	14
May	8.87	42	6.66	20	4.70	21	9.05	18	2.65	12	1.71	20
June	7.82	23	7.76	23	8.29	14	15.62	34	9.89	27	0.39	6
July	4.91	15	6.38	8	5.71	12	6.82	20	7.74	28	0.68	4
August	8.81	22	5.13	11	3.78	9	3.39	13	2.80	12	0.10	4
September	8.26	33	7.93	10	3.27	9	4.66	9	4.77	18	0.41	4
October	11.43	24	3.98	11	4.61	13	1.35	6	2.26	10	0.37	8
November	7.92	38	8.18	24	1.63	5	0.79	5	1.97	11	0.35	13
December	4.59	30	9.36	29	5.40	9	0.50	1	0.52	6	0.24	9
Total	95.98	380	106.10	277	53.08	146	47.61	127	37.57	149	7.86	133
Average	0.25		0.38		0.36		0.37		0.25		0.06	

Stat. = Stationary
Amt = Total amount of precipitation in inches for respective months for 10-year period
Fq = Total number of occurrences for respective months for 10-year period
Averages = Average contribution in inches per occurrence

Table 26. Type Distributions of Precipitation in Summer Months During 1944-1953 at Chicago, Moline, and Cairo

Month	Cold front Amt (inches)	Fq	Warm front Amt (inches)	Fq	Stat. front Amt (inches)	Fq	Squall line Amt (inches)	Fq	Warm air mass Amt (inches)	Fq	Cold air mass Amt (inches)	Fq
Chicago												
June	9.35	26	9.26	24	7.20	18	11.01	25	5.99	15	0.22	5
July	6.29	28	2.53	8	3.61	13	11.15	14	9.24	25	1.97	7
August	11.08	33	3.70	10	4.34	14	3.34	11	3.76	11	0.20	4
Moline												
June	5.88	24	14.58	27	8.01	18	17.62	29	5.60	21	0.01	1
July	10.16	26	4.16	8	3.74	10	9.40	17	9.26	25	1.51	5
August	10.05	32	11.20	14	2.50	10	6.29	17	5.15	13	0.36	5
Cairo												
June	10.29	24	1.54	4	5.47	10	12.74	28	18.08	47	0.71	1
July	4.91	18	1.42	4	4.59	11	9.57	17	7.19	37	0.32	6
August	9.60	13	1.33	6	4.26	14	4.58	12	15.32	25	0.49	5

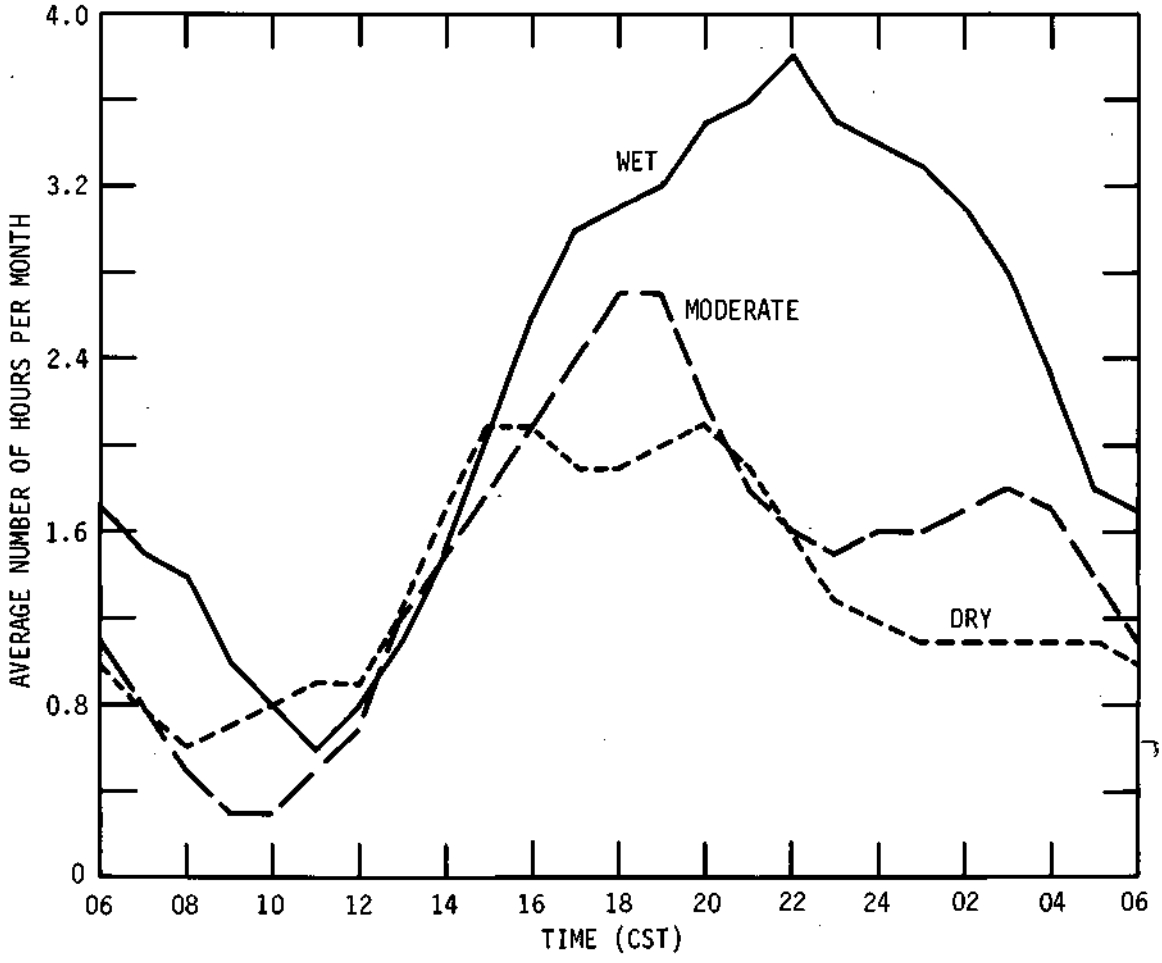

Figure 72. Diurnal frequency of cumulonimbus clouds at Springfield during July-August, 1951-1964

Table 27. Normal Percentage Distribution of July-August Rainfall in Illinois by Synoptic Types

Synoptic type	*Percent of storm days*	*Percent of total rainfall*
Cold front	46	39
Warm front	8	14
Stationary front	13	21
Occluded front	1	2
Low centers	2	7
Air mass storms (Non frontal)	30	17

Table 28. Definition of Synoptic Weather Types Used in METROMEX

Squall Line Storms (SL)

A non-frontal group of thunderstorms accompanied by a trigger mechanism, usually a short wave trough. The convective activity associated with the storm systems was intense, well-organized, and often times was arrayed in a narrow band or line of active thunderstorms.

Squall Zone Storms (SZ)

A mesoscale system of thunderstorms, organized into an area or cluster and independent of a frontal zone. These storms, like squall lines, tended to move across large regions of the Midwest, and an upper-air impulse was usually discernible.

Frontal Storms

Precipitation formed within 120 km (75 mi) of a surface front (cold, CF; static, SF; or warm, WF). There was no synoptic evidence that this precipitation was associated with a squall line or squall zone which, on occasion, moved 40 km (25 mi) or more ahead of the fronts.

Pre-Frontal and Post-Frontal Storms (P&PoF)

Precipitation associated with a frontal structure but at a distance of 120 to 240 km (75 to 150 mi) ahead or behind a front (cold, static, or warm).

Air Mass Storms (AM)

A shower or thunderstorm generated within an unstable air mass. No large scale or mesoscale synoptic causes were evident. The resulting convective activity was usually widely scattered to scattered and weak.

Low Pressure Storms (LOW)

A cyclonic storm situated so close to the research circle that it was not possible to associate the precipitation with a frontal or mesoscale weather structure. These systems are rare during the summer months.

Table 29. Frequency of METROMEX Synoptic Weather Types, June-August 1971-1975

	Number of rainstorms									
	SL	*SZ*	*CF*	*SF*	*WF*	*P&PoF*	*AM*	*LOW*	*Total*	*Rain days*
1971	5	17	7	5	1	4	6	2	47	40
1972	11	11	6	4	3	9	24	1	69	44
1973	12	16	6	2	3	4	21	1	65	46
1974	7	19	15	6	3	8	21	1	80	50
1975	13	20	12	2	4		18		69	48
1971-1975	48	83	46	19	14	25	90	5	330	228
Average	9.6	16.6	9.2	3.8	2.8	5.0	18.0	1.0	66	46

pensate for the areal extent differences. Average percent of the 2000-mi^2 area encompassed by storm rainfall is shown for each synoptic type in table 31. This allows estimation of the areal coverage of rainfall within the network for any storm type. Squall line storms typically produce rainfall over 76% of the network, as compared to 7% for air mass storms.

Table 32 presents the frequency distribution of rainfall motion sorted by synoptic weather type. The squall line storms showed a preponderance of motion from the WSW, whereas the cold front storms showed a nearly equal preference for WSW and WNW motion.

Figures 73 through 79 present a variety of rainfall patterns for the various synoptic weather types, sorted in most cases by storm motions. For example, figure 73a shows the pattern based on all squall line storms. Squall line storms moving from the southwest result in the pattern shown in figure

Table 30. Storm Average Point Rainfall for All Gages and for Gages with Rain, 1971-1975

	1971	1972	1973	1974	1975	All storms 1971-1975
	Point average rainfall (cm)					
SL	1.24	0.98	1.37	0.72	1.43	1.19
SZ	0.46	0.26	0.25	0.31	0.38	0.34
CF	0.07	0.56	0.32	0.43	0.15	0.30
WF	0.41	0.11	0.20	0.25	0.02	0.16
SF	0.13	0.28	0.30	0.77	0.22	0.39
P&PoF	0.05	0.02	0.23	0.05		0.07
AM	0.03	0.04	0.01	0.01	0.02	0.02
LOW	0.24	0.02	0.03	0.10		0.13
	Point average per storm (cm) for gages with rain					
SL	1.30	1.34	1.75	1.02	2.01	1.57
SZ	0.76	0.56	0.56	0.66	0.64	0.64
CF	0.23	1.50	1.04	1.14	0.56	0.94
WF	0.58	0.25	0.79	0.41	0.15	0.41
SF	0.36	0.74	0.71	2.67	0.56	1.09
P&PoF	0.38	0.15	0.53	0.23		0.33
AM	0.43	0.33	0.18	0.15	0.30	0.28
LOW	0.64	0.23	0.15	0.61		0.51

Table 31. Average Percent of Area with Storm Rainfall by Synoptic Types, 1971-1975

	1971	1972	1973	1974	1975	1971-1975
SL	95.0	72.9	78.3	70.4	71.4	75.7
SA	60.5	46.5	43.7	47.3	60.8	52.4
CF	29.2	37.2	30.9	37.6	26.9	32.6
WF	69.7	47.1	26.4	62.5	14.0	38.1
SF	39.0	38.0	40.0	28.7	39.4	35.7
P&PoF	11.7	12.6	44.1	20.1		19.9
AM	5.7	11.0	4.3	5.7	6.0	6.9
LOW	37.6	16.3	17.2	17.2		25.2

Table 32. Frequency of Rainstorm Motions by Synoptic Types, 1971-1975

	Number of storms								
	SL	SZ	CF	WF	SF	P&PoF	AM	LOW	Total
SSW	5	3	1	4		2	9		24
SW	9	23	3	3	3	1	21	1	64
WSW	15	24	11	1	6	8	11	1	77
WNW	7	14	12	1	5	4	9	1	53
NW	9	8	8	2	3	5	18	2	55
NNW	0	3	7	0	0	3	6	0	19
NNE		2	1				1		4
NE									
ENE									
ESE							1		1
SE		1			1		1		3
SSE		2				1	1		4
Stationary	1	1					1		3
Indeterminate	2	2	3	3	1	1	11		23
Total	48	83	46	14	19	25	90	5	330

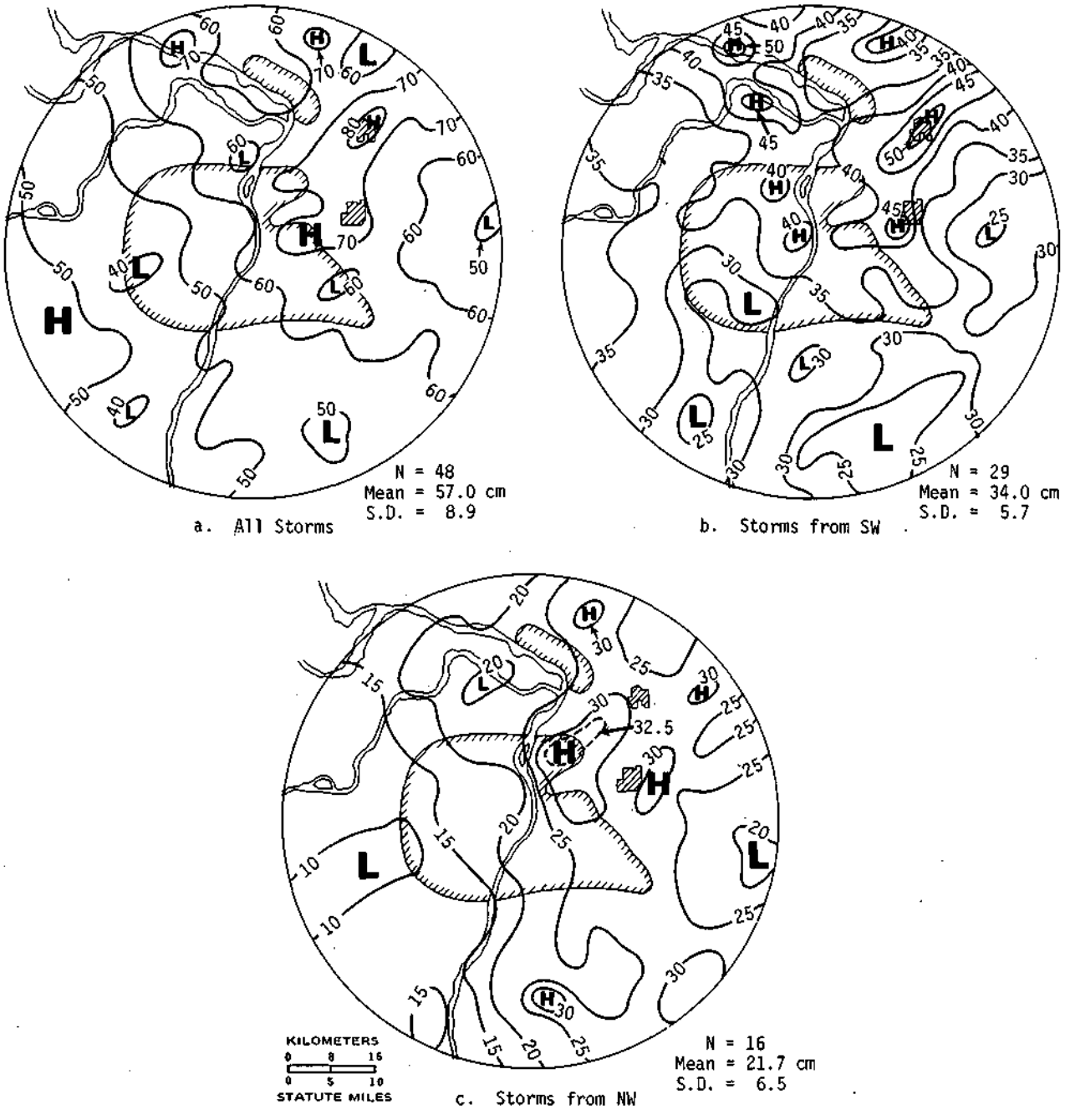

Figure 73. Rainfall patterns for squall line storms, 1971-1975

73b, and those moving from the northwest are shown in figure 73c. Comparison of the patterns on these figures reveals the general magnitude of rainfall production from these basic types, as well as the type of total rainfall patterns they produce. Comparison of the squall storms and cold front patterns (figures 73, 74, and 75) with the air mass pattern for all storms (figure 79a) shows the tremendously greater production of precipitation from these organized summer systems than from the isolated shower category.

Another expression of fixed area (network) rain-

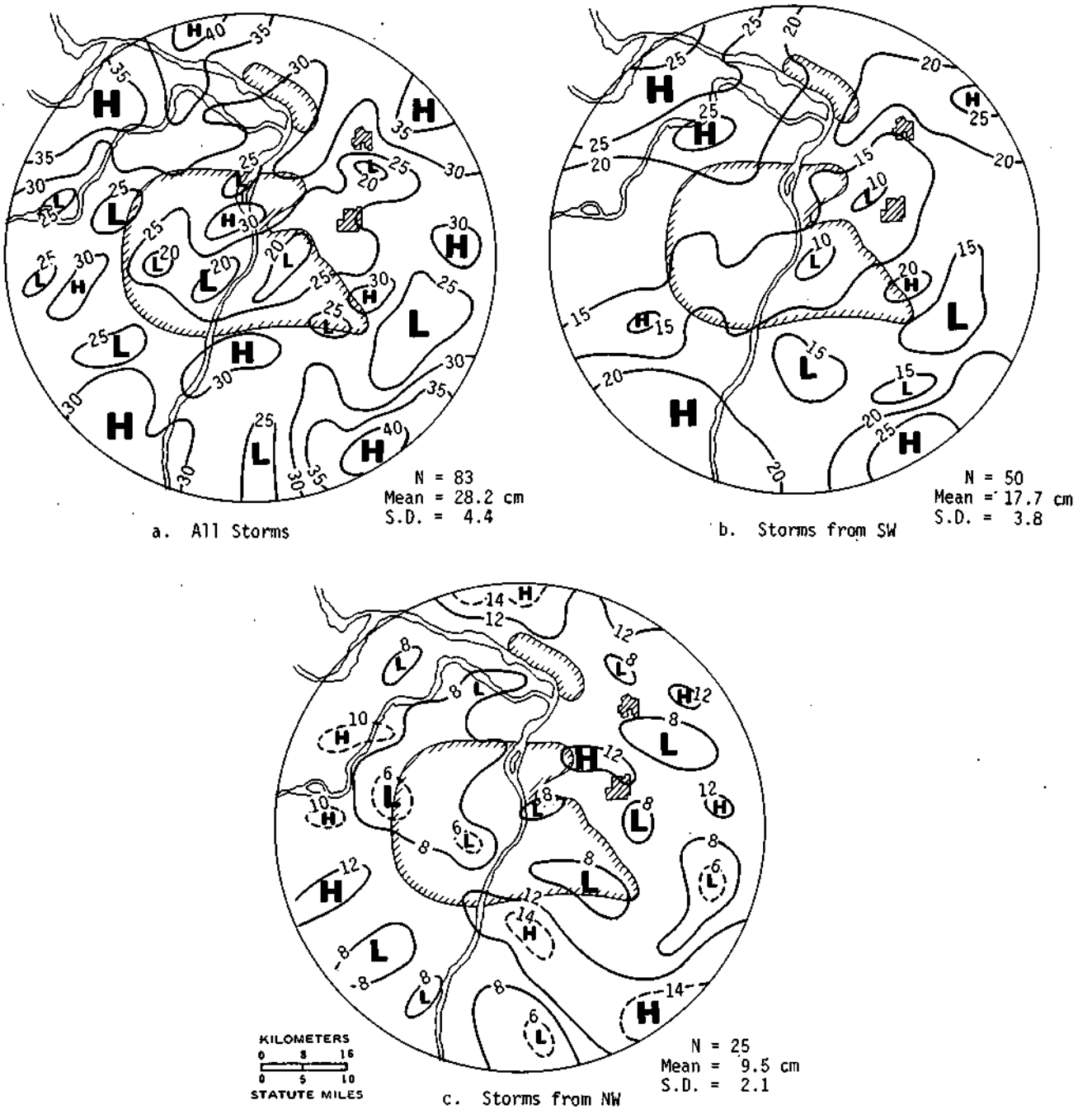

Figure 74. Rainfall patterns for squall zone storms, 1971-1975

fall with the synoptic weather types was presented by Huff (1966). The five years (1960-1964) of air mass rainfall in the Little Egypt Network were combined and expressed as a percent of the network average period for this 550-mi^2 area (figure 80).'This pattern revealed spatial variations in the air mass rainfall ranging from 120% of the mean in the northwest to less than 80% a few miles away. The network 5-year average was 14.8 inches. This pattern further illustrates some of the evaluation problems to be faced in dealing with this type of storm condition in a fixed area.

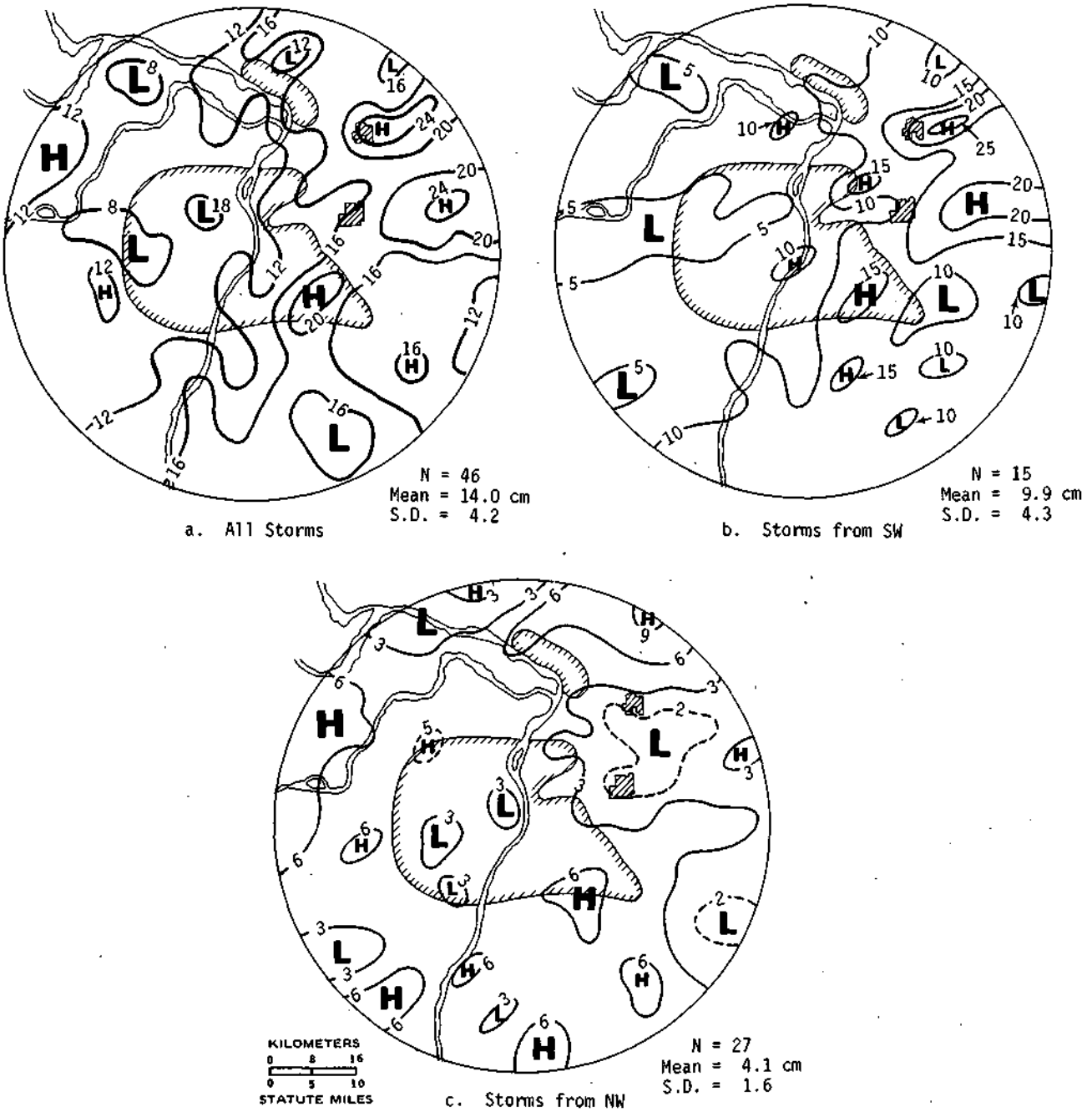

Figure 75. Rainfall patterns for cold front storms, 1971-1975

Huff and Shipp (1969) used the central Illinois network of 400 mi^2 to study the correlation patterns around a central gage. Figure 81 presents the correlation patterns with three basic synoptic types for May-September storms for an 11-year period. There were 195 frontal storms, 73 air mass storms, and 28 low center passages in the sample. The correlation differences are striking with a great change in the air mass storm values across distances of 10 miles or less. Correlation patterns indicate a general southwest-northeast orientation although this is not evident in the air mass pattern.

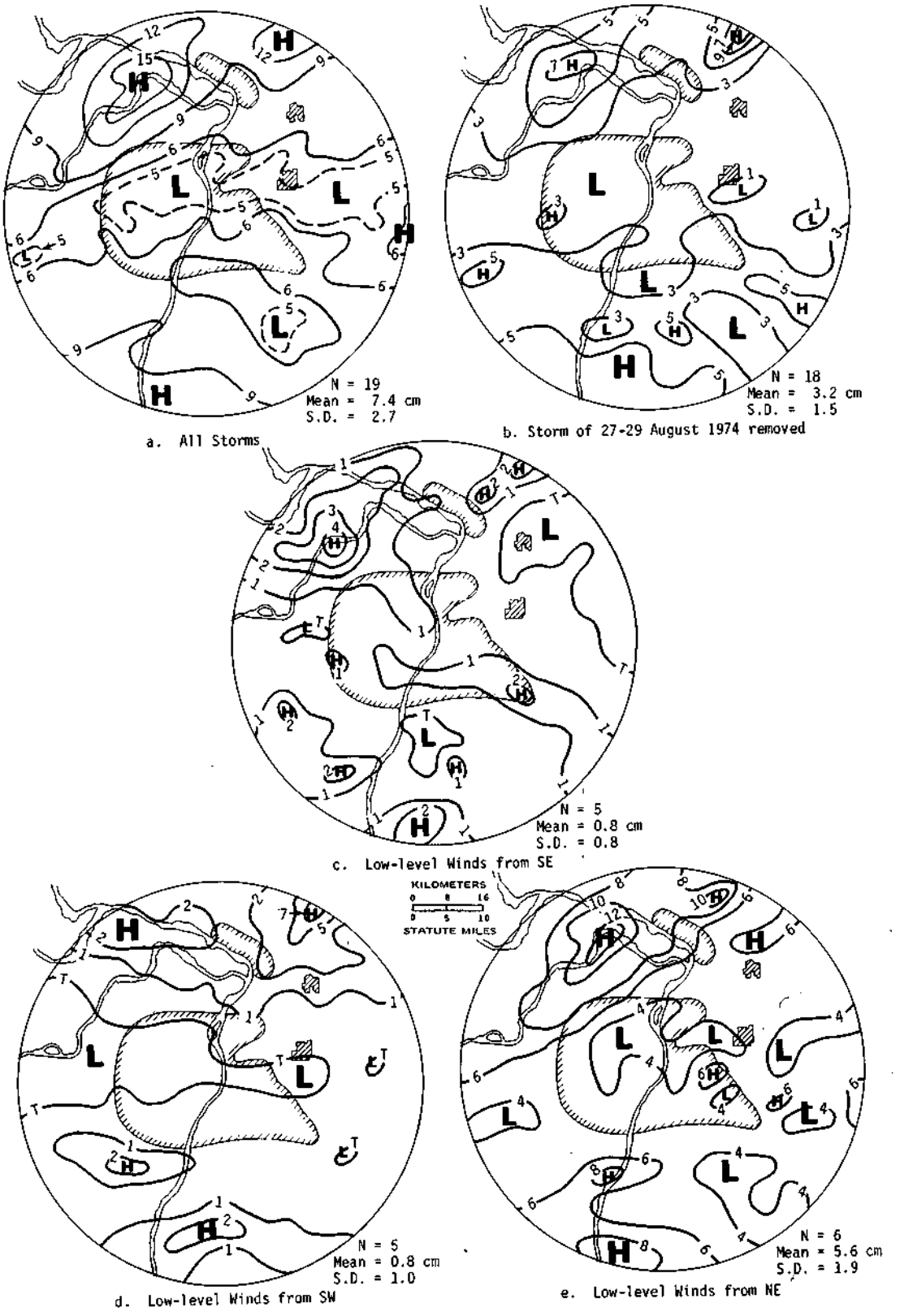

Figure 76. Rainfall patterns for static front storms, 1971-1975

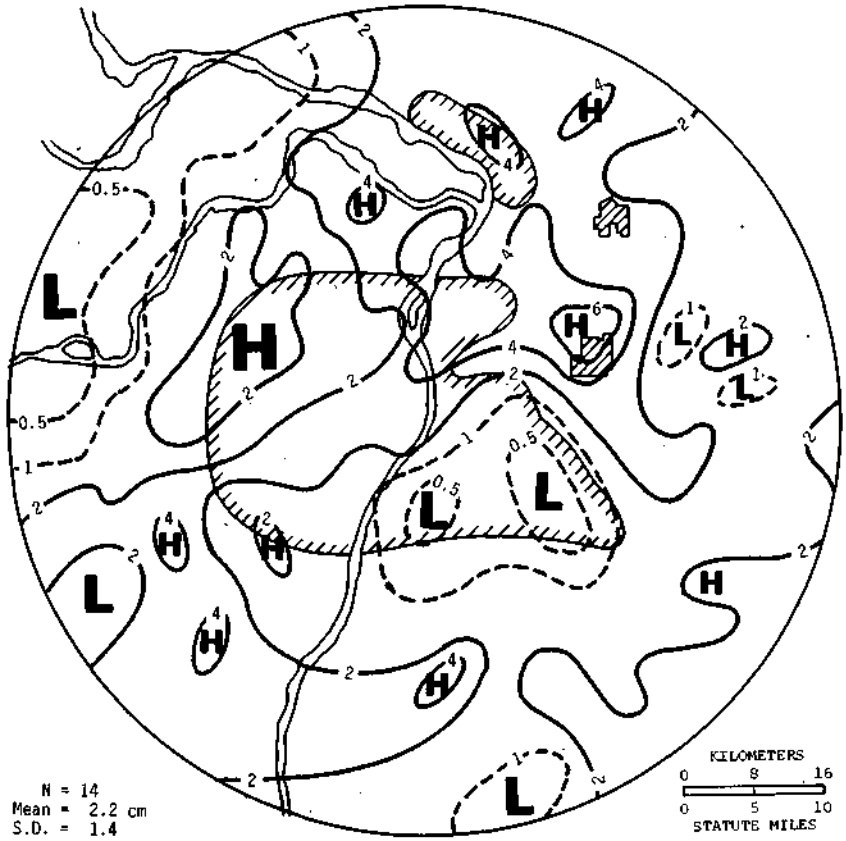

Figure 77. Rainfall pattern for warm front storms, 1971-1975

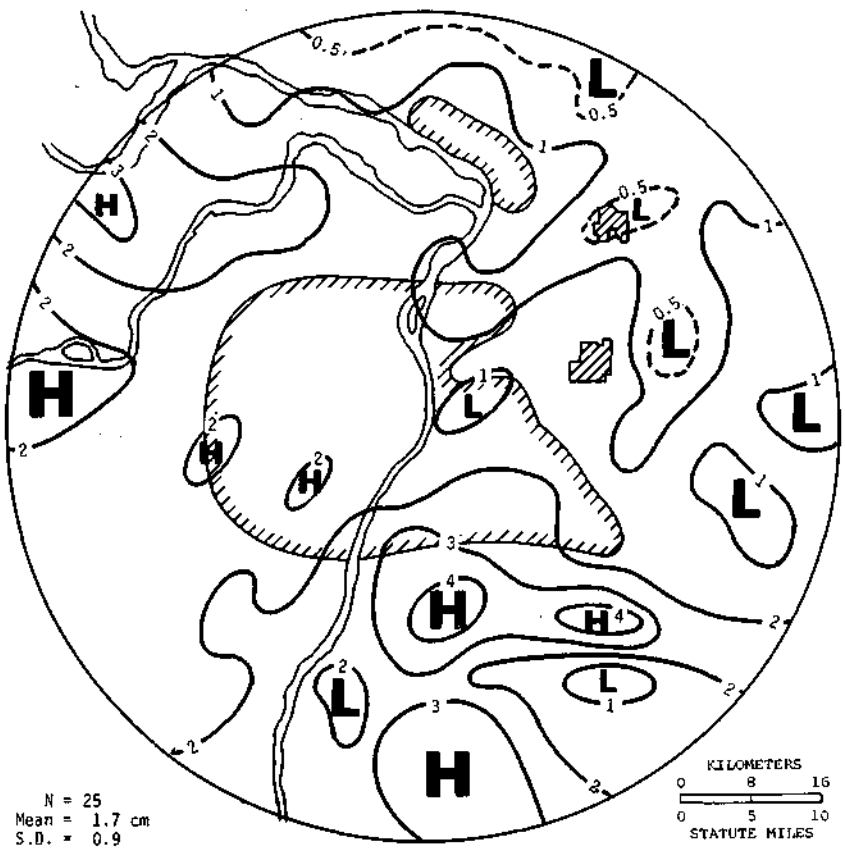

Figure 78. Rainfall pattern for pre- and post-frontal storms, 1971-1975

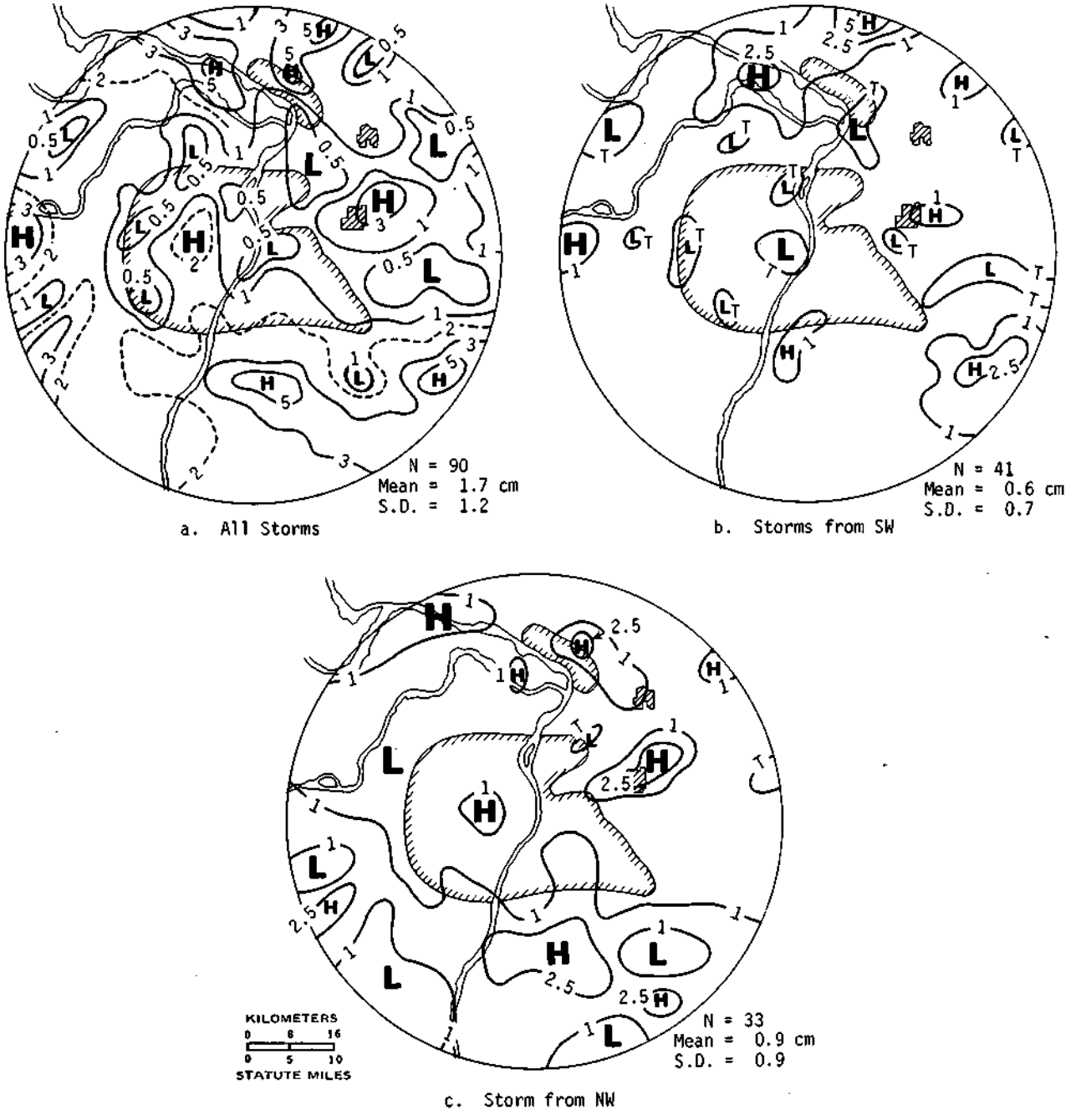

Figure 79. Rainfall patterns for air mass storms, 1971-1975

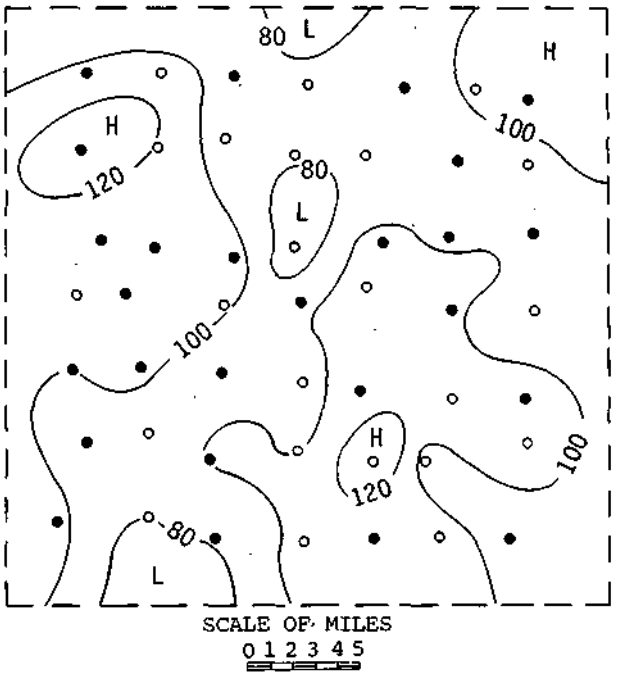

Figure 80. Percent of average network rainfall in summer air mass storms on Little Egypt Network

Pre-Rain Conditions and Forecasting

Important studies relating to the forecasting of warm season precipitation are ongoing (1980) as part of three projects: OSET (Operational Seeding Evaluation Techniques), VIN (Virginia, Illinois, NOAA project), and PACE (Precipitation Augmentation for Crops Experiment). Much of the recent Survey research relating to forecasting of warm season precipitation and thunderstorm conditions was performed as a part of a multi-year project aimed at developing a plan for a hail suppression experiment in Illinois (Changnon and Morgan, 1976). That report and related papers present much useful information on forecasting pre-rain and pre-storm conditions in Illinois.

Huff and Vogel (1977) in their studies of summer droughts in Illinois present useful information on the climatology of upper air temperatures, humidity, and saturation depths. Their results appear in tables 3 3 and 34 for Peoria (central Illinois) and Salem (southern Illinois).

Ackerman (in Ackerman, et al., 1978) in a detailed study of the atmospheric conditions prior to summer rain in the St. Louis area presented typical pre-rain profiles of temperature and dewpoints. Figure 82 presents the average profiles of tempera-

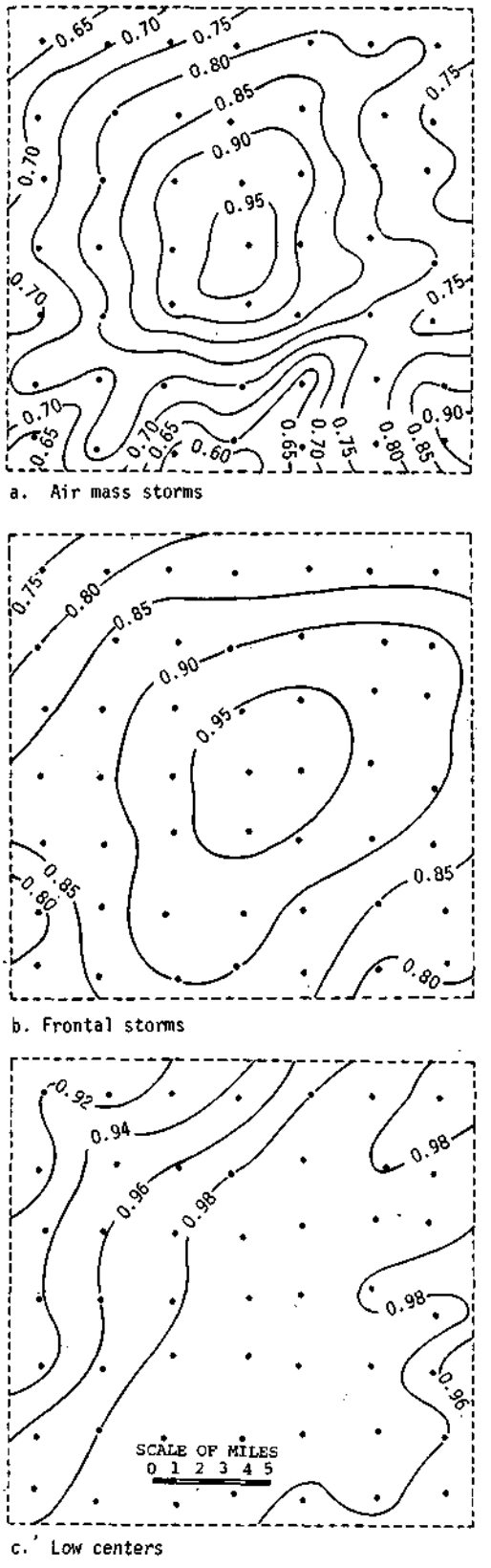

Figure 81. Correlation patterns of synoptic types in May-September storms on East Central Illinois Network

Table 33. Mean Monthly Temperatures at Peoria and Salem for 0600 and 1800 CST during June to August 1971-1975

	Mean temperature (C°)				
	Sfc-850	850-700	700-500	Sfc-700	Sfc-500
Salem 0600 CST					
Very dry	18.0	11.1	−0.9	14.5	8.2
Moderately dry	18.3	10.5	−2.2	14.3	7.6
Near normal	18.7	11.8	−0.3	15.1	8.1
Above normal	18.5	10.7	−2.2	14.5	9.2
Much above normal	18.3	11.0	−1.3	14.6	8.1
Salem 1800 CST					
Very dry	22.0	11.7	−0.3	16.9	10.0
Moderately dry	21.3	11.0	−1.7	16.2	9.0
Near normal	21.8	11.5	−0.7	16.7	9.7
Above normal	22.1	12.4	0.3	17.3	10.4
Much above normal	21.3	11.7	−0.6	16.5	9.6
Peoria 0600 CST					
Very dry	18.2	11.3	−1.4	14.6	8.1
Near normal	17.5	10.0	−2.7	13.6	7.1
Above normal	16.5	9.7	−2.4	13.0	6.7
Much above normal	17.5	10.3	−2.0	13.8	7.4
Peoria 1800 CST					
Very dry	21.9	11.9	−0.6	17.0	9.9
Near normal	20.7	10.5	−2.1	15.6	8.5
Above normal	20.2	10.6	−1.4	15.6	8.6
Much above normal	20.6	10.8	−1.3	15.7	8.9

Table 34. Mean Monthly Relative Humidity and Saturation Deficit at Peoria and Salem for 0600 and 1800 CST for June to August 1971-1975

	Mean relative humidity (%)					Mean saturation deficit (g/kg)				
	Sfc-850	850-700	700-500	Sfc-700	Sfc-500	Sfc-850	850-700	700-500	Sfc-700	Sfc-500
Salem 0600 CST										
Very dry	68.0	51.0	35.0	59.7	49.7	4.8	5.3	4.0	5.0	4.6
Moderately dry	67.0	54.0	49.0	61.0	56.0	4.9	4.8	3.0	4.9	4.1
Near normal	72.4	57.2	41.2	55.6	55.6	4.3	4.7	3.5	4.4	4.0
Above normal	70.5	54.0	38.5	52.0	52.5	4.8	5.3	4.2	5.0	4.6
Much above normal	71.8	52.0	38.3	62.0	56.5	4.3	5.3	3.8	4.7	4.3
Salem 1800 CST										
Very dry	52.6	47.3	32.0	48.0	42.0	9.5	5.9	4.4	7.4	6.3
Moderately dry	56.0	56.0	43.0	55.0	50.0	8.4	5.0	3.4	6.9	5.5
Near normal	59.2	55.8	39.0	56.8	49.6	8.0	5.1	3.9	6.7	5.6
Above normal	62.5	55.0	38.5	57.5	50.0	7.5	5.4	4.3	6.7	5.7
Much above normal	61.8	51.5	37.3	56.3	48.8	7.1	5.6	4.0	6.4	5.5
Peoria 0600 CST										
Very dry	69.0	57.0	40.0	60.2	52.2	5.8	5.7	3.5	5.7	4.8
Near normal	71.0	57.0	46.0	64.0	57.0	4.1	4.5	3.0	4.2	3.7
Above normal	65.7	50.7	37.3	58.0	50.7	4.6	5.0	3.6	4.8	4.2
Much above normal	69.4	55.2	40.8	62.2	53.8	4.5	4.8	3.4	4.6	4.1
Peoria 1800 CST										
Very dry	57.0	50.6	38.2	52.0	46.8	8.5	5.8	3.9	7.4	5.7
Near normal	62.0	57.5	41.5	59.0	52.0	6.8	4.6	3.5	5.9	4.9
Above normal	56.0	49.7	37.0	51.0	45.7	7.8	5.4	3.9	6.8	5.6
Much above normal	63.6	57.6	42.4	59.6	52.4	6.7	4.8	3.5	5.9	5.0

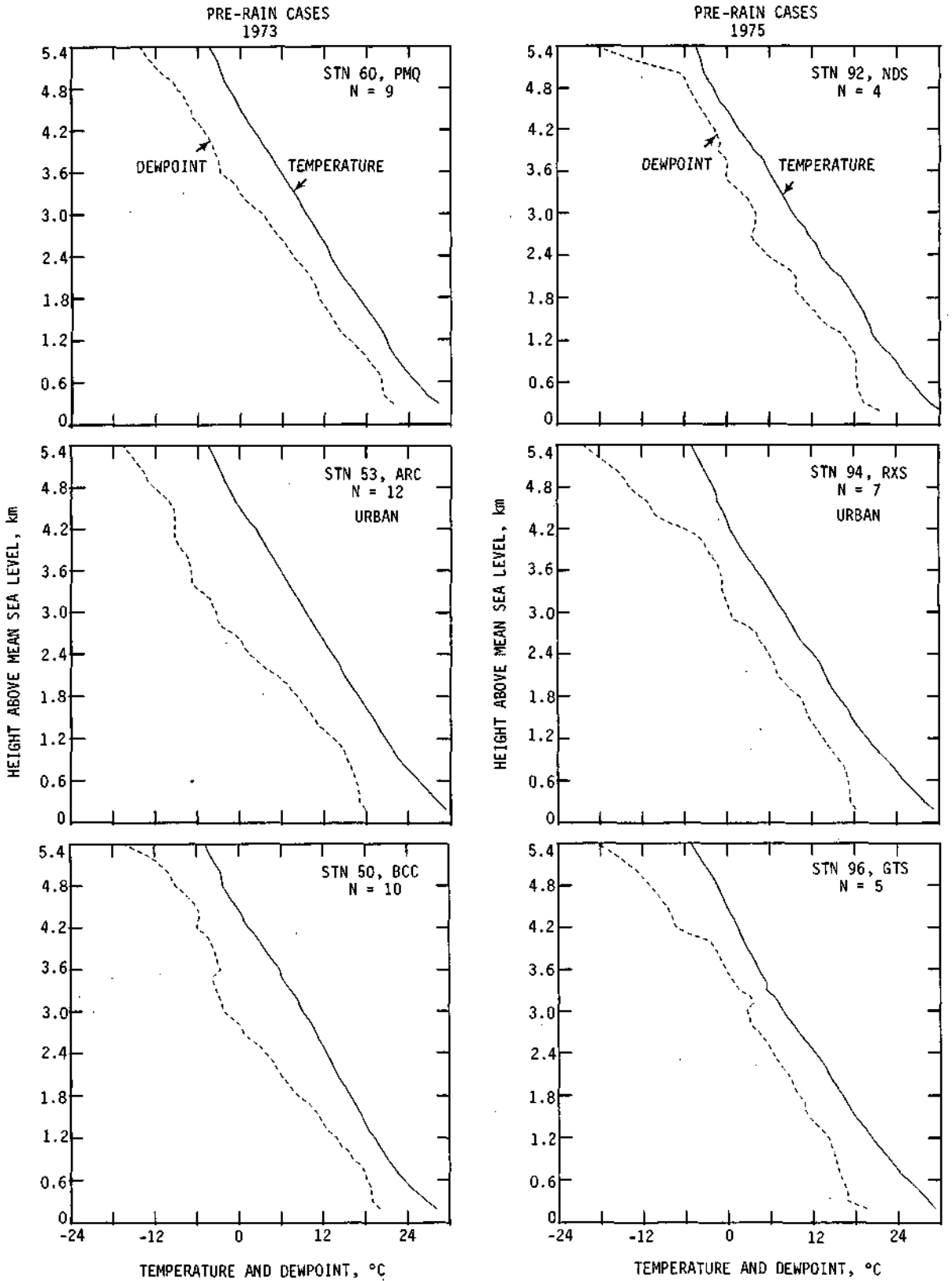

Figure 82. Average profiles of temperature and dewpoint in pre-rain cases at St. Louis in summer

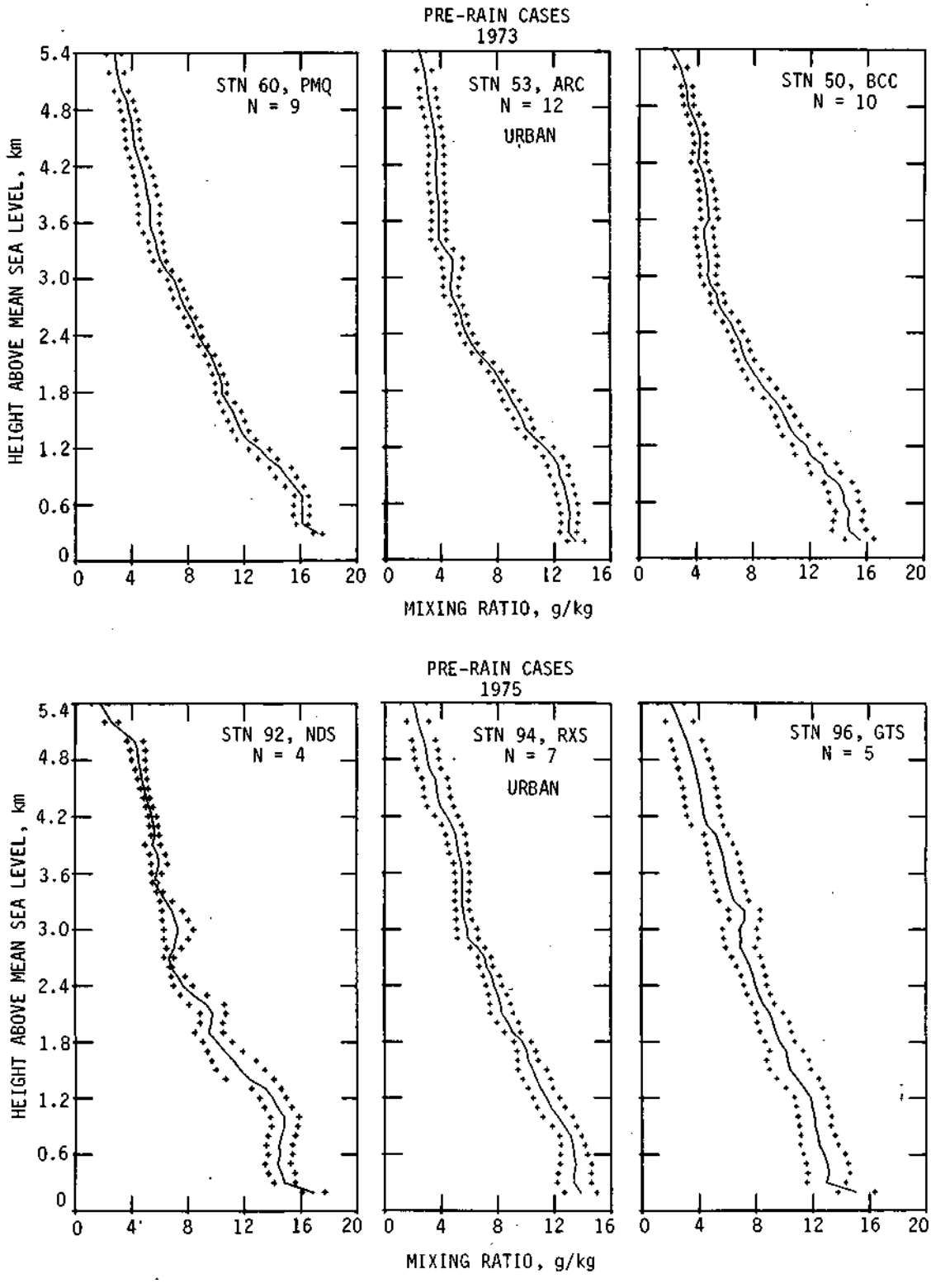

Figure 83. Average profiles of mixing ratio in pre-rain cases at St. Louis in summer

ture and dewpoint for urban stations (middle of figure) and rural stations near St. Louis. Figure 83 presents similar urban and rural profiles of the mixing ratio for pre-rain cases.

Achtemeier and Morgan (1975) presented results on thunderstorm forecasts for central Illinois, based largely on the use of surface weather data. Their analysis proceeded with the view that differential advection of thermodynamic properties, adiabatic heating and mechanical lifting may act in any combination to destabilize the lower troposphere prior to the onset of Illinois convection. When convective instability is released through isolational heating and subsequent destabilization within the subcloud layer, maximum activity occurs during hours of maximum temperature in the absence of local destabilization or triggering mechanism. Local effects often occur with the random distribution of showers within a favorable air mass. However, it is also well known that convection seldom occurs randomly. Complex lines and groups of convective showers often occur adjacent to areas completely shower or cloud free and yet all within the same air mass. This tendency for organization of mesoscale convection is especially evident in the upper Midwest during midsummer when the synoptic scale systems are quite weak. Convergence and mechanical lift within the low-level moist layers deepen the moist layers and destabilize the air mass, making it locally more favorable for convection. Mechanical lift is operative at times, whereas adiabatic destabilization is effective with plenty of sunshine during the warmest hours.

A major data set of thunder and no-thunder days in the summer of 1972 was examined. The best results were obtained with a thunderstorm forecast algorithm threshold of 200 m for 7 grid-points. The thunder/no-thunder days were correctly identified in 54 of the 58 days with one false alarm and three failures. The study area is shown in figure 84, and the contingency tables and selected thresholds are presented in figure 85.' Results give strong proof that thunder days can be reliably distinguished in central Illinois from no-thunder days, on the basis of the areal coverage of the modified cumulative lift.

To properly estimate predictive capabilities of the modified cumulative lift (TFA), Achtemeier and Morgan (1975) created a scenario of aircraft

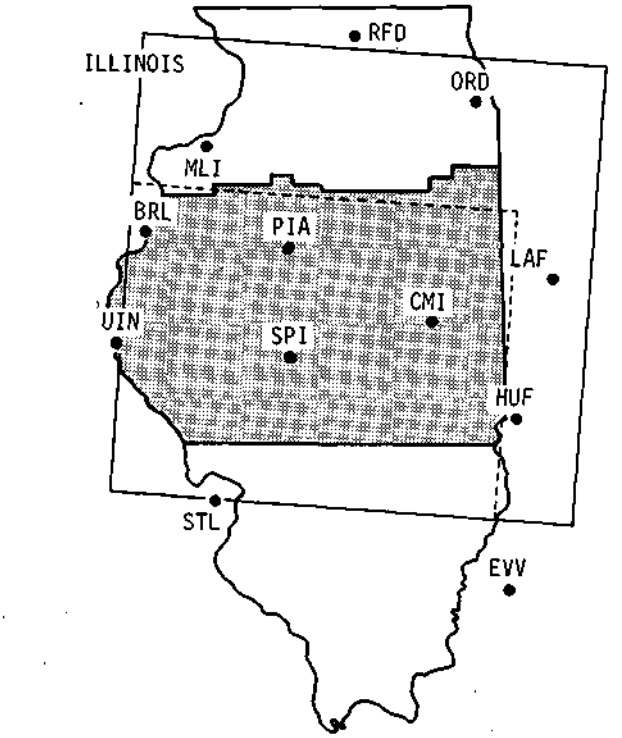

Figure 84. Map of Illinois showing the area of the thunder day calendar (shaded); sites of 12 stations included in the objective analysis, and an outline of the analysis grid (area bounded by the dashed lines was included in the comparative studies with the thunder day calendar)

operations in a weather modification experiment, presuming a minimum of 2 hours to get a weather modification aircraft aloft with a maximum flight time of 4 to 5 hours. Other operational criteria were set forth and a total of 37 decision events were found for the 31 thunder days used. Results are presented in figure 86 for the 7 thunder with hail periods and the 21 thunder (no hail) day periods for the 200-m and 300-m thresholds. Both sets of curves suggest that cumulative lift is generally predictive of increases in echo top height and intensity of thunder activity over central Illinois.

Further information on this general method for a dynamic destabilization model is given in Changnon and Morgan (1976). The approach relies upon hourly monitoring of the surface weather conditions and less frequent monitoring of upper air conditions to produce reasonably accurate 2- to 4-hour predictions of the locations and onset times of convection in central Illinois. The frequent updating of this technique allows circumvention of the mesoscale numerical predictive models which are complicated by boundary and initial conditions.

NT = NO-THUNDER DAY TD = THUNDER DAY

	CL(TFA) <200	CL(TFA) >200	TOTAL	
NT	7 (20)	20 (7)	27	x = 4
TD	0 (2)	31 (29)	31	
TOTAL	7 (22)	51 (36)	58	
NT	12 (26)	15 (1)	27	x = 7
TD	1 (3)	30 (28)	31	
TOTAL	13 (29)	45 (29)	58	
NT	18 (26)	9 (1)	27	x = 10
TD	4 (8)	27 (23)	31	
TOTAL	22 (34)	36 (24)	58	
NT	23 (27)	4 (0)	27	x = 15
TD	13 (20)	18 (11)	31	
TOTAL	36 (47)	22 (11)	58	

	CL(TFA) <300	CL(TFA) >300	TOTAL	
NT	17 (24)	10 (3)	27	x = 4
TD	4 (6)	27 (25)	31	
TOTAL	21 (30)	37 (28)	58	
NT	22 (27)	5 (0)	27	x = 7
TD	3 (12)	28 (19)	31	
TOTAL	25 (39)	33 (19)	58	

Figure 85. Contingency table for the Cumulative Lift (CD and Thunderstorm Forecast Algorithm (TFA) thresholds of 200m and 300m observed for at least 1 hour at a minimum of x gridpoints (TFAs shown in parentheses)

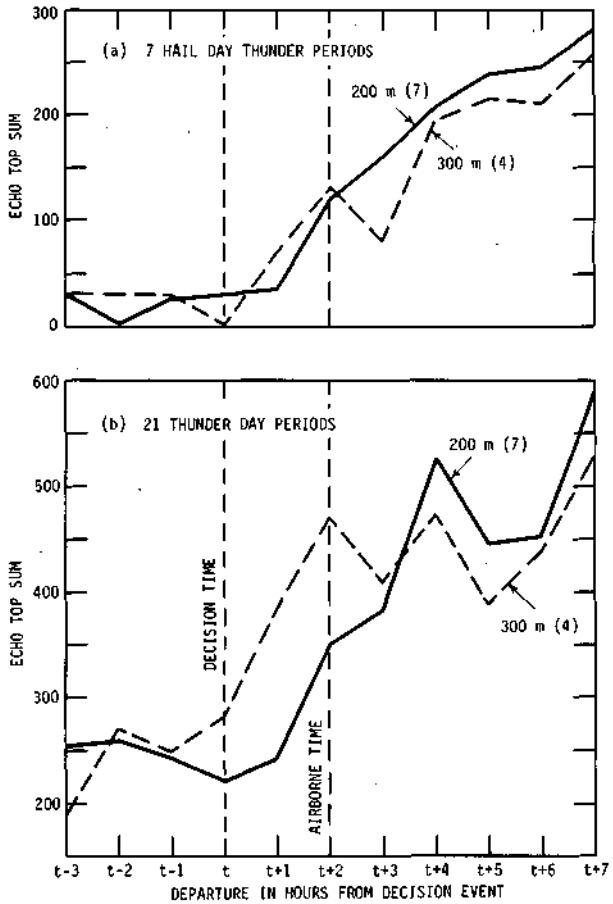

Figure 86. Sums by hour of maximum reported echo top heights above 30,000 ft relative to the decision time when the TFA threshold is exceeded for a specified number of gridpoints

Prediction of July-August Rainfall

The results for various crop-yield-weather models reveal that it would be very useful and important to know in advance the amount of rainfall expected in the July-August period, or in either of these 2 months. Such information would permit the utilization of the optimum seeding approach (including no-seeding) for any given summer. Forecasting skill available now or in the foreseeable future is not capable of predicting the July and/or August rainfall amounts 30 to 60 days in advance. The need for predictive knowledge led to a limited climatological study at five locations (each with long records) of the 1-month relationships in monthly rainfall and mean temperatures for June-July and for July-August (Changnon and Huff, 1971). If non-random relationships existed, conditional probability forecasts could be derived using knowledge of the past month's weather conditions.

The frequency distributions of the various June-July relations and July-August relations for Urbana is shown in table 35. Probabilities can be derived from the various frequencies shown in table 35. For example, one useful operational seeding situation would concern, given that a wet July has occurred, what will August experience? Examination of the results indicate that when July is wet and hot, the likelihood of a dry August predominates. In general, an inverse relationship exists for

Table 35. Region 3 (Urbana) Monthly Weather Relationships, 1889-1962

JUNE		JULY								
Rain	Temp	Rain →	Wet			Normal			Dry	
		Temp →	Hot	Normal	Cool	Hot	Normal	Cool	Hot	Normal	Cool
Wet	Hot								6		
	Normal			2			2	2		2	
	Cool			1	2		2	2			4
Normal	Hot		5			2	1		2		
	Normal		2	1	2		3				1
	Cool				1	1	2		1		1
Dry	Hot					2	1		3	2	
	Normal				4		2	1	2		
	Cool			2	2		1	1		1	

JULY		AUGUST								
Rain	Temp	Rain →	Wet			Normal			Dry	
		Temp →	Hot	Normal	Cool	Hot	Normal	Cool	Hot	Normal	Cool
Wet	Hot		1			1	1		2	2	
	Normal				2					1	2
	Cool				6		3		2		2
Normal	Hot			1	1		1				
	Normal		2		1		3	2	1		
	Cool		3	1	1		2	3	1	2	
Dry	Hot			2	1	2	2		5		1
	Normal			1		1	2		1		
	Cool		1	1				1	1	2	

	Temperature, °F			Rain, inches		
	Hot	Normal	Cool	Wet	Normal	Dry
June	>74.0	70.8–74.0	<70.8	>4.7	2.9–4.7	0.4–4.6
July	>76.3	74.3–76.3	<74.3	>3.9	2.4–3.9	0.2–2.3
August	⩾74.5	72.3–74.4	<72.3	>4.0	2.6–4.0	0.2–2.6

most combinations. However, persistence is indicated when a wet-cool July has occurred, since a wet August is most likely. Examination of the frequencies in table 35 for both wet and dry conditions in the preceding months reveals that there is generally a marked tendency for a certain rain combination to follow given rain-temperature combinations in the preceding month, particularly when the prior month's rainfall was extreme (wet or dry).

ORGANIZED STORM SYSTEMS AND SUBSYSTEM ENTITIES

Well-Organized Lines of Cells

Much of the information presented heretofore about 'storms' or rain events has pertained to these events inside a fixed area. In this section, the characteristics of storm events are viewed as to their actual total lifetime, generally over Illinois or larger areas. As would be expected, much of the information has been derived from radar portrayals. Statistics presented in this section were determined from 3-cm radar operations, and, consequently, are subject to limitations imposed by precipitation attenuation. Length and width of storm systems, particularly width, will be underestimates of the true dimensions. However, the measurements are useful for relative comparisons between various storm types. Furthermore, the 3-cm data are quite adequate for determining speed, direction of movement, orientation, acceleration of convective entities, and other storm characteristics.

Figures 87 and 88 present illustrations of organized line activity typical for Illinois (Stall and Huff, 1971). Organized lines are most often not a uniform straight line of equally sized cells, but more typically take on a pattern such as shown in figure 87. The radar range marks are 20 miles and the line shown is about 120 miles long with a variety of large and small cells. A schematic of typical array of three thunderstorm cells in a portion of an organized line is shown in figure 88. This is as viewed from the southeast since most lines move from westerly directions. One typically finds older cells to the north and developing cells to the south, or on the right flank of existing cells.

Further examples of radar-depicted organized lines appear in figure 89. Shown are two time sequences of lines moving across central Illinois from a radar based at Champaign (CMI). Examination of figure 89a shows cells (in a line) moving at different relative speeds, but yet in an organized fashion.

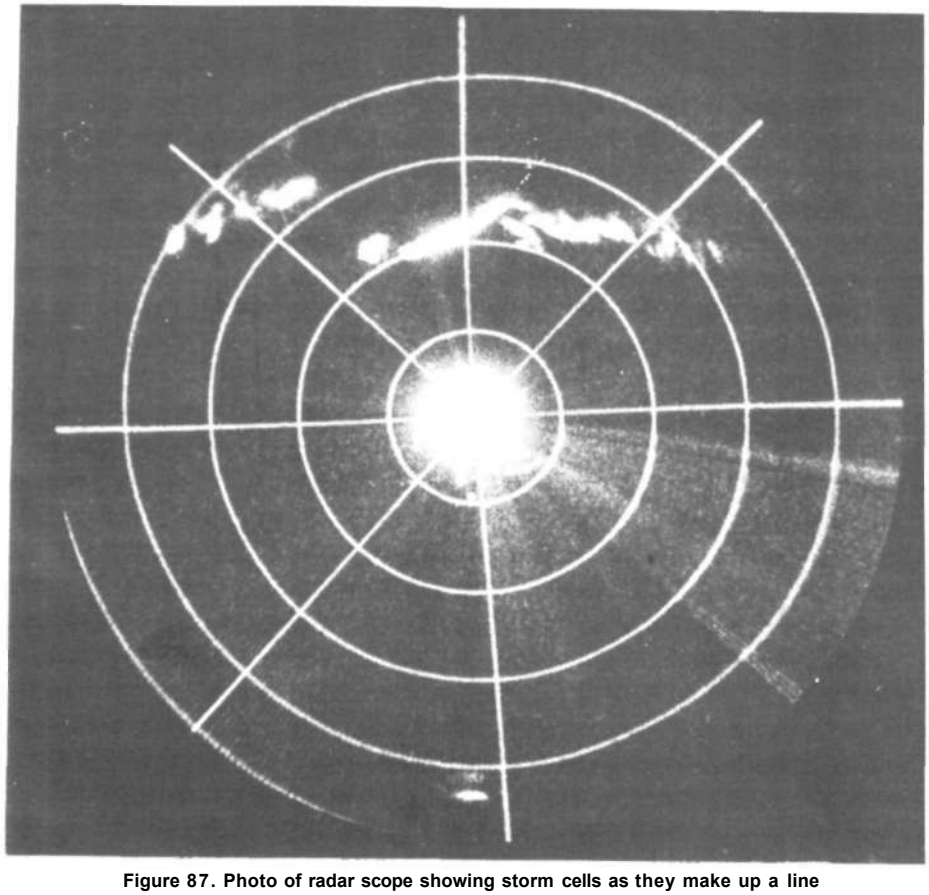

Figure 87. Photo of radar scope showing storm cells as they make up a line of thunderstorm activity

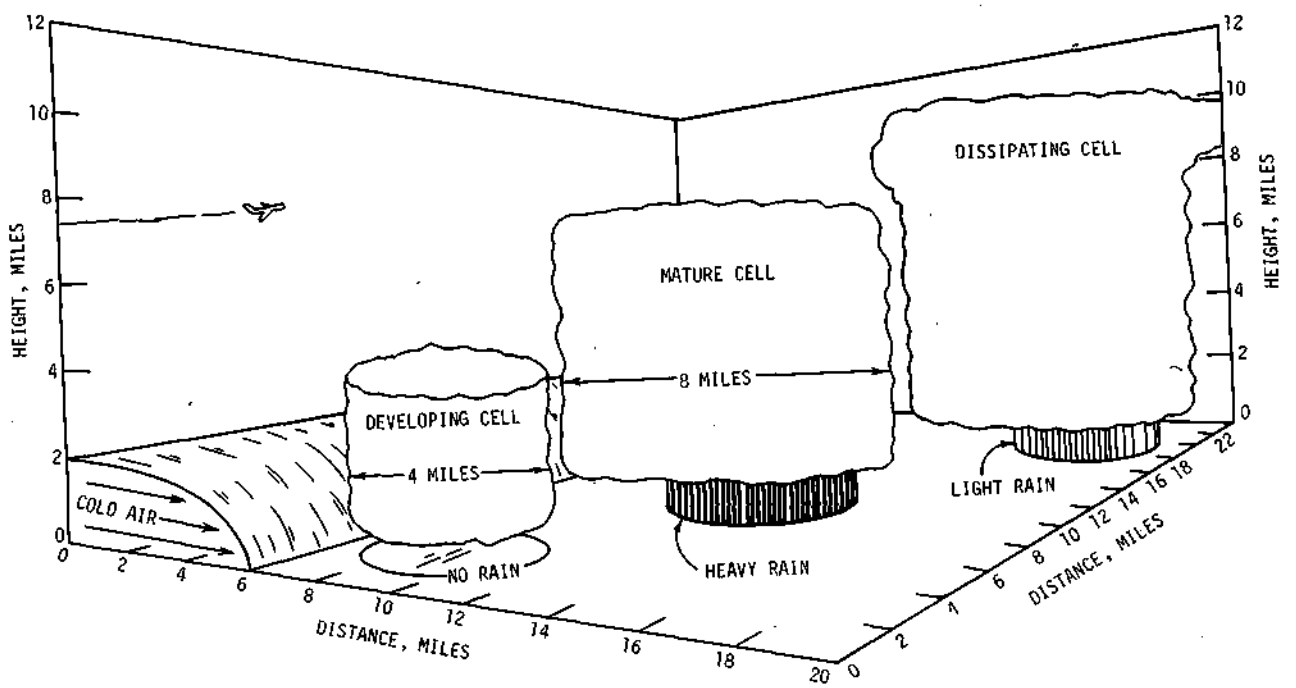

Figure 88. Schematic drawing of thunderstorm cells

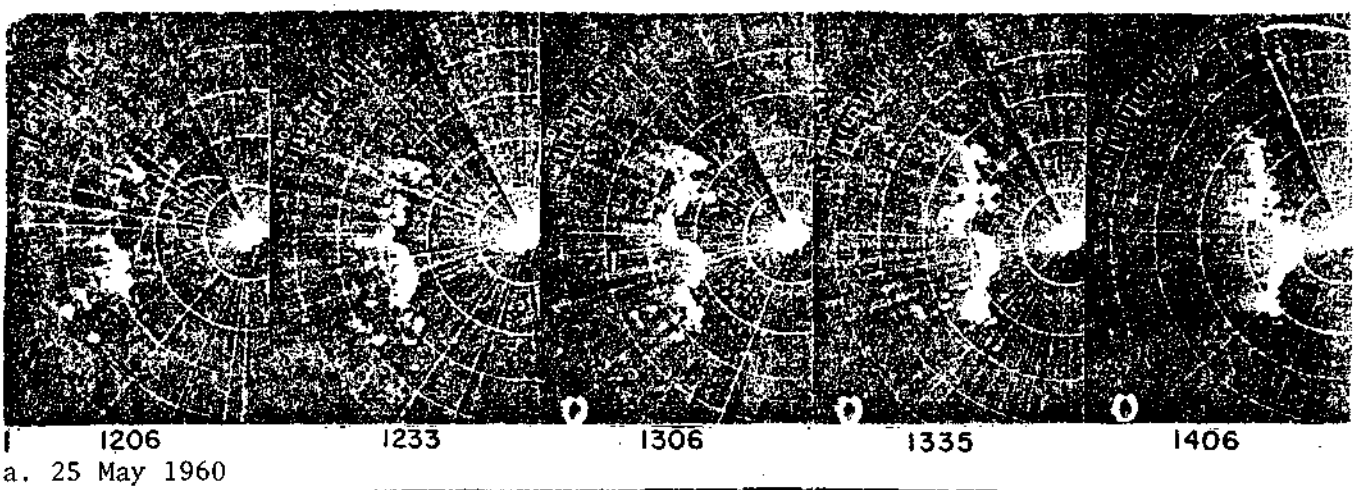

a. 25 May 1960

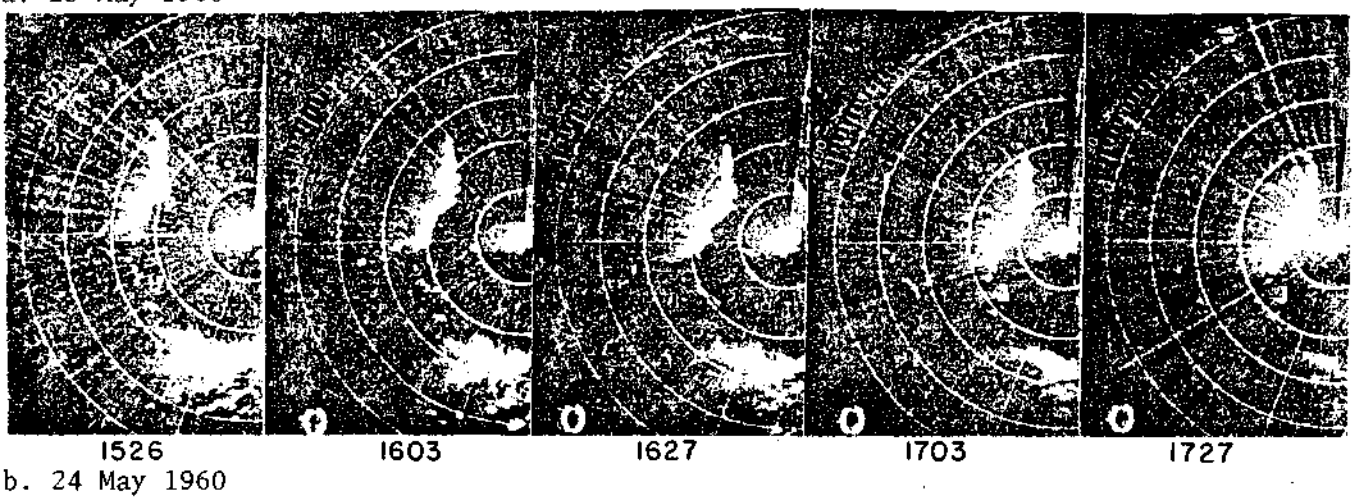

b. 24 May 1960

Figure 89. Radar lines in central Illinois, 250-nautical-mile range

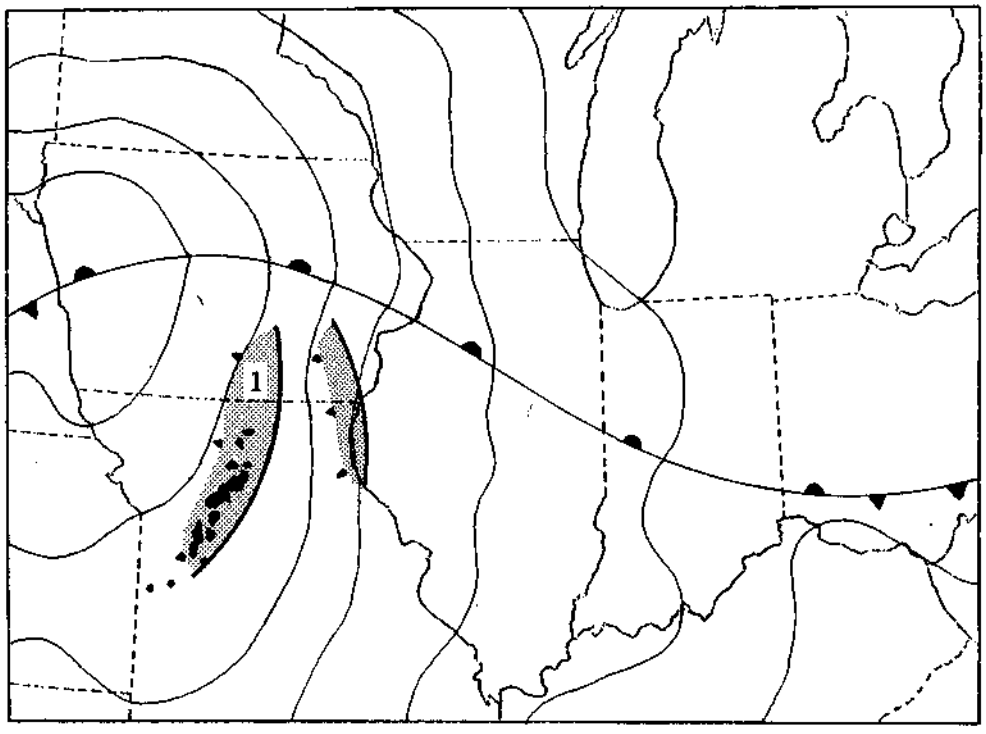

Figure 90. Radar synoptic composite 0600 CST, 16 May 1960

Note the flanking small cells that were growing along the right flanks, the right rear, and in advance of this line. The line revealed in figure 89b is a more solid wedge of precipitation remaining spatially coherent with time. Notable in this line are the new small echoes growing on the right flank, as well as a large area of lighter rain oriented west-east and south of the line moving from the WNW.

Wilk (1961) studied multiple lines in the Midwest using radar and satellite data. One of his case studies is presented as figures 90 through *96,* based on radar and synoptic composites developed over an 18-hour period. These figures show the evolution of two rather heavy squall lines across central Illinois during the morning hours (combining into one by 1200), followed by the line of precipitation along and just ahead of the cold front. These reveal the complexity (and intensity) that such lines can assume in a strong convective period. More detail on the development and evolution of the patterns is shown in figures 97-99 which pertain only to central Illinois. These show the detailed evolution of the lines.

Much of the detailed information that exists about precipitation lines comes from an extensive climatological study by Changnon and Huff (1961). One year of data were procured from a CPS-9, 3-cm radar located in east-central Illinois. For one large echo, or group of echoes to be classified as a line, the echo presentation had to have a rectilinear appearance with a length of more than 50 miles. Definition of a line, as opposed to a group of small echoes, had to contain at least four echoes with not more than 10 miles between any two echoes. The echoes also had to have sharply defined outlines. Two lines were considered a separate line if they were separated by a distance of 25 miles or more. All 206 lines studied were viewed from their inception until their dissipation.

Results for the 196 lines measured are presented in a series of tables and figures. Figure 100 shows the frequency distribution of the line orientations for every possible orientation. A majority had a SW-NE orientation. Another factor noted in the study was the tendency for lines to 'pivot' or rotate during their duration. The amount of pivoting is shown in table 36, which reveals that 105 lines (half) did not pivot whereas the other 91 lines pivoted, typically 12 degrees or more during their lifetimes. This pivoting is due partially to the relatively more rapid growth along one end of the line. Figure 101 presents the distribution of line movements, showing the preference for motion from the southwest, west, and northwest as expected.

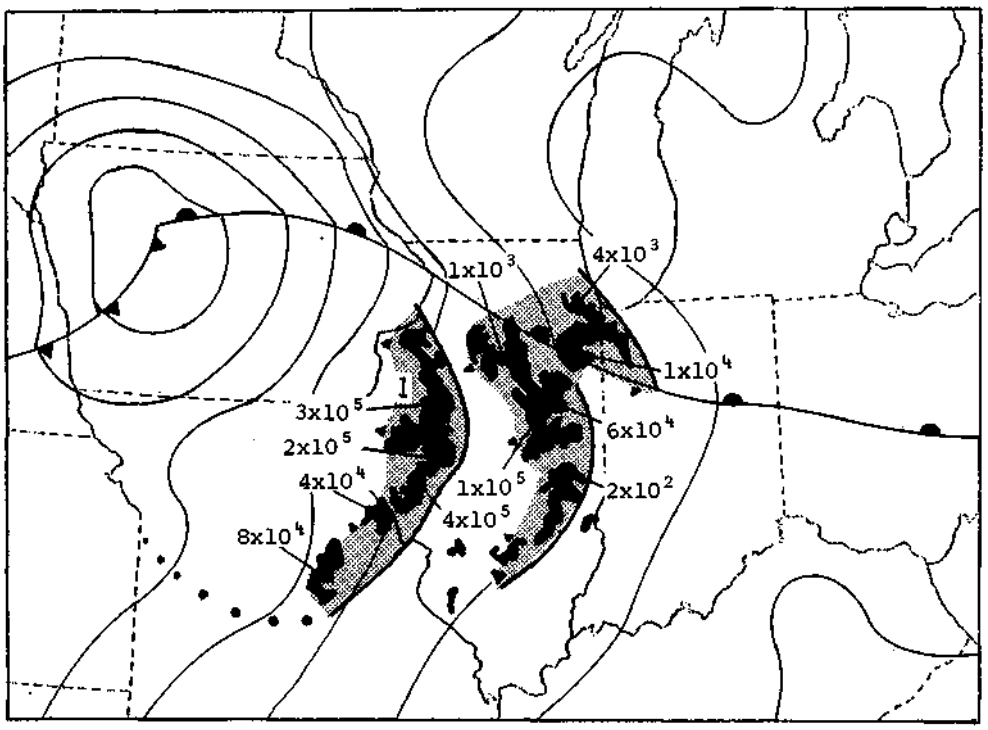

Figure 91. Radar synoptic composite 0900 CST, 16 May 1960

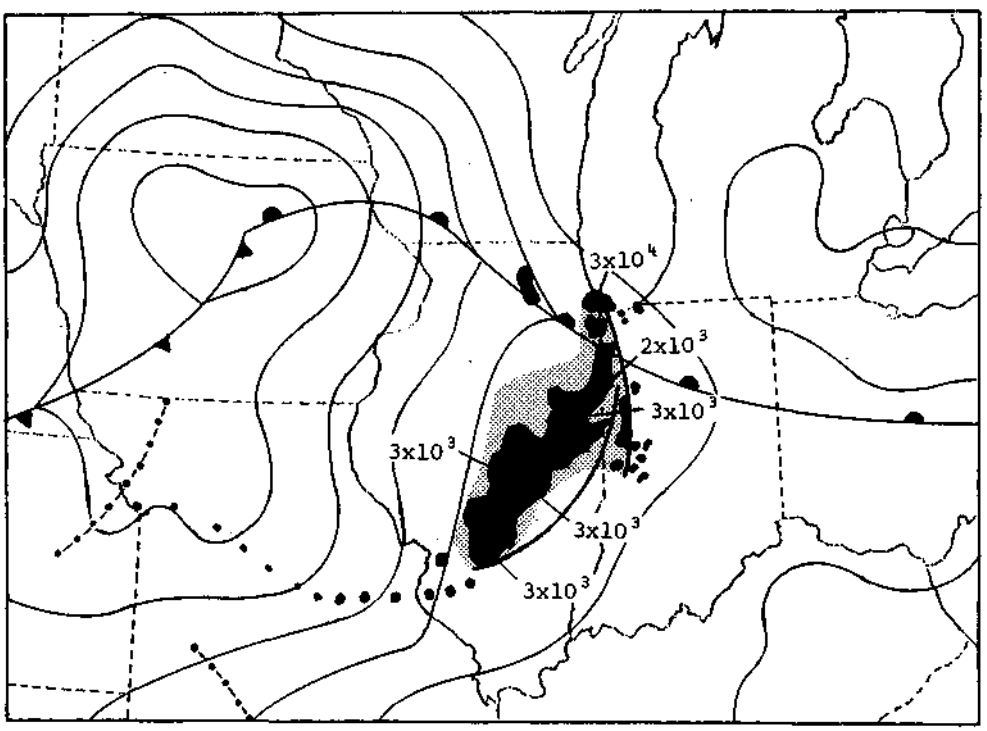

Figure 92. Radar synoptic composite 1200 CST, 16 May 1960

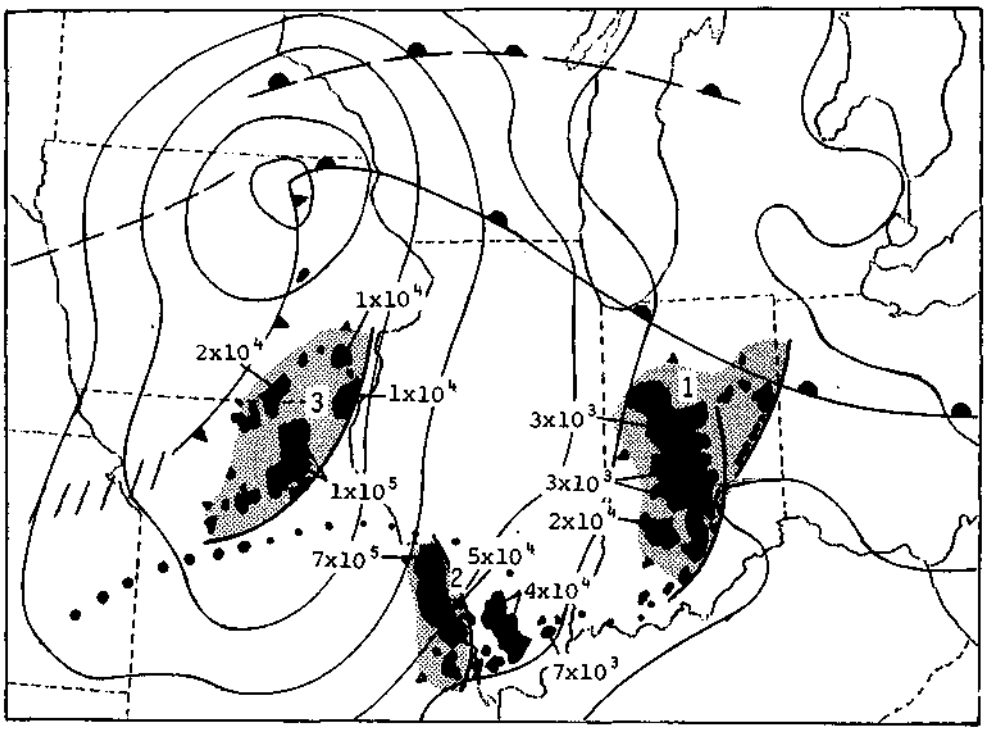

Figure 93. Radar synoptic composite 1500 CST, 16 May 1960

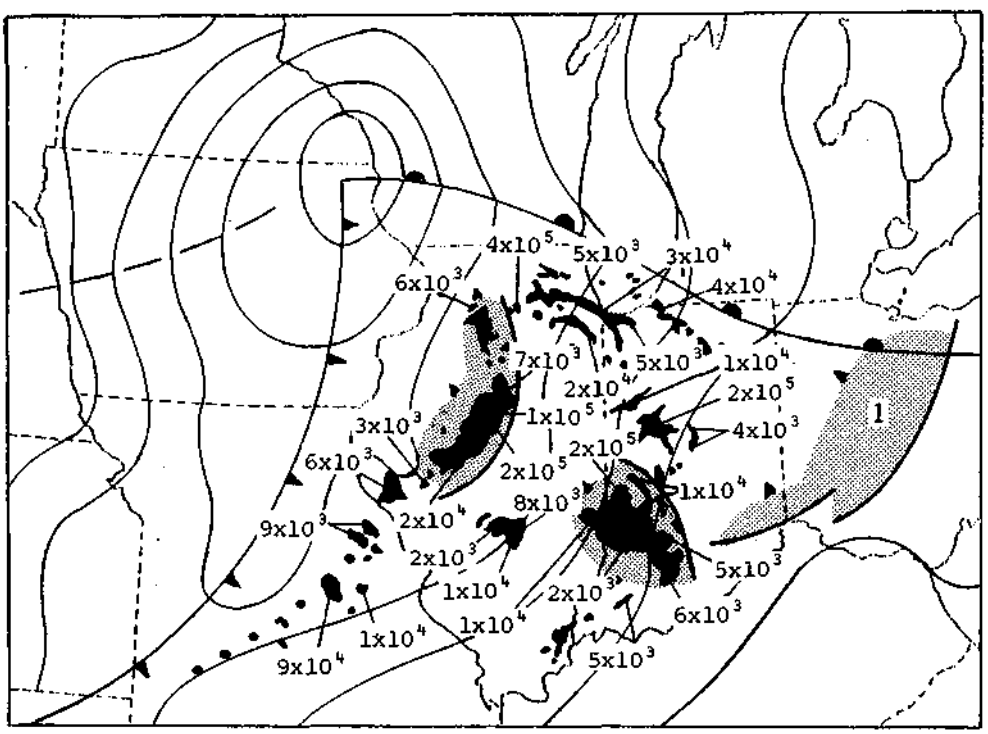

Figure 94. Radar synoptic composite 1800 CST, 16 May 1960

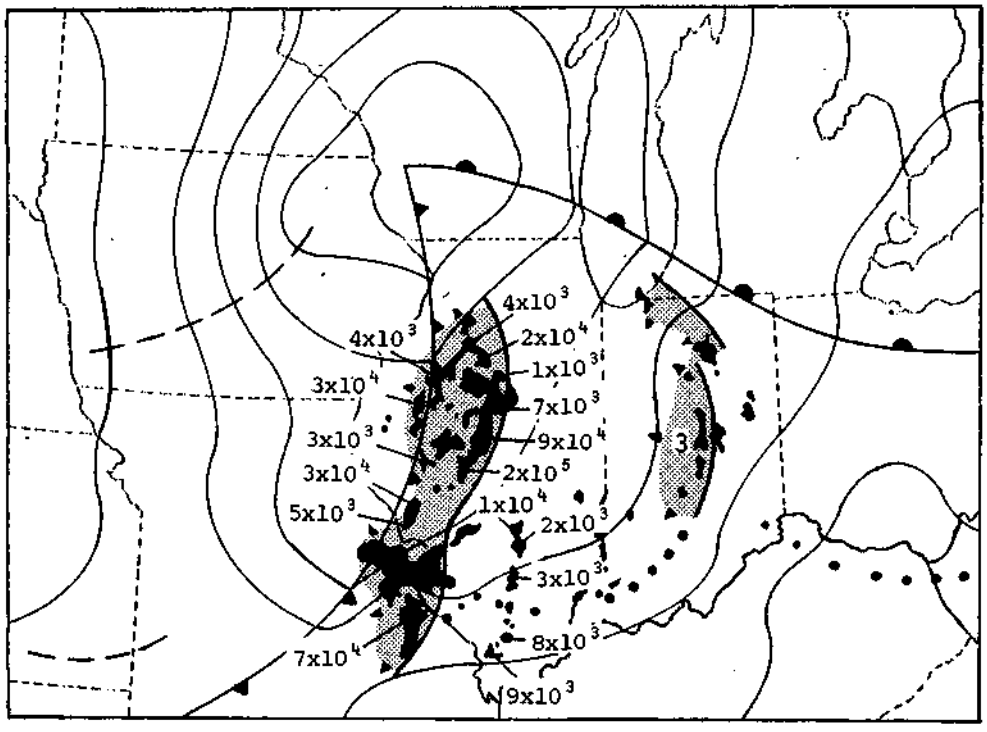

Figure 95. Radar synoptic composite 2100 CST, 16 May 1960

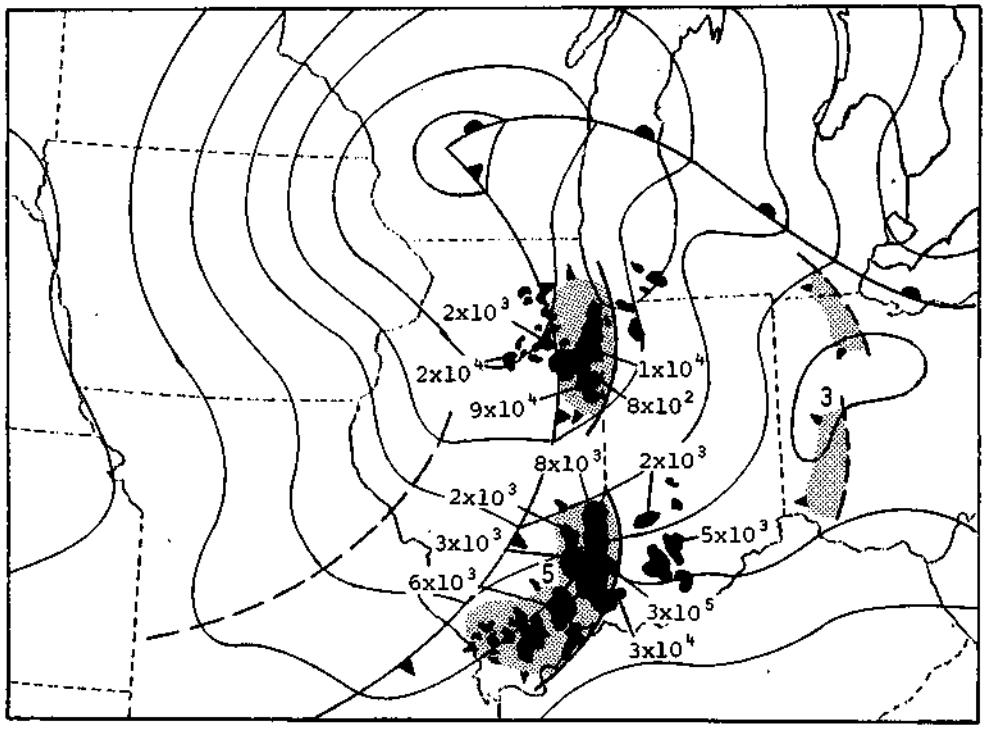

Figure 96. Radar synoptic composite 2400 CST, 16 May 1960

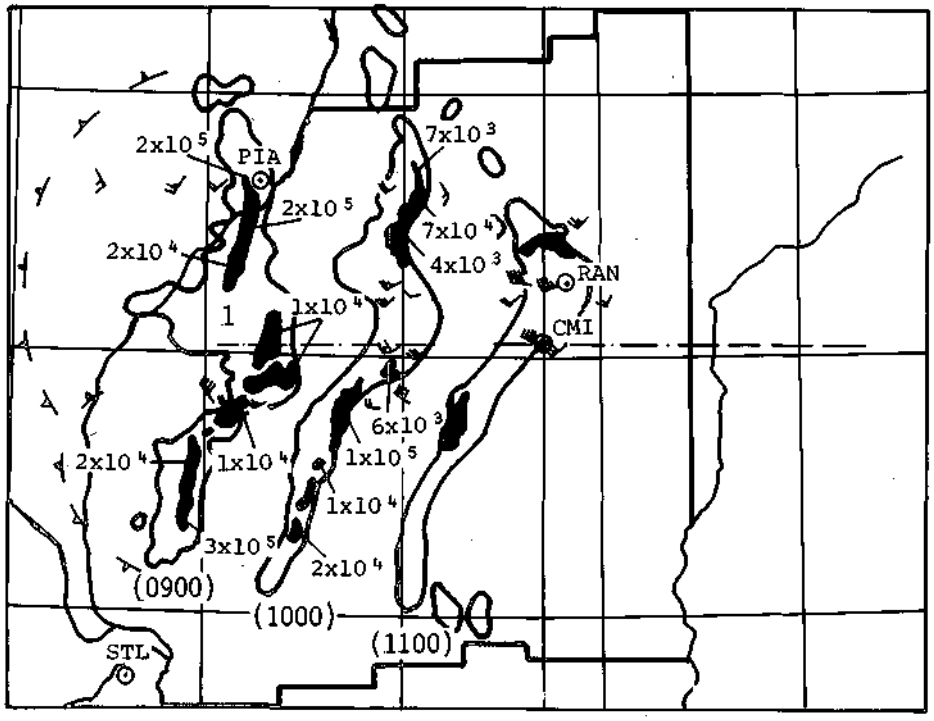

Figure 97. Radar echo composites 16 May 1960

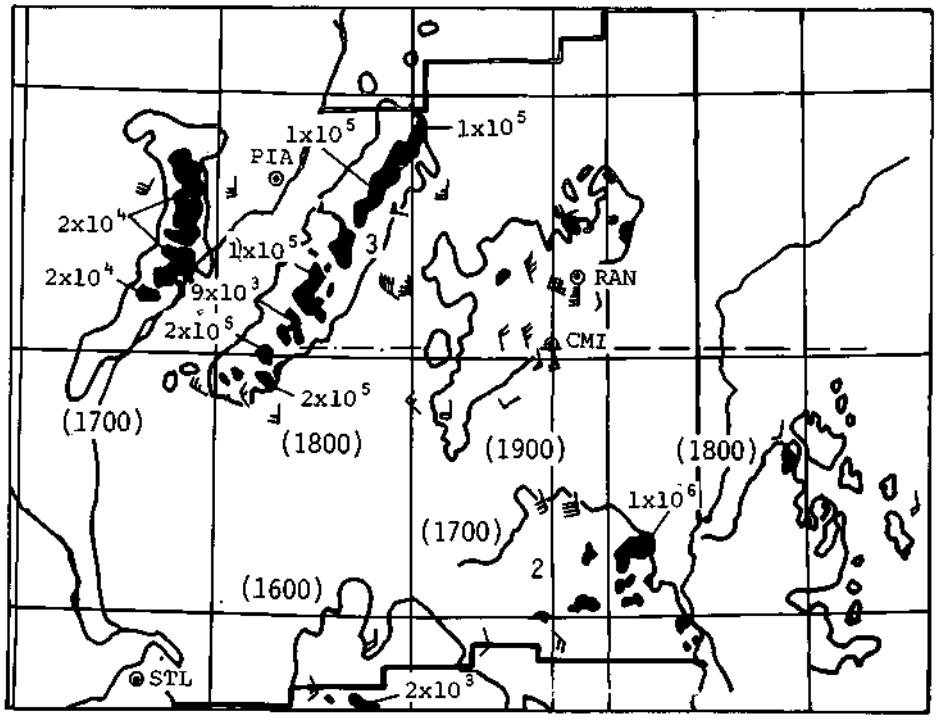

Figure 98. Radar echo composites 16 May 1960

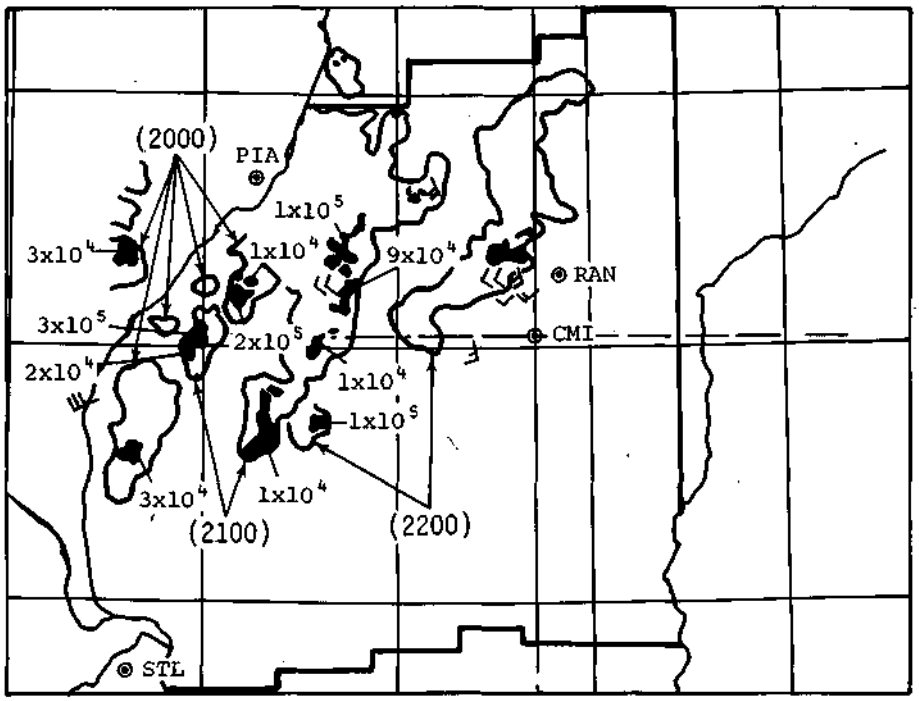

Figure 99. Radar echo composites 16 May 1960

Table 36. Total Amount of Pivoting during Line Duration, Central Illinois

	Number of lines				
Degrees rotation	*Clockwise pivoting*	*Counter-clockwise pivoting*	*Non-pivoting*	*Total*	*Lines with severe weather*
0–3.9	0	0	54	54	3
4–7.9	0	0	31	31	6
8–11.9	6	4	20	30	3
12–15.9	10	13	0	23	1
16–19.9	6	3	0	9	6
20–23.9	7	7	0	14	4
24–27.9	3	8	0	11	3
28–31.9	3	4	0	7	0
32–35.9	1	4	0	5	2
36–39.9	2	2	0	4	2
≥40	2	6	0	8	4
Mean	21°	25°	4°	13°	22°
Median	18°	23°	3°	9°	18°
Greatest	60°	67°	10°	67°	67°
Least	11°	11°	0°	0°	0°

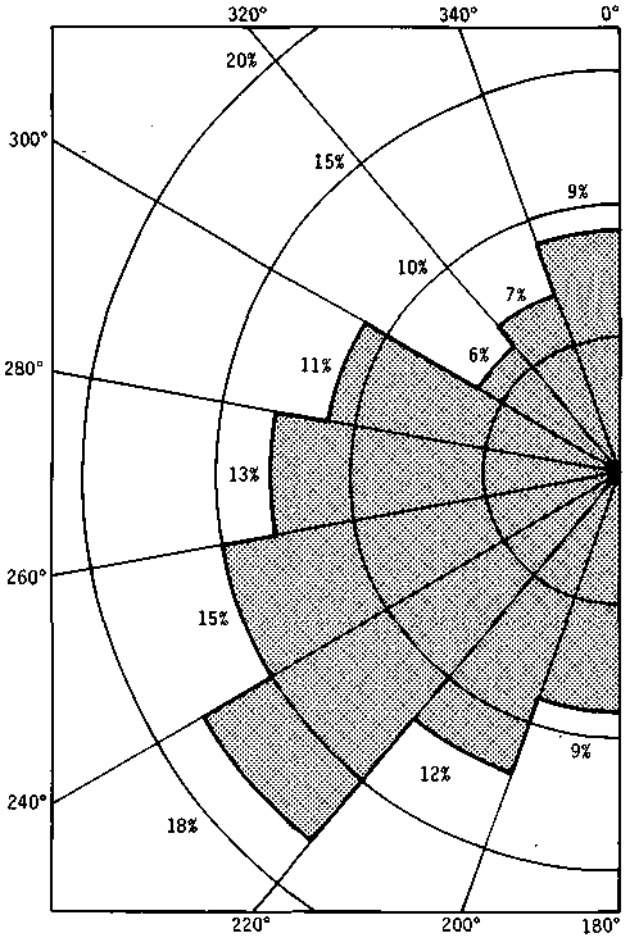

Figure 100. Distribution of line orientations, CPS-9 [frequency in each 20° sector expressed as a percent of total (196) lines, central Illinois]

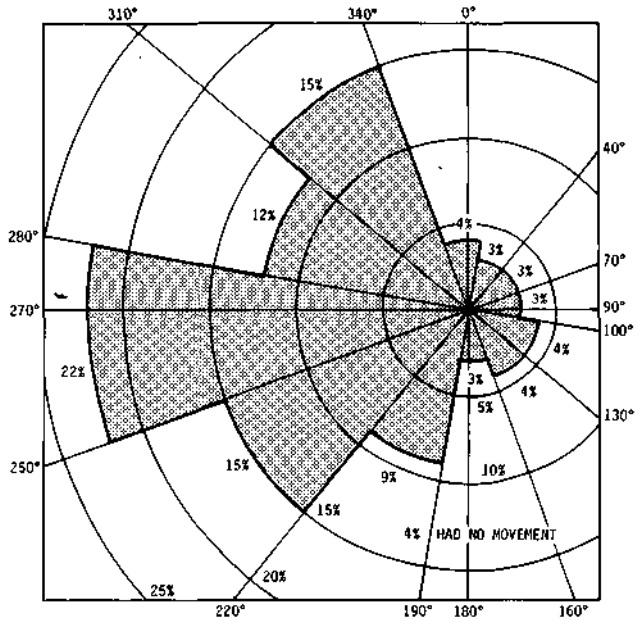

Figure 101. Direction of line movements, CPS-9 [frequency in each 30° sector expressed as percent of total (196) lines]

Table 37 presents the line speed values which reveal that the median value is 24 knots with a wide variety of speeds. Table 38 presents distribution of lines by their lengths, showing the median was 88 nautical miles, and that lines producing severe weather were considerably longer, 125 nautical miles. The widths of lines appear in table 39 showing the median as 7 nautical miles but varying from 37 to 3. Table 40 presents the growth tendencies exhibited during the four equal periods of line duration. These values show preponderance for an increase in line size and intensity during the first quarter. Line durations appear in table 41. These show a mean duration of 2.6 hours, and also show that lines which produced severe weather had much longer durations. The diurnal distribution of the lines appears in table 42. These results are biased by lack of radar operations during the 2000 to 0800 CST period. Within the general operational period there seems to be little diurnal difference. The climatology of monthly line frequencies appears in table 43. These show a preponderance of lines within the spring and summer months with few in August. Also shown are the average number of lines on days when lines occur. In most summer months, at least two or three lines are typical.

Figure 102 presents the location of the center points of the lines studied. In general, no preference for line formation is shown. The median values of 'climatological' or all lines are summarized in table 44 along with median values for lines that produce severe weather (hail, tornadoes, or heavy rainfall rates). Severe weather lines generally are longer lasting, larger, and faster moving than the climatological lines. Schematics of these typical, or average, lines are portrayed in figure 103. The position of the lines in relation to the radar, CMI, is not particularly relevant.

Tables 45 and 46 present information about the behavior and characteristics of lines when severe weather occurred. These are based on the 34 lines that were associated with severe weather. Many of these lines exhibited, in the area of damage, relatively sudden changes in speed, size, or pivoting. Table 46 presents a distribution of damage location along the lines. This indicates that much of the

Table 37. Average Line Speed Sorted by 5-Knot Intervals

Speed, knots	Number of lines: Clockwise pivoting	Counter-clockwise pivoting	Non-pivoting	Total	Lines with severe weather
0–5	0	1	8	9	0
6–10	2	2	11	15	1
11–15	4	4	14	22	0
16–20	4	7	25	36	3
21–25	6	6	8	20	4
26–30	8	8	11	27	5
31–35	7	5	7	19	7
36–40	3	4	9	16	3
41–45	0	7	2	9	3
46–50	2	3	1	6	0
51–55	2	1	3	6	4
56–60	2	0	2	4	2
≥61	0	3	4	7	2
Mean	29	32	24	27	36
Median	28	30	20	24	34
Greatest	56	72	68	72	70
Least	8	0	0	0	8

Table 38. Average Line Lengths Sorted by 20-Mile Intervals

Length, nautical miles	Number of lines: Clockwise pivoting	Counter-clockwise pivoting	Non-pivoting	Total	Lines with severe weather
50–70	8	9	34	51	1
71–90	9	12	28	49	3
91–110	6	8	16	30	10
111–130	4	8	10	22	5
131–150	7	5	8	20	3
151–170	3	4	4	11	2
171–190	1	3	1	5	4
191–210	0	2	1	3	0
211–230	2	0	1	3	3
≥231	0	0	2	2	3
Mean	110	108	94	101	142
Median	96	96	83	88	125
Greatest	221	203	243	243	243
Least	60	51	49	49	70

Table 39. Line Widths Sorted by 4-Mile Intervals

Width, nautical miles	Number of lines: Clockwise pivoting	Counter-clockwise pivoting	Non-pivoting	Total	Lines with severe weather
0-4	6	6	32	44	1
4.1-8	11	18	43	72	10
8.1-12	12	15	19	46	10
12.1-16	6	5	4	15	10
16.1-20	1	5	4	10	3
20.1-24	0	1	2	3	0
24.1-28	2	1	0	3	0
≥28.1	2	0	1	3	0
Mean	11	10	8	9	11
Median	9	9	6	7	9
Greatest	37	26	33	37	20
Least	3	3	3	3	4

Table 40. Comparison of Growth Tendencies in Each Quarter Period of Line Duration Expressed as a Percent of All 196 Lines

Growth tendency	Quarter periods: First	Second	Third	Fourth
Increase (I)	58	32	26	10
Neutral (N)	21	37	28	19
Decrease (D)	21	31	46	71
Growth tendency coded in descending order of frequency	IND	NID	DNI	DNI

Table 41. Duration of Lines Sorted into ½-Hour Intervals with Number per Interval Expressed as a Percent of Total Lines

Duration, in hours	Number of lines: Clockwise pivoting	Counter-clockwise pivoting	Non-pivoting	Total	Lines with severe weather
0.5-1.0	10	17	35	26	0
1.1-1.5	19	10	26	20	3
1.6-2.0	10	14	11	12	12
2.1-2.5	15	12	2	7	6
2.6-3.0	8	8	10	9	9
3.1-3.5	12	6	3	5	6
3.6-4.0	8	4	3	4	22
4.1-4.5	5	10	3	5	12
4.6-5.0	0	4	1	2	0
5.1-5.5	2	4	1	2	6
5.6-6.0	2	2	2	2	6
6.1-6.5	2	0	1	1	6
6.6-7.0	0	4	0	1	6
≥7.1	7	5	2	4	6
Total lines	40	51	105	196	34
Mean	3.2	3.4	2.1	2.6	4.3
Median	2.5	2.5	1.4	2.0	4.0
Longest	9.0	15.0	7.8	15.0	8.0
Shortest	1.0	1.0	0.5	0.5	1.5

Table 42. Time of Line Formation in the 0600 to 2300 CST Period Expressed as a Percent of Total Lines

Hour ending (CST)	*Clockwise pivoting*	*Counter-clockwise pivoting*	*Non-pivoting*	*Total*	*Lines with severe weather*
07	0	0	2	1	6
08	5	16	5	7	3
09	12	8	5	7	3
10	0	12	8	8	3
11	13	4	7	8	6
12	10	4	7	7	12
13	15	13	6	10	17
14	3	4	11	8	6
15	10	8	8	8	6
16	8	13	7	9	11
17	2	4	10	8	6
18	10	8	7	8	9
19	10	0	4	4	0
20	0	4	4	2	3
21	2	0	5	3	3
22	0	0	2	1	3
23	0	2	2	1	3
Maximum 1-hour period	12–13	07–08	13–14	12–13	12–13
Maximum 2-hour period	11–13	07–09	13–15	12–14	11–13
Maximum 3-hour period	10–13	07–10	13–16	12–15	11–14

Table 43. Monthly Line Frequency Data

	Aug	*Sep*	*Oct*	*Nov*	*Dec*	*Jan*	*Feb*	*Mar*	*Apr*	*May*	*Jun*	*Jul*
Number of days radar operation	22	7	25	20	21	27	24	24	21	26	26	21
Number of days with lines	3	3	14	8	7	4	2	5	11	14	20	18
Percent of operational days with lines	14	43	56	40	33	15	8	21	52	54	77	86
Lines per month	5	5	37	15	13	6	4	19	32	34	62	88
Average number lines on days with lines	2–	2–	3–	2	2	2–	2	4	3	2+	3	5
Maximum number of lines on one day	3	2	8	3	3	2	3	7	8	5	12	16

Table 44. Comparison of Line Data (Medians) for Lines Associated with Severe Weather with Data from Climatological Lines

Lines	*Duration, hours*	*Length, nautical miles*	*Width, nautical miles*	*Orientation, degrees*	*Pivot per hour, degrees*	*Speed, knots*	*Direction of movement, degrees*
Climatological	2.0	88	7	255	4	24	265
Severe weather	4.0	125	9	240	5	34	265

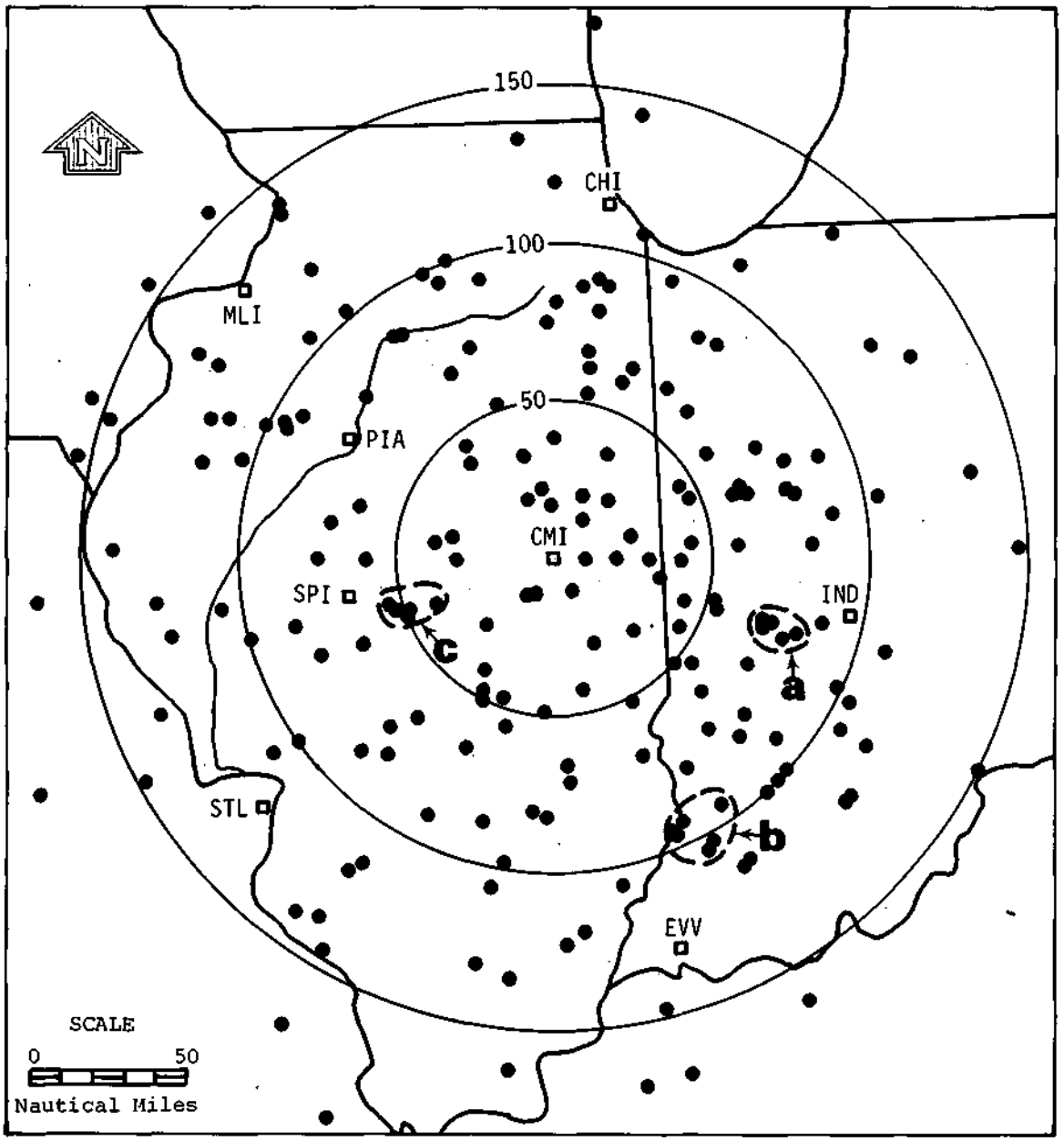

Figure 102. Location of center points of lines at time of first appearance, CPS-9

Table 45. Sudden Changes in Portions of Lines near the Damage Area at the Time of Damage Produced by Severe Weather

	Type of Change							
	No change	*Intersection of lines*	*Increase pivot*	*Increase speed*	*Increase size*	*Increase in speed and pivot*	*Increase in speed and size*	*Increase in speed, size, and pivoting*
Number of lines	4	2	3	9	1	10	4	1
Percent of total severe weather lines	12	5	9	26	3	30	12	3

Table 46. Location of Damage along Major Axis of Lines Associated with Severe Weather

	Along entire line	*Left end*	*Left and center*	*Center*	*Right and center*	*Right end*
Number of lines	3	19	5	1	1	5
Percent of total lines with severe weather	9	55	15	3	3	15

damage occurred on the 'left end,' as viewed from the radar (which is typically the more southerly end).

Less Organized Groups of Cells

Less vigorous, less well organized groups of cells also occur in Illinois. These often appear on a radar as semi-random entities and upon close monitoring, one finds small groups of cells that typically develop and move along with some interaction between cells. These are typically within the squall zone class *{see* table 28). An example of the precipitation pattern derived from such a semi-organized but small groups of cells is shown in figure 27a. The precipitation can be heavy, as in this case, often depending upon the number of flanking cells that grow and merge around the initial shower or storm entities.

Ackerman and Greenman (1978) presented a description of the evolution of such a multicellular convective cloud mass in Illinois. The cloud complex they studied was part of a small but 'active' line that propagated westward, or upwind. The initial echo of the complex (figure 104), labeled as mother cloud, developed a few miles southwest of an older multicellular complex. Most of the new cells occurred as a series of feeder cells forming successively on the southwest end of the mother cloud mass shown in figure 104. There is very little translation of the individual echoes during their development. The time history of the top of the radar echoes shown in figure 104 appears in figure 105, along with the rain rate. As the feeder clouds developed, they moved in and merged with the mother cloud, forming many arrays of cells as shown in figure 104. Dynamic interaction between the feeder cells and the main cloud were suggested by the time histories of the summits of the main echo. As each new feeder cell developed (echoes A through D), the descent of the mother cloud either ceased or perceptively slowed.

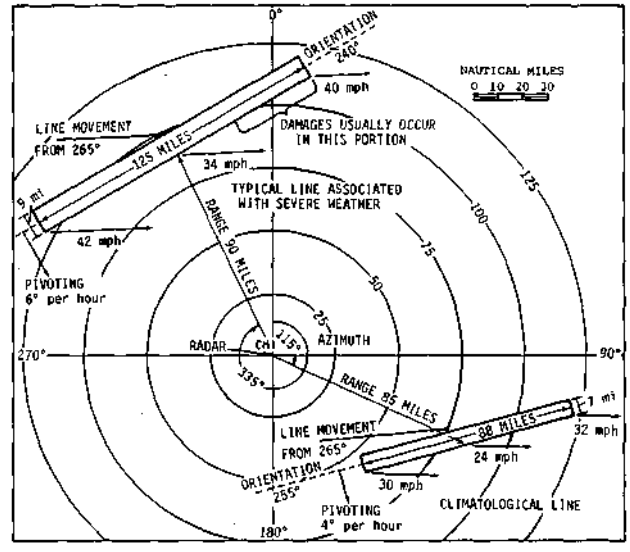

Figure 103. Pictorial illustration of typical radar-depicted lines as synthesized from median measurements

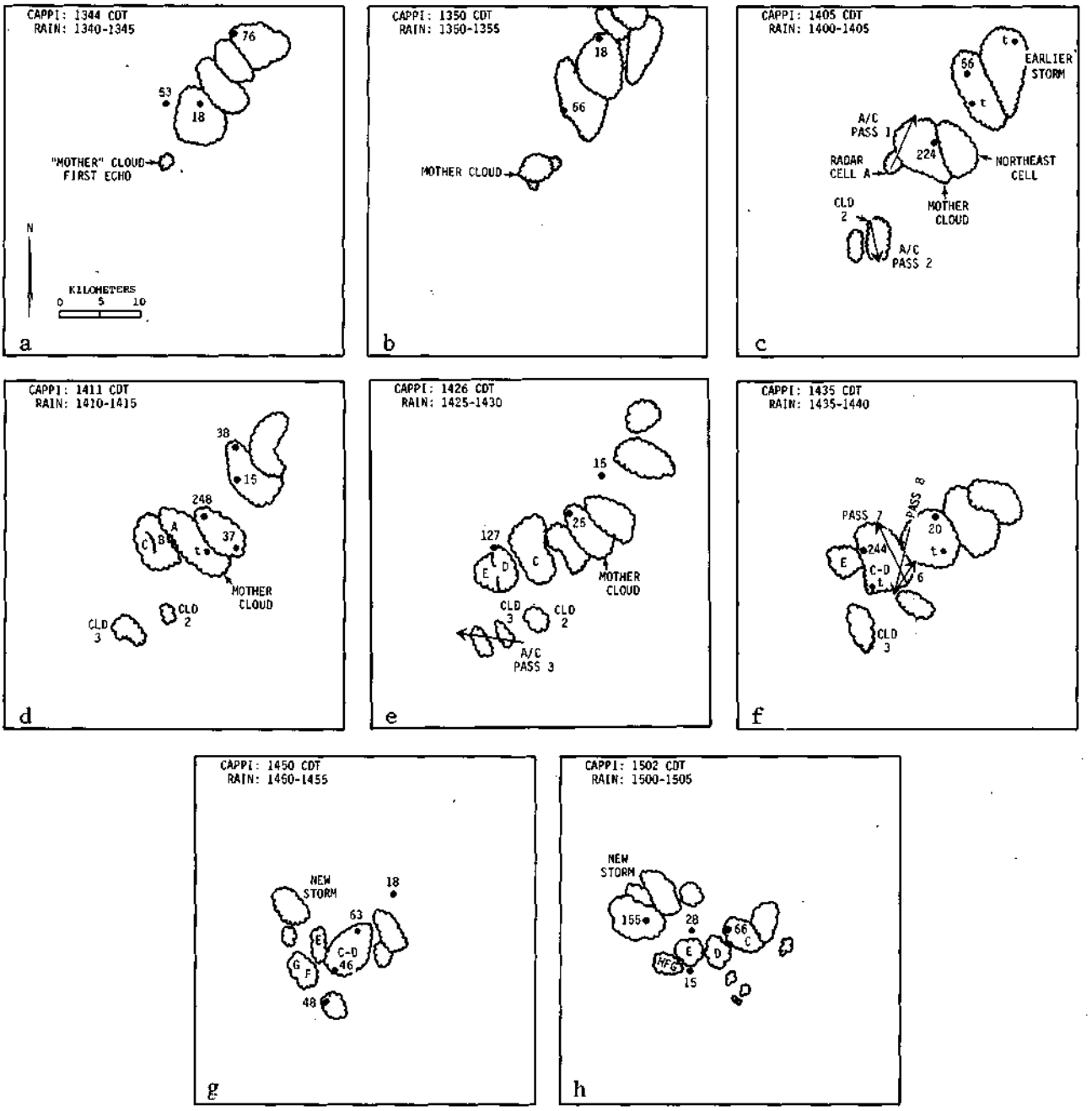

Figure 104. Radar echoes and surface rainfall at 8 times during the life cycle of the storm studied [Scalloped outline gives 5000-ft CAPPI limits; rainfall is in 5-min rates (10^{-2} cm/h); airplane traverses shown by arrows in (c), (e), and (f)]

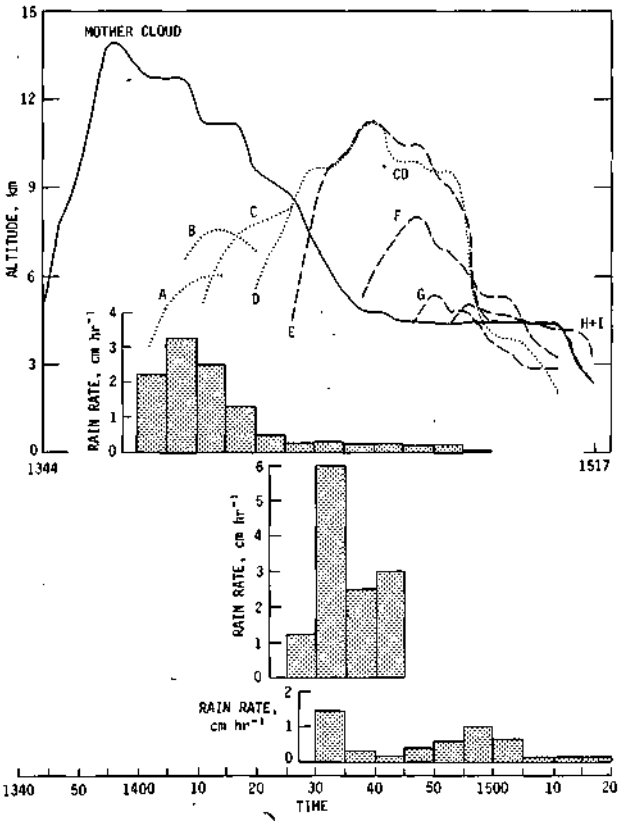

Figure 105. Radar echo tops (line graphs) and 5-min rain rates (bar graphs) versus time, CDT

INDIVIDUAL STORM CELLS

Introduction

A wide variety of Water Survey studies have concerned individual storm cells, as defined by radars and by dense networks of recording raingages. The radar studies have extensively examined both the vertical and the horizontal properties of these cells. These cells at the surface might be defined often as rainfall cores. Since there is a great amount of information about 'cells,' the information has been presented in two sections, one about their vertical characteristics as reflected in radar data, and one about their horizontal characteristics as measured by radar and by dense networks of raingages.

Figures 106 through 108 help define what a rain cell may be in Illinois. Figures 106 and 107 are 3-dimensional storm re-creations (based on RHI radar data for a thunderstorm in central Illinois and separated by 10 minutes in time). The storm had a multicellular nature with tops extending to above 30,000 feet in a complex intertwined nature. Ten minutes later (figure 107) the structure of the large thunderstorm (which produced damaging hail and heavy rainfall) had changed greatly. Several cells descended to the surface with their tops below 10,000 feet, and new cells of 0.5- to 1-mile diameter developed and grew in the left central portion of the storm.

Figure 108 shows the rainfall pattern produced at the ground by the typical small thunderstorm cell, based on recording raingage data. Rainfall traces from this storm at three selected raingages

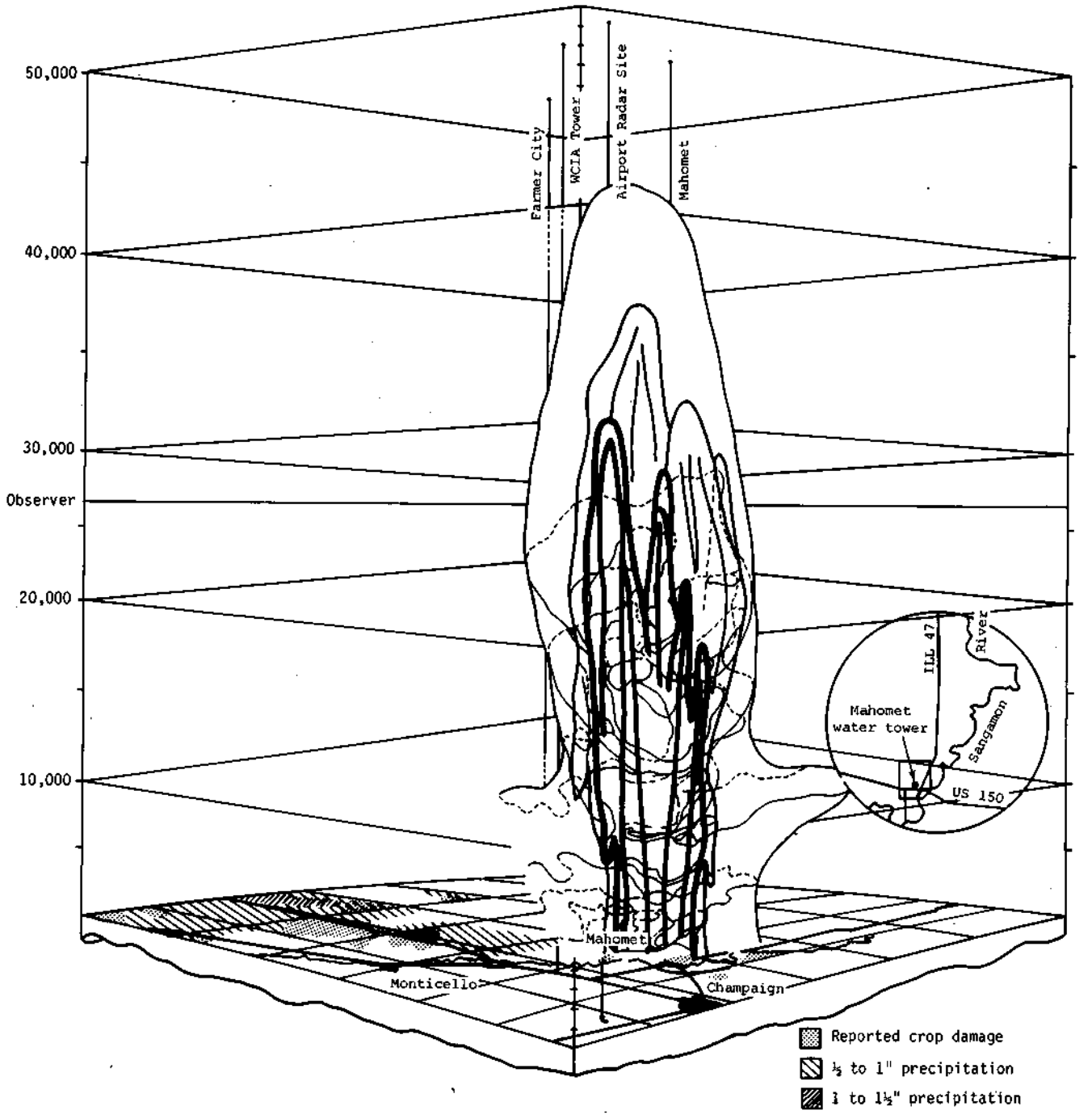

Figure 106. Radar echo composite 2120 CST, 8 September 1960

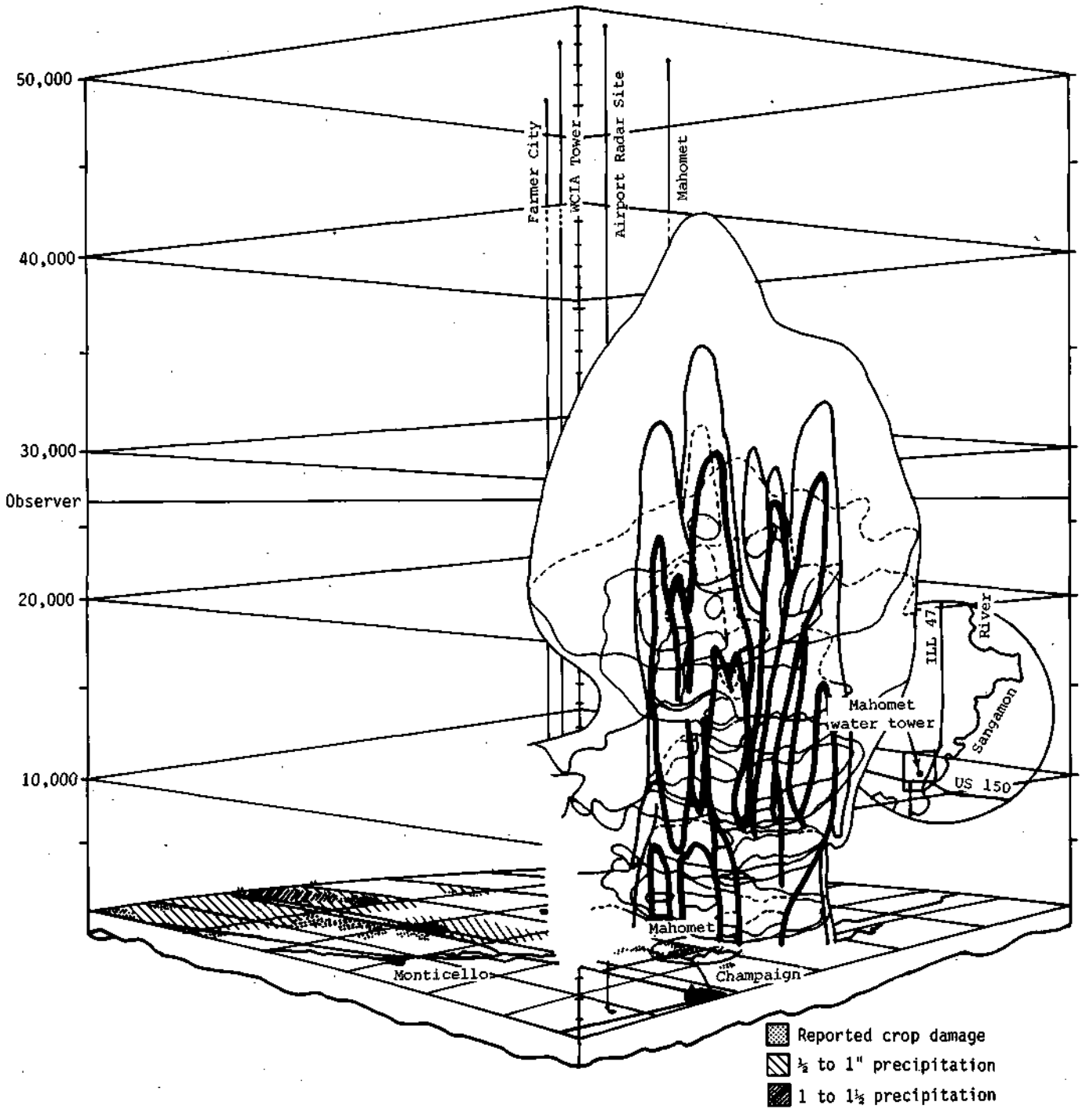

Figure 107. Radar echo composite 2130 CST, 8 September 1960

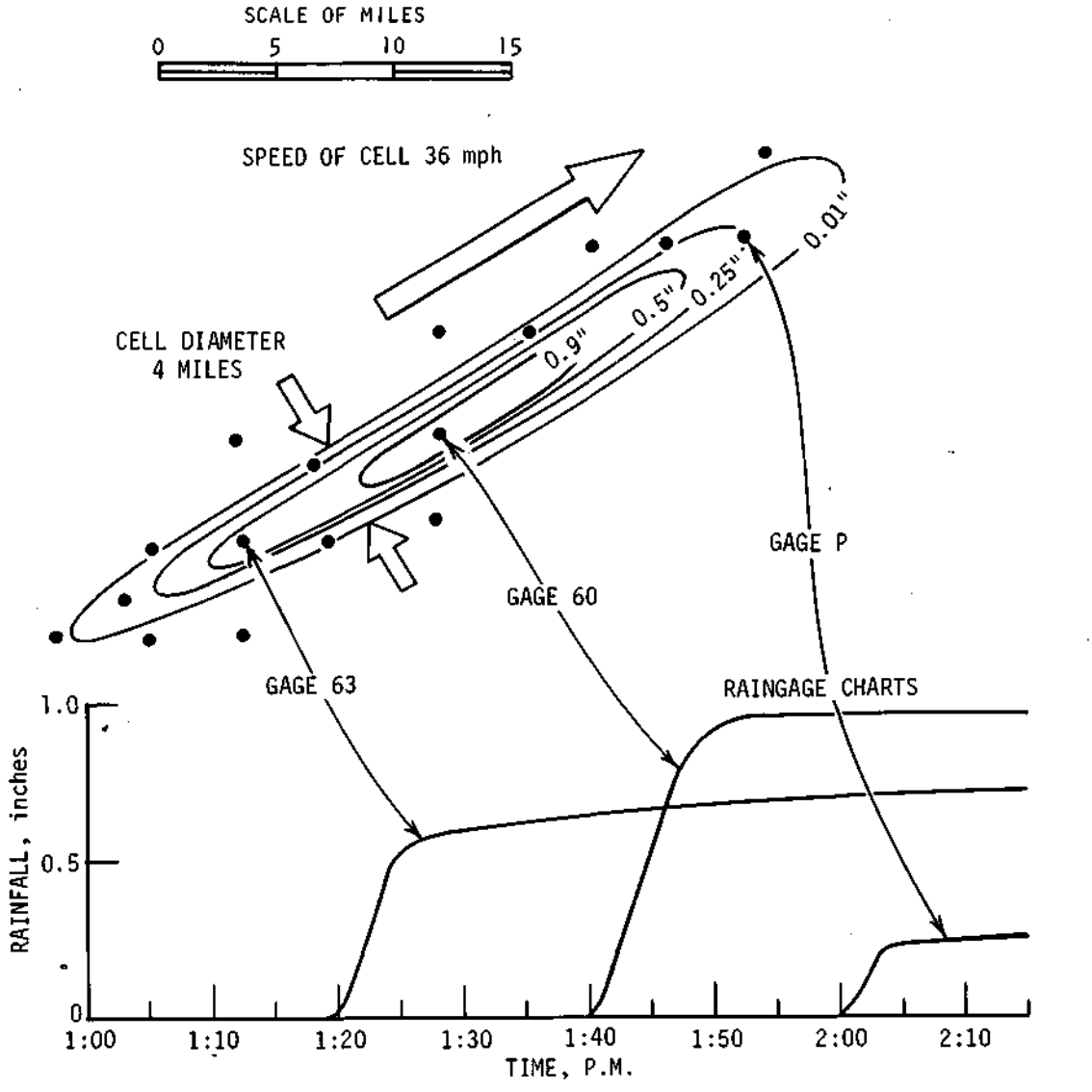

Figure 108. A single storm cell's size, speed, and magnitude for storm of 2 June 1965 on Little Egypt Raingage Network in southern Illinois

along its main axis are presented. Essentially, the cell shown in figures 106-107 had a surface diameter of approximately 6 miles, comparable to that shown in figure 108. This indicates that a thunderstorm cell which has a single core at the surface may be produced by a series of very small convective elements aloft in the rain-producing cloud mass.

Vertical Characteristics

One set of observations of 'first echoes,' defined as the first appearance of measurable precipitation by radar and indicating the formation of detectable precipitation aloft, was made in central Illinois with a 3-cm, CPS-9 radar (Semonin et al., 1962). The pattern of first echoes detected between 10 and 40 miles from the radar in east central Illinois is shown in figure 109. The data came from 1960 and 1962, and the distribution appears to be quite random. The frequency distribution of the tops of first echoes appears in figure 110. This shows a predominance of tops between 10,000 and 14,000 feet. When the initial echo top is related to the height of the freezing level, it was noted that 56% of all the first echoes formed as all-water echoes, pointing to the importance of the coalescence mechanism in summer rainfall.

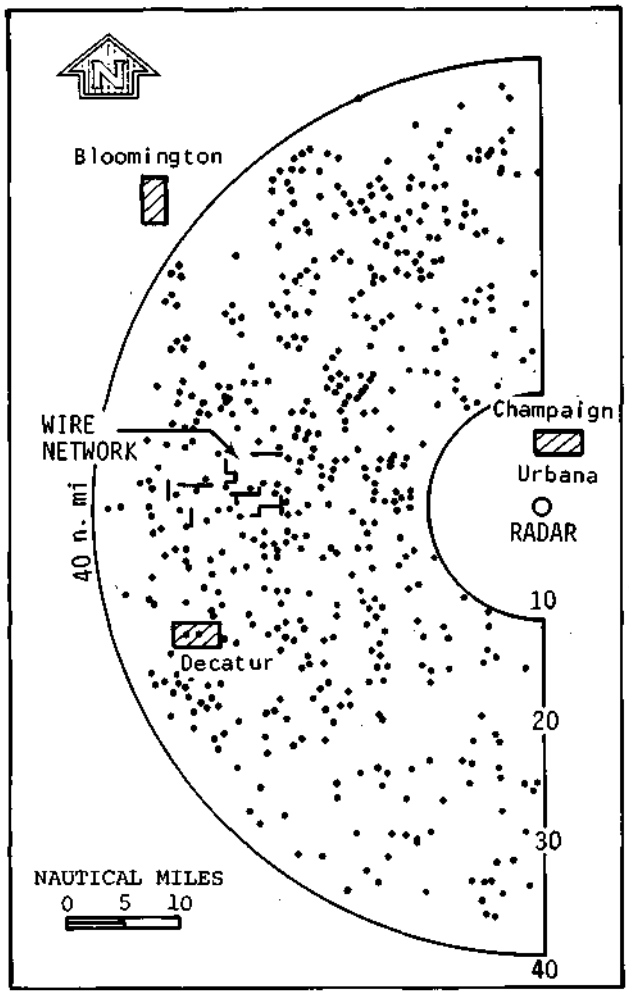

Figure 109. Location of first echoes from 10 June to 30 August 1960 and from 1 May to 6 August 1962 during operational periods

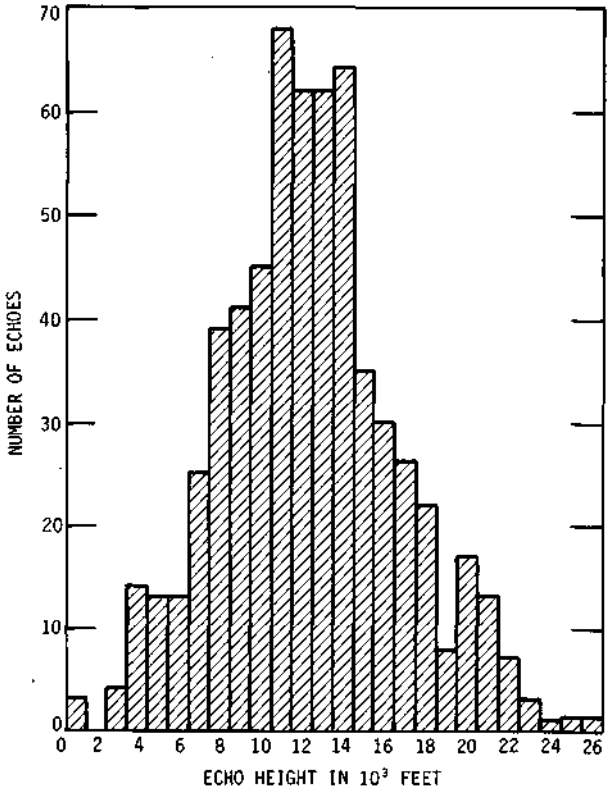

Figure 110. Frequency distribution of the tops of first echoes for the years 1960 and 1962

The METROMEX program at St. Louis also focused on the incidence of first echoes, primarily as an indicator of local effects on precipitation (Changnon, 1978). The pattern, based on regional frequencies of first echoes as shown in figure 111, indicates greater incidences of first echoes during July-August 1973 in the urban and industrial areas. This is based on 811 first echoes. The average tops, bases, and heights for first echoes over each of the physiographic and land use areas shown in figure 111 appear in table 47. The echoes are also separated according to whether they were associated with organized systems (lines) or were isolated echoes. The results for echoes in organized systems show that those over the urban area, bottomlands, and hill areas were much the same, although the urban first echo had a slightly lower base and taller top. All had lower bases than the typical rural echo with the base at 3.2 km and a top at 6.7 km (table 47). The isolated echoes had markedly lower tops and bases than did the first echoes with organized systems. The results do show that echoes forming over different types of natural surfaces tend to have varying and systematic differences.

Echo Growth. An interesting sequence revealing the structure of the first echo of an isolated storm and its ensuing feeder first echoes is shown in figure 112 (Vogel, 1975). This shows a cross-section through an air mass thunderstorm with its multiple cells building and dissipating as they move from left to right (west to east) through the core of the storm. This is very common in many semi-isolated summer storms.

In a hail study, Changnon (1972) compared profiles of 3 hail echoes and 48 no-hail echoes from a June day in central Illinois. Table 48 presents the analysis of the no-hail echoes sorted into four classes based on the top heights of first echoes. It is important to realize that on any given day, first echoes can exhibit a wide variety of tops as illus-

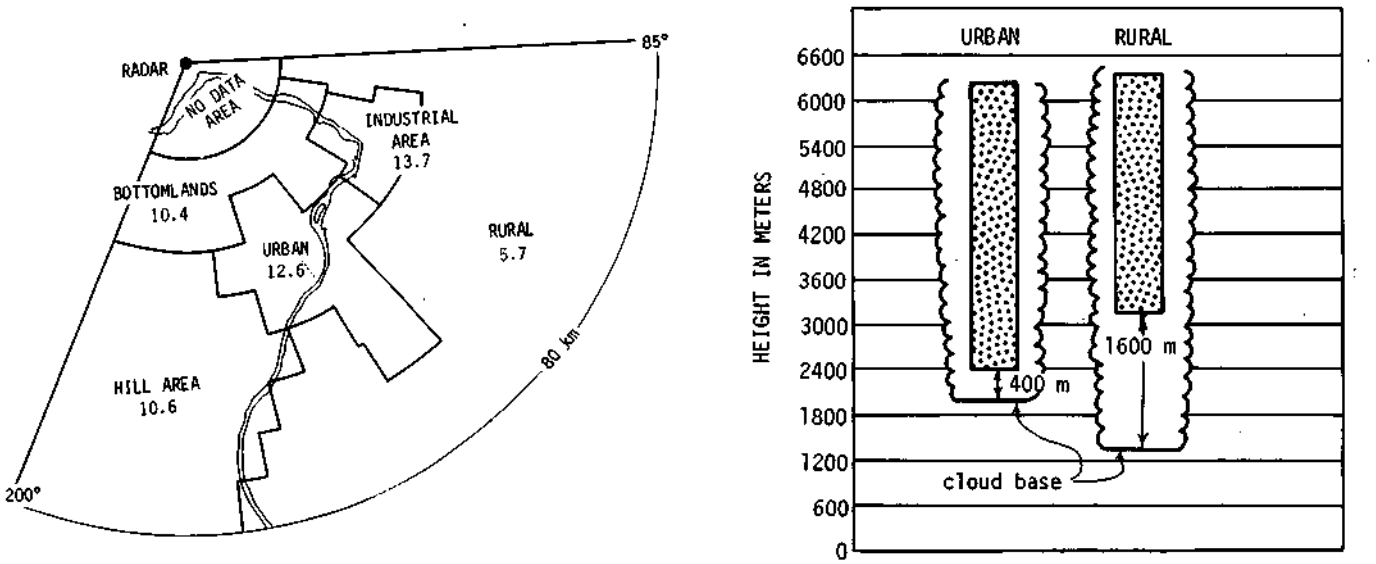

a. Average regional values of first echoes, expressed as number per 100 square kilometers in July-August 1973

b. Average bases and tops of urban and rural first echoes and clouds (bases only)

Figure 111. First echo frequencies in different land use-physiographic areas

trated in this case. Many of the first echoes do not reach the ground and dissipate before precipitation occurs, as shown by the classes of first echoes that began in the 10,000- and 20,000-foot levels. The echoes on this day are modeled in figure 113. The total profiles of the three hail echoes are shown along with the models of the no-hail echoes found in each height category. From the time of first formation, precipitation typically reaches the ground within 4 to 8 minutes.

Behavior of Echo Tops. An extensive study of hail and no-hail echoes (Changnon and Morgan, 1976) led to many comparisons of the behavior of echo tops. Maximum echo tops for the summer months, plotted on a diurnal basis, appear in figure 114. The hail echoes show systematically higher

Table 47. Average Heights (thousands of meters) of First Echo Tops and Bases in July-August 1973 Based on Degree of Organization of Rain Echoes and on Land Use-Physiographic Regions

	Hill	*Bottomland*	*Urban*	*Rural*	*All*
*Organized Systems**					
Frequency of echoes	241	36	54	95	426
Tops	6.4	6.5	6.6	6.7	6.5
Bases	2.9	2.8	2.7	3.2	3.0
Vertical extent	3.5	3.7	3.9	3.5	3.5
*Isolated Echoes***					
Frequency of echoes	113	16	75	181	385
Tops	4.8	4.7	4.9	4.8	4.9
Bases	2.1	2.1	1.7	2.2	2.1
Vertical extent	2.7	2.6	3.2	2.6	2.8
All Echoes					
Frequency of echoes	354	52	129	276	811
Tops	5.9	5.9	5.6	5.5	5.7
Bases	2.6	2.6	2.1	2.6	2.5
Vertical extent	3.3	3.3	3.5	2.9	3.2

* *Cold front and squall lines*
** *Air mass and squall zones*

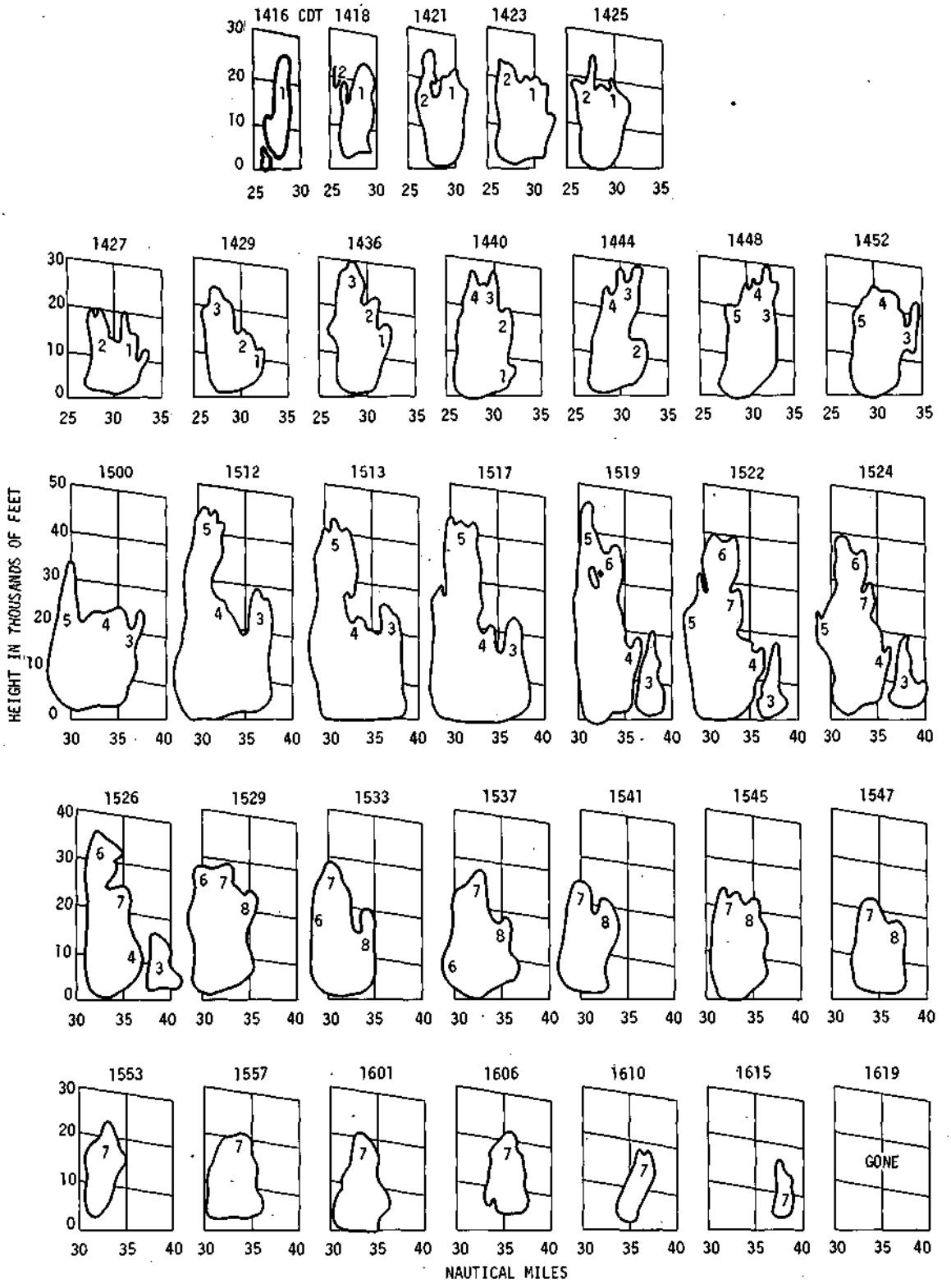

Figure 112. A 2-hr sequence of vertical cross sections through echo 1 from 3-cm RHI data

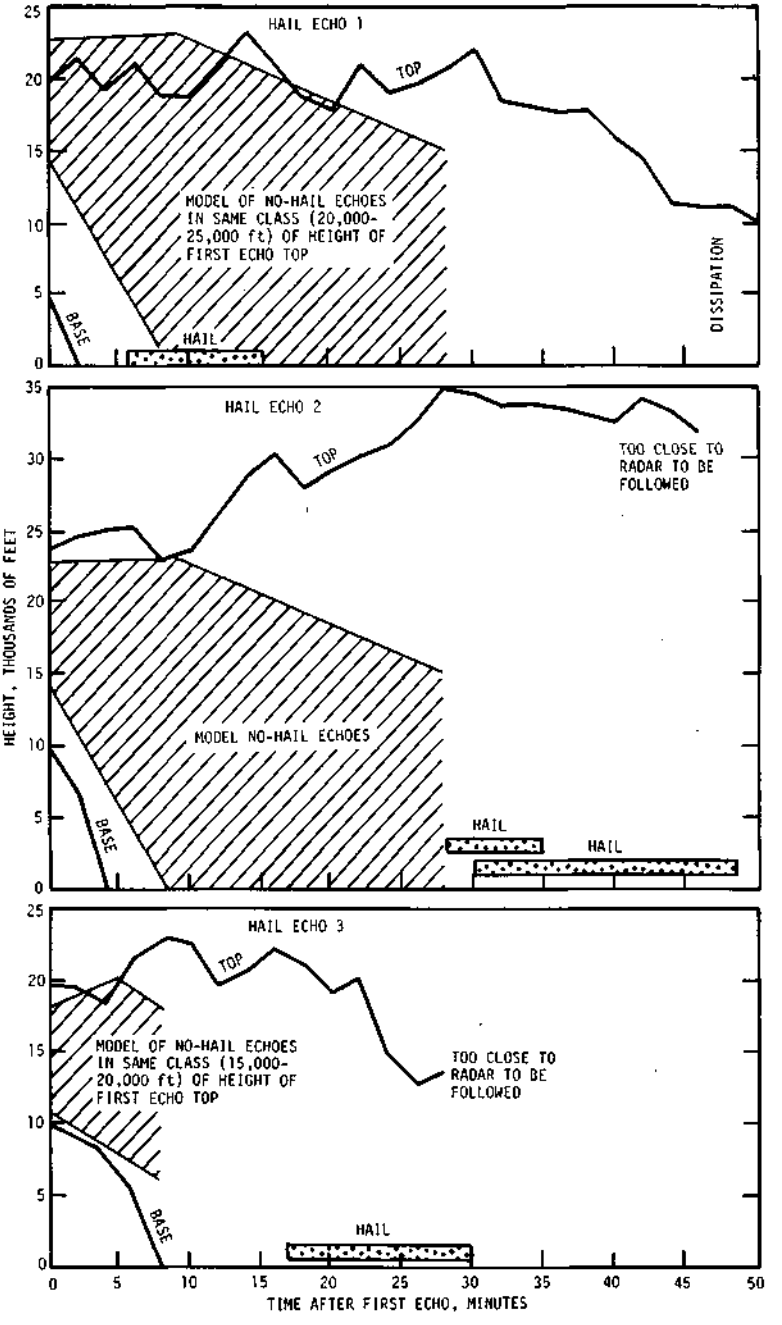

Figure 113. Profiles of three hail-producing echoes on 22 June 1969 in central Illinois

Table 48. Average Values for Four Classes of No-Hail Echoes on 22 June 1969

	Values for given echo class based on height of first echo top (thousands of feet)			
	10-15	*15-20*	*20-25*	*25-30*
Number of echoes	3	14	23	8
First echo dimensions *(thousands of feet)*				
Top	14.0	17.9	22.6	26.2
Base	9.0	10.7	14.2	17.4
Depth	5.0	7.2	8.4	8.8
Time first echo base to ground *(minutes)*	*	*	8.5	6.5
Maximum echo stage				
Height *(thousands of feet)*	16.0	20.3	23.0	26.2
Time after first echo *(minutes)*	2.0	4.5	6.0	0.0
Dissipation stage				
Height *(thousands of feet)*				
Top	13.7	18.0	15.0	20.0
Base	8.0	6.0	0.0	0.0
Time after first echo *(minutes)*	5.0	8.0	28.0	23.0

* *Did not reach ground*

tops in all hours than no-hail echoes. Both classes reveal a midday minimum in their tops with maximum echo tops generally achieved around 1600. A secondary maximum slightly after midnight is also obvious. The average heights of the hail and no-hail echoes during the March-August period are shown in figure 115. These show a systematic increase from March to July followed by a slight decrease in average echo heights in August. The relation between maximum daily echo height and warm layer thickness for hail and no-hail days (using a large sample of data from Illinois and selected data from Colorado) are shown in figure 116. The maximum height of echoes achieved on a given day is generally a function of the thickness of the warm layer, and the thicker warm layers are apt to be associated with hail days.

Towery and Changnon (1970) also made a series of studies of echo tops for hail and no-hail echoes during their lifetimes. Comparison of those for all echoes appears in figure 117a. Systematic differences are shown throughout echo lifetime. A similar comparison of hail and no-hail echo tops for three major synoptic weather types is shown in figure 117b. Cold front echoes show systematically higher tops if they produce hail, whereas in stationary front conditions there is less systematic difference between tops of hail and no-hail echoes. In the low-air mass category, the hail echoes are slightly taller, but both classes are generally lower throughout their lifetime than those with any other synoptic class.

Merging Echo Tops. Changnon (1976) studied the tops of echoes in the St. Louis area that merged and did not merge. Since merging appears to be related to rapid increases in rainfall rates and occasionally the development of severe storms, the behavior of merging echoes is of considerable importance in Illinois. The definition of merger used in this study is that merged echoes had originally been separated by more than 8 km and had persisted for 10 minutes or longer as separate echoes. There were 702 echoes recorded in July-August 1973. All of the 190 merged echoes grew vertically and 93% had durations greater than 30 minutes. Mergers occurred largely in the first quarter of echo lifetime. As shown in table 49, the average of the maximum 5-minute growth values of merged echoes was 2700 meters, compared with much lower values for the other classes. Forty percent of the merged echoes had a maximum 5-minute growth greater than 3000 meters, compared with only 18% for all other echoes.

Table 50 presents information on the amount of echo top change during 10 and 20 minutes after the merger. These reveal the impact of the merging on echo behavior and indicate the strength of storm dynamics. Seventy percent of the merged

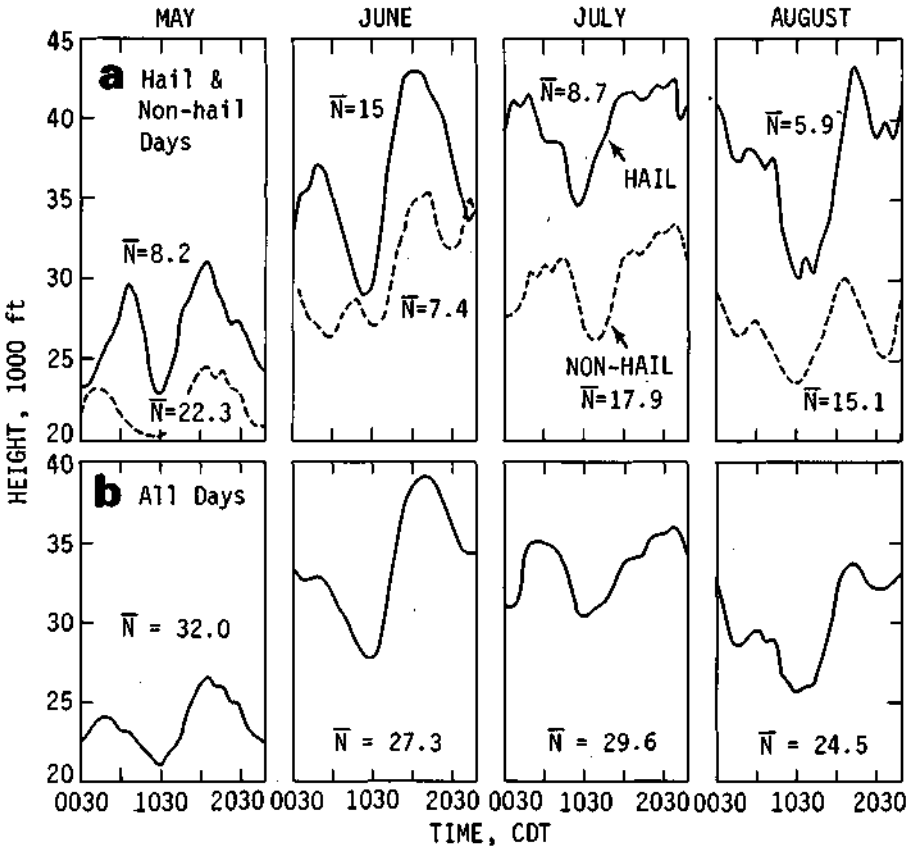

Figure 114. Average hourly echo heights for hail and non-hail days (a) and for all days (b) in central Illinois

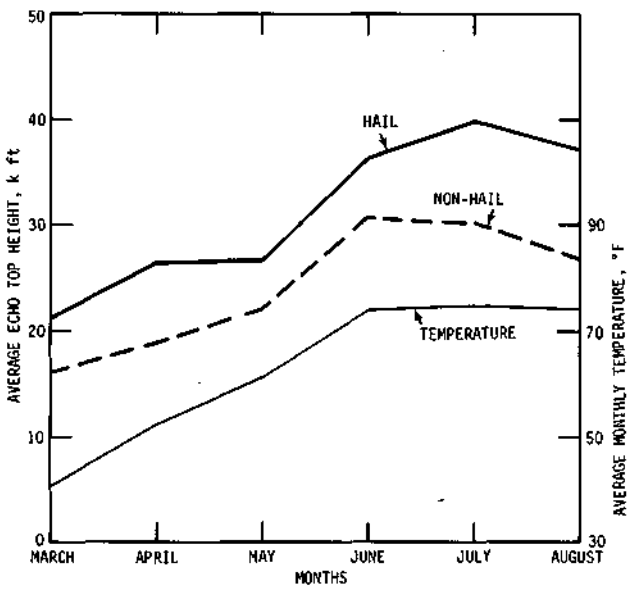

Figure 115. Seasonal variations of average maximum echo height, and comparison with monthly temperatures in central Illinois

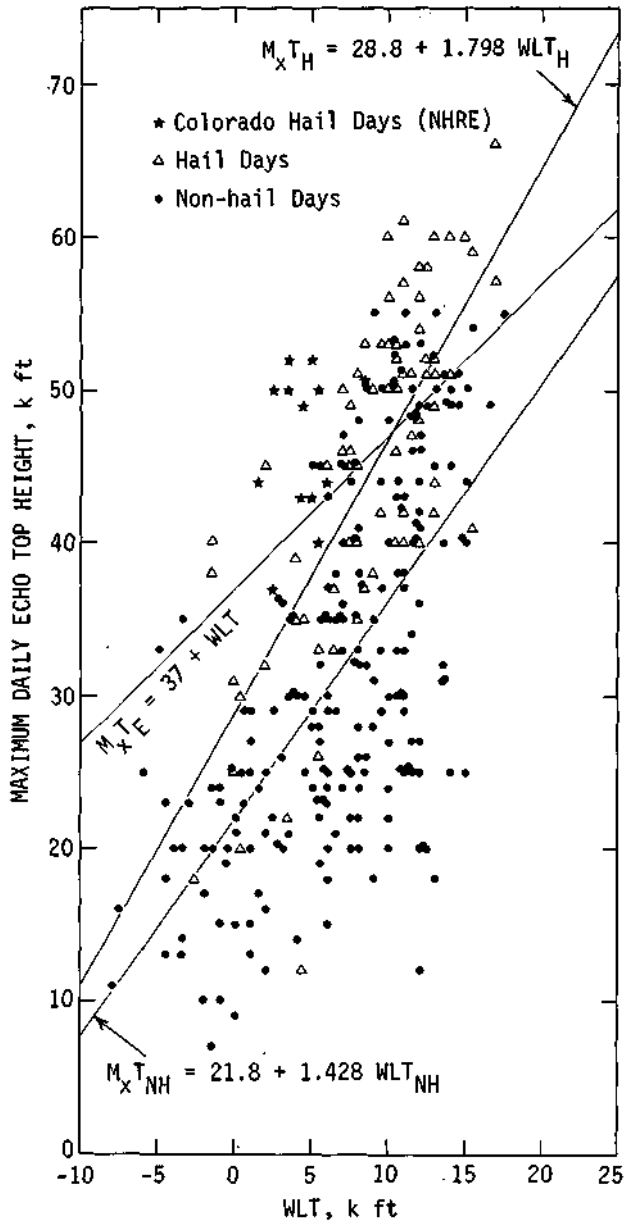

Figure 116. Maximum daily echo top height versus warm layer thickness for hail and non-hail days in central Illinois and Colorado

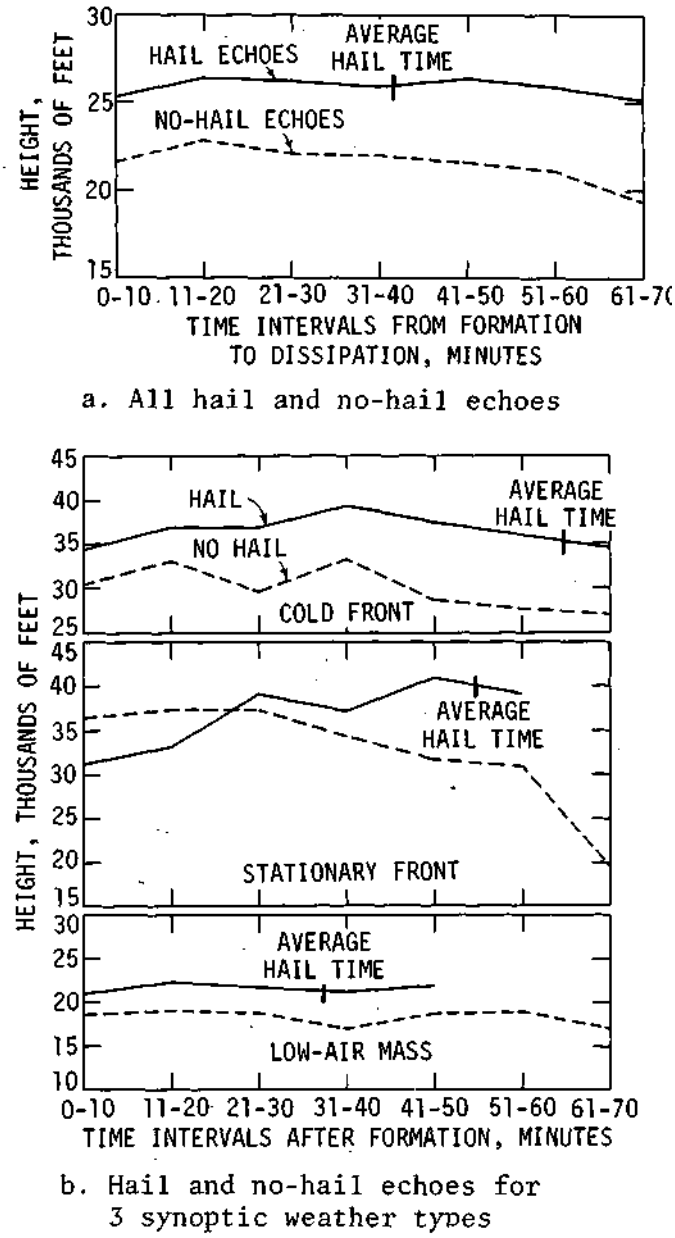

Figure 117. Height curves for hail and no-hail echoes

echoes grew in height during the 10 minutes after merger. The daily differences between the characteristics of the 190 merger echoes and the 420 non-merging echoes is shown in table 51. In every instance the merger echo values were higher with durations being 222% of the non-merger values. Differences in initiation heights were slight. Basically, merger echoes were larger throughout their lifetimes, grew faster, and lasted longer than echoes which did not merge. Figure 118 presents the average time-height profiles for urban and rural echoes and merger and non-merger echoes. The greater height and longer life of the merged echoes is clearly apparent.

Echo Volumes. Grosh (1978a) made a study of echo volumes, sometimes in relation to echo tops, utilizing 75 echoes from 5 summer days in 1974 at St. Louis. Figure 119 presents the derived model echoes. Shown are the mean echo heights, the echo volume, and the calculated rain flux. The clear rela-

Table 49. Statistics on the Maximum 5-Minute Growth of Echo Tops for Echo Classes

	All echoes	*Echoes with vertical growth*	*Echoes of ≥30 min*	*Merged echoes*	*Urban echoes*
Average *(m)*	1500	2400	2400	2700	3000
	Frequency of growth values per category expressed as percent of totals (m)				
<300	41	0	12	6	12
300–1500	23	38	25	18	16
1500–3000	18	31	27	36	18
3000–4500	10	17	19	22	28
4500–6000	6	9	12	9	16
6000–7500	2	5	5	9	10

Table 50. Statistics for Change in Echo Heights after Merger

Time after merger (min)	*Average top change (m)*	*Number of echoes expressed as percent of total*			
		Increase in height	*Decrease in height*	*No height change*	*Echo dissipated*
10	+1500	74	12	14	0
20	+1200	55	20	12	13

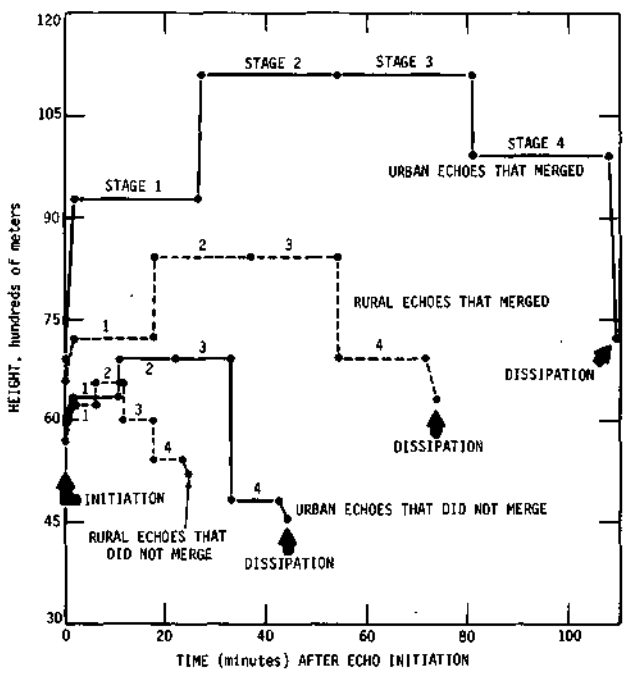

Figure 118. Time-height profiles for urban and rural echoes

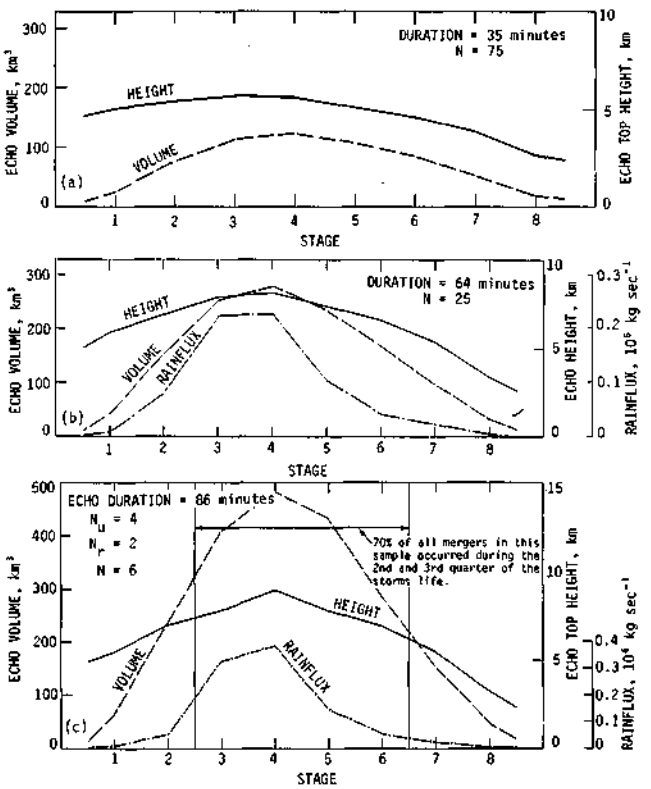

Figure 119. Model echoes for (a) all echoes, (b) echoes with gaged rain, and (c) merged echoes

Table 51. Comparison of Merged Echoes and Non-Merged Echo Characteristics
Based on Data from 14 Periods with Both Types

	Average percentage, merged ÷ non-merged values	*Number of merged echoes in each merger ÷ non-merger percentage class, expressed as percent of total (190) merged echoes*					
		50–100%	*100–150%*	*150–200%*	*200–250%*	*250–350%*	*>350%*
Duration	222	9	13	15	17	13	33
Height							
Initiation	104	51	40	8	0	1	0
Stage 1	125	28	48	20	2	2	0
Stage 2	140	21	37	36	5	1	0
Stage 3	144	22	38	37	0	3	0
Stage 4	139	21	42	31	6	1	0
Dissipation	117	27	51	13	9	0	0
Maximum height	152	18	23	44	12	3	0
Maximum 5-min growth	150	23	27	28	13	9	0

tionship between rain flux and echo volume is shown, and echo top height is shown to be a reasonable estimator of volume. Figure 120 shows the relationship between the maximum 3-minute growth of echo height and volume as a function of the maximum echo volume attained in these 75 echoes. Clearly, the maximum volumetric growth attained in echo lifetime is closely related to the maximum volume that the echo attains. Grosh also studied the relationship between echo variables and rain production. Figure 120 d presents the relationship between average echo volume and average echo height and indicates a strong relationship (R =+0.93). Figure 120c shows the fairly good relationship between average echo volume and echo rain mass (R = +0.82). Grosh also related the rain mass and echo top heights as shown in figure 120e. The correlation coefficient was +0.68.

Echo Tops and Severe Weather. Extensive studies of maximum echo tops associated with various forms of severe weather, including heavy rainfall in Illinois, are reflected in figure 121 (Grosh, 1978b). Here, maximum daily echo heights achieved in central Illinois are plotted in relation to the incidence of severe storms. It is shown that frequency of severe weather is low until maximum echo tops in summer begin to exceed 50,000 feet. The likelihood of severe weather grows rapidly after echo tops exceed 55,000 feet. Such findings have been used to define and limit the operational periods for weather modification operations in Illinois.

Modeling Studies. Semonin (1977) utilized a 1-dimensional (Hirsch) cloud model in the study of 10 years of Illinois sounding data. As part of this effort, the model was used to predict echo tops. Results for updraft speeds for 1 m/sec and an updraft radius of. 5 km are shown in figure 122. Those initial conditions gave the highest correlation between observed echo tops and model predicted tops. The monthly characteristics of the predicted clouds are shown in table 52. The most suitable period from the viewpoint of adequate cloud mass frequency occurs from June through August. Table 53 presents results indicating that

Table 52. The Characteristics of the 2.5 km Radius Updraft Model Predicted Clouds
with Depth ≥ 3000 m and Penetrating the Freezing Level

	Mar	*Apr*	*May*	*Jun*	*Jul*	*Aug*	*Sept*	*Oct*
Top height, *(m)*	7545	9510	9037	9599	10035	10130	9961	7711
Top temperature (°C)	−36.9	−42.0	−40.1	−39.2	−40.4	−42.3	−43.2	−33.9
−20°C height *(m)*	5758	6315	6864	7311	7647	7668	7225	6656
0°C height *(m)*	2982	3477	3985	4329	4635	4640	4210	3678
Base temperature (°C)	+4.1	+7.2	+9.6	+12.9	+14.5	+14.0	+11.8	+8.6
Base height *(m)*	2182	2090	2063	1882	1878	1970	1683	2056
Number/month	1.1	3.1	6.5	9.8	9.8	11.4	4.1	1.8

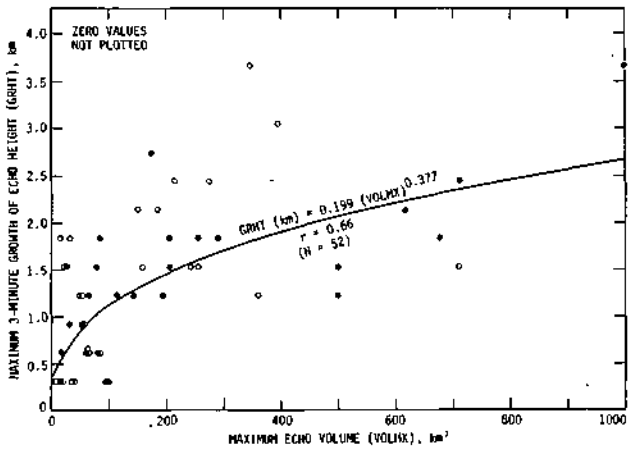

a. Maximum 3-min growth of height related to volume

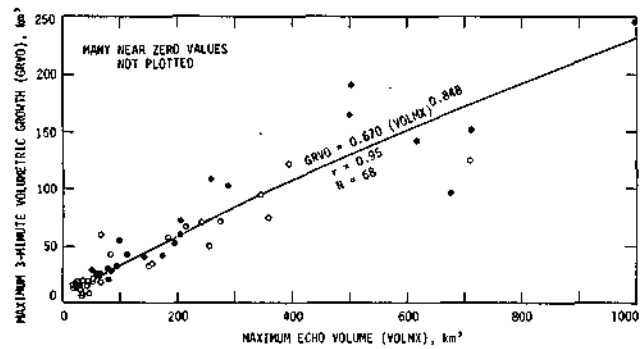

b. Maximum 3-min growth of height as a function of maximum echo volume

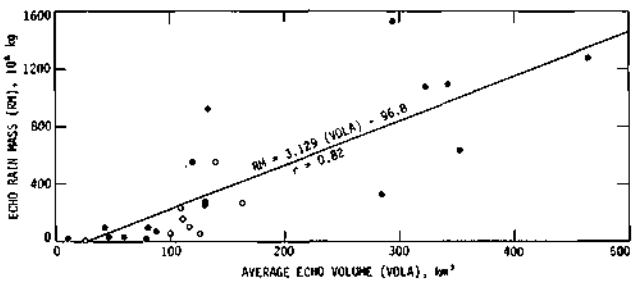

c. Average echo volume and rain mass

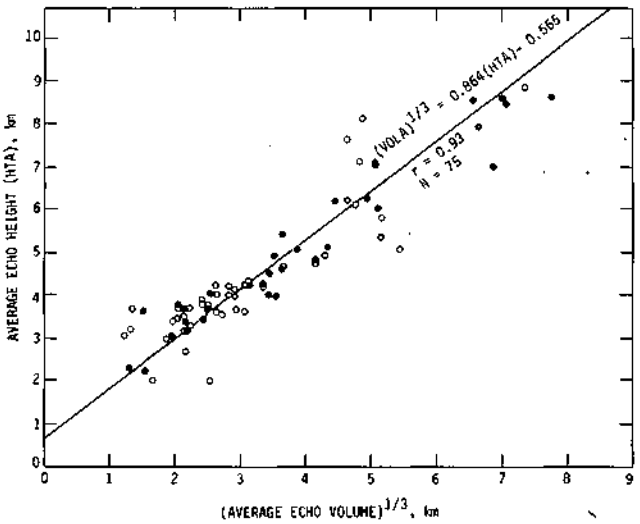

d. Average echo volume and height

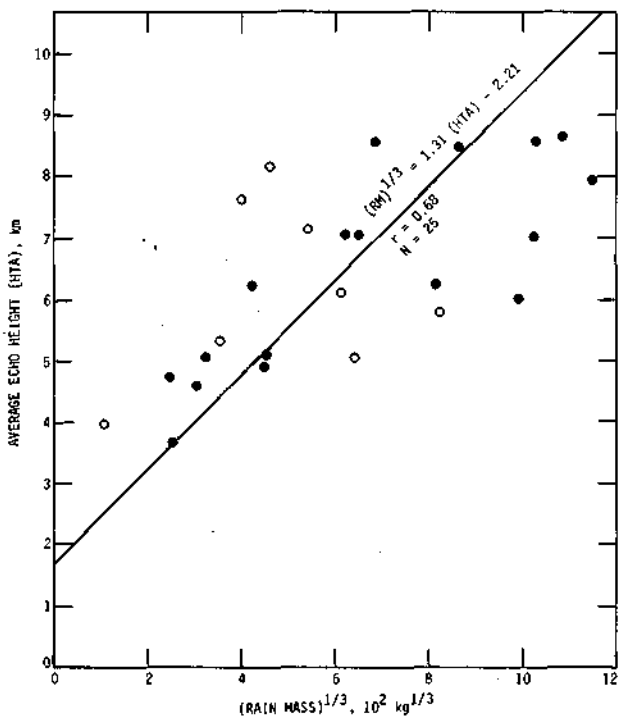

e. Average echo height and rain production

Figure 120. Relationships between echo height and volume and various other parameters (Open dots are rural cases, closed dots urban cases)

PERCENT OF RAIN DAYS WITH TALL ECHOES

	Maximum echo top height, feet				
	≥60,000	*≥55,000*	*≥50,000*	*≥45,000*	*≥40,000*
Spring[x]	0	1	3	8	12
Summer[xx]	3	10	30	47	62
Spring + Summer	1	5	16	26	36

[x]Spring = March, April, and May
[xx]Summer = June, July, and August

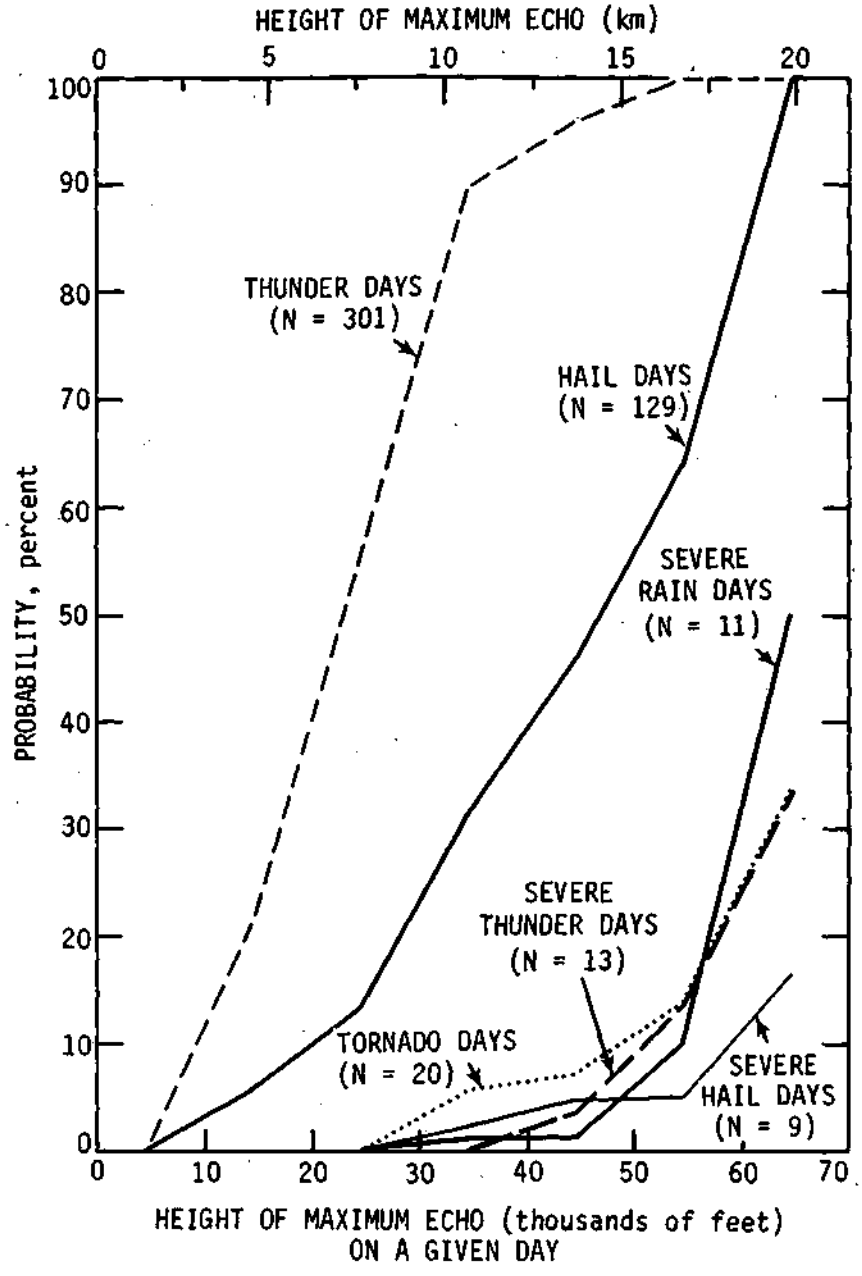

Figure 121. Daily severe weather probabilities as a function of maximum radar echo top heights for spring and summer

Table 53. Percentage of Possible Soundings with High Cloud Bases (HCB), with Clouds ≥ 400 m, and the Percentage of Those Clouds ≥ 3000 m Deep Penetrating the Freezing Level

	HCB	*≥ 400 m*	*≥ 3000 m*
March	37.1	44.5	3.5
April	31.7	57.3	10.3
May	30.6	63.5	21.0
June	19.7	74.7	32.7
July	13.2	84.5	31.6
August	10.6	83.5	36.8
September	37.7	54.0	13.7
October	43.9	47.1	5.8

more than 80% of the days in July and August have clouds (as calculated) of greater than 400-meter depths, and about one-third of the days of July and August have clouds with depths greater than 3000 meters that penetrate the freezing level.

Radar Reflectivity Values Aloft. Considerable study has been made of the reflectivity profiles of Illinois storms (Wilk, 1961; Changnon, 1972). Primary attention was given to the differences between portions of echoes producing hail and those not producing hail. Figure 123a shows the relative number of occurrences of various reflectivities based on all types of echoes. At 10,000 feet above the freezing level, one finds the value of 60 for 10^4, indicating that there are six times more values of 10^4 at that height than at 10^6 which had a value of 10 (as compared to 60). A relative maximum of 40

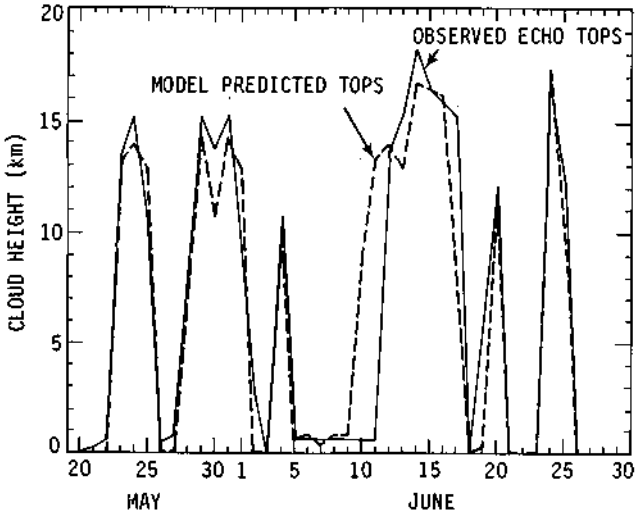

Figure 122. Comparison between model-predicted cloud tops and radar-observed storm tops in central Illinois

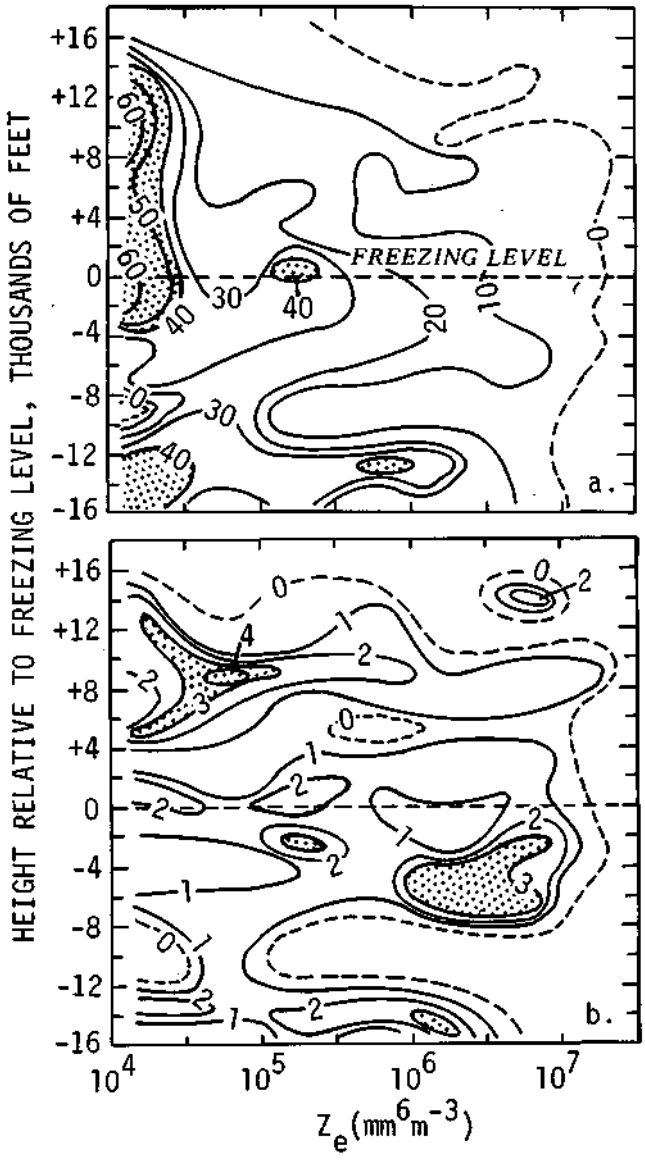

Figure 123. Relative number of reflectivity occurrences for given intervals, 1967 season, associated with (a) no-hail and hail reports and (b) hail reports only

in the frequency is shown for 10^5 at the freezing level. A similar graph based on hail reflectivity values associated with surface hail reports is shown in figure 123b. These show a maximum number of occurrences at about 10,000 feet above the freezing level in the $10^{4.5}$ to $10^{5.5}$ range. This appears to be a feature of several individual hailshaft echoes.

Although figure 123 gives hope of detecting hail-producing storms according to their reflectivity profiles, figure 124 tends to show that it is not easy. Here, the reflectivities associated with hail are expressed as a percent of all reflectivity values. Near $10^{5.5}$, only 2.5 to 3% of all the strong reflectivities at 5000 to 20,000 feet above the freezing level were associated with hail. In general, many high reflectivities occurred without hail appearing at the ground. Further investigations of the reflectivities aloft, generally from 5000 to 10,000 feet above the surface, are shown in figure 125. Forty-two percent of the hail events were associated with reflectivities equal to or greater than 50 dbZ. This graph shows that a 10-cm reflectivity value of 40 dbZ appears to be a reasonable threshold indicating the presence of potential hail-producing cells in Illinois.

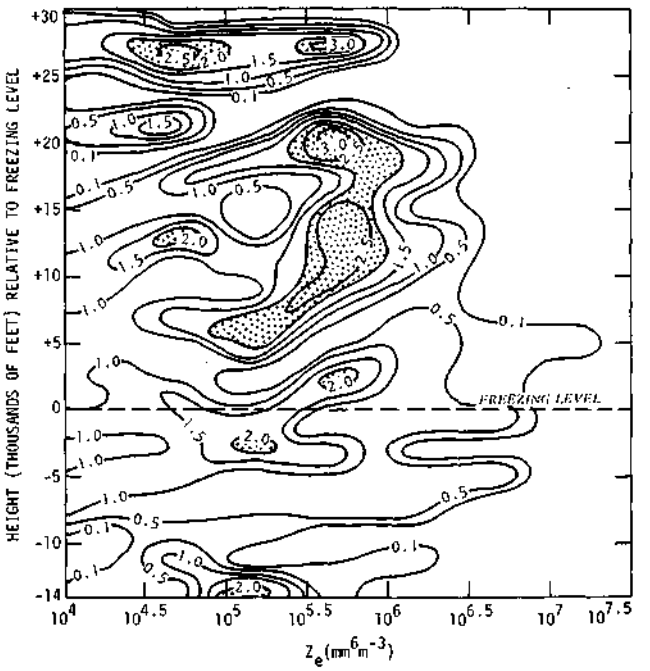

Figure 124. Number of each height-reflectivity combination associated with hail, expressed as a percent of all reflectivity values above hail reports

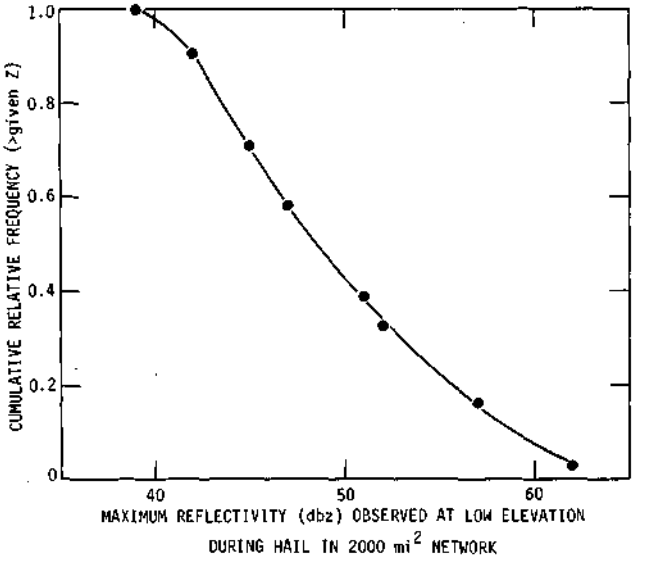

Figure 125. Cumulative relative frequency distribution of maximum reflectivities during hail

Horizontal Cell Characteristics

Radar Echoes. Huff (1978c) studied the intense centers of echoes from 3 5 summer storm days in the St. Louis region. The echo centers were classified as either moving or quasi-stationary and their mean values are shown in table 54.

Changnon and Morgan (1976) made several studies of echoes in a fixed network, relevant to the potential seeding aircraft operations. The data within a 2000 mi^2 area of Illinois were inspected for various circumferences of cellular echoes. The distribution of the circumferences of echo bases (at about 5000 feet) is shown in figure 126. Fifty percent of the echoes had circumferences of 200 miles with some echoes having circumferences in excess of 3 50 miles. This has particular importance to aircraft which must circumnavigate echoes as part of their seeding.

Another operational aspect for a fixed area relates to length of time echoes are present over a region. Data from 18 summer convective periods in a central Illinois area (2000 mi^2) are shown in figure 127. This gives some estimate of the persistence or duration of echo activity in a potential experimental region.

Towery and Changnon (1970) made a study of the echoes associated with hail-producing storms in central Illinois. Selected results are presented to

Table 54. Statistical Summary of FPS-18 Echo Center Properties

Echo type	N	Duration (minutes)	Maximum intensity (dbz)	Path length (km)	Speed (knots)
Means for moving centers					
Urban effect	221	29	43	14	20
Potential urban effect	145	22	42	11	21
No effect	359	20	39	8	21
Hill effect	178	28	43	10	19
Means for quasi-stationary centers					
Urban effect	123	15	40		
Potential urban effect	77	9	36		
No effect	227	9	37		
Hill effect	96	10	38		

provide horizontal echo information relative to central Illinois. Figure 128 presents distribution of echo direction sorted by three speed categories. Further information on the direction of echo motion is in figure 129. Here, directions are sorted according to the synoptic weather class associated with the echoes. The post cold frontal, air mass type frequently produces fast moving small echoes moving towards the ESE. Cold fronts (including squall lines) have a double vector maximum.

Figure 130 presents information about the tendency for echoes to 'turn' during their lifetime with the frequency and the average turning shown. More than 60% of all echoes turn either left or right. Table 55 presents comparison of characteristics of hail echoes and no-hail echoes from the 2-year study period. Very little difference is shown in the time of occurrence, direction, and speed averages. Hail echoes appear to have a stronger reflectivity at the time of the formation and remain stronger and taller throughout their lifetime. Table 56 presents a summary of echo characteristics for three basic synoptic classes. Hail echoes with cold fronts are not basically different in many of their characteristics.

Raincells. Raincells are convective entities of rainfall definable in space and time at the surface. An example was presented in figure 108. It is important, however, to consider some of the instantaneous, or near instantaneous protrayals of surface raincells. Stout (1960) presented 1-minute rainfall maps from a very dense central Illinois raingage network. The 1-minute isohyetal maps (rain rates in inches per hour) during a 14-minute period are

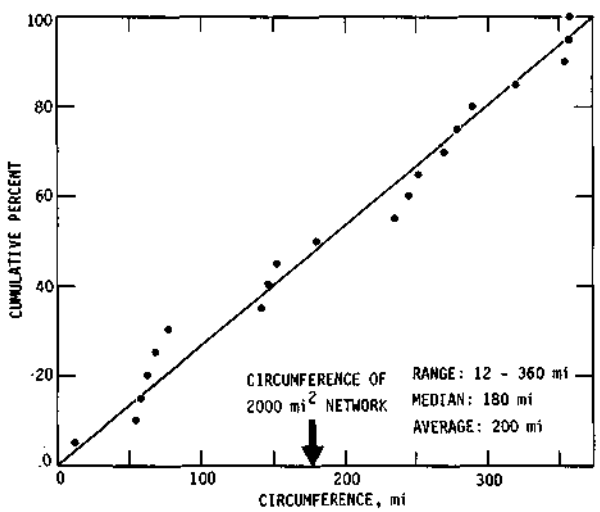

Figure 126. Cumulative relative frequency distribution of the circumferences of main echoes during hail periods

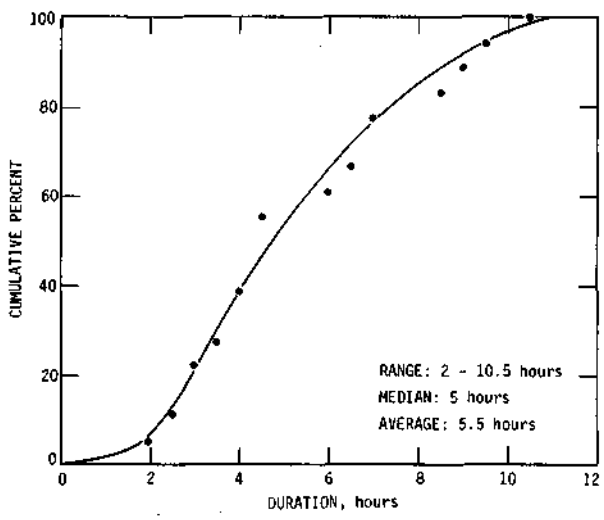

Figure 127. Cumulative relative frequency distribution of the duration of echoes for 18 hail dates over 2000 mi^2 network

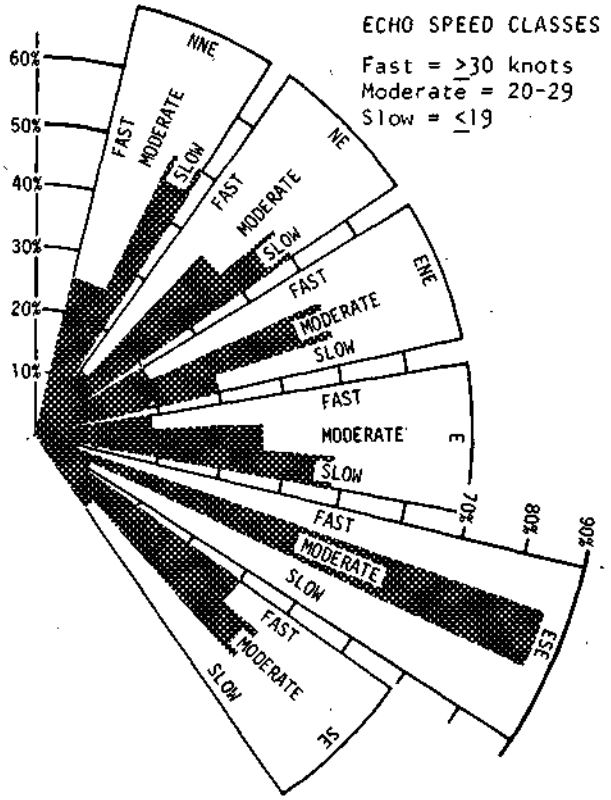

Figure 128. Percent of occurrence of the 3 echo speeds (as averaged over whole echo life) for each direction of motion of all hail echoes

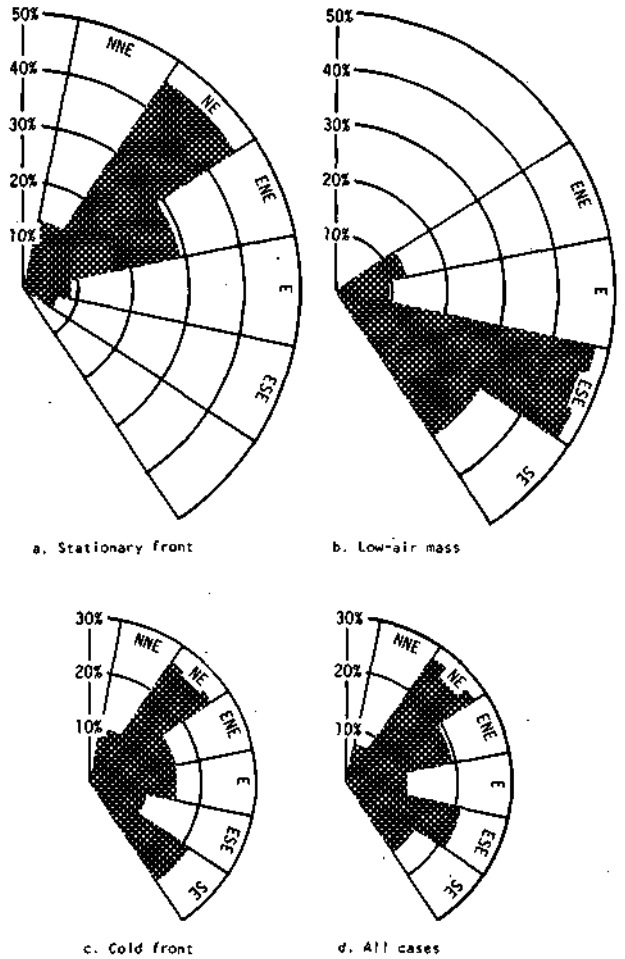

Figure 129. Percent of occurrence of hail-echo motion (toward which the echoes were moving) for each synoptic weather category and for all cases

presented in figure 131. These show the rapidly changing character of surface rainfall, essentially with the merging after 1605, such that two apparent cores at 1609 had become one heavy cell by 1613. These are the phenomena that are being studied over their lifetimes and labeled as 'raincells.'

Schickedanz (1974) provided a definition for objectively determining raincells from dense networks of the Water Survey. Raincell results from 1971-1975 summers at St. Louis (Schickedanz, 1978) are now discussed. It should be noted that many of the values presented offer information on raincells from different land use areas, with L = St. Louis, SI = St. Louis industrial area, W = the Wood River industrial area', H = hill-lands, B = bottom-lands, and C = control or rural lands without any major physiographic features. Table 57 presents comparison of raincell volumes over the 5-year METROMEX period. These have been sorted according to different path lengths of the raincells. Table 58 presents similar rainfall volume values for raincells, but sorted according to synoptic types. Raincells with squall zones and squall lines were much larger producers of precipitation than those with the other types, with air mass being the smallest. Analyses of the volume of raincells by time of day are presented in table 59. Figure 132 presents information on the five summer initiation patterns of raincells in the St. Louis network. The summer pattern is based on values above 70; in the non-analyzed areas values range from 32 to 70. These offer some indication of the point frequencies of raincell initiations.

Further information on the characteristics of raincells is provided in tables 60-62. Table 60 shows the distribution of raincell orientations from three sources. One is a set of cells associated with hailstorms on the Central Illinois Network of 1600 mi^2 in 1965. The second and largest set is from the

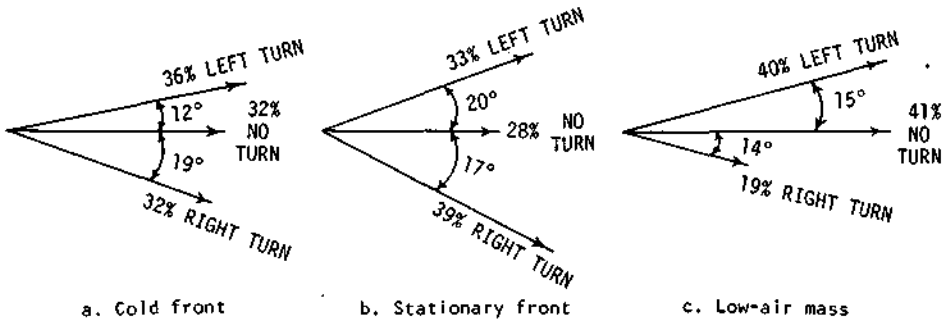

Figure 130. Percent of occurrence of hail echoes turning and not turning and average degrees of turns for each synoptic weather category

Table 55. Comparison of Characteristics of Hail Echoes and No-Hail Echoes

*Echo characteristic**	*Hail*	*No-hail*
Preferred time of occurrence *(CST)*	1200–1800	1200–1800
Average direction of movement *(degrees)*	81.9	85.9
Average speed *(knots)*	23.8	24.2
Average reflectivity at formation $(mm^6 m^{-3})$	6.1×10^2	5.5×10^2
Average reflectivity at hail time $(mm^6 m^{-3})$**	7.3×10^4	1.6×10^4
Average height at formation *(feet)*	25,300	22,000
Average height at hail time *(feet)***	26,900	21,700
Average height at dissipation *(feet)*	25,000	18,500

** All values based on the 50 no-hail echoes and on the 50 hail echoes that formed in range, except the height values which are based on the 35 hail echoes that formed and dissipated in range*

*** Average hail time was 44 minutes after formation*

Table 56. Summary of Echo Characteristics for Each Synoptic Classification

Echo characteristic	*Cold front*	*Stationary front*	*Low-air mass*
Average speed *(knots)*	30	21	25
Average duration prior to hail *(minutes)*	59	49	32
Average total duration *(minutes)*	90	83	75
Preferred direction of motion	NE	NE	ESE
Preferred direction of turn	Left	Right	No turn
Average number of degrees turn (when turning) in preferred direction	12	17	0
Preferred time of day (CST)	1200–2400	1200–1800	0000–1800
Average reflectivity at formation $(mm^6 m^{-3})$	5.6×10^2	5.1×10^2	4.6×10^2
Average reflectivity at hail time $(mm^6 m^{-3})$	2.6×10^5	4.6×10^5	5.2×10^4
Average top height for echo duration *(thousands of feet)*	38	36	19
Average top height at hail time *(thousands of feet)*	37	38	20

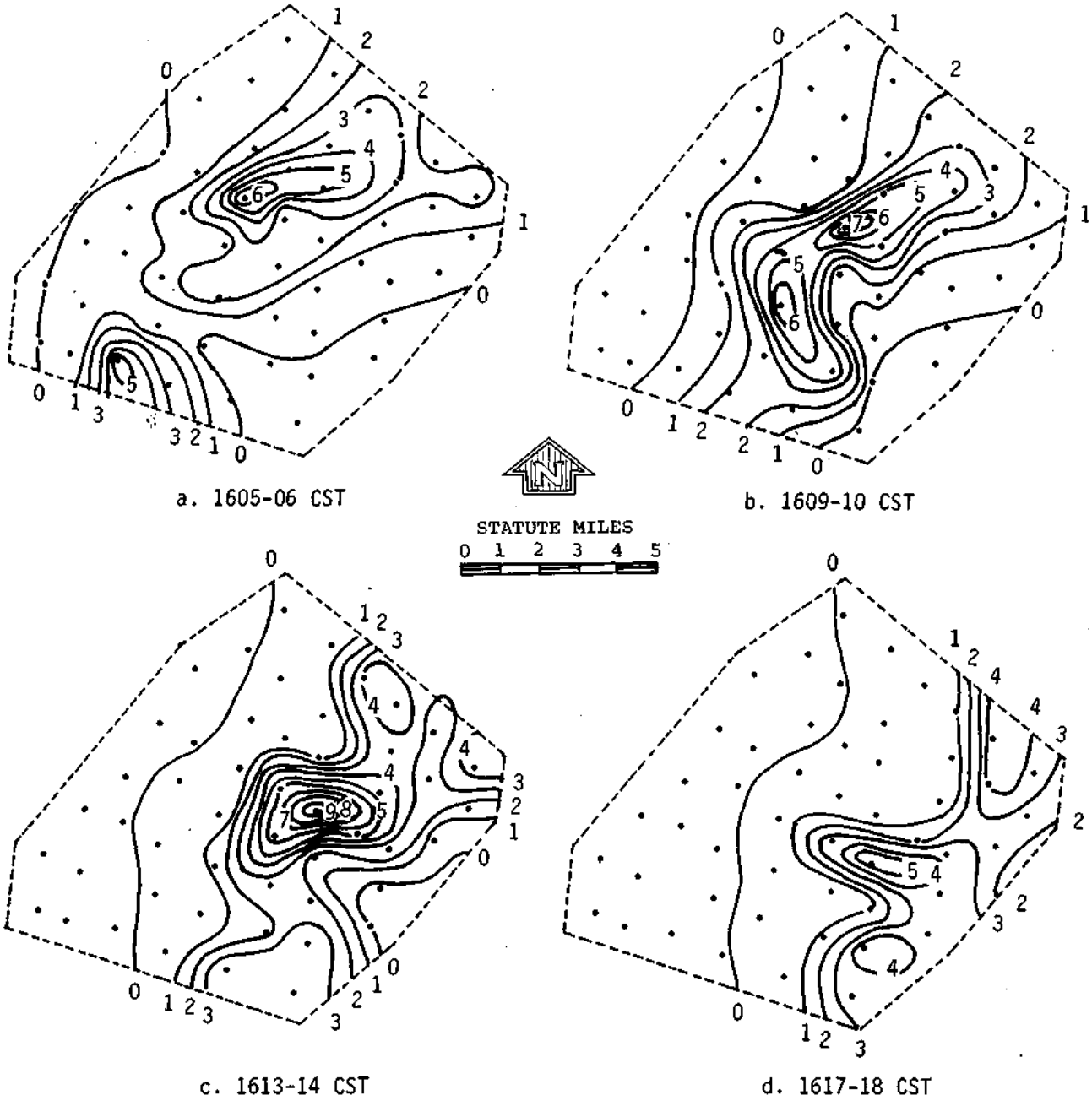

Figure 131. One-minute rain maps (rate in inches/hour) on 100 mi^2 network in central Illinois, 25 June 1953

Table 57. Comparison of Average Volume from Effect and No-Effect Cells Stratified According to Path Length, METROMEX

	L	SI	W	H	B	C
			≤6.4 km			
1971	8.5(25)	10.9(60)	11.3(66)	13.7(101)	3.5(−49)	6.8
1972	14.2(92)	17.7(139)	11.7(58)	7.7(4)	12.8(73)	7.4
1973	15.8(74)	18.4(102)	16.9(86)	11.7(29)	9.6(5)	9.1
1974	6.0(5)	7.8(37)	5.8(2)	7.4(30)	5.4(−5)	5.7
1975	9.2(33)	11.2(62)	7.9(14)	5.5(−20)	8.3(20)	6.9
1971–1975	9.4(38)	11.7(72)	8.8(29)	8.1(19)	7.5(10)	6.8
			≤12.8 km			
1971	16.5(60)	23.3(126)	17.5(70)	19.9(93)	8.2(−20)	10.3
1972	18.8(70)	18.1(63)	12.2(10)	12.9(16)	16.2(46)	11.1
1973	27.0(125)	30.8(157)	19.7(64)	16.8(40)	14.6(22)	12.0
1974	9.1(26)	11.8(64)	6.7(−7)	9.2(28)	7.5(4)	7.2
1975	14.2(58)	16.1(79)	10.7(19)	9.7(8)	10.5(17)	9.0
1971–1975	15.0(65)	17.7(95)	10.9(20)	12.0(32)	10.6(16)	9.1
			≤19.3 km			
1971	21.2(88)	30.2(167)	35.9(218)	19.4(72)	13.2(17)	11.3
1972	31.7(142)	37.8(189)	14.8(13)	13.2(1)	18.5(41)	13.1
1973	30.4(134)	39.7(205)	23.2(78)	25.3(95)	15.0(15)	13.0
1974	11.2(40)	14.2(78)	8.0(0)	10.9(36)	7.9(−1)	8.0
1975	18.6(82)	23.2(127)	13.1(28)	14.7(44)	11.0(8)	10.2
1971–1975	19.5(91)	25.0(145)	14.2(39)	15.4(51)	11.7(15)	10.2
			All cells			
1971	26.5(114)	40.8(229)	50.5(307)	23.6(90)	13.2(6)	12.4
1972	46.2(216)	63.7(336)	51.3(251)	22.1(51)	18.8(29)	14.6
1973	37.6(163)	50.5(253)	27.1(90)	30.8(115)	15.3(7)	14.3
1974	13.4(56)	18.3(113)	8.0(−7)	11.1(29)	8.4(−2)	8.6
1975	22.3(114)	28.3(172)	14.6(40)	18.8(81)	12.1(16)	10.4
1971–1975	24.8(125)	34.2(211)	19.5(77)	19.1(74)	12.3(12)	11.0

Note: Volume is measured in hectare-meters; effect-control difference is given in parentheses expressed as % of control

Table 58. Comparison of Average Rainfall Volume from Effect and No-Effect Cells According to Synoptic Type for Summer 1971-1975, METROMEX

	L	SI	W	H	B	C
Volume (hectare-meters)						
Squall zone	17.4(93)	28.8(220)	11.7(30)	18.0(100)	10.6(18)	9.0
Squall line	33.3(107)	51.5(220)	37.2(131)	26.3(63)	16.3(1)	16.1
Air mass	11.4(34)	27.1(219)	13.5(59)	9.8(15)	12.3(45)	8.5
Cold front	21.8(86)	29.0(148)	20.7(77)	20.4(74)	11.6(−1)	11.7
Static front	7.9(55)	10.4(104)	8.9(75)	10.7(110)	8.4(65)	5.1
Sample size						
Squall zone	516	150	163	108	217	1530
Squall line	584	205	117	119	171	1382
Air mass	64	9	19	27	37	237
Cold front	254	69	65	43	76	647
Static front	196	70	51	43	45	538

Note: Effect–control differences are expressed as % of control in parentheses

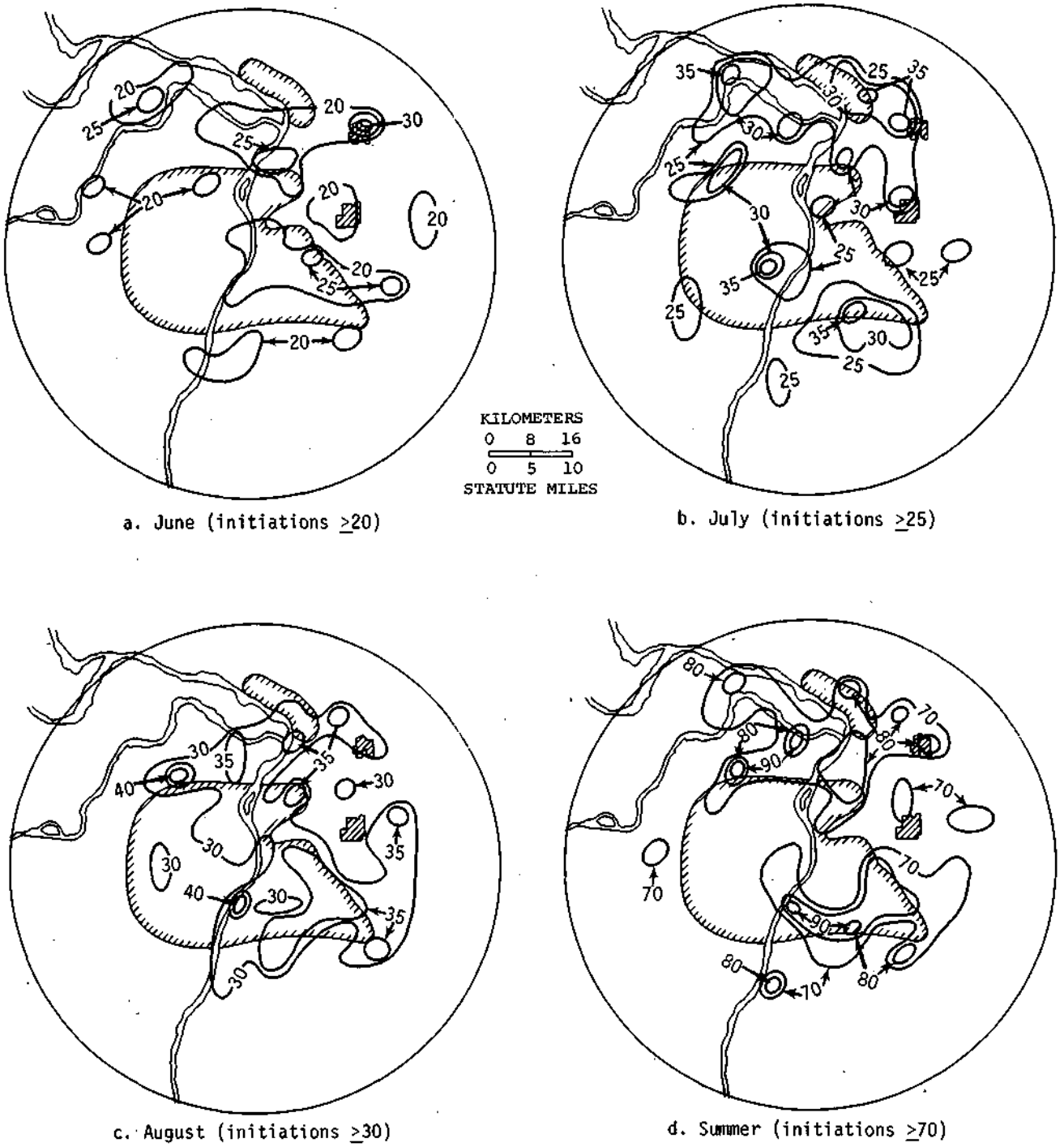

a. June (initiations ≥20)

b. July (initiations ≥25)

c. August (initiations ≥30)

d. Summer (initiations ≥70)

Figure 132. Monthly and seasonal patterns of complete raincell initiation at METROMEX, 1971-1975

Table 59. Comparison of Average Rainfall Volume from Effect and No-Effect Cells According to Time of Day for Summer 1971-1975, METROMEX*

	L	SI	W	H	B	C
0001-0600	15.1(97)	20.1(161)	11.4(49)	12.0(57)	8.1(5)	7.7
0601-1200	13.0(52)	14.5(69)	12.3(43)	13.9(62)	8.8(2)	8.6
1201-1800	40.4(171)	59.5(299)	27.4(84)	28.1(89)	16.9(14)	14.9
1801-2400	22.8(89)	33.8(180)	23.7(96)	22.1(84)	14.4(19)	12.0

** Volume (hectare-meters)*
Note: Effect-control differences are expressed as % of control in parentheses

Shawnee-Little Egypt Network in southern Illinois, and were analyzed for the summer of 1965 on this 1500-mi^2 network. The third set from the METROMEX network includes those cells measured in conjunction with several case studies of heavy rainstorms in 1972-1973. All sets show an average movement from the WSW. The major portion of the cells traveled from the SW through W to WNW. These are also the orientations most frequently found with total storm rainfall in Illinois, particularly in heavy rainstorms (Huff and Vogel, 1976; Vogel and Huff, 1977; Huff, 1977).

Tables 61 and 62 indicate typical dimensions of raincells in Illinois. In compiling these tables, only raincells with lengths of 6 miles or more were used. This eliminates most of the weaker, short-lived convective entities which are usually light rain producers. These tables indicate that the more substantial cells have an average length of 10 to 12 miles and a width of about 4 miles, except for the hailstorms which show lengths of 16 to 17 miles and widths of 6 to 7 miles, on the average. Most of the cells have lengths less than 25 miles and widths not exceeding 12 miles. The widths are close

Table 60. Illinois Raincell Orientations

Orientation, degrees	Number of cells: Raincells with hail*	All raincells** in southern Illinois	METROMEX raincells†
180-189 (S)	1	1	1
190-199	0	0	0
200-209	0	1	2
210-219	1	2	2
220-229 (SW)	8	22	3
230-239	5	28	5
240-249	22	20	4
250-259 (WSW)	18	29	11
260-269	11	77	10
270-279 (W)	5	69	4
280-289	1	10	3
290-299	0	5	8
300-309	0	5	1
310-319 (NW)	1	5	1
320-329	1	3	1
330-339	0	1	1
340-349	0	2	1
350-359	0	7	0
Total	73	287	58
Average	252°	262°	261°

** Raincells with hail in CIN (40 X 40 mi) in May-September 1965 (some complete and some crossed the network)*
*** Raincells in June-August 1965 completely defined in Shawnee-LEN network, 25 X 60 miles*
† Raincells in selected heavy storms in 1972-1973 in METROMEX circular network, diameter 50 miles

Table 61. Illinois Raincell Lengths, Based on 5- to 15-Minute Rain Amounts

Length, miles	Number of cells: Raincells with hail	Southern Illinois raincells**	METROMEX raincells†
6–10	3	168	26
11–15	9	75	17
16–20	6	39	7
21–25	4	3	7
26–30	1	1	0
31–35	3	1	0
36–40	1	0	0
41–45	0	0	1
46–50	0	0	0
51–55	0	0	0
56–60	0	0	0
Totals	27	287	58
Average	17	11	12
Median	16	10	12

** Raincells with hail in 40 X 40 mi network 1968*
***All completely within network (20 X 60 mi) in June-August 1965*
† All completely within METROMEX network (50 mi diameter), selected heavy storms, 1972-1973

approximations of the true diameters of the cells. However, the cell lengths are to some degree overestimates of the true cell dimension, since they include the path swept out by rain over periods of 5 to 15 minutes. For example, the relatively large sample of southern Illinois cells in table 61 were based on 15-minute amounts. Assuming an average speed of 20 mph among these cells, the average cell length of 11 miles would be closer to 6 miles at a given time. This would indicate an average length to width ratio of 1.5 to 1, which agrees quite well with other related studies at the Water Survey. Stall and Huff (1971) showed that the average summer thunderstorm cell has an area of 15 to 30 mi^2. Huff in an extension of an earlier storm rainfall shape study (Stout and Huff, 1962) has calculated that total storm rainfall in heavy storms of this size (single-cell storms) has an average length to width ratio of about 1.7 to 2.0

Table 62. Illinois Raincells Widths (at Maturity)

Widths, miles	Number of cells: Raincells with hail*	Raincells in southern Illinois**
1–3	5	120
4–6	34	135
7–9	9	28
10–12	12	3
13–15	5	1
16–18	3	0
19–21	2	0
22–24	1	0
25–27	1	0
28–30	1	0
Totals	73	287
Average	7	4
Median	6	4

** In CIN during May-September 1968, all with hail, network 40 X 40 miles*
*** In Shawnee-LEN during June-August 1965*

Motion of Cells. Collection of data on the motion of radar echoes and raincells during the METROMEX program allowed the derivation of information on the frequency of their direction. Figure 133 shows the frequency distribution and the direction of motion of 250 radar echoes and over 3000 raincells, as measured in the St. Louis area. The prevailing motion is westerly (260-280°) with a secondary maximum from the southwest. Importantly, raincells and echoes moved from every direction.

Hiser and Bigler (1953) studied the determination of wind data from radar echoes. Table 63 presents correlation coefficients they obtained between isolated echoes and wind direction and speed in various layers. Similar correlations for cells inside squall lines are shown in table 64. Basically, the

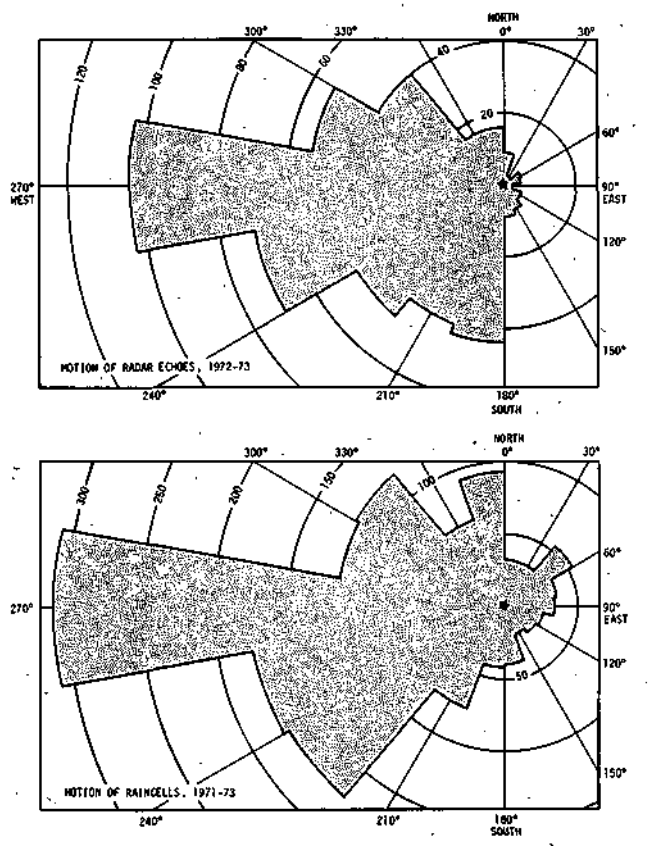

Figure 133. Direction of motion of radar echoes and raincells at St. Louis

Table 63. Correlation Coefficients for 34 Cases of Isolated Echoes

	Direction	*Speed*
Wind layers		
2000-20,000 ft	0.87	0.72
2000-26,000 ft	0.90	0.67
6000-30,000 ft	0.88	0.60
Specific levels		
6000 ft	0.84	0.44
10,000 ft	0.75	0.62
20,000 ft	0.82	0.54

Table 64. Correlation Coefficients for 35 Cases of Elements of Squall Lines

	Direction	*Speed*
Wind layers		
2000-20,000 ft	0.79	0.72
2000-26,000 ft	0.84	0.73
6000-30,000 ft	0.82	0.72
Specific levels		
6000 ft	0.56	0.44
10,000 ft	0.80	0.68
20,000 ft	0.63	0.64

movement of echoes, whether isolated or in squall lines, provides more reliable estimates of the winds at the 10,000-foot level than at lower or higher levels. Figure 134 illustrates a typical case in which a fair correlation was obtained between the movement of elements of a squall line and the mean winds in the layer from 2000 to 26,000 feet. The difference between the propagation of the squall lines and the movement of the individual cells is an important factor to note in this figure — it is typical.

Merging. The prior section on the vertical characteristics of cells presented results about tops of merging radar echoes. Merging of cellular entities displayed in the horizontal has also been studied utilizing both PPI radar data and surface raincell data. An example from a case study at St. Louis is presented in figure 135 (Changnon and Semonin, 1975). Here, the patterns of the raincells and the associated echoes are shown for a series of mergers as viewed in the horizontal. This represents a series of mergers of adjacent cellular entities which would not be classed as feeder cells, but rather as individual storm cell entities moving or growing together.

Patterns of raincell mergers in five separate summers, as defined by surface raingage data, are shown in figure 136. These offer some estimate of the distribution and frequency of these events in a given summer over a 2000-mi^2 area. The diurnal distributions of raincell mergers in the five summers in the St. Louis area are shown in figure 137. This shows how the frequency changes later in the day (when fewer cell entities develop).

In the St. Louis studies, the Water Survey analysis of mergers of horizontal echoes has been based on the interaction of distinctly separate radar echo systems. An echo 'system' was defined initially as an echo entity separated in space from other echoes in the system, and having one or more intensity centers within it. The merger was based on two such systems merging.

Mergers, as determined from surface raincells in the dense raingage network at St. Louis, hinged on the delineation of a raincell itself. Raincells were essentially a closed isohyetal entity within an enveloping isohyet consisting of one or more con-

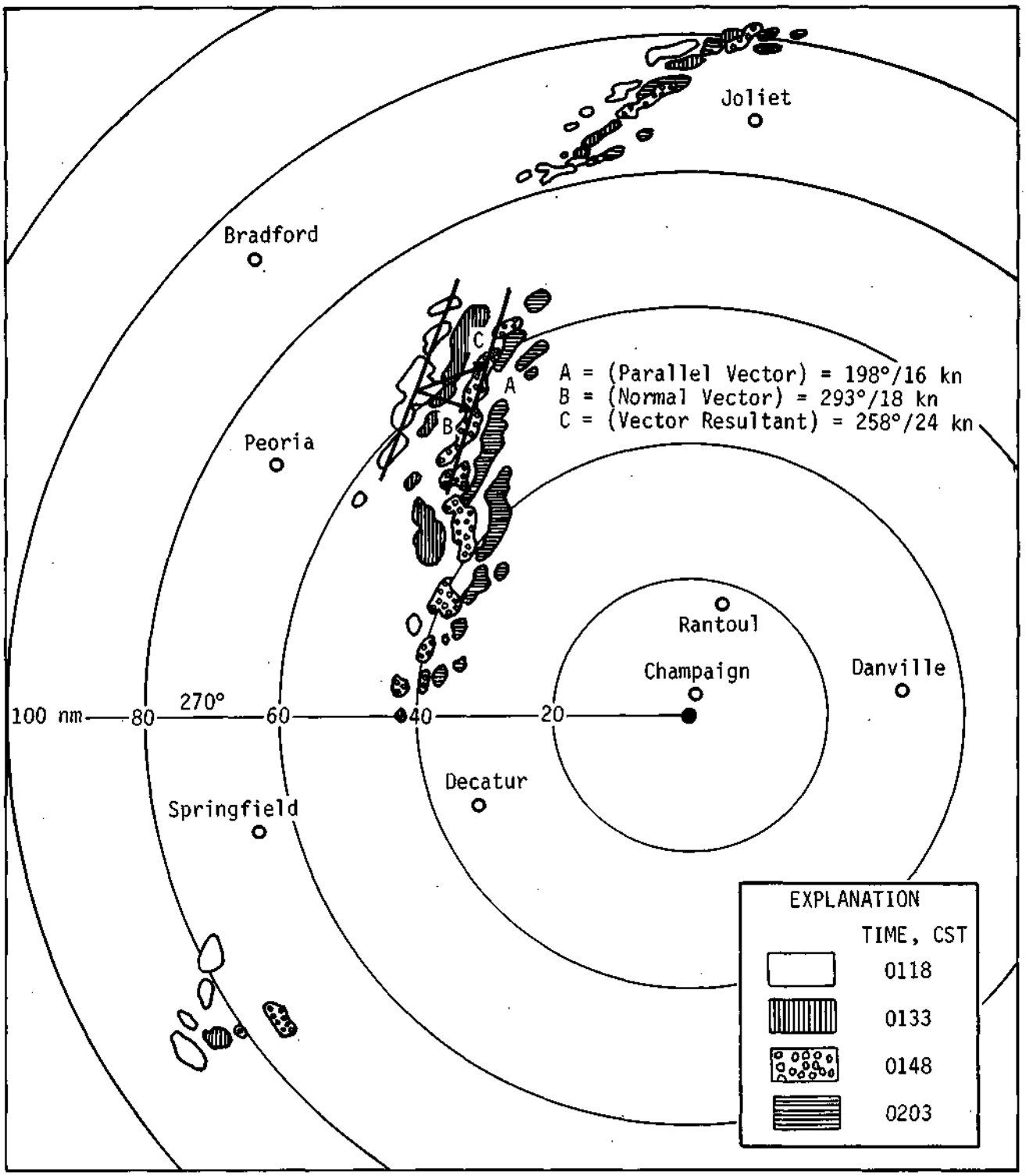

Figure 134. Squall line sequences for 9 August 1952

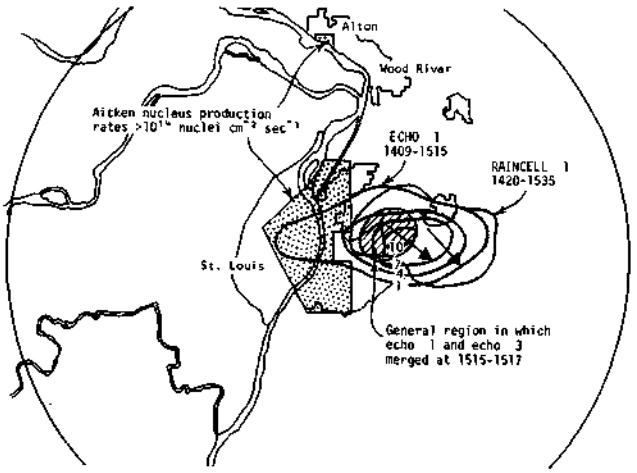

a. Life histories of echo 1 and associated raincell 1

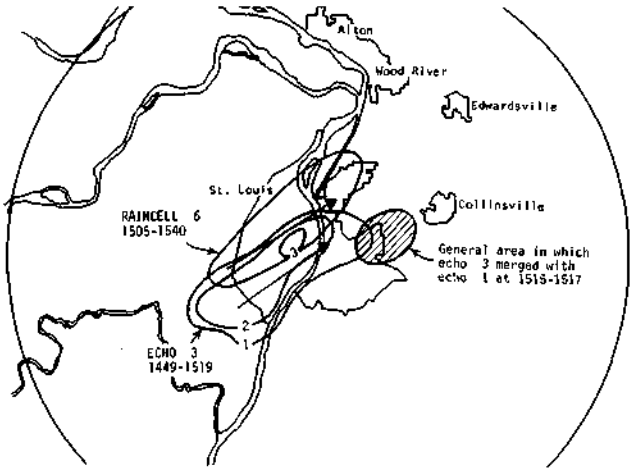

b. Life histories of merged echo 5 and associated raincell 1

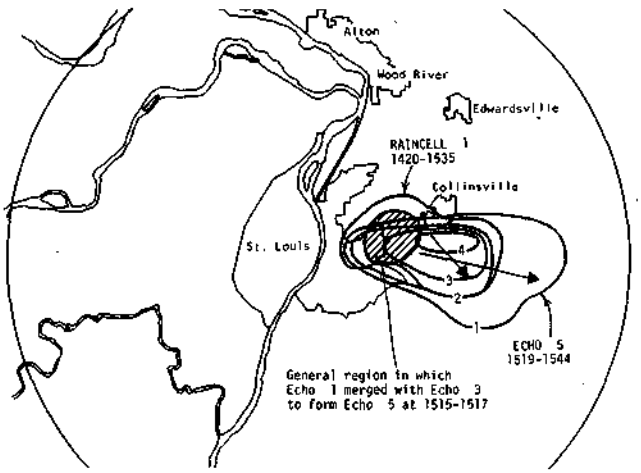

c. Life histories of echo 3 and associated raincell 6

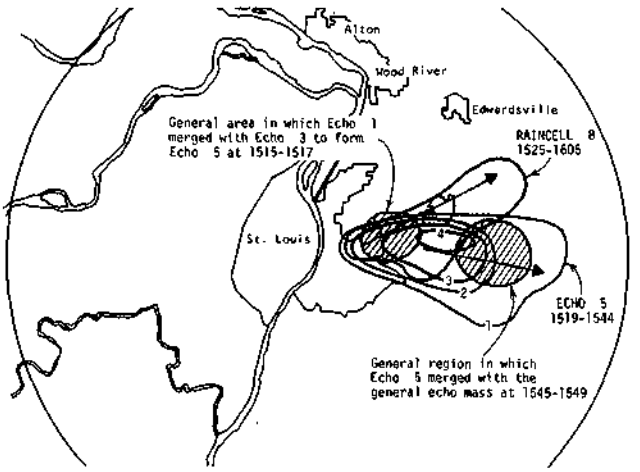

d. Life histories of merged echo 5 and associated raincell 8

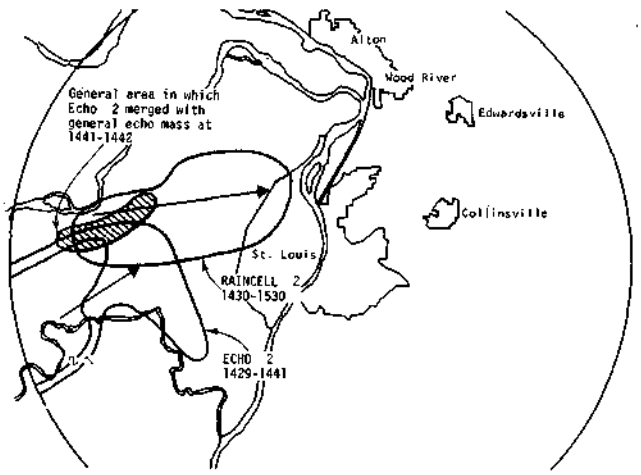

e. Life histories of echo 2 and associated raincell 2

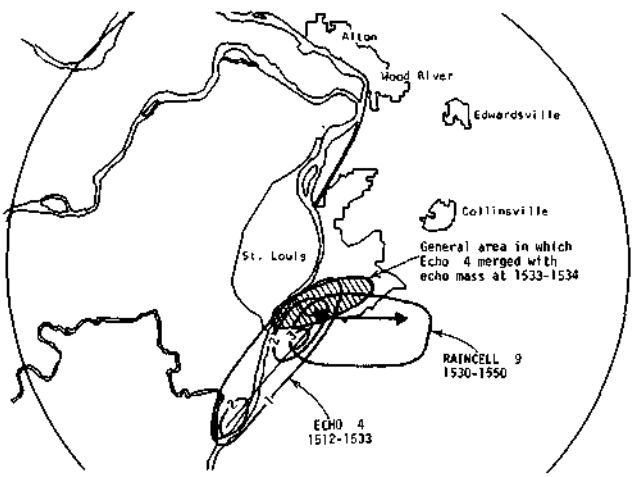

f. Life histories of echo 4 and associated raincells 4 and 9

Figure 135. Sequence of raincells and related echoes and their mergers on 13 August 1973

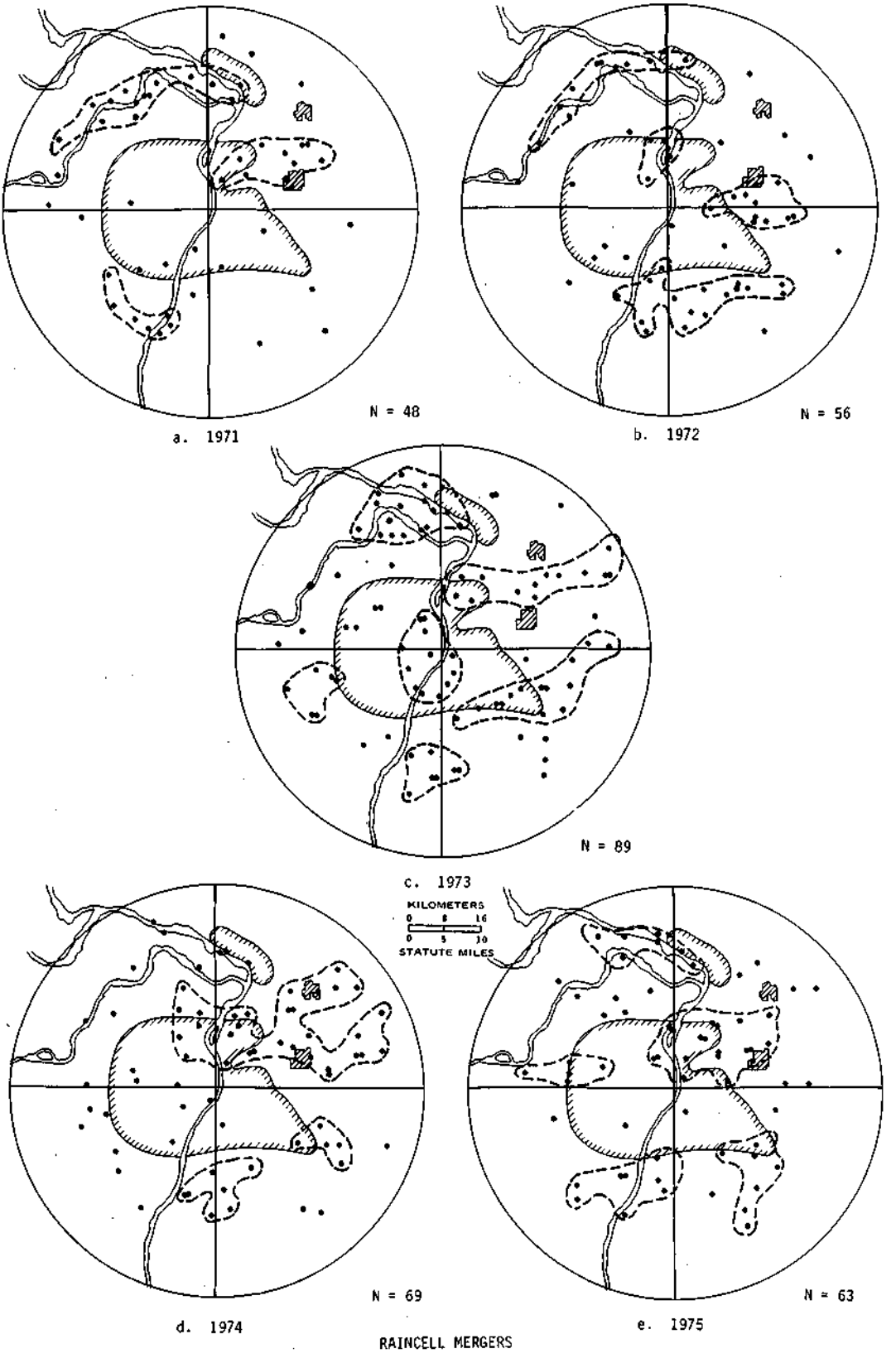

Figure 136. Raincell mergers during summers 1971-1975 at St. Louis

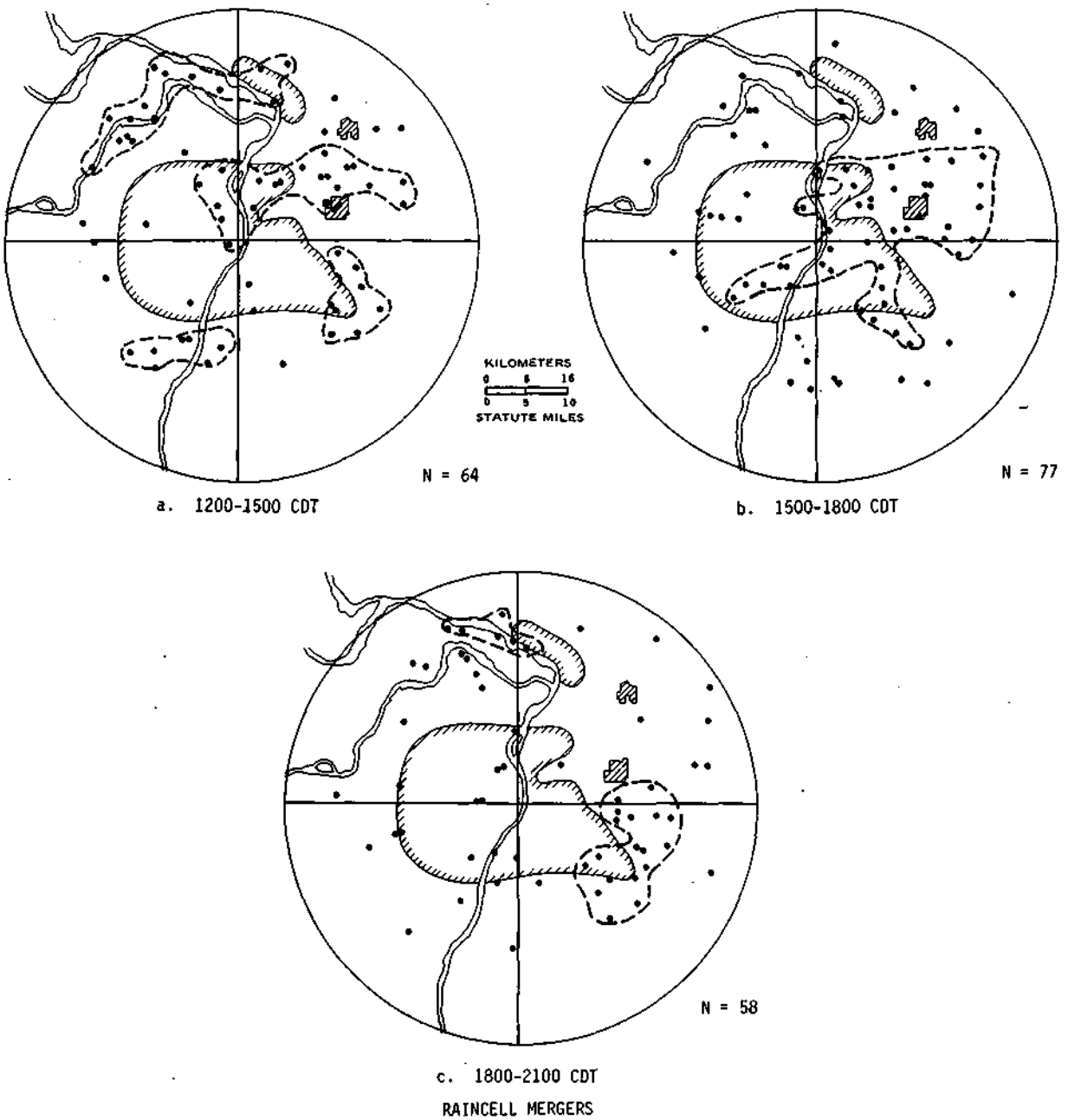

Figure 137. Diurnal distribution of raincell mergers 1971-1975 at St. Louis

vective entities which might be single or multicellular. The raincells in a multicellular storm system incorporated an isolated area of significantly greater rainfall intensity than the system isohyet. Thus, mergers of raincells could involve separate rainfall cores within a multicellular system or could be the merger of two separate isolated cells. In both the surface raincell analysis (Huff and Vogel, 1977) and the RHI radar analysis (Changnon, 1976), a merger required that the two raincells or radar echoes had to exist at least 10 minutes prior to their merger and had to have been separated by more than 8 km before they meshed to form a 'merger.'

Mergers can be of *three basic kinds.* First is the 'system merger' when a collection of cells (storms)

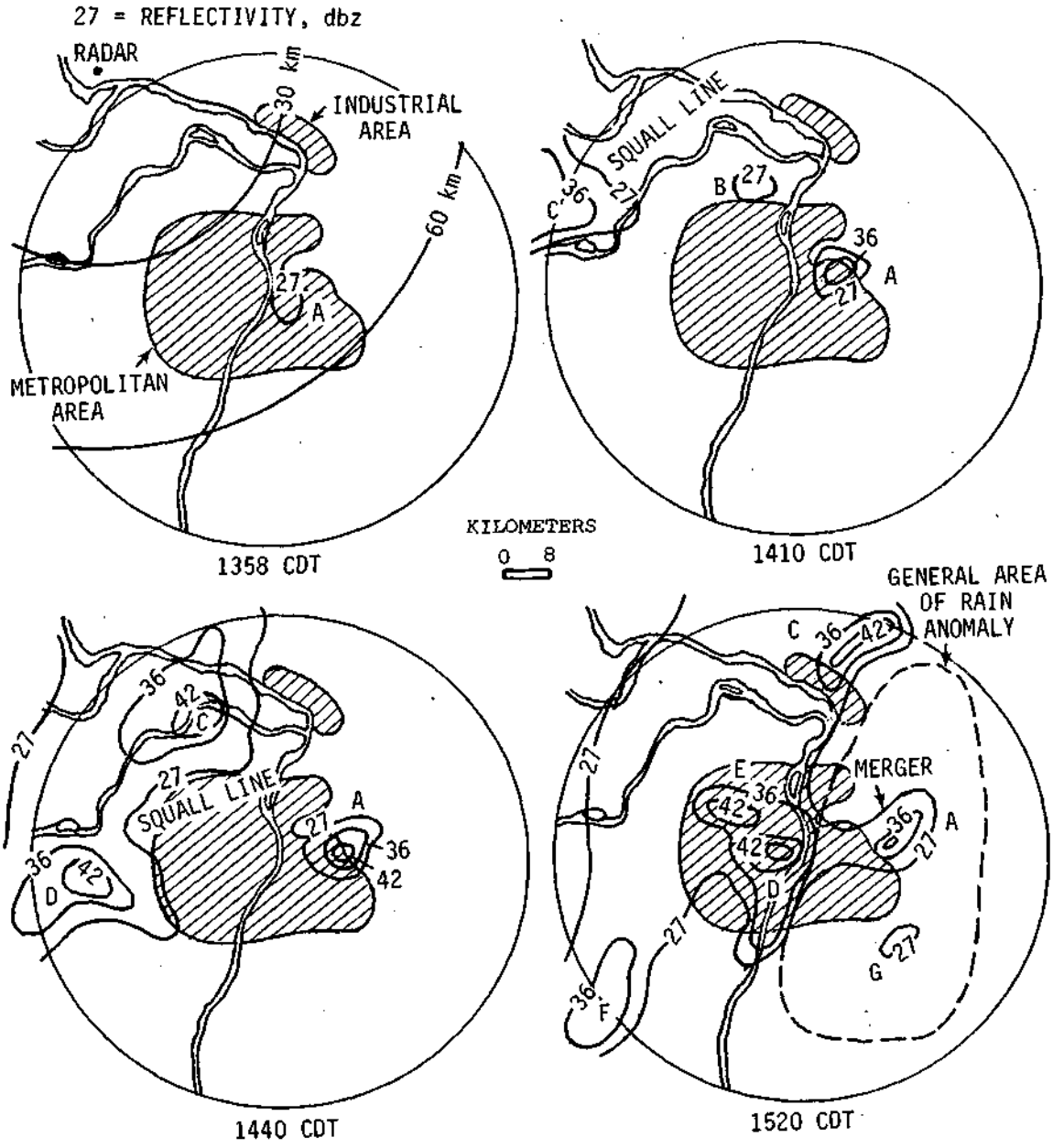

Figure 138. Radar echo merging on 13 August 1973 at St. Louis

with a given unity of motion grow so as to interact with another group of cells, forming a larger system. This merger is illustrated in figure 138. Second is the 'storm merger.' This is caused by two isolated showers or storms that move independently such that they merge due to differential motions (speed and/or direction; cells A and B in figure 141 are an example). The third merger is the 'feeder storm' type. It involves an existing storm and a series of small feeder storms that move into the core storm (note echoes C, D, E on figure 141) (Changnon, 1976).

Examples of mergers as viewed in the horizontal plane are presented in the St. Louis case study shown in figures 138-141. Figure 138 shows a typical case in which echoes develop in front of an

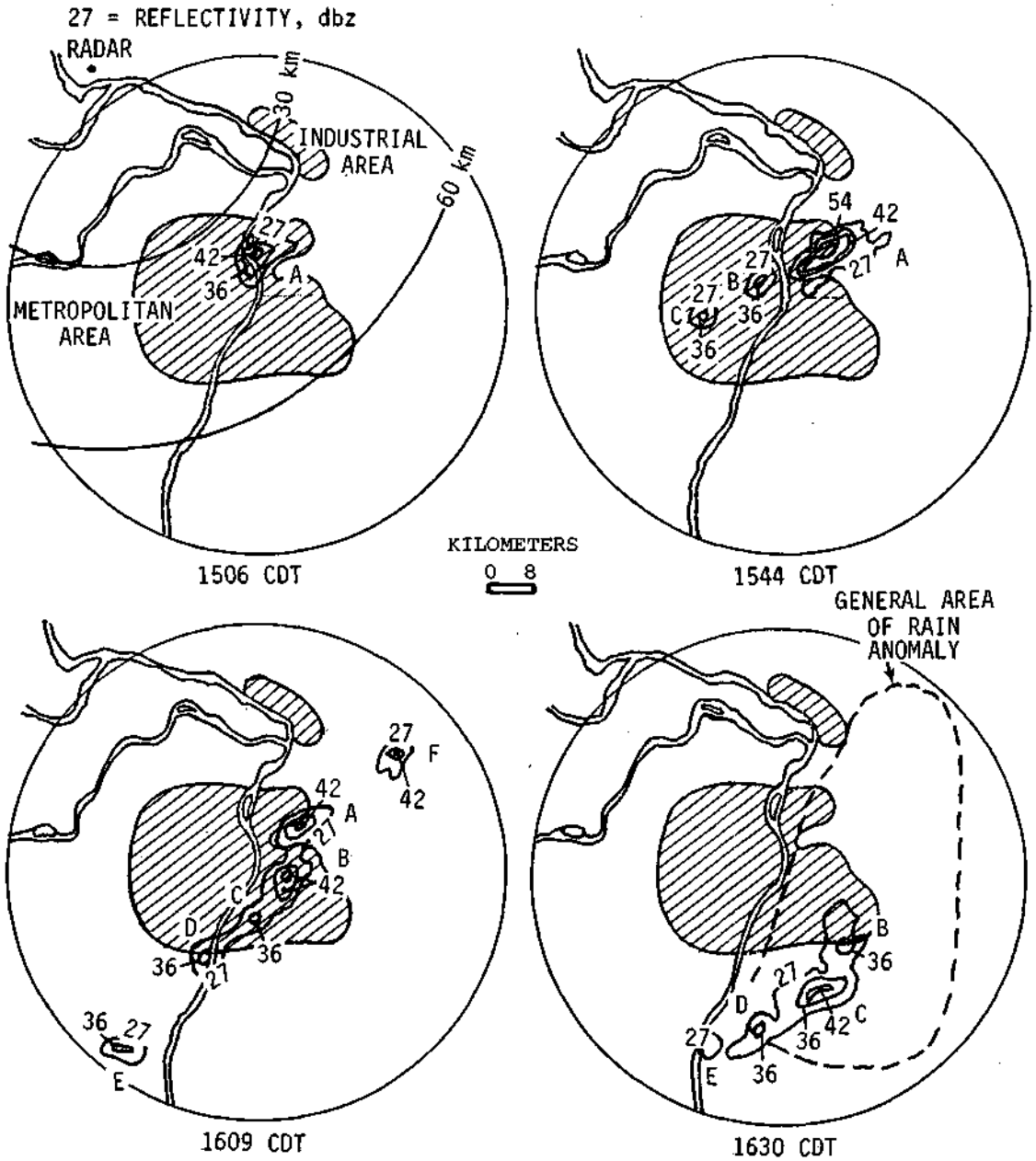

Figure 139. Development of a squall line shown by radar echoes on 12 August 1973

approaching line and because of little or no movement are eventually intercepted as part of the moving line. Another typical case is shown in figure 139 which shows the formation of a group of cells which eventually grow together to form a small squall line. Figure 140 illustrates a situation in which isolated cells grow and die but eventually develop peripheral feeder cells that merge and cause a larger entity, as shown by echo D. Still another illustration of merging is shown in figure 141. Repeated generation of cells over an area, such as St. Louis, with a subsequent slowing of the downwind motion in older cells, allows new cells, which are classed as feeders, to merge on the upwind edge and eventually form an elongated large cell.

The raincell mergers in the METROMEX area

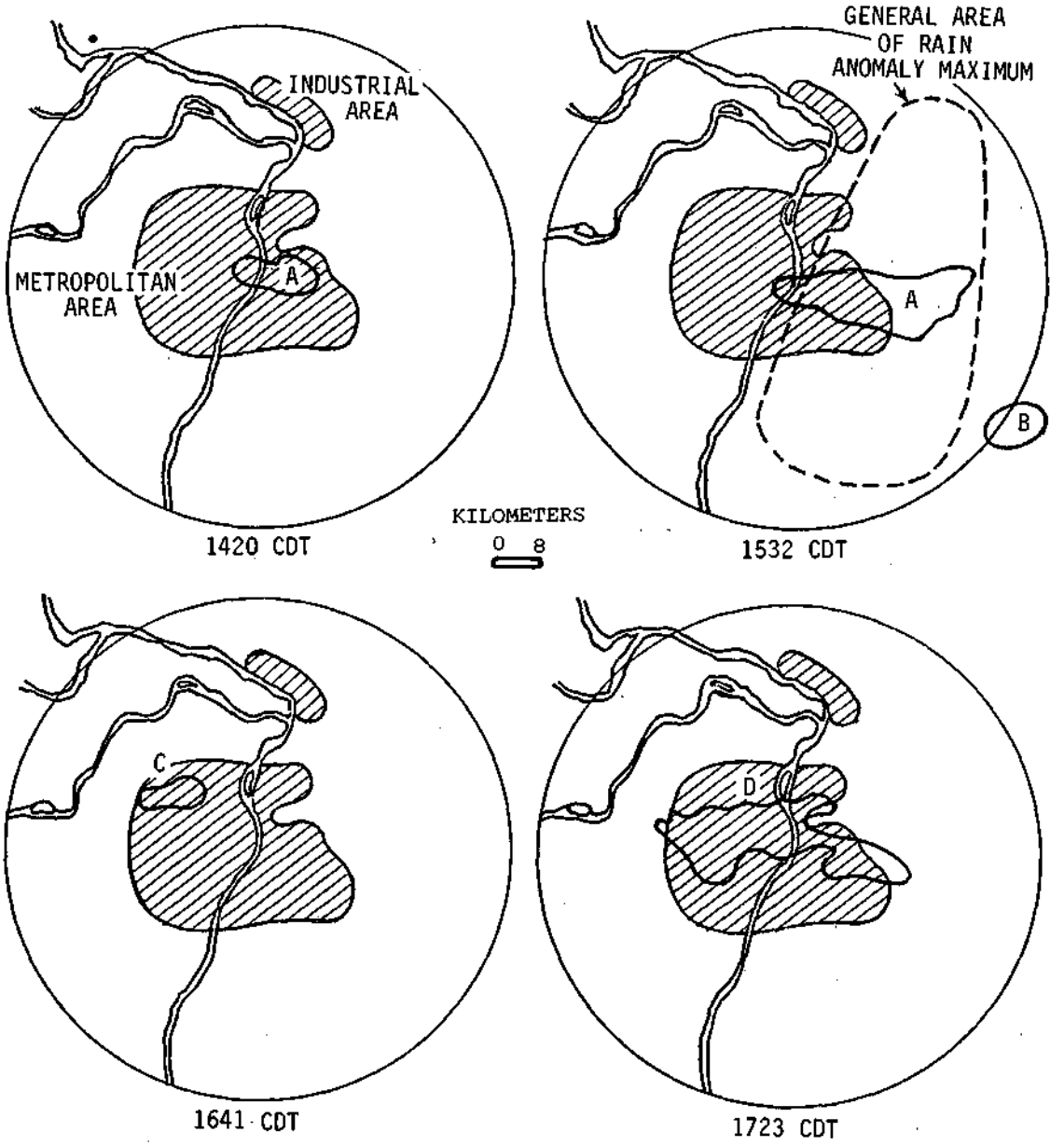

Figure 140. Development of isolated storm echoes over St. Louis on 10 August 1973

for 5 summers are shown in table 65 (Huff and Vogel, 1977). It was found that 78% of the mergers was followed by. an increase in rainfall intensity and 82% by an increase in the area of rainfall. Another presentation of the change in echoes and of raincell intensity and area following the merger of surface raincells is shown in figure 142. In more than 80% of the mergers, a marked increase in echo area and rainfall intensity followed.

Figure 143 shows a further comparison of changes that occur in rainfall intensity when mergers of relatively intense raincells occur. Shown are the frequency distribution curves derived for 1) maximum rainfall intensity following mergers, 2) the most intense of the two merging cells 5 minutes prior to merger, and 3) the less intense of

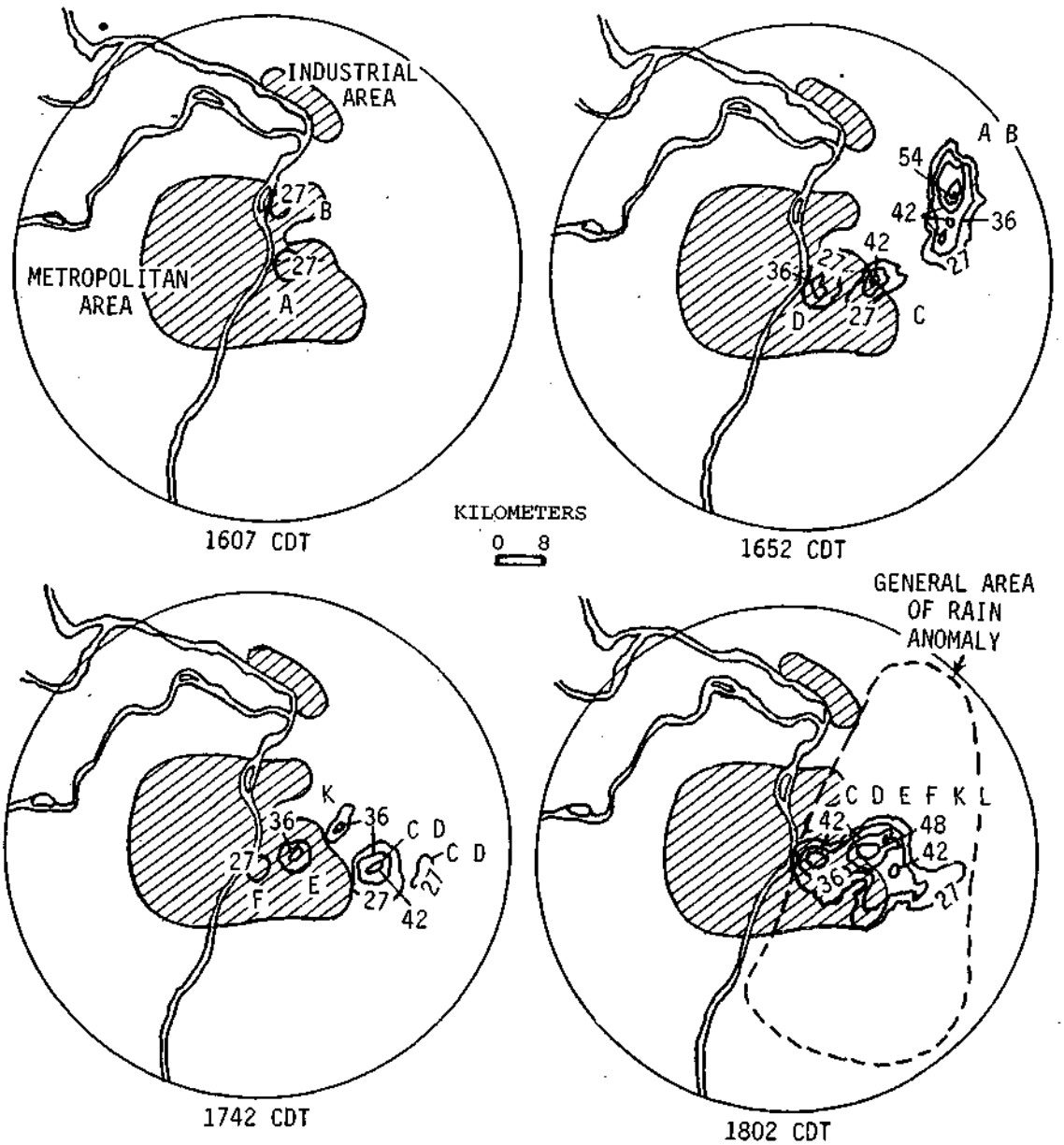

Figure 141. Development of isolated echoes over St. Louis which merged on 11 August 1972

the merging cells. These distributions provide a measure of the peak intensity of the merged entities, and the intensity characteristics of the cells responsible for the merger. Figure 144 shows the frequency distributions derived from the area measurements prior to and following cell mergers. The upper curve shows a distribution of maximum areas associated with the merged entities, and the lower curve shows a similar distribution for the total area included in the two cells producing the merger. The upper curve indicates that approximately 5% of the merged entities had areas of 1300 km^2 or more. This reduces to 240 km^2 at the 75% level.

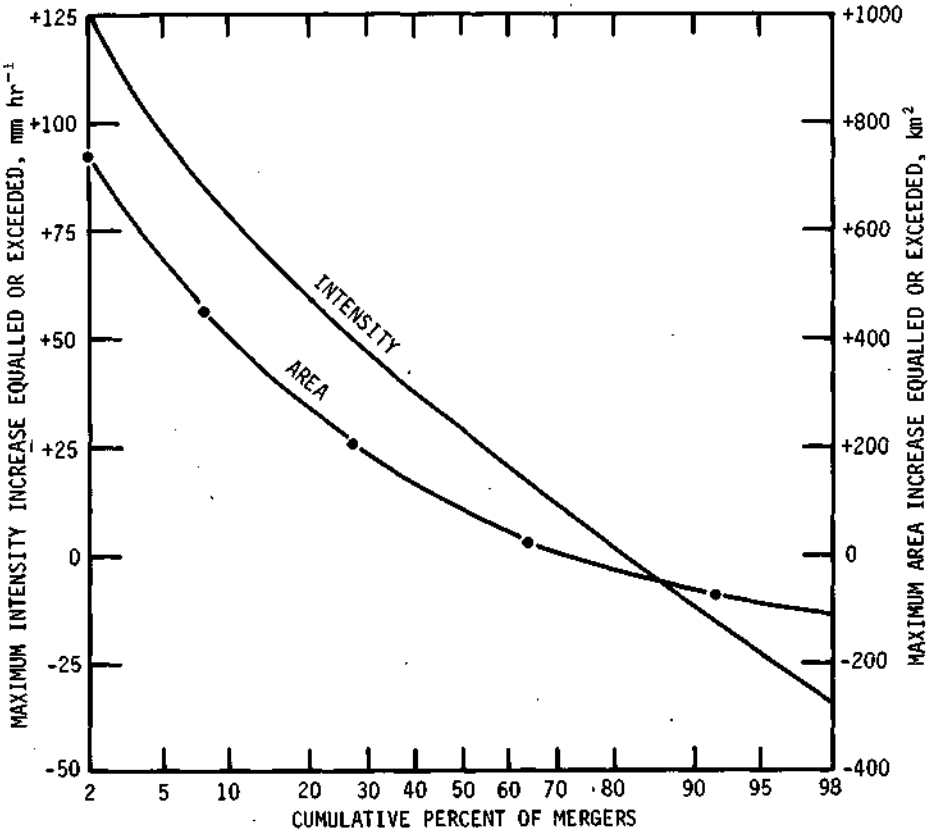

Figure 142. Frequency distribution of maximum increase in intensity and area following surface raincell mergers, summers 1971-1975, METROMEX

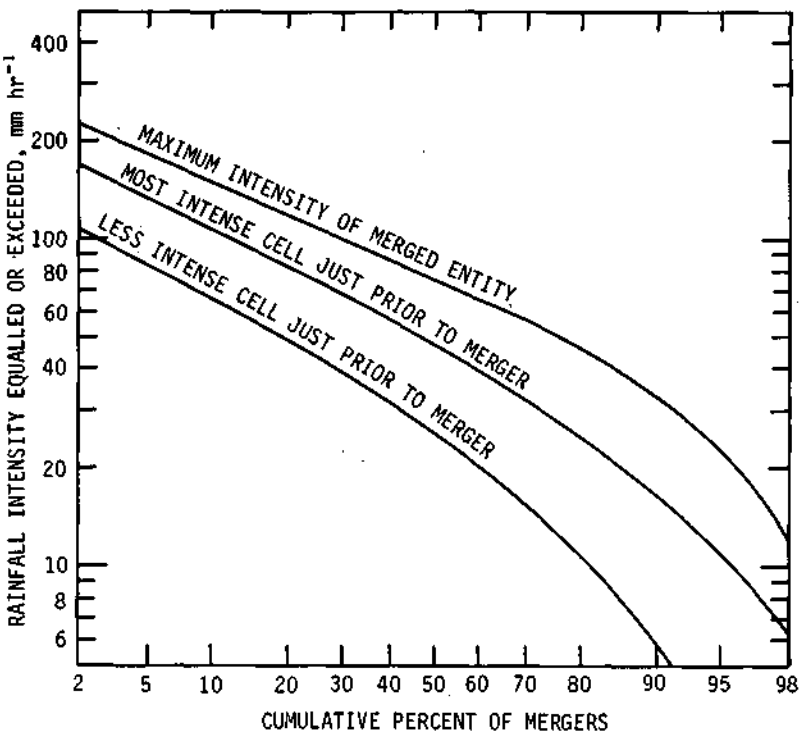

Figure 143. Frequency distribution of rain intensity prior to and following mergers, METROMEX, 1971-1975

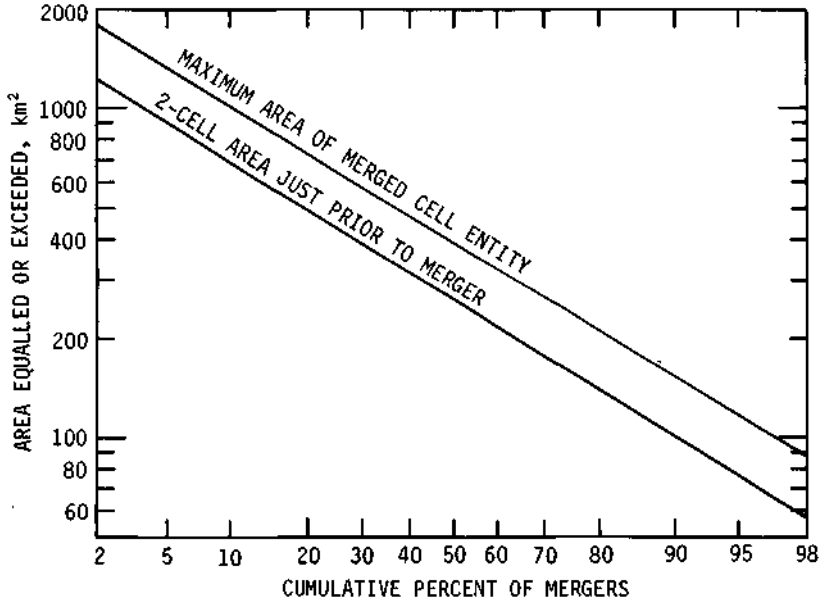

Figure 144. Frequency distribution of raincell areas prior to and following mergers, METROMEX, 1971-1975

Table 65. Statistics of Rainfall Mergers for Summers of 1971-1975, METROMEX

Number and percent of mergers with intensity increase	254	(78)
Number and percent of mergers with no change in intensity	25	(8)
Number and percent of mergers followed by intensity decrease	46	(14)
Number and percent of mergers followed by area increase	266	(82)
Number and percent of mergers followed by no area change	25	(8)
Number and percent of mergers followed by area decrease	34	(10)
Median duration of merger-involved cells		
Oldest cell prior to merger *(min)*	26	
Newest cell prior to merger *(min)*	13	
Merged cell *(min)*	33	
Median of maximum intensity change after merger, *mm/br* and %	27	(57)
Median of maximum area change after merger, km^2 and %	90	(37)
Maximum intensity change among all cases, *mm/br*	190	
Maximum area change among all cases, km^2	1119	

CLOUD CHARACTERISTICS

Cloud Dimensions

Aircraft flights were made in the St. Louis area in the summers of 1972-1973 to measure cloud base heights. Heights of some 200 cumuliform clouds were measured. The cumulative frequency of the cloud base heights at St. Louis is shown in figure 145. The median cloud base height is 3800 feet, with heights ranging from less than a 1000 up to 6000 feet. The Springfield values shown in figure 145 were calculated from surface measurements and models. In general, most summer cloud bases in Illinois are between 3000 and 5000 feet above the surface (Changnon and Morgan, 1976).

A comparative study of echo tops (based on 3-cm RHI data) and their visual cloud tops (as photographed and measured by cloud cameras) focused on data from the summers of 1953 and 1954. Figure 146 presents comparisons of the growth of echo tops and their associated visual cloud tops (Changnon and Bigler, 1957). In most instances, the visual cloud top is 3000 to 4000 feet above the echo top, but often closer during the vigorous growth periods. Also, there is a suggestion that cloud top growth continues for several minutes after the echo top growth has ended. In general, the only reasonable estimate of cloud tops of taller clouds can be made by using the echo top statistics presented in earlier sections on vertical cell characteristics.

Cloud Base Updrafts

In METROMEX (St. Louis area), cloud base flights were made to release unique tracer materials (such as lithium chloride and indium) into updrafts of convective clouds to study scavenging processes. However, updrafts were also studied. The tracer objective required that measurements of updraft speed and size be obtained. The updraft measurements were made from an instantaneous vertical speed indicator during careful aircraft operations.

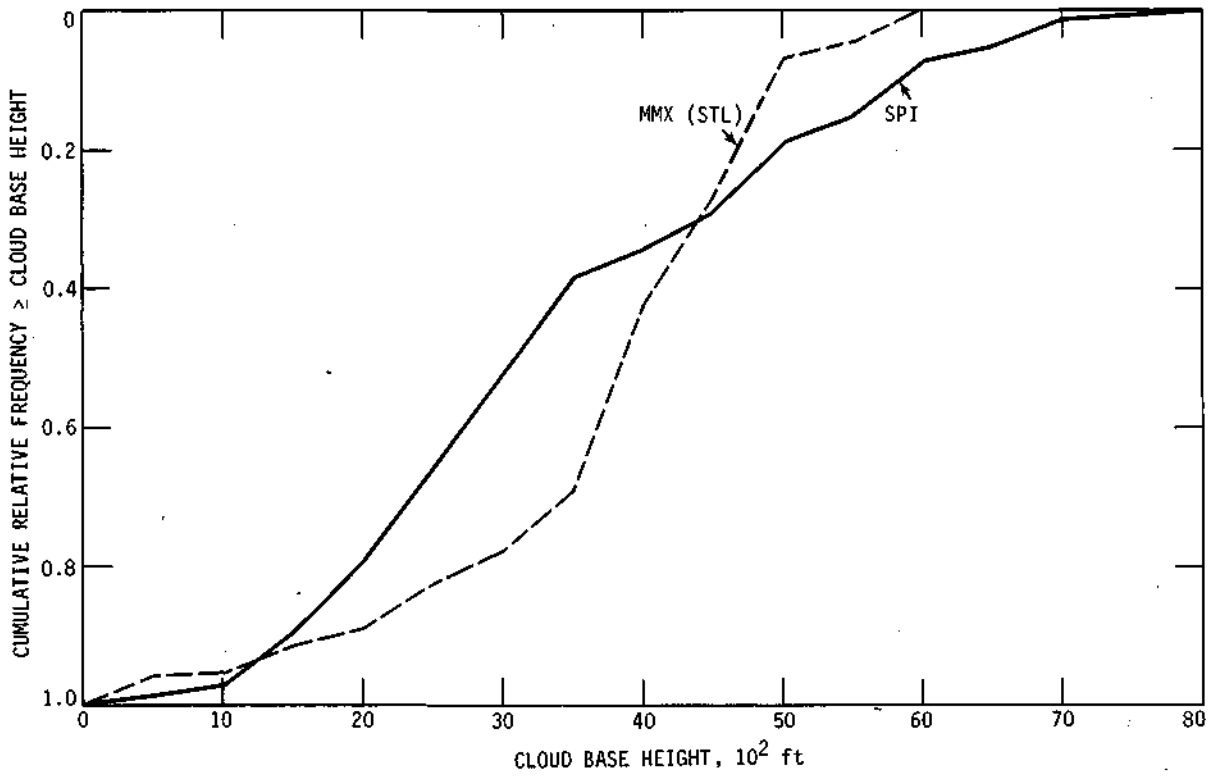

Figure 145. Cumulative relative frequency of cloud base heights at Springfield and St. Louis

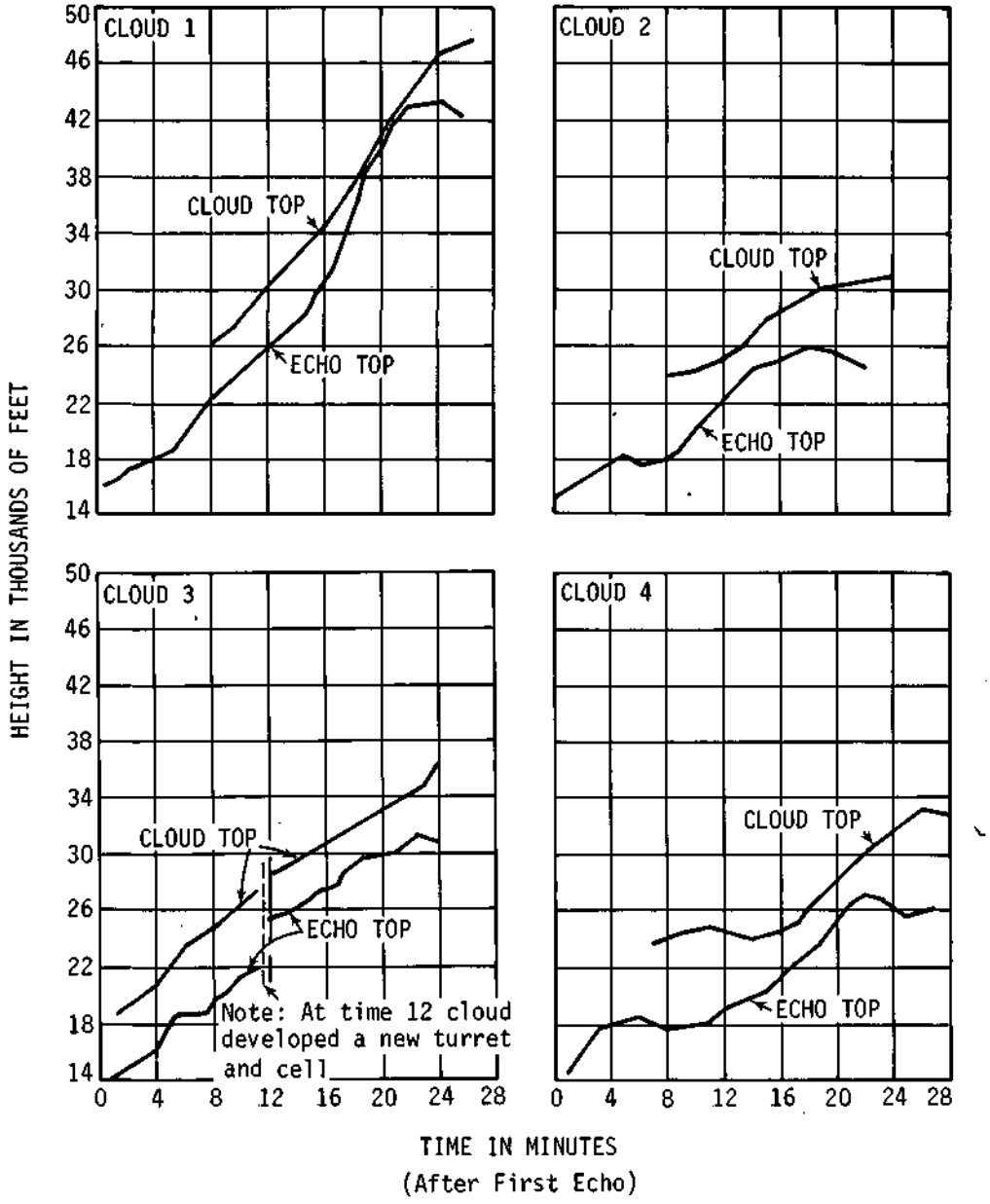

Figure 146. Visual cloud top-radar echo top growth relationship graphs for four clouds in central Illinois

Cloud base updraft data were derived from data on 15 days during 1972 and 1973, and *69* updrafts were measured, each with cumulonimbus clouds. The analysis of the data focused upon speeds in relation to the location of the updraft, positioned with respect to the direction of the movement of the storm cloud cells. Results of the analysis are presented in table 66. Seventy percent of the 51 updrafts for which the position was known occurred ahead of the echoes (downwind) and most were located on the right front. Their average speed was 2.3 m/sec. The 'unknown' category in table *66* refers to the updrafts that were measured but could not be located relative to echo position. These data are from Changnon and Morgan (1976). Further information on updrafts will be found in the tracer release texts of this section. The tracer releases for three different types of storm cases are shown, revealing both the placement and type of updrafts.

Table 66. Cloud Base Updraft Data of Illinois Thunderstorms Stratified by Their Position Relative to the Radar Echo Movement

	Left front	*Right front*	*Left rear*	*Right rear*	*Unknown*	*All*
Number of updrafts	14	24	6	7	18	69
Average speed, m/sec	2.5	2.3	2.3	2.0	3.4	2.5
Median speed, m/sec	2.5	1.7	2.5	1.3	3.6	2.5
Maximum speed m/sec	6.1	5.5	3.1	3.1	7.1	7.1
Number of updrafts ≤1.5 m/sec	6	12	0	4	3	25
Number of updrafts 1.5-2.5 m/sec	0	4	2	0	3	9
Number of updrafts 2.5-3.8 m/sec	5	3	4	3	2	17
Number of updrafts 3.8-5.1 m/sec	0	1	0	0	5	6
Number of updrafts ≥5.1 m/sec	3	4	0	0	5	12

In-Cloud Characteristics

As part of the METROMEX program (Semonin, 1978), many cumulus congestus clouds were penetrated and the liquid water content was measured. Data for more than 175 clouds on 26 summer days in 1971-1975 were obtained. The clouds outer dimensions, as estimated by flight crews, ranged between 1.7 and 3.7 km in depth with their cloud bases between 1 and 2 km above the surface. Liquid water values (LWC), as shown in table 67, were normalized to total cloud depth within a class of 100, with 90 to 100 meaning the upper 10% of the cloud. LWC increased upward through these convective clouds, reaching 1.5 grams per cubic meter (g/m^3) in the upper 30% of cloud depth. Cloud penetrations at lower levels were insufficient to give an adequate breakdown for each 10% of depth. Results measured by other participants in METROMEX indicated average LWC for cumulus congestus to be between 0.4 and 0.7 g/m^3.

Another facet of the aircraft operations in the summers of 1971-1975 in METROMEX included penetration of cumulus and cumulus congestus clouds at altitudes of around 200 meters below cloud tops to measure condensation nuclei (CN). Data were gathered on 14 days and 127 clouds were penetrated. These were sorted according to rural clouds (unaffected by urban air) and urban clouds (potentially affected by urban air), as shown in table 68. The median CN values show great differences between the rural and urban clouds, with slightly higher LWC in the urban clouds (Semonin, 1978).

Near the Freezing Level. During the summer of 1973, an intensive field measurement program was conducted to study summer cloud characteristics near the freezing level. One important part of the program was the in-cloud measurement of a number of meteorological variables. Several results focus on measurements of bulk water near the freezing level (Ackerman, 1974). Measurements of 123 clouds were taken with a JW, a total water content meter, and a Cambridge systems dewpoint hygrometer mounted aboard an Aerocommander aircraft.

Figure 147 shows the measurements from a penetration through a cloud with a simple structure, as reflected by the generally smooth and symmetrical spatial distributions of all conditions. A more complex cloud with a rain shaft near its edge is shown in figure 148. However, most main rainshafts occurred in the center of the clouds studied. In most cases, when the total water content was found to be very large, the cloud water content was small.

The average value of the cloud water and precipitation water was calculated for each cloud unit,

Table 67. Average Liquid Water Content as a Function of Height in Natural Clouds Observed in METROMEX

Penetration altitude (% of cloud depth)	*Liquid water content (g/m^3)*
90-100	1.61
80-89	1.48
70-79	1.50
60-69	1.01
50-59	1.07
40-49	1.02
30-39	
20-29	0.59
10-19	
0-9	

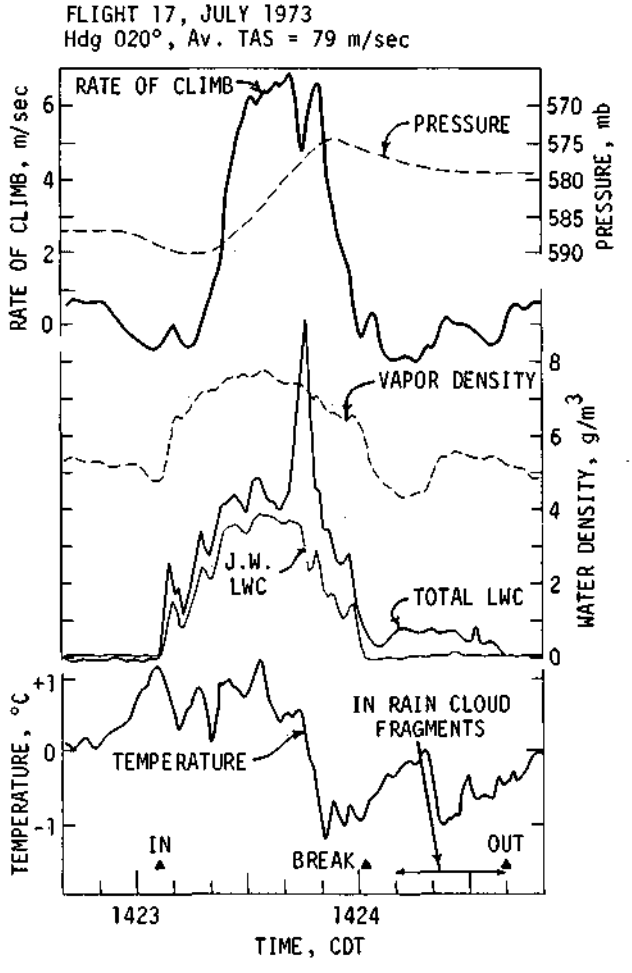

Figure 147. Measurements from a vigorous, broad cumulus congestus [Data smoothed by 5 point running mean (200 m) in Illinois]

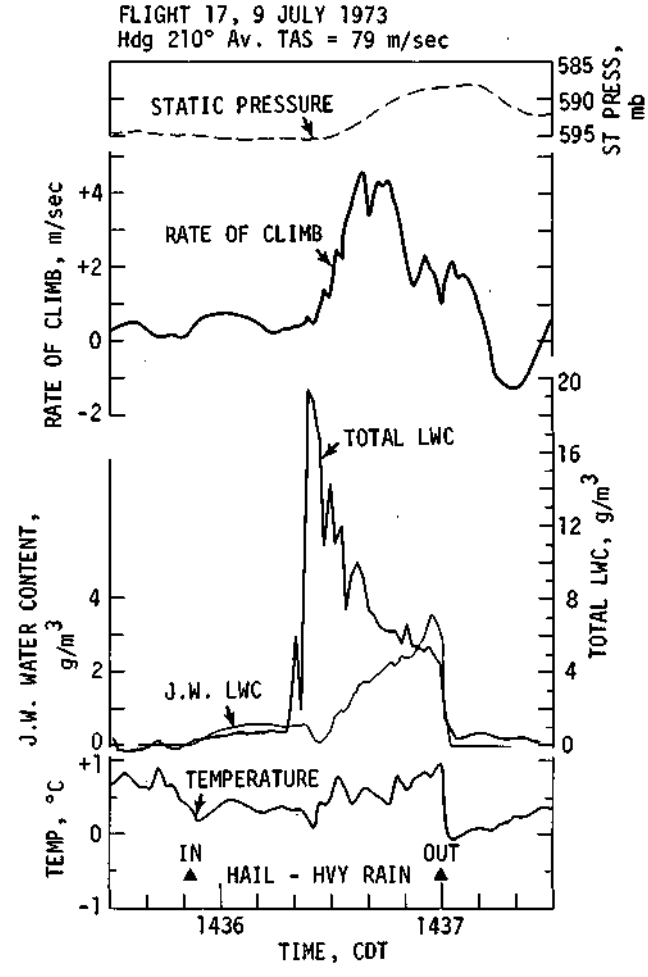

Figure 148. Measurements from a "precipitating" but still growing cloud [Note the differences in the scales of the cloud and total liquid water contents; data averaged over 120 m, in Illinois]

and the cloud water fraction was defined as the ratio of the average of cloud water content and total water content. In none of the cloud units was the water dispersed totally in small drops (figure 149), although in a few instances this condition was approached. The frequency distribution in figure 149 shows that in over 80% of the samples, less than half of the condensate in a cloud unit was in the form of cloud droplets.

Tables *69* and 70 contain many in-cloud results for various cloud types studied in the summer of 1973 (Changnon and Morgan, 1976). They present the following information: cloud type, number of clouds in sample; mean rate of climb (ROC) time in minutes; percent of total cloud penetration time prior to entering the updraft; percent time in updraft; percent of total cloud penetration time after leaving the updraft; cloud width in nautical miles; updraft width; peak rate of climb; peak Johnson-Williams (JW) water content in the updraft; peak

Table 68. The Median Condensation Nuclei and Liquid Water Content in Unaffected and Urban-Affected Clouds

	Median CN (cm^{-3})	*Median LWC* (g/m^3)
Unaffected clouds	1500	0.98
Affected clouds	3750	1.10

Table 69. Median Cloud and Updraft Parameters Stratified by Cloud Type, Based on Penetrations near 0°C Level

Type	Clouds	ROC time (min)	% Time before UD	% Time in UD	% Time after UD	Cloud width (n mi)	UD width (n mi)	Peak ROC (m/sec)	Peak JW in UD (g/m^3)	Peak JW out UD (g/m^3)	Peak RUS in UD (g/m^3)	Peak RUS out UD (g/m^3)	Peak Vap D in UD (g/m^3)	Peak Vap D out UD (g/m^3)
1	72	0.33	19	44	21	2.2	0.9	4.2	1.5	1.7	9.7	10.9	5.5	5.5
2	20	0.46	20	37	23	3.4	1.2	7.0	1.6	0.8			5.6	4.9
3	22	0.38	8	44	23	2.3	1.0	5.8	1.2	1.4	12.4	10.1	5.9	6.2
4	15	0.33	40	42	8	3.1	0.9	6.0	2.4	2.8	9.8	12.1	5.7	6.2
5	20	0.42	12	34	11	3.4	1.1	8.0	1.7	2.0	11.1	10.1	5.8	5.7
6	4	0.50	38	16	46	2.6	1.4	4.4	2.0	2.1	10.2	11.9	4.8	5.0
7	3	0.25	18	51	49	2.2	0.7	3.7	0.9		7.7		5.6	
8	7	0.58	19	60	21	2.8	1.5	5.5	1.5	0.9	9.5	12.1	5.7	
Total	163													
Median		0.46	26	44	31	3.6	1.2	6.1	1.7	1.9	11.0	13.0	5.6	5.6

Table 70. Mean Values of Various Cloud and Updraft Parameters Stratified by Cloud Type, Based on Penetrations near 0°C Level

Type	Clouds	ROC time (min)	% Time before UD	% Time in UD	% Time after UD	Cloud width (n mi)	UD width (n mi)	Peak ROC (m/sec)	Peak JW in UD (g/m^3)	Peak JW out UD (g/m^3)	Peak RUS in UD (g/m^3)	Peak RUS out UD (g/m^3)	Peak Vap D in UD (g/m^3)	Peak Vap D out UD (g/m^3)
1	72	0.39	25	47	28	2.3	1.1	5.2	1.7	1.7	10.3	11.1	5.8	5.6
2	20	0.48	29	42	29	3.9	1.3	6.6	1.7	0.9			5.6	5.2
3	22	0.47	21	47	32	4.1	1.2	7.7	1.5	1.9	13.3	11.4	5.9	6.2
4	15	0.44	34	45	20	3.3	1.2	6.4	2.4	2.8	11.3	15.5	5.6	6.0
5	20	0.52	28	41	31	4.1	1.5	9.3	1.8	2.0	13.8	10.0	5.7	5.7
6	4	0.44	44	18	38	3.9	1.2	4.5	2.1	2.1	10.0	14.6	5.0	5.0
7	3	0.28	14	43	42	1.8	0.7	3.5	1.4		8.5		5.7	
8	7	0.52	15	54	31	2.8	1.4	5.8	1.4	0.9	11.0	14.5	5.6	
Total	163													
Average		0.44	26	42	32	3.3	1.2	6.1	1.8	1.8	11.2	12.8	5.6	5.6
Median		0.46	26	44	31	3.6	1.2	6.1	1.7	1.9	11.0	13.0	5.6	5.6

1 Cumulus congestus — towering cumulus
2 Cumulus congestus adjacent to thundershowers
3 Front feeders
4 Trunk feeders
5 Congestus showers — cumulonimbus calvus
6 Cumulus cells in layers
7 Squall line back feeders
8 Cumulus congestus going to cumulonimbus calvus

JW water content outside the updraft (when peak in the cloud was not located in the updraft); peak Ruskin liquid water in the updraft; peak Ruskin liquid water outside the updraft (peak in the cloud not located in updraft); peak vapor density in the updraft; peak vapor density outside the updraft (peak in the cloud not located in the updraft).

Examination of the mean values, stratified by cloud type in table 69, reveals little difference in the first five cloud types (which were the only types with more than 10 clouds in each sample). Median values are not too different from the mean values shown in table 70. An overview of all clouds reveals that a typical growing cloud at the 0°C level is 3 nautical miles in diameter with a centrally located updraft with a diameter of 1 nautical mile which has a speed of 6 m/sec (1200 ft/min). Essentially the updraft occupies about half of the cloud. Peak JW, Ruskin, and vapor density values of 1.8, 12, and 5.6 g/m^3, respectively, can be expected at this level in the typical cloud.

Table 71 presents an analysis of the location of the updrafts found within the clouds at the 0°C level. For each cloud type, the location of the updraft, in percent of cloud from the edge of cloud and for a particular quadrant, is given relative to north. For instance, for cloud type 1, the updraft edge is located 26% of the way from the cloud edge in the 0 to 90° quadrant. There is a great tendency for the updraft to be located slightly toward the west side of the clouds; note the large numbers for the 0 to 90 to 180° quadrants. This is especially true for cloud types 2 through 5 which were all associated with precipitation echoes. However, if one looks at the type 1 clouds (cumulus congestus-towering cumulus), the updraft is almost symmetrically located within the clouds.

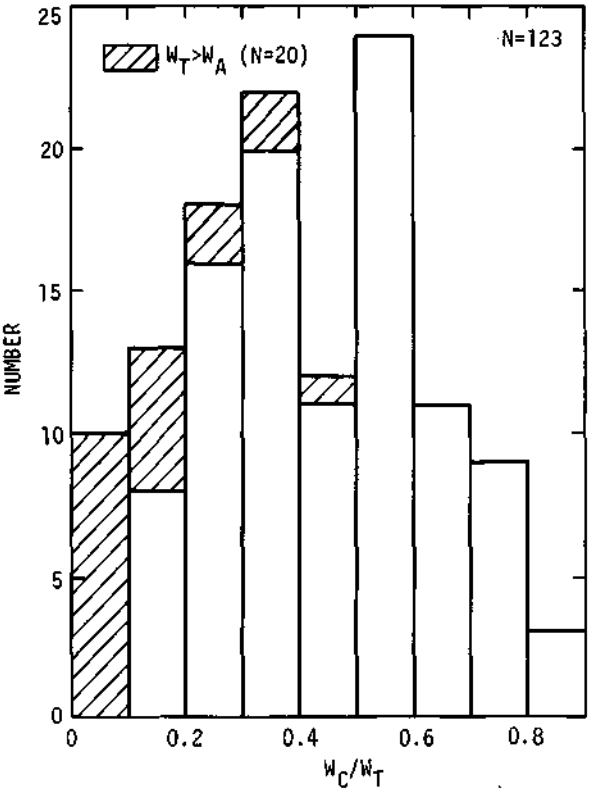

Figure 149. Frequency distribution of the fraction of condensate in cloud droplets (ratio of cloud water to total condensate) in the pooled sample

Although the earlier described cloud base updraft data were not based on the same clouds as the mid-cloud updraft study, the results taken together suggest that mid-cloud updrafts are about twice as strong as those found at cloud base. This suggests that the smaller and often greater number

Table 71. Location of Updraft (in Percent of Cloud) from Edge of Cloud for Given Quadrants

Cloud type	*Number of clouds*	*Cloud quadrant* 0-90°	91-180°	181-270°	271-360°
1	67	26.1	28.2	23.5	22.9
2	16	37.0	27.0	14.2	15.5
3	19	33.5	26.8	24.6	18.7
4	14	28.7	43.6	31.0	25.4
5	15	27.1	26.8	30.0	13.5
6	1	60.0		0	
7	3	28.1	39.0	8.5	44.0
8	7	33.8	31.2	20.2	23.1
Total of clouds	142				
Weighted average of all clouds		29.3	29.4	23.4	21.0

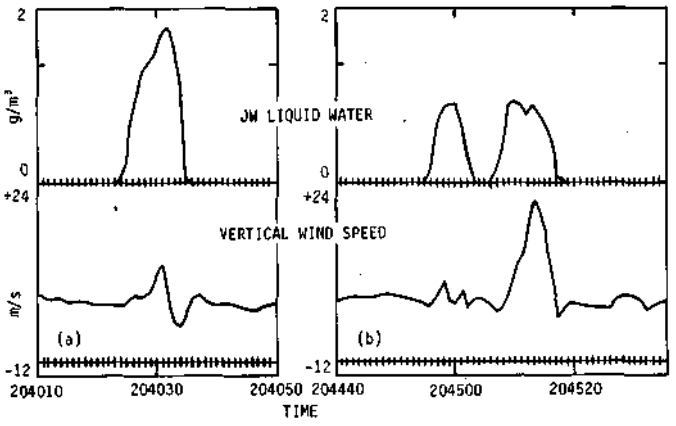

Figure 150. Liquid water and updraft profiles for cloud 13/1 (a) and 14/1 (b) on 21 July 1977

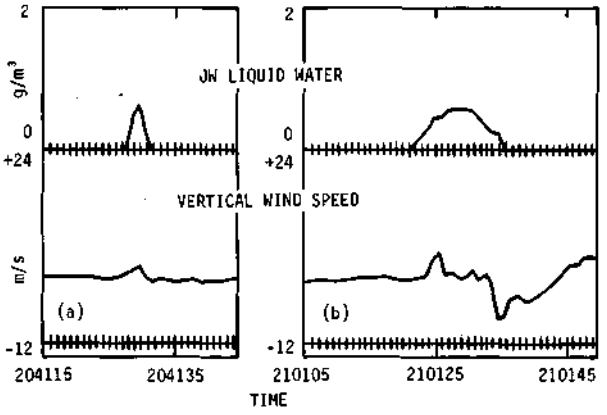

Figure 151. Liquid water and updraft profiles for cloud 2/1 (a) and 3/1 (b) on 22 July 1977

(and weaker) of updrafts at cloud base may consolidate at mid-cloud levels to provide larger and stronger updrafts (Changnon and Morgan, 1976). Conceptual modeling of the updraft locations also suggests that the updrafts are often slightly tilted from east to west as they extend upward inside Illinois cumulus clouds. This is based upon the fact that the cloud base updrafts are most often located on the front (east) side of the echoes, whereas the mid-level updrafts were found to be most often slightly displaced into the western quadrants of the cloud.

At the —10°C Level. During the afternoon of two summer days (21 and 22 July 1977) aircraft were used to penetrate convective clouds in central and southern Illinois at near the —10°C isotherm level and a large variety of cloud measurements were made (Sax et al., 1978).

One of the wettest clouds observed on 21 July is reflected in figure 150a which shows the water content and vertical velocity at 2040 GMT. The cloud boundaries are clearly defined in the water profile with water contents in excess of 1.5 g/m^3. Figure 150b shows the same cloud 4 minutes later with slightly less liquid water and a still weak updraft. Several minutes later, the updraft had become substantial, reaching 20 m/sec.

In contrast to the clouds penetrated on 21 July, the content of cloud water and strength of updrafts were much lower in cloud towers penetrated on 22 July 1977. Figure 151 shows the velocity and cloud water profiles for two penetrations (on 22 July) of clouds behind the cold front. Figure 152 shows the size distributions of cloud droplets for two towers penetrated on 21 July, and one tower on 22 July. The general shape of their distributions is similar for all clouds with an appreciable percentage (greater than 20%) of the total drop concentration contained in sizes larger than 20 microns in diameter.

These somewhat limited observations at the —10°C level suggest that summertime convective clouds in Illinois developing in moist air in advance of a weak cold front have microphysical characteristics quite similar to those for comparable clouds in Florida. The Illinois towers are characterized by high cloud water contents, moderate updrafts, and in initial penetrations, by low concentrations of graupel ice. Clouds found developing in the dry air behind the front had very weak updrafts, low concentrations of cloud water, and an abundance of ice in the form of graupel.

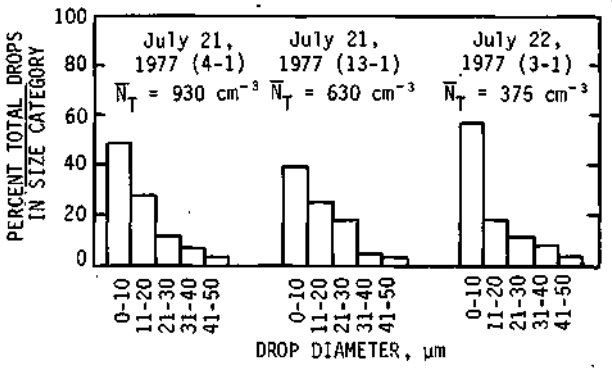

Figure 152. Cloud droplet size distributions for towers 4/1 and 13/1 on 21 July 1977 and 3/1 on 22 July 1977 (from formvar data)

Airflow Trajectories in and around Convective Clouds

A primary effort in the METROMEX program concerned the use of relatively unique tracers released by aircraft into cloud base updrafts. The results of ensuing analysis of surface rainwater to measure these tracers were used to make inferences about the airborne scavenging, by clouds and rainfall, of airborne pollutants. Primarily, the tracer efforts done in St. Louis used either lithium, which is a hygroscopic material, or indium which is an inert material. On several dates, one or both of these tracers were released into cloud base updrafts in a manner exactly comparable to cloud base seeding for cloud modification. Results from these pseudo-seeding missions offer information about the release of seeding materials and their dispersion within clouds. Three case studies from different synoptic types with varying cell organization were chosen for presentation (Changnon and Semonin, 1975).

Tracer Releases on 11 August 1972. A good understanding of the tracer releases on this date can be obtained by comparing the aircraft flight track with the corresponding raincell patterns at different times during the release. Storms on 11 August were in a squall area of the air mass type, for which the total storm rainfall is shown in figure 27a.

The first of the 5-minute flight-rain patterns (for 1630-1635 CDT) is shown in figure 153. At this time, the aircraft pilot reported burning lithium into a weak updraft related to cell 3 which had a rainshaft approximately 6 miles east of the updraft (and aircraft position). Following the aircraft tracks in subsequent periods (figure 153) shows that strong updrafts were occurring on the west, or upwind flank, of the developing storm where new towers were growing, thus reflecting a backside feeder situation. The lithium tracer material was released for nearly an hour into the rear updrafts of this storm.

Figure 154 is an isohyetal map that includes all the rainfall potentially affected by the tracer releases. The boundary of the rain chemistry network where tracer could be measured (at each dot) is also shown in figure 154. The lithium deposition pattern is shown in figure 155 with iso-deposition lines drawn for intervals of 500, 1000, and 2000 pg/cm^2. Also portrayed are selected isohyetal lines and hailfall points. A reasonably good relationship exists between the heaviest deposition and the heavier rainfall values. The envelope that includes the flight track during the 67-minute tracer release is also shown. Seventy percent of the lithium released could be accounted for in the surface network measurements.

Tracer Releases on 23 July 1973. Both indium and lithium tracers were released into flanking cells of a squall line passing through St. Louis on 23 July 1973. The wind direction shown (figure 156) is approximately at flight level at 1600 CDT. The lithium release was into updrafts found along the right flank of a major squall line cell moving from WSW to ENE.

The relationships between airplane location, updrafts, and the rainfall rate elements are shown in figure 157. The measured updraft speeds, combined with the height of rain generation and of raindrop falling speeds, suggest an interval of 20 to 30 minutes between water vapor entering these convective clouds and subsequent deposition as rain. Such calculations indicate that the tracers should have been deposited over the extreme northern portion of the chemistry network. The aircraft releasing the tracers was flying in a strong updraft, as shown in figure 157.

Figure 158 reveals the pattern of lithium deposited as corrected for dry deposition since other lithium sources were known to exist in the area. The tracer deposition was not uniform. Heaviest lithium depositions were in the cells very close to the updraft releases of the aircraft.

Tracer Releases on 12 August 1973. Another type of weather condition in which tracers were released occurred on 12 August *1973,* when a squall line developed in the St. Louis area. The total rainfall for this storm event is shown in figure 30b. The release of lithium began at 1545 (as shown on figure 159) and continued for 36 minutes.

The aircraft flew in a strong, greater than 1000 ft/min, updraft. It was an extremely smooth frontal updraft typical of those found in organized squall lines. The aircraft essentially flew a race track pattern (figure 159) parallel and in front of the relatively straight N-S front edge of the storm system.

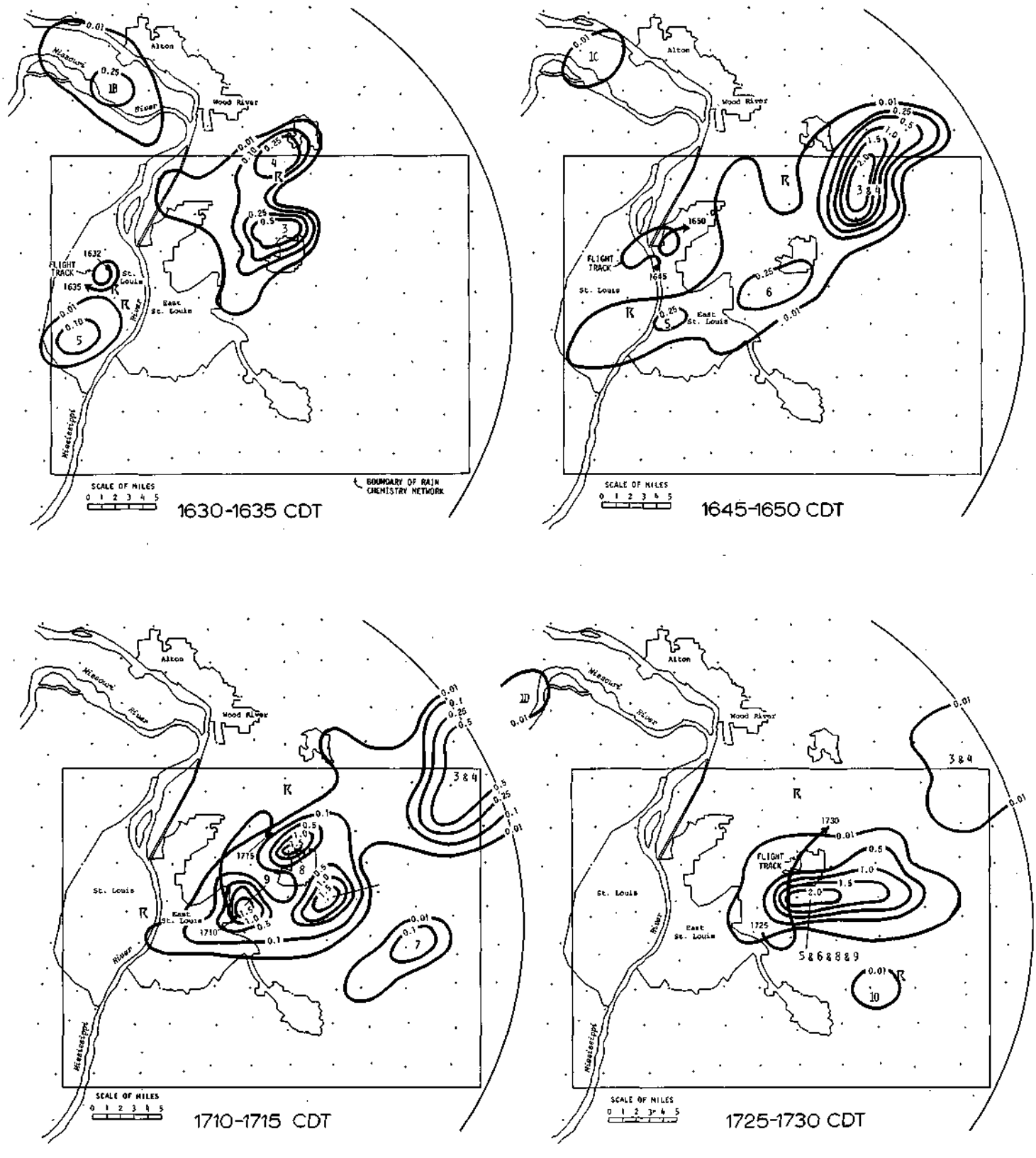

Figure 153. Flight tracks and rainfall during tracer releases for selected times on 11 August 1972

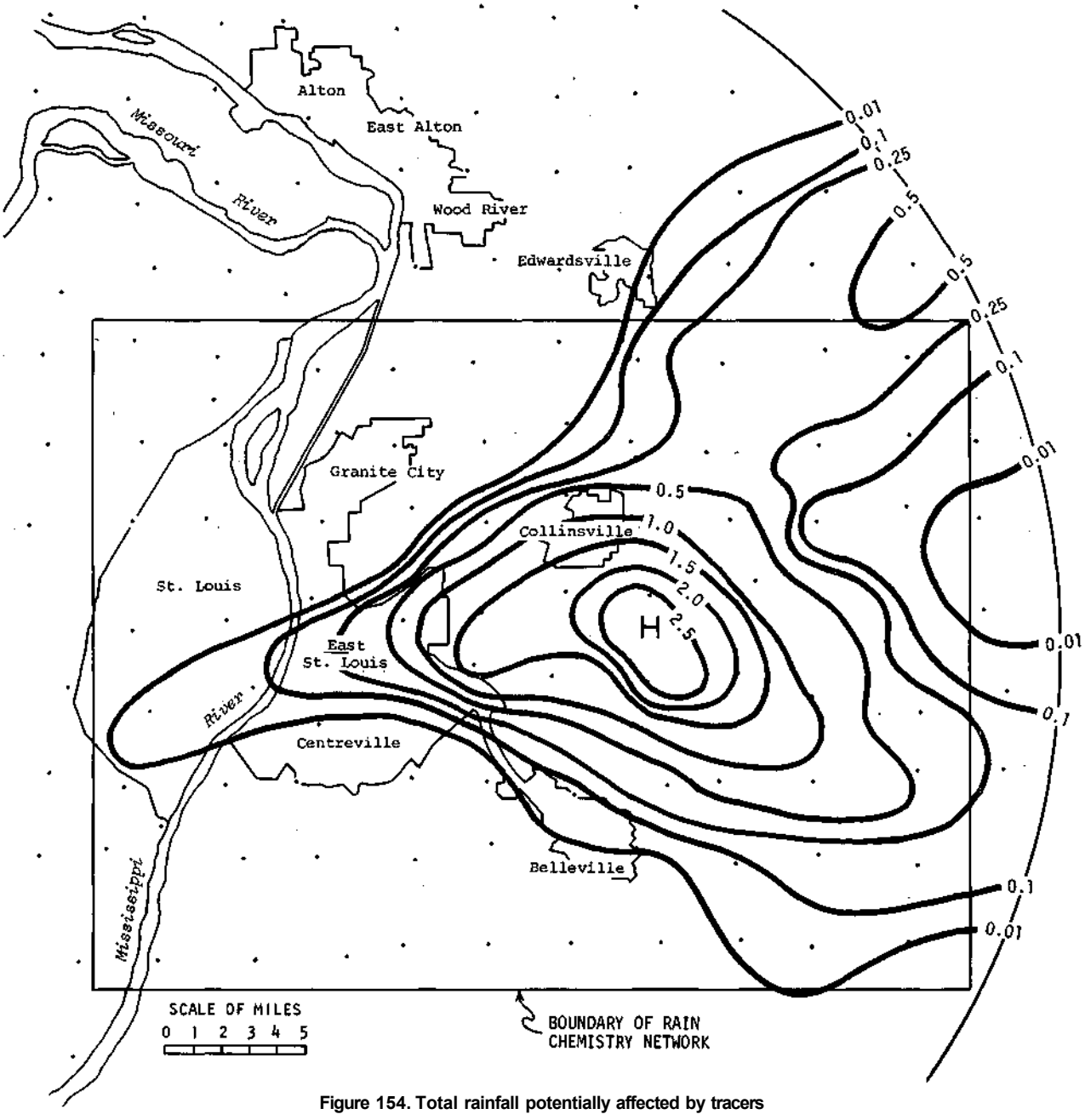

Figure 154. Total rainfall potentially affected by tracers

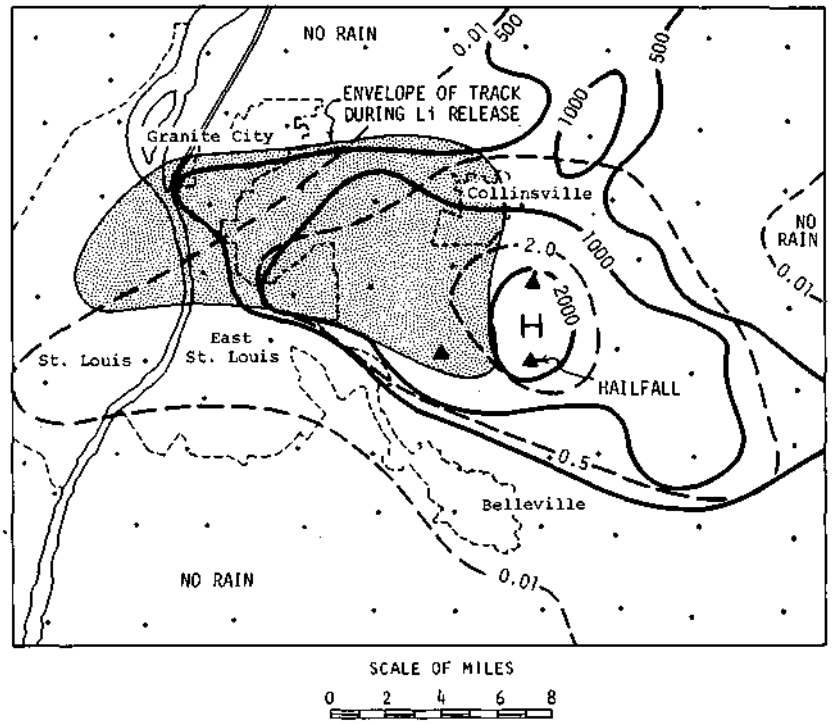

Figure 155. Lithium pattern and rainfall on 11 August 1972

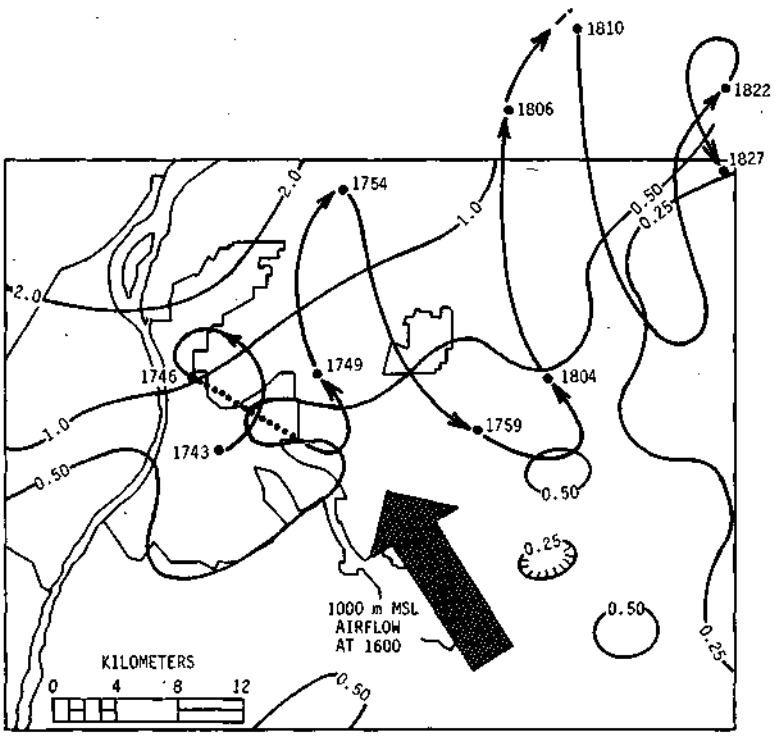

Figure 156. Rainfall in the Chemistry Network after start of tracer releases (Li was released along entire aircraft track and In was released over dotted portion only; wind direction shown is approximately that of flight level at 1600, 23 July 1973)

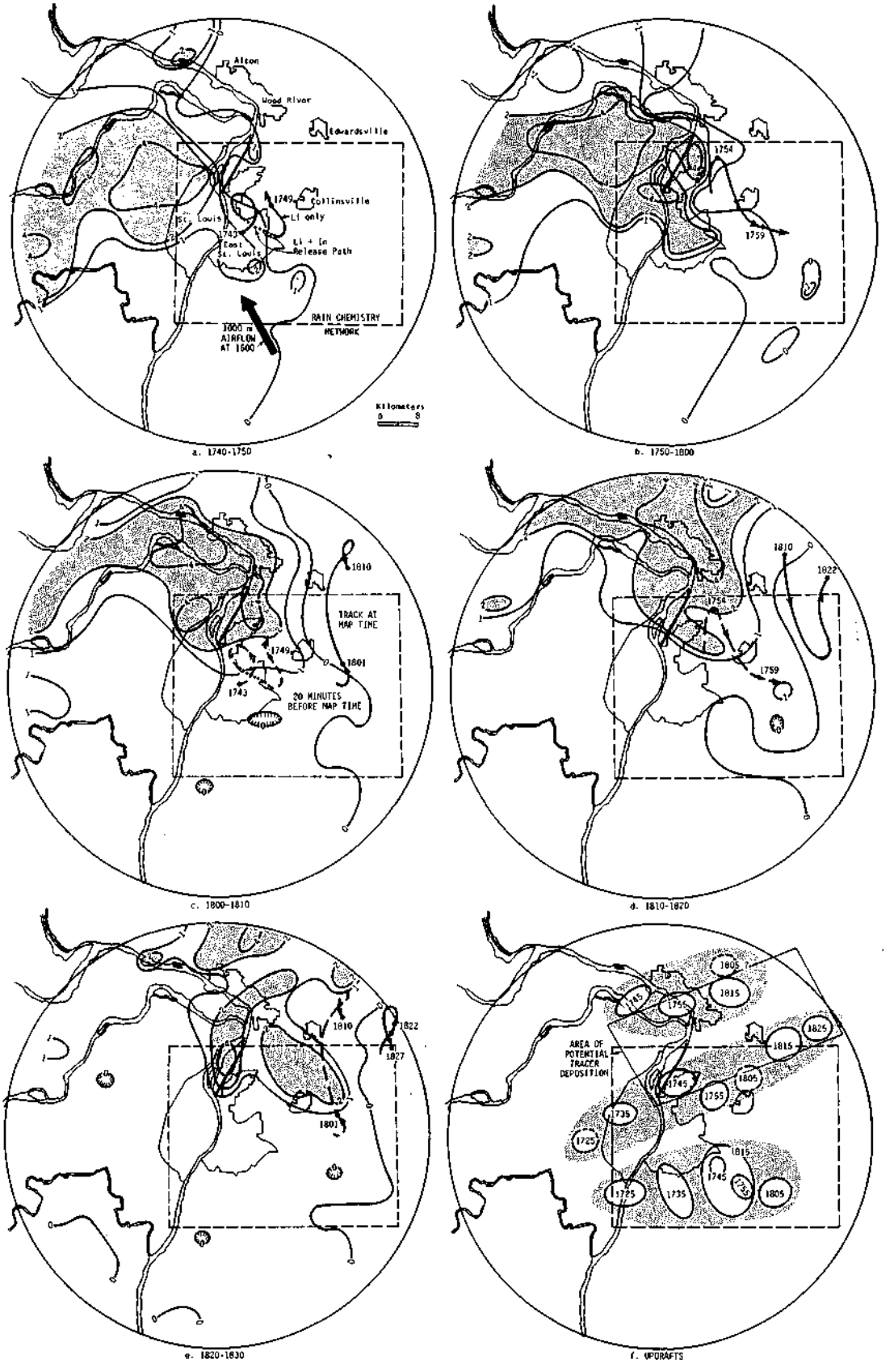

Figure 157. Rainfall rate (in/hr) distributions for successive 10-minute periods during the squall line, and updraft positions inferred from the rainfall rate distributions

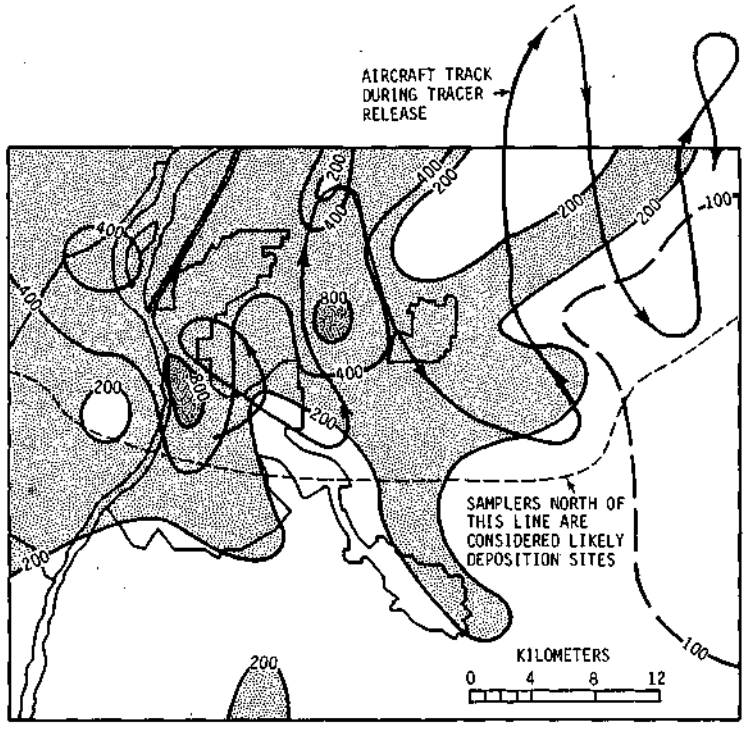

Figure 158. Soluble Li deposition (pg/cm^2) for dry deposition

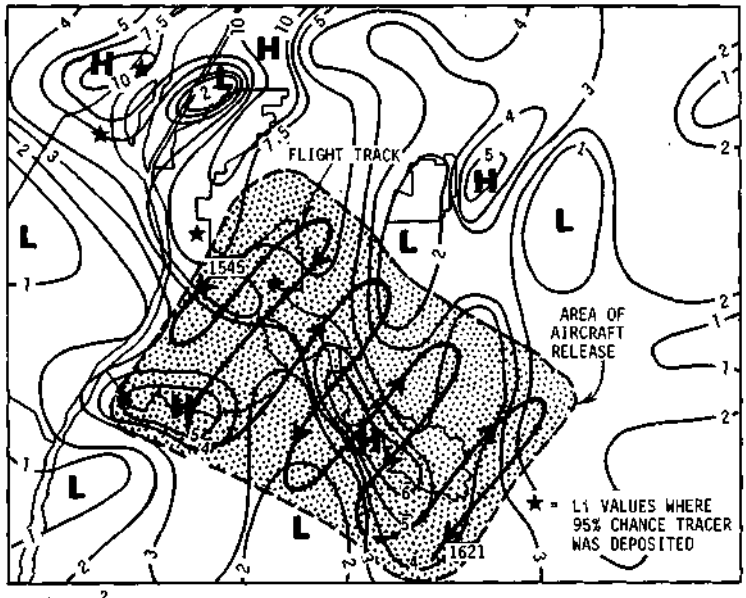

Figure 159. Corrected deposition of Li and aircraft release track

Comparison of the release track and the surface lithium pattern shows there were highs (deposition values >6) directly below and likely related to the lithium release and the subsequent rainfall along the track of the airplane. Although the inflow was relatively laminar and unchanging with time along the front edge of the line, the lithium pattern is highly variable. High values (>5) existed at three locales well north of the release track. Starred" values shown in figure 159 were calculated at the 95% likelihood to be values affected by the tracer release. These were in areas where cells and heavy rain existed or developed during orafter the release. In this case and in several other tracer case studies, it appeared that the tracers were being exposed to both in-cloud and between-cloud processes.

Summary. The tracer studies of some 15 summer rain cases at St. Louis revealed at least two important facts. In multicellular situations, the tracers released in well-defined updrafts of a given storm were found to be diffused or mixed into the air of other cells often 10 to 20 miles away and deposited by a variety of cells. This suggests considerable between-cloud exchange.

Another important result concerned tracers released in very isolated clouds where the rainfall in tracer amounts could be carefully monitored. In most of these cases, relatively small amounts of the tracers were found at the surface, commonly only 10 to 25% of that released. This suggests that either the materials were not released totally in the updrafts (a low amount getting into the target cloud), or that the tracer was passing on through the cloud without being captured in the rainfall process.

Cloud Frequencies

Figures 160 and 161 present average annual patterns of various major cloud types in Illinois (Changnon and Huff, 1957). These are based on surface observations for 1948-1955 at the stations shown.

The monthly frequencies of cumulus and cumulonimbus at Chicago and St. Louis are shown in figures 162 and 163. These show the monthly number of hours with occurrence, and the average number of tenths coverage over the 7-year period. Dividing these two values provides an approximation of the average monthly coverage. The average monthly values of all the major cloud types at six of the stations in and around Illinois are shown in table 72. Considerable regional differences are revealed.

The diurnal distributions of various cloud types at Springfield (central Illinois) for January and July are shown in figure 164. The major early afternoon maximum of cumulus is quite obvious with a double maximum of Cb which corresponds well with the thunderstorm distribution (figures 20 and 21).

One part of the Illinois cloud climatology done by Changnon and Huff (1957) related to studying mathematical relationships between surface-measured cloud amounts and precipitation. Table 73 presents the seasonal correlation coefficients (note May-September) for various cloud types and monthly precipitation at a point (Springfield), and at an 8-station area around Springfield. Note that the amount of Cb has a correlation of +0.7 with the area rainfall, and that As has a correlation of +0.8.

Another presentation relating cloud cover and precipitation is shown in table 74. Here, for various seasons and stations, the medians of low cloudiness (largely cumuliform) are shown for days of moderate to heavy rainfall. In summer at Springfield, and for daily rainfalls of 0.26 to 1 inch, low clouds are 206% of normal.

Table 75 shows the frequency distribution of low clouds on days with precipitation in excess of 0.25 inch. Data for four cloud observing stations have been combined to provide 'average Illinois' statistics. Columns 2 and 3 show the average daily cloudiness, expressed in terms of normal, which is equaled or exceeded for the cumulative percent of precipitation days given in column 1. For example, on 10% of the days with precipitation ≥ 1 inch, the average daily cloudiness is $\geq 338\%$ of normal. Analyses of the monthly frequencies of days with measurable rain and monthly frequencies of hours with clouds are summarized in table 76 and figure 165. Table 76 shows correlation coefficients between the major cloud types and the frequency of measurable rainfall at Springfield in all months. This reveals the amount of year-to-year variation that can be obtained between the incidence of clouds and the frequency of precipitation. Scattergrams for the seasonal precipitation frequency of precipitation in

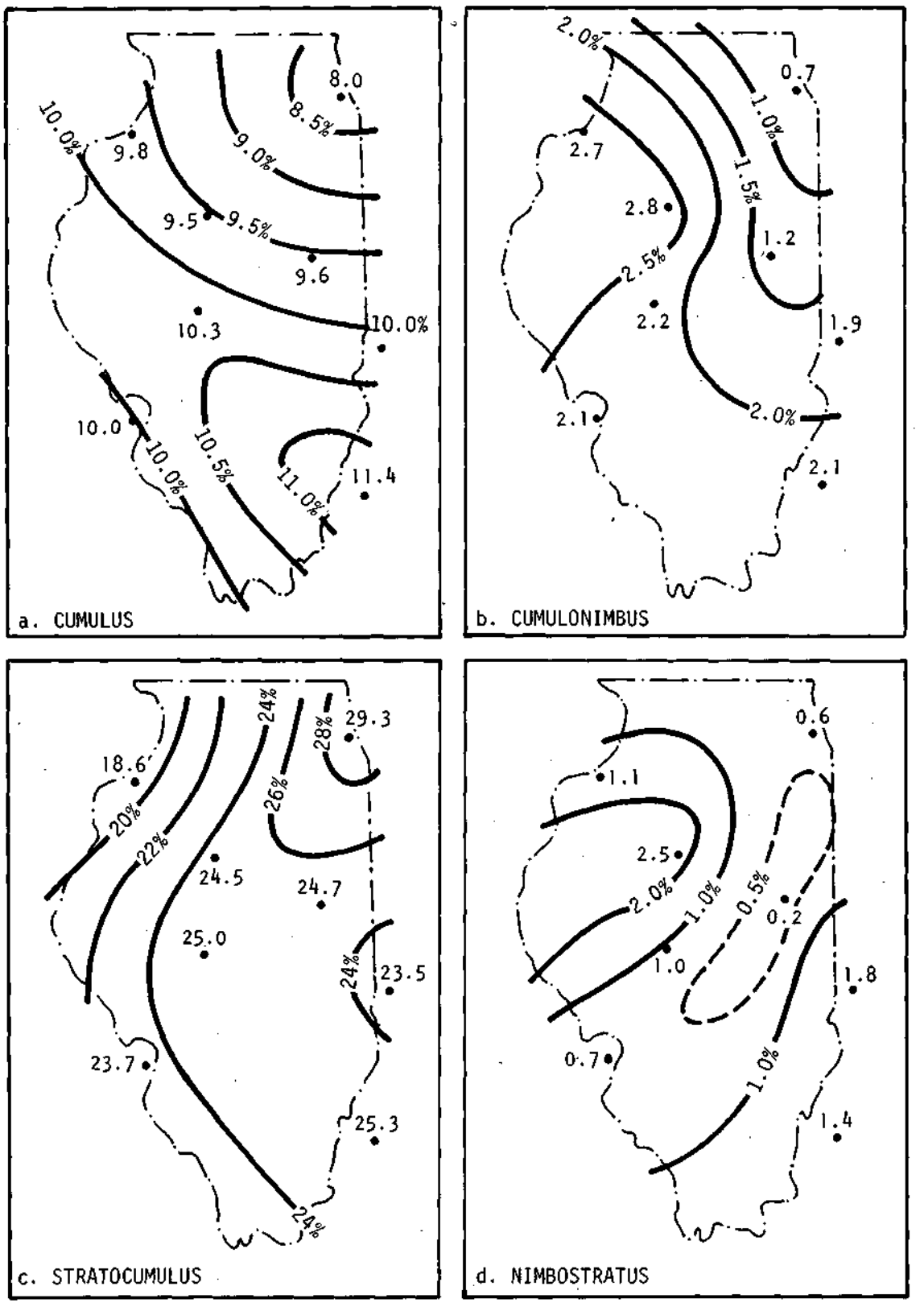

Figure 160. Average annual occurrences of low cloud types expressed as percent of total possible occurrences

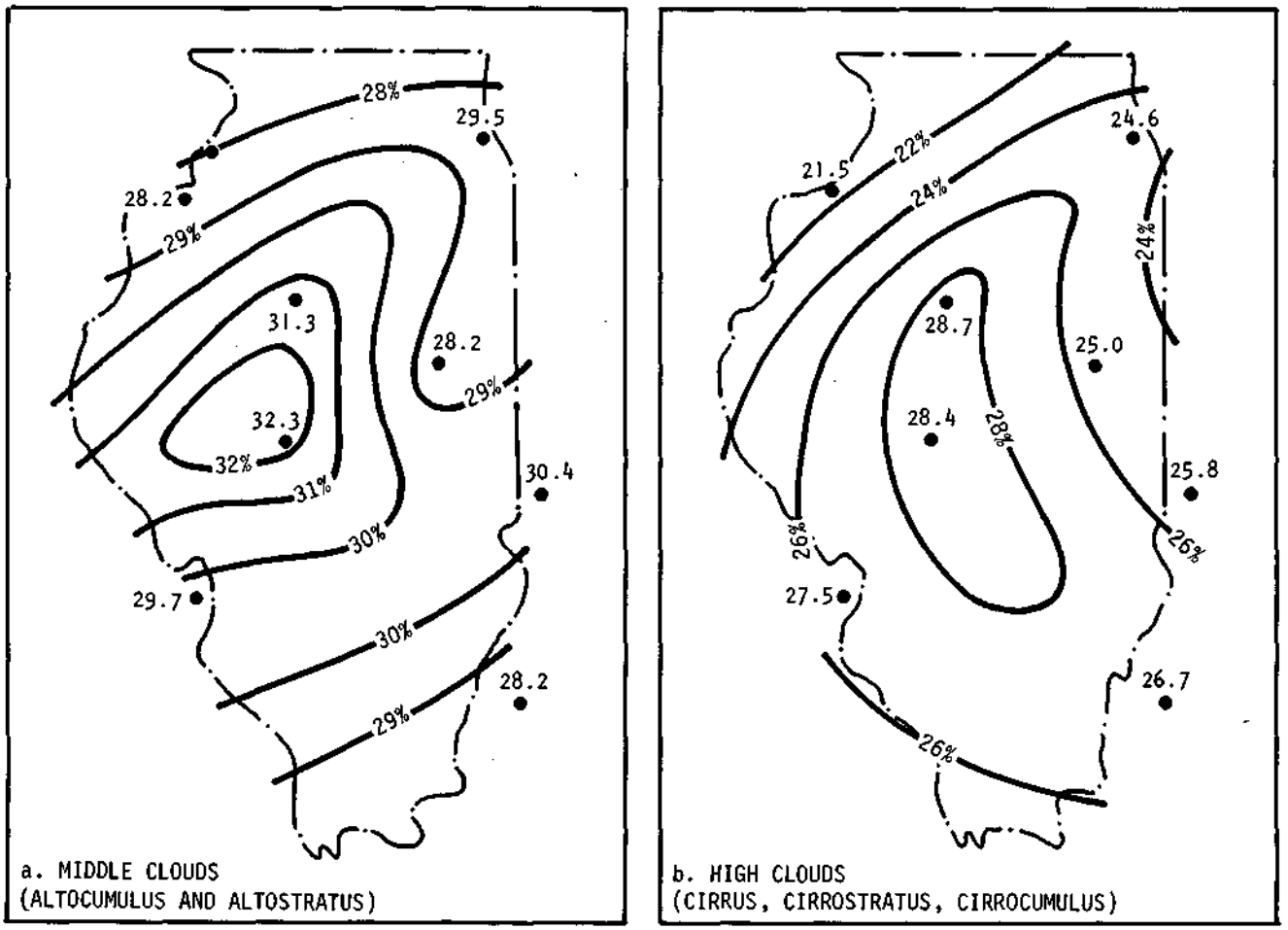

Figure 161. Average annual occurrences of middle and high cloud types expressed as percent of total possible observations

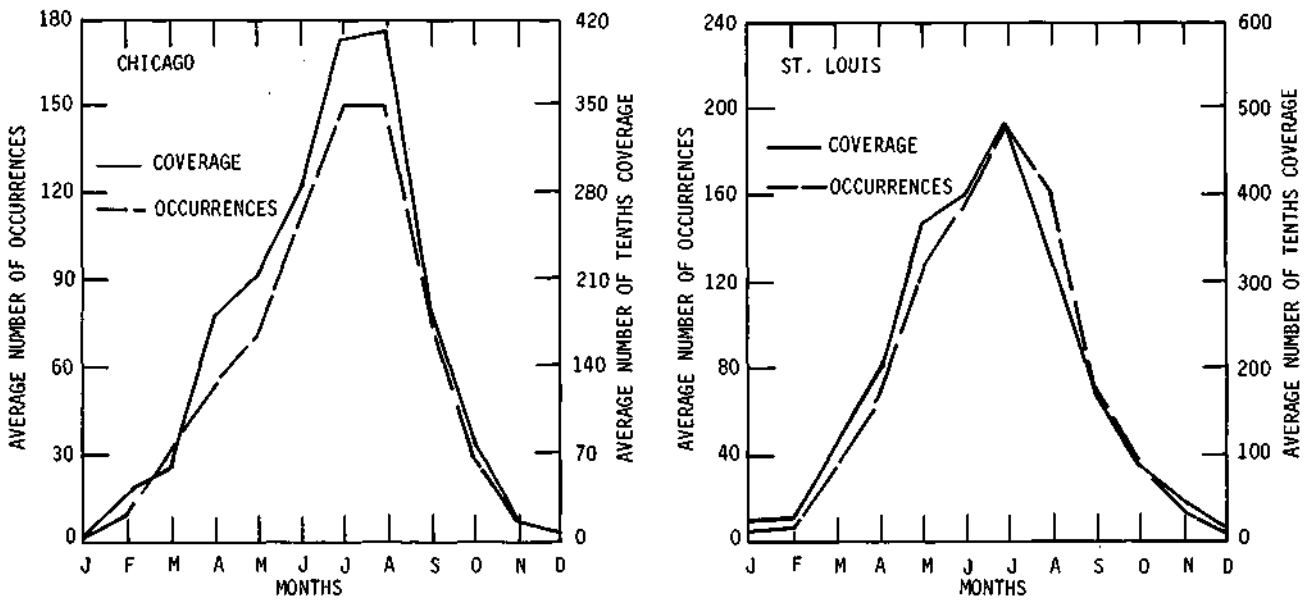

Figure 162. Comparison of average monthly occurrences and average tenths coverage of cumulus, 1949-1955

Table 72. Average Monthly and Annual Number of Tenths Coverage

	J	F	M	A	M	J	J	A	S	O	N	D	Annual
Cumulus													
CHI	6	40	58	108	209	282	407	423	193	83	10	3	1812
MLI	21	32	178	305	462	435	453	475	194	111	73	23	2670
SPI	26	46	119	191	398	342	477	369	226	140	66	14	2408
STL	23	24	116	198	367	399	475	309	169	90	46	14	2169
EVV	56	73	198	241	522	673	770	664	343	188	95	52	3722
RAN	35	67	199	291	483	618	725	597	301	173	94	21	3688
Cumulonimbus													
CHI	0	0	7	29	33	54	45	44	22	7	0	0	222
MLI	6	9	46	100	162	283	259	194	112	65	30	0	1229
SPI	11	21	55	108	120	217	190	129	159	57	20	0	1036
STL	2	9	42	87	55	157	164	116	70	29	11	2	798
EVV	21	10	51	99	90	226	174	135	82	17	12	18	924
RAN	4	9	31	43	100	156	183	93	55	29	12	4	728
Stratocumulus													
CHI	2347	2052	2005	1639	1336	786	579	904	739	1386	1959	2093	17,757
MLI	1355	1270	1337	1202	1022	632	452	573	632	1114	1434	1383	12,061
SPI	1796	1667	1668	1533	1003	740	376	528	506	906	1639	1826	13,550
STL	1808	1236	1242	1138	951	545	348	384	435	837	1323	1892	11,618
EVV	2063	1698	1609	1409	998	566	346	367	419	949	1580	1964	13,622
RAN	1514	1543	1544	1414	1211	807	417	495	514	823	1536	1497	12,918
Nimbostratus													
CHI	54	16	82	32	30	9	3	21	12	20	35	24	353
MLI	138	137	169	39	136	19	2	19	3	50	59	84	850
SPI	119	79	67	54	55	4	1	3	6	28	61	102	544
STL	25	37	59	69	68	3	5	22	2	36	25	54	419
EVV	106	90	52	53	49	24	0	0	1	17	95	88	483
RAN	10	16	5	15	17	10	0	6	0	68	21	0	173
Altocumulus													
CHI	628	778	736	993	1217	1116	1377	1302	1132	797	749	186	11,802
MLI	632	816	692	682	982	1026	941	1076	805	724	744	611	9536
SPI	981	893	835	952	1190	1011	1216	1451	986	943	825	1005	12,390
STL	770	623	794	755	921	716	896	1056	696	652	576	661	8850
EVV	1097	1070	1020	1306	1546	1491	1489	2071	1313	984	1011	1099	15,012
RAN	771	965	691	931	1282	1331	1497	1579	1349	1019	826	901	12,790
Altostratus													
CHI	296	270	262	329	261	215	164	145	153	168	169	284	2323
MLI	482	383	334	451	210	225	102	163	123	175	277	446	3075
SPI	176	88	119	113	84	84	47	55	53	102	161	173	1013
STL	420	291	286	304	331	254	192	274	125	146	246	325	2907
EVV	330	248	446	284	333	220	183	141	141	128	274	268	2874
RAN	354	379	458	417	586	543	365	358	268	418	271	318	4432
Cirriform													
CHI	955	686	653	1012	1070	1570	1246	1130	822	749	890	774	11,393
MLI	731	519	561	708	714	1041	804	705	560	549	779	588	8237
SPI	749	670	563	925	992	1221	1307	1083	721	760	805	802	10,864
STL	760	718	738	1014	1145	1327	1062	916	614	569	721	749	10,323
EVV	1164	1331	1344	1787	2145	2645	2531	2071	1327	1340	1138	1098	19,799
RAN	1462	1320	1211	1894	2111	2804	2500	1961	1370	1279	1411	1301	20,757

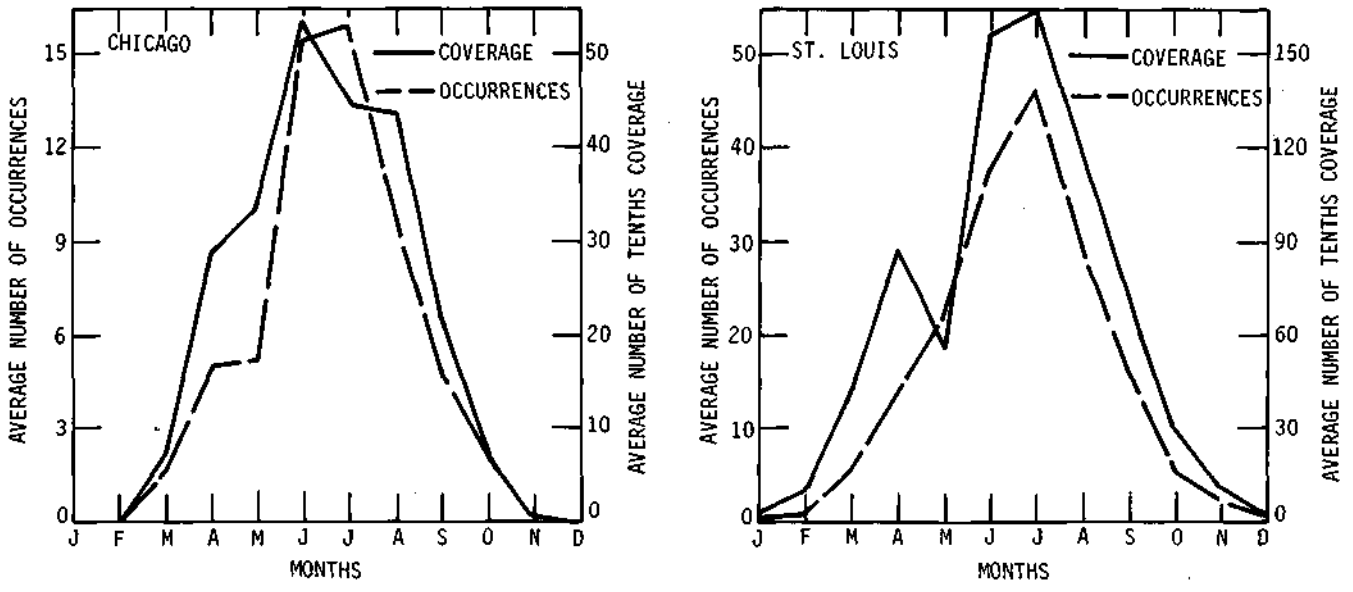

Figure 163. Comparison of average monthly occurrences and average tenths coverage of cumulonimbus, 1949-1955

Table 73. Seasonal Correlation Coefficients between Cloud Amounts and Monthly Precipitation at Springfield

	Correlation coefficients for point and areal mean precipitation					
			October-November and			
Cloud type	*May-September*		*March-April*		*December-February*	
	Point	*Area**	*Point*	*Area**	*Point*	*Area**
Cb	0.59	0.70	0.42	0.50	0.22	0.24
Cu	0.17	0.20	0.33	0.36	0.21	0.21
Sc	0.27	0.37	0.20	0.16	0.04	−0.16
Cu,Sc,Cb	0.41	0.51	0.29	0.27	0.13	0.03
St,Fs	0.25	0.33	0.44	0.41	−0.05	−0.02
As	0.76	0.80	−0.03	−0.01	−0.04	−0.15
Ac	0.34	0.37	−0.12	−0.02	−0.15	−0.22
Ci,Cc,Cs	0.60	0.60	0.17	0.30	−0.22	−0.12

** 8-station average of monthly precipitation over 30-mile radius about Springfield*

Table 74. Median Low Cloudiness, Expressed as Percent of Normal, for Various Values of Daily Precipitation

Period	*Chicago*	*Moline*	*Springfield*	*St. Louis*	*All stations*	*Number of cases*
Daily precipitation of 0.26 to 1.00 inch						
Winter	134	155	166	221	160	90
Spring	152	159	186	140	155	152
Summer	129	175	206	139	163	152
Fall	214	251	234	243	224	95
Annual	140	175	187	186	172	489
Daily precipitation over 1.00 inch						
Winter	128	188	175	260	193	13
Spring	220	196	182	228	208	26
Summer	260	195	124	174	183	40
Fall	203	197	167	319	215	19
Annual	210	194	179	242	201	98

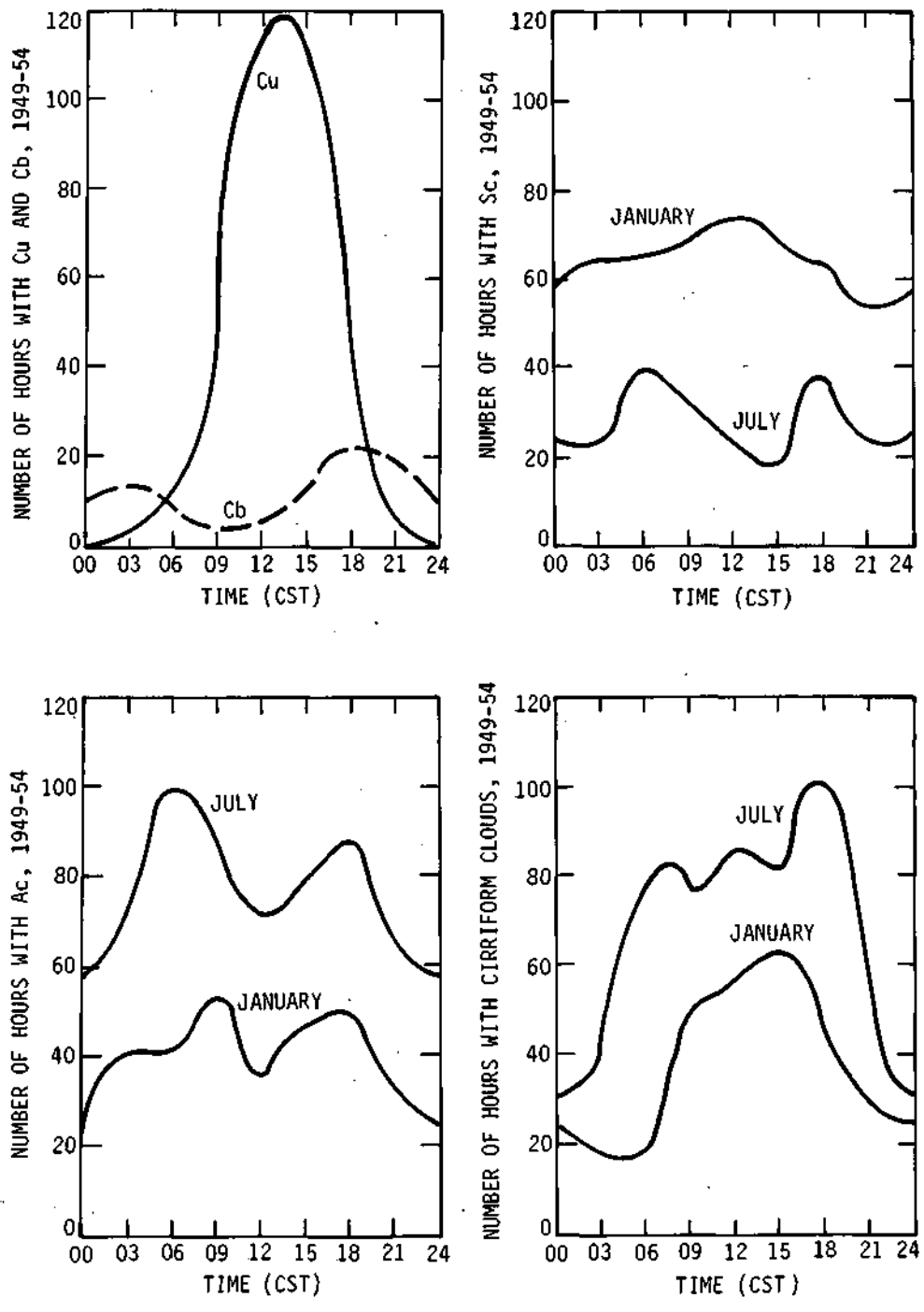

Figure 164. Diurnal distribution of cloud types at Springfield

Table 75. Distribution of Low Clouds on Days with Precipitation Exceeding 0.25 Inch during 1951-1955

Cumulative percent of wet days	*Percent of normal cloudiness equaled or exceeded for given daily precipitation (inches)*	
	0.26-1.00	*over 1.00*
5	350	414
10	322	338
20	272	276
30	241	244
40	203	216
50	172	201
60	145	184
70	118	142
80	104	124
90	72	93
95	48	74

Table 76. Correlation between Major Cloud Types and Precipitation Frequencies at Springfield

	Correlation coefficients for given cloud groups		
Year	*Low clouds (Cb,Cu,Sc)*	*Middle clouds (As,Ac)*	*High clouds (Ci,Cs,Cc)*
1949	0.19	–0.10	0.01
1950	0.50	0.22	–0.09
1951	0.25	–0.31	0.08
1952	0.93	0.37	0.22
1953	0.83	0.09	–0.21
1954	0.65	0.44	0.14
1955	0.54	0.82	0.36
Combined	0.54	0.16	0.04

days and the monthly frequency of cloud types in hours is shown in figure 165. Relationships, at best, are not strong.

Relationships between cirrus, cumulonimbus, and rainfall were also investigated since the development of precipitation may be implemented by the presence of cirriform clouds acting to seed (ice crystal) the lower level cumuliform clouds. Two conditions associated with the development of cumulonimbus clouds were investigated: 1) *CuCb conditions,* those when continuous hourly observations of cumulus existed from 1200 CST until the first Cb was reported with no cirriform clouds reported during that day and prior to the Cb; and 2) *CiCb conditions,* those when continuous hourly observations of cirriform clouds existed from 1100 CST until Cb were first reported, either with or without Cu in prior hours. Then, the average rainfall associated with the Cb under each of these two conditions was determined for five stations, as shown in table 77.

In Springfield, the average rainfall with prior cirrus (CiCb) was 0.26 inch, as compared to 0.15 inch with no prior cirrus (CuCb). Results in table 77 reveal that the prior presence of cirrus does occur with conditions that produce heavier rainfall. Whether more rain is a result of prior cirrus seeding or is just reflecting that a stronger convective condition exists when prior cirrus appear is not known.

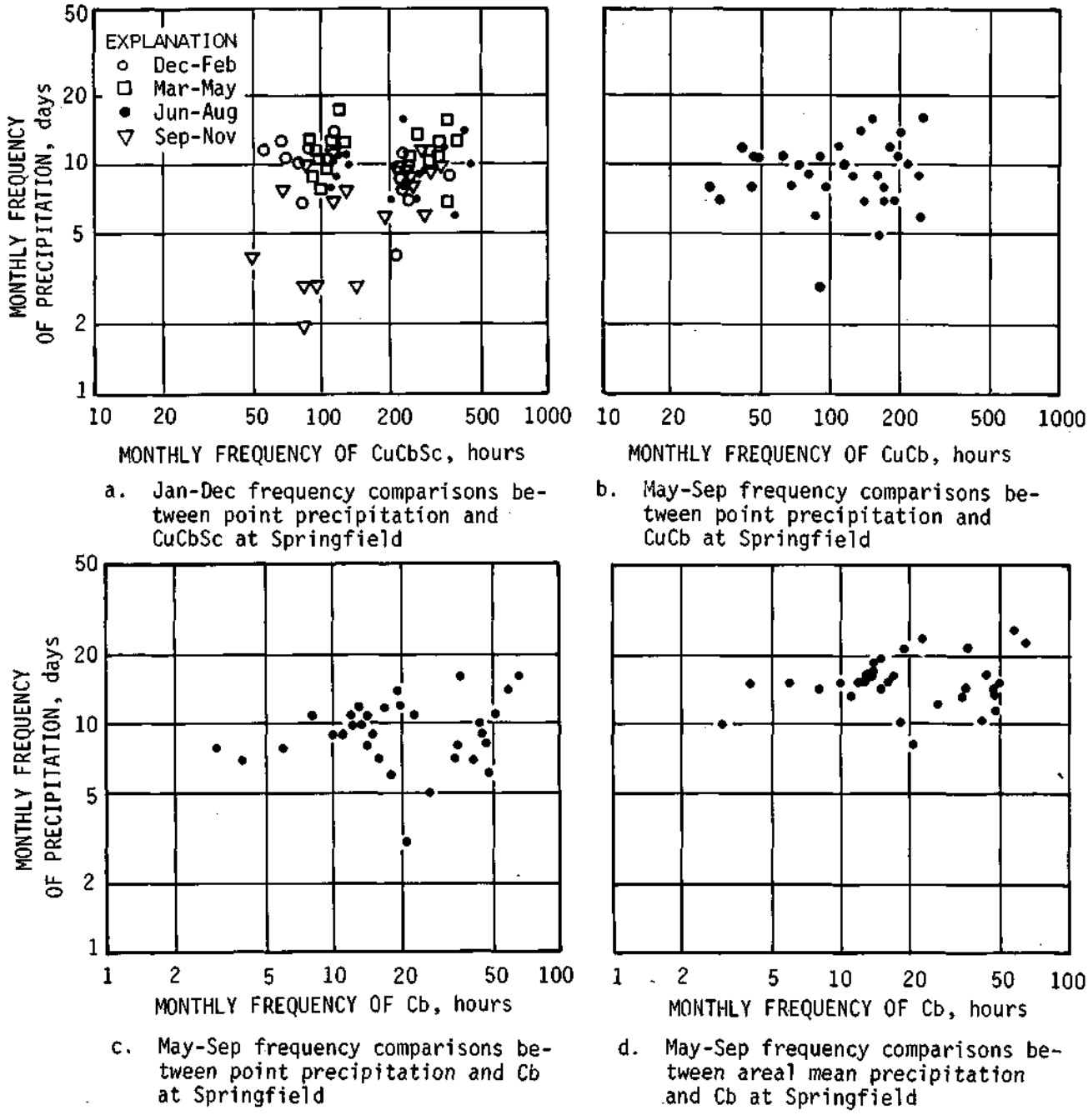

a. Jan-Dec frequency comparisons between point precipitation and CuCbSc at Springfield

b. May-Sep frequency comparisons between point precipitation and CuCb at Springfield

c. May-Sep frequency comparisons between point precipitation and Cb at Springfield

d. May-Sep frequency comparisons between areal mean precipitation and Cb at Springfield

Figure 165. Seasonal frequencies of rain days and hourly frequencies of clouds at Springfield

Table 77. Cumulonimbus Relationships to Daily Precipitation

	Daily prior condition			
	CuCb		*CiCb*	
	Number of cases	*Average rainfall per case, inches*	*Number of cases*	*Average rainfall per case, inches*
Chicago	10	0.34	19	0.45
Springfield	24	0.15	44	0.26
Moline	40	0.25	29	0.30
St. Louis	44	0.16	62	0.18
Rantoul	27	0.32	42	0.33

REFERENCES

Achtemeier, Gary L. 1978. *Model cloud distributions in an anisotropic environment.* Preprint Conference on Cloud Physics and Atmospheric Electricity, July 31-August 4, Issaquah, Washington, AMS, Boston, pp. 467-474.

Achtemeier, Gary L., and Griffith M. Morgan, Jr. 1975. *A short-term thunderstorm forecast system: Step 1, exploitation of the surface data.* Preprint Ninth Conference on Severe Local Storms, Norman, Oklahoma, AMS, Boston, pp. 18-24.

Ackerman, B. 1974. *The partition of liquid water near the freezing level.* Preprint Conference on Cloud Physics, Tucson; AMS, Boston, pp. 300-304.

Ackerman, B., S. A. Changnon, Jr., G. Dzurisin, D. F. Gatz, R. C. Grosh, S. D. Hilberg, F. A. Huff, J. W. Mansell, H. T. Ochs, III, M. E. Peden, P. T. Schickedanz, R. G. Semonin, and J. L. Vogel. 1978. *Summary of METROMEX, volume 2: Causes of precipitation anomalies.* Illinois State Water Survey Bulletin 63, 395 p.

Ackerman, B., and Herbert A. Greenman. 1978. *The evolution of a multicellular convective cloud mass: A case study.* Preprint Conference on Cloud Physics and Atmospheric Electricity, July 31-August 4, Issaquah, Washington, AMS, Boston, pp. 655-660.

Changnon, S. A. 1978. *Vertical characteristics and behavior of radar echoes. In* Summary of METROMEX, Volume 2: Causes of Precipitation Anomalies, by B. Ackerman et al., Illinois State Water Survey Bulletin 63, pp. 274-279.

Changnon, S. A. 1976. *Effects of urban areas and echo merging on radar echo behavior.* Journal of Applied Meteorology, v. 15(6):561-570.

Changnon, S. A. 1972. *Illinois radar research for hail suppression applications, 1967-1969.* Illinois State Water Survey Report of Investigation 71, 23 p.

Changnon, S. A. 1968. *Climatology of hourly occurrences of selected atmospheric phenomena in Illinois.* Illinois State Water Survey Circular 93, 28 p.

Changnon, S. A. 1967. *Weather probabilities in Illinois.* University of Illinois Agronomy Series, Urbana, 5 p.

Changnon, S. A. 1963a. *Monthly and semi-monthly distributions of hail daysin Illinois.* Research Report 17, CHIAA, Chicago, 21 p.

Changnon, S. A. 1963b. *Precipitation in a 550-square-mile area of southern Illinois.* Transactions Illinois Academy of Science, v. 56(4):165-187.

Changnon, S. A. 1962a. *Singularities in severe weather events in Illinois.* Research Report 13, CHIAA, Chicago, 19 p.

Changnon, S. A. 1962b. *Regional characteristics of severe summer hailstorms in Illinois.* Research Report 14, CHIAA, Chicago, 19 p.

Changnon, S. A. 1960. *A method for determining dry period probabilities as applied to Illinois.* Meteorological Monograph, AMS, Boston, pp. 113-118.

Changnon, S. A. 1958. *Water resources and climate, section 1.* Atlas of Illinois Resources, Illinois Division of Industrial Planning and Development, Springfield, 58 p.

Changnon, S. A. 1957. *Thunderstorm-precipitation relations in Illinois.* Illinois State Water Survey Report of Investigation 34, 24 p.

Changnon, S. A., Jr., and S. G. Bigler. 1957. *On the observation of convective clouds and the radar-precipitation echoes within them.* Bulletin American Meteorological Society, v. 38:279-283.

Changnon, S. A., and F. A. Huff. 1971. *Evaluation of potential benefits of weather modification on agriculture.* Contract INT-14-06-D-6843, Final Report, Parts 1 and 2, October, 136 p.

Changnon, S. A., and F. A. Huff. 1961. *Studies of radar-depicted precipitation lines.* Contract AF 19(604)-4940, Scientific Report 2, February, 63 p.

Changnon, S. A., and F. A. Huff. 1957. *Cloud distribution and correlation with precipitation in Illinois.* Illinois State Water Survey Report of Investigation 33, 44 p.

Changnon, S. A., F. A. Huff, and P. T. Schickedanz. 1975. *A High Plains climatography.* Illinois State Water Survey Special Report, Contract 14-06-D-7197, 119 p.

Changnon, S. A., F. A. Huff, P. T. Schickedanz, and John L. Vogel. 1977. *Summary of METROMEX, volume 1: Weather anomalies and impacts.* Illinois State Water Survey Bulletin 62, 260 p.

Changnon, S. A., and Griffith M. Morgan, Jr. 1976. *Design of an experiment to suppress hail in Illinois.* Illinois State Water Survey Bulletin 61, 194 p.

Changnon, S. A., and R. G. Semonin, Editors. 1975. *Studies of selected precipitation cases from METROMEX.* Illinois State Water Survey Report of Investigation 81, 329 p.

Changnon, S. A., R. G. Semonin, and F. A. Huff. 1976. *A hypothesis for urban rainfall anomalies.* Journal of Applied Meteorology, v. 15(6):544-560.

Chiang, I. M. 1961. *An analysis of selected synoptic elements of the climatology of Illinois, period from 1945-1959.* Masters thesis, Department of Geography, Southern Illinois University, Carbondale, 75 p.

Grosh, Ronald C. 1978a. *Lightning and precipitation — The life history of isolated thunderstorms.* Preprint Conference on Cloud Physics and Atmospheric Electricity, July 31-August 4, Issaquah, Washington; AMS, Boston, pp. 617-624.

Grosh, Ronald C. 1978b. *Operational prediction of severe weather.* Technical Letter 27, Illinois State Water Survey, Miscellaneous Publication 51, 3 p.

Hiser, H. W. 1956. *Type distributions of precipitation at selected stations in Illinois.* Transactions American Geophysical Union v. 37:421-424.

Hiser, H. W., and S. G. Bigler. 1953. *Wind data from radar echoes.* Contract N 189s-88164, Technical Report 1, 18 p.

Huff, F. A. 1978a. *Characteristic properties of midwestern flash flood storms.* Preprint Conference on Flash Floods, Los Angeles; AMS, Boston, pp. 29-33.

Huff, F. A. 1978b. *The synoptic environment of flash flood storms.* Preprint Conference on Flash Floods, Los Angeles; AMS, Boston, pp. 10-16.

Huff, F. A. 1978c. *Radar analysis of urban effects on rainfall. In* Summary of METROMEX Volume 2: Causes of Precipitation Anomalies. Illinois State Water Survey Bulletin 63, pp. 265-273.

Huff, F. A. 1977. *Distribution of heavy raincells. In* Summary of METROMEX Volume 1: Weather Anomalies and Impacts, Illinois State Water Survey Bulletin 62, pp. 182-192.

Huff, F. A. 1971. *Distribution of hourly precipitation in Illinois.* Illinois State Water Survey Circular 105, 23 p.

Huff, F. A. 1970. *Sampling errors in measurement of mean precipitation.* Journal of Applied Meteorology, v. 9:35-44.

Huff, F. A. 1969a. *Climatological assessment of natural precipitation characteristics for use in weather modification.* Journal of Applied Meteorology, v. 8(3):401-410.

Huff, F. A. 1969b. *Precipitation detection by fixed sampling densities.* Journal of Applied' Meteorology, v. 8:834-837.

Huff, F. A. 1968. *Area-depth curves — A useful tool in weather modification experiments.* Journal of Applied Meteorology, v. 7:940-943.

Huff, F. A. 1967a. *Time distribution of rainfall in heavy storms.* Water Resources Research v. 3(4):1007-1019.

Huff, F. A. 1967b. *Rainfall gradients in warm season rainfall.* Journal of Applied Meteorology v. 6:435-437.

Huff, F. A. 1966. *The effect of natural rainfall variability in verification of rain modification experiments.* Water Resources Research v. 2(4):791-801.

Huff, F. A. 1963. *Atmospheric moisture-precipitation relations.* ASCE Journal of Hydraulics v. 89(HY6):93-110.

Huff, F. A., and S. A. Changnon, Jr. 1973. *Precipitation modification by major urban areas.* Bulletin American Meteorological Society v. 54:1220-1232.

Huff, F. A., and S. A. Changnon, Jr. 1966. *Development and utilization of Illinois precipitation networks.* International Association of Scientific Hydrology, Symposium on Design of Hydrological Networks Publication No. 67, pp. 97-125.

Huff, F. A., and S. A. Changnon, Jr. 1964. *A model 10-inch rainstorm.* Journal of Applied Meteorology v. 5:587-599.

Huff, F. A., and S. A. Changnon, Jr. 1963. *Drought climatology of Illinois.* Illinois State Water Survey Bulletin 50, 68 p.

Huff, F. A., and S. A. Changnon. 1960. *Hail climatology of Illinois.* Illinois State Water Survey Report of Investigation 38, 46 p.

Huff, F. A., S. A. Changnon, and D. M. A. Jones. 1975. *Precipitation increases in the low hills of southern Illinois: Part 1. Climatic and network studies.* Monthly Weather Review v. 103(9):823-829.

Huff, F. A., and W. L. Shipp. 1969. *Spatial correlations of storm, monthly and seasonal precipitation.* Journal of Applied Meteorology v. 8(4):542-550.

Huff, F. A., and W. L. Shipp. 1968. *Mesoscale spatial variability in midwestern precipitation.* Journal of Applied Meteorology v. 7(5):886-891.

Huff, F. A., and J. L. Vogel. 1977. *Assessment of weather modification in alleviating agricultural water shortages during droughts.* Illinois State Water Survey Final Report, ENV 74-24367, 113 p.

Huff, F. A., and J. L. Vogel. 1976. *Hydrometeorology of heavy rainstorms in Chicago and northeastern Illinois.* Illinois State Water Survey Report of Investigation 82, 63 p.

Morgan, Griffith M., Jr., David A. Brunkow, and Robert C. Beebe. 1975. *Climatology of surface fronts.* Illinois State Water Survey Circular 122, 48 p.

Sax, Robert I., Jane C. Eden, and Bernice Ackerman. 1978. *Single-level microstructure of pre-fronial and post-frontal Illinois cumuli.* Preprint Conference on Cloud Physics and Atmospheric Electricity, July 31-August 4, Issaquah, Washington; AMS, Boston, pp. 324-329.

Schickedanz, P. T. 1978. *Surface raincell analyses. In* Summary of METROMEX, Volume 2: Causes of Precipitation Anomalies, Illinois State Water Survey Bulletin 63, pp. 280-314.

Schickedanz, P. T. 1974. *Inadvertent rain modification as indicated by surface raincells.* Journal of Applied Meteorology v. 13(8):891-900.

Schickedanz, P. T. 1973. *Climatic studies of extra-area effects from seeding.* PEP, Phase I, Contract 14-06-D-7197, Technical Report 5, 53 p.

Schickedanz, P. T., and F. A. Huff. 1971. *The design and evaluation of raincell modification experiments.* Journal of Applied Meteorology v. 10:502-514.

Semonin, R. G. 1978. *Cloud Characteristics. In* Summary of METROMEX, Volume 2: Causes of Precipitation Anomalies, Illinois State Water Survey Bulletin 63, pp. 236-239.

Semonin, Richard G. 1977. *Illinois seeding opportunities as indicated by a 1-D model.* Preprint Sixth Conference on Inadvertent and Planned Weather Modification, Champaign-Urbana; AMS, Boston, pp. 266-269.

Semonin, R. G., D. W. Staggs, and G. E. Stout. 1962. *Cloud electrification studies in Illinois.* National Science Foundation G-17038, Annual Report. April, 13 p.

Stall, John B., and Floyd A. Huff. 1971. *The structure of thunderstorm rainfall.* Preprint 1330, ASCE National Water Resources Engineering Meeting, Phoenix, January, 30 p.

Stout, G. E. 1960. *Observations of precipitation variability.* Transactions Illinois Academy of Science v. 53(1,2): 11-19.

Stout, G. E., and F. A. Huff. 1962. *Studies of severe rainstorms in Illinois.* ASCE Journal of Hydraulics Division v. 88(HY4):129-146.

Towery, N. G., and S. A. Changnon. 1970. *Characteristics of hail producing radar echoes in Illinois.* Monthly Weather Review v. 98(5): 346-353.

Vogel, J. L. 1975. *Air mass storms of 10 August 1973. In* Studies of Selected Precipitation Cases from METROMEX, Illinois State Water Survey Report of Investigation 81, pp. 191-231.

Vogel, J. L., and F. A. Huff. 1978. *Relation between St. Louis urban precipitation anomaly and synoptic weather factors.* Journal of Applied Meteorology v. 17:1141-1150.

Vogel, J. L., and F. A. Huff. 1977. *Relation between surface winds, storm movement, and rainfall. In* Summary of METROMEX Volume 1: Weather Anomalies and Impacts, Illinois State Water Survey Bulletin 62, pp. 53-62.

Wilk, K. E. 1961. *Research concerning analysis of severe thunderstorms.* Contract AF 19(604)-4940, Final Report, December, 68 p.

Wilson, J. W., and S. A. Changnon. 1971. *Illinois tornadoes.* Illinois State Water Survey Circular 103, 58 p.